Calcium signalling in a fluid transporting epithelium

A thesis submitted for the degree of
Doctor of Philosophy at the University of Glasgow

By

Matthew MacPherson

Division of Molecular Genetics
Institute of Biomedical and Life Sciences
University of Glasgow
Glasgow
G11 6NU
UK

January 2001

ProQuest Number: 13818779

All rights reserved

INFORMATION TO ALL USERS
The quality of this reproduction is dependent upon the quality of the copy submitted.

In the unlikely event that the author did not send a complete manuscript
and there are missing pages, these will be noted. Also, if material had to be removed,
a note will indicate the deletion.

ProQuest 13818779

Published by ProQuest LLC (2018). Copyright of the Dissertation is held by the Author.

All rights reserved.
This work is protected against unauthorized copying under Title 17, United States Code
Microform Edition © ProQuest LLC.

ProQuest LLC.
789 East Eisenhower Parkway
P.O. Box 1346
Ann Arbor, MI 48106 – 1346

GLASGOW
UNIVERSITY
LIBRARY
12206
COPY 1

The research reported within this thesis is my own work except where otherwise stated, and has not been submitted for any other degree.

Matthew MacPherson

Abstract

The *Drosophila* Malpighian tubule is an ideal model epithelium for the study of fluid transport and cell signalling. This thesis has aimed to develop further the tubule for the study of calcium signals in response to a variety of stimuli, and their relation to fluid transport. To do this an 'integrative' approach combining molecular genetic and pharmacological studies with physiological assays of tubule function was used.

The expression of several calcium channel genes (*DmcaIA*, *DmcaID*, *trp*, *trpl* and *trpγ*), and several genes encoding molecules involved in the regulation of calcium signalling (*inaC*, *pkc53e*, *inaD*, *norpA and plc-21e*) was surveyed by Reverse Transcriptase-PCR. All these genes, with the exception of *inaD*, are expressed in tubules.

CAP_{2b} is a neuropeptide that stimulates an increase in fluid secretion rate and also a sharp increase in $[Ca^{2+}]_i$, exclusively in the principal cells of the tubule. Through the examination of CAP_{2b}-stimulated fluid secretion and CAP_{2b}-stimulated rises in $[Ca^{2+}]_i$, as well as studies using fluorescently labelled calcium channel antagonists, verapamil- and nifedipine-sensitive calcium channels were shown to be involved in stimulated fluid secretion and calcium signalling. By immunocytochemistry, α1 subunits were localised to main segment principal cells. Additionally, cGMP was shown to stimulate a prolonged rise in $[Ca^{2+}]_i$ through the influx of extracellular calcium via nifedipine and verapamil sensitive channels.

The role of transient receptor potential channels (TRP, TRPL) in CAP_{2b}- and thapsigargin-stimulated $[Ca^{2+}]_i$ rises was examined using *Drosophila trp* and *trpl* mutants expressing aequorin. Analysis of the CAP_{2b}-stimulated calcium signal, found an attenuation of the signal elicited in *trpl* mutants, but both attenuation and potentiation of signal in different *trp* mutants.

Alongside results obtained using TRP and TRPL antagonists, this suggested a major role for TRPL in the production of the CAP_{2b} calcium response. Furthermore, TRP and TRPL were localised to main segment principal cells by immunocytochemistry.

Finally, the effect on calcium signalling of molecules further downstream in the signal transduction pathway was examined using mutants containing the nitric oxide synthase gene under heat shock control. Although no effect on calcium responses to either CAP_{2b} or cGMP was observed following heat shock-induced ectopic expression of NOS, there was a significant if inconsistent rise in unstimulated fluid secretion. Further experiments suggested this to be due to a rise in intracellular cGMP. Together the results presented here suggest an involvement of phenylalkylamine (PAA)- and dihydropyridine (DHP)-sensitive calcium channels and TRP and TRPL in the production of the CAP_{2b} calcium response.

Overall, this thesis demonstrates the amenability of the Malpighian tubule for the study of calcium signalling and goes some way to revealing the calcium regulatory mechanisms lying within.

Abbreviations

APS	ammonium persulphate
ATP	adenosine triphosphate
ATPase	adenosine triphosphatase
BCIP	5-bromo-4-chloro-3-indolyl-phosphate
BDGP	Berkeley *Drosophila* Genome Project
b p	base pairs
BSA	bovine serum albumin
CAP_{2b}	cardioacceleratory peptide
cDNA	complementary DNA
CNG	cyclic nucleotide gated channel
d	days
dATP	2' deoxyadenosine triphosphate
dCTP	2' deoxycytosine triphosphate
dGTP	2' deoxyguanosine triphosphate
dNTP	2' deoxy(nucleotide) triphosphate
dTTP	2' deoxythymidine triphosphate
dUTP	2' deoxyuridine triphosphate
DEPC	diethyl pyrocarbonate
DHP	dihydropyridine
DMF	dimethylformamide
DNA	deoxyribonucleic acid
DTT	dithiothreitol
EDTA	ethylenediamine tetra acetic acid (disodium salt)
EM	electron microscopy
ER	endoplasmic reticulum
EtBr	ethidium bromide
g	gram
HEPES	N-([2-hydroxyethyl]piperazine-N'-[2-ethanesulphonic acid])
INAC	inactivation no-after potential C
INAD	inactivation no-after potential D
$InsP_3$	Inositol 1,4,5-trisphosphate

kb	kilobases
kDa	kiloDaltons
M	molar
max.	maximum
mg	milligram
ml	millilitre
mm	millimetre
mM	millimolar
min	minute
mRNA	messenger RNA
MOPS	3-[N-morpholino]propane-sulphonic acid
NBT	nitro-blue-tetrazolium
ng	nanograms
nM	nanomolar
OLB	oligo-labelling buffer
OreR	Oregon R
PAA	phenylalkylamine
PBS	phosphate buffered saline
PCR	polymerase chain reaction
PKC	protein kinase C
PLC	phospholipase C
PtdIns(4,5)P_2	phosphatidyl inositol bisphosphate
RNA	ribonucleic acid
RNase	ribonuclease
rpm	revolutions per minute
rp49	*Drosophila* ribosomal protein 49
ROC	receptor operated channel
RT-PCR	reverse transcriptase polymerase chain reaction
RYR	ryanodine receptor
s	second
SDS	sodium dodecyl sulphate
SOC	store operated channel
TEMED	N,N,N',N'-tetramethylethylenediamine
Tris	2-amino-2-(hydroxymethyl)-1,3-propanediol
u	unit
UAS	upstream activation sequence

UV	ultraviolet
V-ATPase	vacuolar H^+ adenosine triphosphatase
VOC	voltage operated channel
X-gal	5-bromo-4-chloro-3-indolyl-β-D-galactopyranoside
µCi	microCurie
µg	microgram
µl	microlitre
µM	micromolar
°C	degrees Celsius

Table of Contents

Results

Index of Figures

Chapter 1

Chapter 3

Chapter 4

Chapter 5

Chapter 6

Figure

Index of Tables

Chapter 2

Appendix

Acknowledgements

I would like to express my sincere thanks to the following people:
Dr. Shireen Davies for her supervision during the course of the Ph.D, and for support, encouragement, and some top class meals and entertainment.
Prof. Julian Dow for extra supervision, much advice and encouragement, and top class meal and entertainment support.
Dr. Douglas Armstrong and Dr. Howard Prentice for advice and support throughout my Ph.D.
Dr. Charles Zuker for the kind gift of anti-TRP antibody.
Dr Craig Montell, for the find gift of anti-TRPL antibody.
Dr Roger Hardie, for the kind gift of the *trp* and *trpl* mutant flies, and for electroretinogram verification of *trp* and *trpl* phenotypes.
The staff and students of the Dow/Davies lab past and present, Dr. Adrian Allan, Dr. Juan Du, Kate Broderick, Irene Durrant, Maria Giannakou, Shirley Graham, Martin Kerr, Ross McLennan, Valerie Pollock, Laura Kean, Jonathon Radford, Tony Southall, Leah Torrie, Kimberley Burns, Dr. Angela Gawthrop, and Dr.Fiona Claire O'Connell.
Ian Morrison, Hugh Jarvis and Alan MacFarlane for support, many laughs and good times.
All my extended family for their support.
To John and Jenny Drummond for much love, kindness and friendship.
Dr. Sean MacPherson and Dr. Linda Brown for support, encouragement and for being an excellent and loving brother.
My Mum and Dad, who I love very much, for their love, kindness, support, encouragment and countless other things.
And to Adrian Allan for letting me copy his acknowledgements and simply changing the names.

1.1 The *Drosophila melanogaster* Malpighian Tubule.

1.1.1 A model for epithelial fluid transport and calcium signalling.

One of the aims of this project is to further develop the *Drosophila melanogaster* Malpighian tubule as a model epithelium for the study of fluid transport and cell-specific signalling pathways. The morphology and development of this tissue has been comprehensively reviewed (Wessing and Eichelberg, 1978; Skaer, 1993), and more recently, it has been reviewed regarding its current importance in the field of 'integrative' physiology (Dow and Davies, in press). As well as a detailed study of cell-specific calcium signalling events in this epithelium, this project demonstrates the suitability of this small organ to genetic and physiological studies. The wealth of information, and abundance of scientific 'tools' concerning *Drosophila* (1000's of mutants, transgenics, the *Drosophila* genome project) make the Malpighian tubule an ideal tissue to study cell signalling events in an organotypic context i.e. in a whole, intact organ.

In this project I have investigated the calcium signalling events initiated by neurohormones and their subsequent effects on fluid secretion both in wild-type and signalling mutants. Malpighian tubules from other insect species have long been used for the study of neurohormonal control and fluid secretion(Maddrell, 1981; Maddrell, 1991; Maddrell and O'Donnell, 1992); and in 1994, Dow *et al*, demonstrated that the tubules of *Drosphila melanogaster* were amenable to physiological study, with the development of an assay for measurement of fluid secretion (Figure 1.2).

1.1.2 The Morphology of the Malpighian tubule.

The Malpighian tubule is the fly's fluid transporting osmoregulatory organ, and is analogous to the vertebrate renal system. Each fly has four tubules, arranged into two pairs, an anterior and posterior, connected to the gut by a ureter. The anterior pair is distinguishable by its prominent initial segment. The tubules were initially thought to be divided into three segments, an initial, a main and a lower (Wessing and Eichelberg, 1978) (Figure 1.1A). More recently, the tubule has been shown to be further divisible into six segments: The initial, transitional and main segments and the lower tubule, upper and lower ureter (Sozen *et al*, 1997) (Figure 1.1B). Here the systematic analysis of over 700 P{GAL4} enhancer trap lines was used to define genetically distinct regions or cells of the tubule. Such a method had previously been used to examine the mushroom bodies in *Drosophila* brains (Yang *et al*, 1995), and the nature of spatial expression and effects of P-elements is neatly demonstrated by the disruption of the spatial expression of the alkaline phosphatase gene (Yang *et al*, 2000). The regions of the tubule correspond to different functions or physiological properties. For example, the main segment performs a secretory role, whereas the lower tubule is involved in reabsorption, and the intial segment is thought to be involved in calcium transport (Dube *et al*, 2000).

In fluid secretion assays there was no observable difference between the antererior and posterior tubules (Dow *et al*, 1994), however it was recently demonstrated that they do have different calcium transporting properties which are conferred by the initial segments (Dube *et al*, 2000).

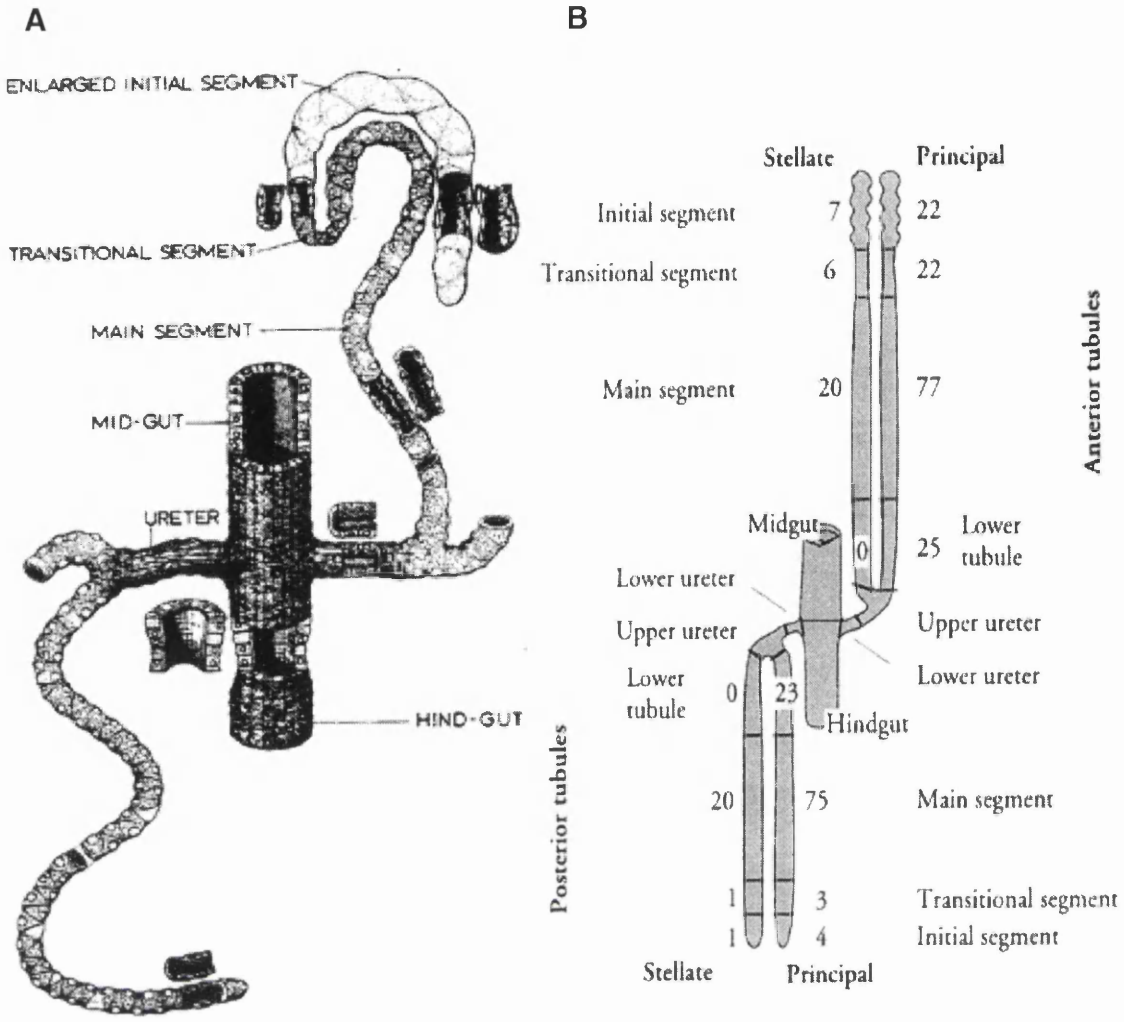

Figure 1.1: Morphology of the Malpighian tubule.

A) The classsical morphology of the Malpighian tubules, showing main, initial and transitional segments, and attachment of the tubule pairs to the gut. [Figure is taken from Wessing and Eichelberg, 1978. The Genetics and Biology of *Drosophila*, eds Ashburner and Wright. Academic, London, Vol. 2c, pp. 1-42]

B) Summary of tubule regional architecture. The different subregions of the tubule are indicated and the numbers of principal and stellate cells in each region are shown. [Figure is taken from Sozen, Armstrong, Yang, Kaiser and Dow, 1997. *Proc. Natl. Acad. Sci. USA*. 94, 5207-5212]

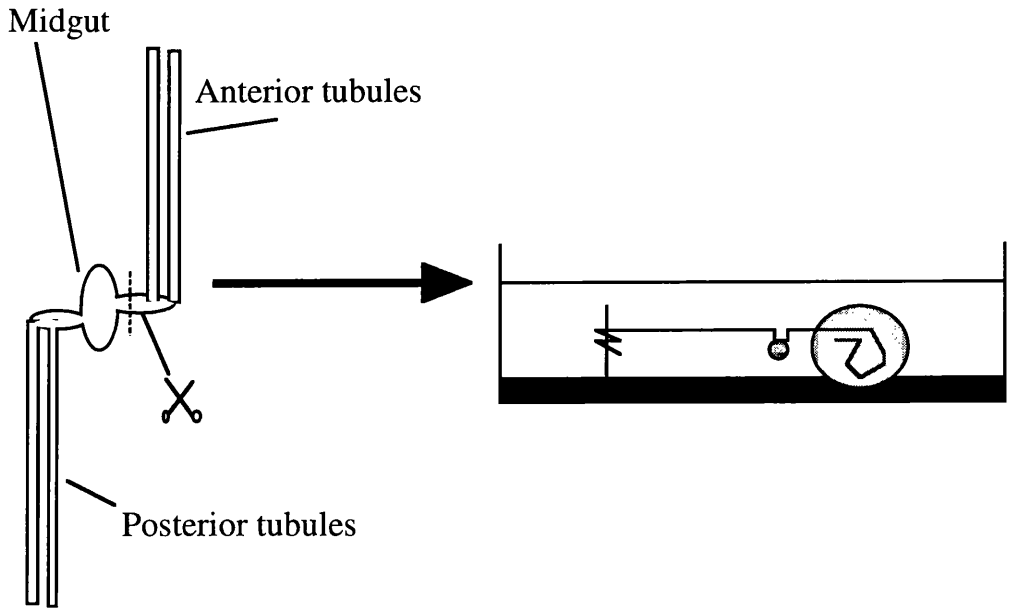

Figure 1.2: Measurement of fluid secretion in *Drosophila* Malpighian tubules. Malpighian tubules were dissected from the fly in Schneider's insect culture media (Gibco BRL). Tubules were dissected and separated as pairs by severance of the ureter. One tubule was wrapped around an anchoring pin whilst the other remained in a drop of 1:1 mixture of Schneider's:*Drosophila* saline, under mineral oil. As the tubule secretes a bubble of secreted fluid is formed at the ureter. This bubble can be 'tweaked' off with a finely pulled glass rod and the diameter measured.

1.1.3 The Cells of the Malpighian tubules.

There are two main cell types in the Malpighian tubule, namely the principal cells and the stellate cells (Figure 1.4). These cells are remarkably invariant in number within different segments of the tubule, and between tubules from different flies. In addition to these cells, there are small bar-shaped cells, genetically related to the stellate cells in the initial segment of the tubule. There are also very small cells, thought to be neuroendocrine cells, in the lower tubule and ureter (Sozen *et al*, 1997). It is speculated that the small neuroendocrine cells secrete hormones involved in the control of secretion and reabsorption in the tubules. Through the use of the aforementioned P{GAL4} enhancer trap lines it is apparent that the principal cells in the main segment can be further subdivided into at least two cell types (Sozen *et al*, 1997). This illustrates the diversity of cell types and complexity of this tiny organ.

Apart from the obvious morphological differences between principal and stellate cells they have also been shown to be involved in separate functions within the main segment. Separate control of anion and cation transport in the tubule has been demonstrated (O'Donnell *et al*, 1996), where different neuropeptides were shown to activate either anion or cation transport by the tubules. Therefore, it was speculated that the different pathways might be confined to the principal and stellate cells. This was demonstrated by the measurement of chloride currents using vibrating probes, which measure the tiny disturbances in electric field surrounding a tissue. 'Hotspots' of chloride current were observed only around the stellate cells in the main segment, implying the presence of a chloride transport pathway specifically in these cells (O'Donnell *et al*, 1998).

The transport of cations takes place in the principal cells where cation transport is energised by a H^+-pumping vacuolar ATPase (for review see Dow, 1999). The transport of cations into the lumen of the tubule drives the flux of

water into the lumen by osmosis. Previously it was described how P{GAL4} enhancer traps can be used to examine the genetic organisation of a tissue. However, if the P-element integrates close to a known gene, it inherits that gene's temporal and spatial expression (Davies *et al*, 1996; Yang *et al*, 2000). In this way it was found that *vha55* gene encoding the vacuolar ATPase B-subunit is strongly expressed in the principal cells of the main segment (Davies *et al*, 1996), indicating that the proton pumping vacuolar V-ATPase works to drive fluid secretion exclusively in these cells.

1.1.4 Cell signalling in the Malpighian tubule.

In this project I investigated the calcium signalling events stimulated by the neuropeptide Cardioacceleratory peptide (CAP_{2b}). CAP_{2b} was originally isolated from the tobacco hornworm, *Manduca sexta*. It was originally named due to the effect on *M. sexta* heart. The amino acid sequence of the *M. sexta* CAP_{2b} is pyro-ELYAFPRVamide (Huesmann *et al*, 1994), and a similar peptide has been isolated from *Drosophila* (Davies *et al*, 1995). However, more recently, a gene encoding a peptide containing the AFPRVamide sequence has been discovered in the *Drosophila* genome, and has been found to have effects similar to CAP_{2b} in *Drosophila* tubules (Kean *et al*, submitted). CAP_{2b} was found to increase the fluid secretion rate in *Drosophila* Malpighian tubules through an increase in intracellular cGMP concentration (Davies *et al*, 1995). The existence of a nitric oxide (NO)/cGMP signalling pathway was known in the tubule (Dow *et al*, 1994), and it was subsequently found that CAP_{2b} works through the NO/cGMP pathway (Davies *et al*, 1997). NO is synthesised through the conversion of L-arginine to L-citrulline by Nitric oxide synthases (NOS) (Marletta, 1994). In *Drosophila* a gene encoding a nitric oxide synthase (*dNOS*) has been discovered, which encodes a 152 kDa protein (Regulski and Tully, 1995). The expression of this gene has been demonstrated in the Malpighian tubules (Davies *et al*, 1997), and CAP_{2b} has been shown to increase DNOS activity in the

tubule. How then does the CAP_{2b} signal the activation of DNOS? DNOS contains putative binding sites for flavin adenine dinucleotide (FAD), flavin mononucleotide (FMN), nicotinamide adenine dinucleotide phosphate (NADP), and calmodulin, and when expressed in human 293 embryonic kidney cells was found to be Ca^{2+}/calmodulin dependent. Therefore it is thought that CAP_{2b} stimulates DNOS by an increase in intracellular calcium concentration ($[Ca^{2+}]_i$).

1.1.5 Measuring $[Ca^{2+}]_i$ in *Drosophila* tubules.

Initially, measuring calcium concentrations in the tubule appeared difficult. The cells were too small to allow measurement using ion specific microelectrodes; and fluorescent calcium-sensitive dyes, such as fura-2, were found to be actively excreted by the tubule (Dow and Cheek, unpublished). However, $[Ca^{2+}]_i$ in the cells of the tubule can be measured by transgenic expression of the Ca^{2+}-sensitive luminescent protein aequorin, a method previously used in cell culture and plants (Sheu *et al*, 1993; Knight *et al*, 1991; Brini *et al*, 1995). Aequorin comes from the jellyfish *Aequorea victoria* and is a complex of apoaequorin and coelenterazine. In a fast Ca^{2+}-dependent reaction aequorin is converted to apoaequorin, coelenteramide and CO_2 (Figure 1.3). If aequorin is expressed in cells, one can calculate the instantaneous calcium concentration from the amount of light produced in real time. In the Malpighian tubule, aequorin expression can be driven in specific regions or cells of the tubule by utilizing the GAL4/UAS binary system (Brand and Perrimon, 1993; Kaiser *et al*, 1993) as was demonstrated by Rosay *et al*, 1997 (Figure 1.3).

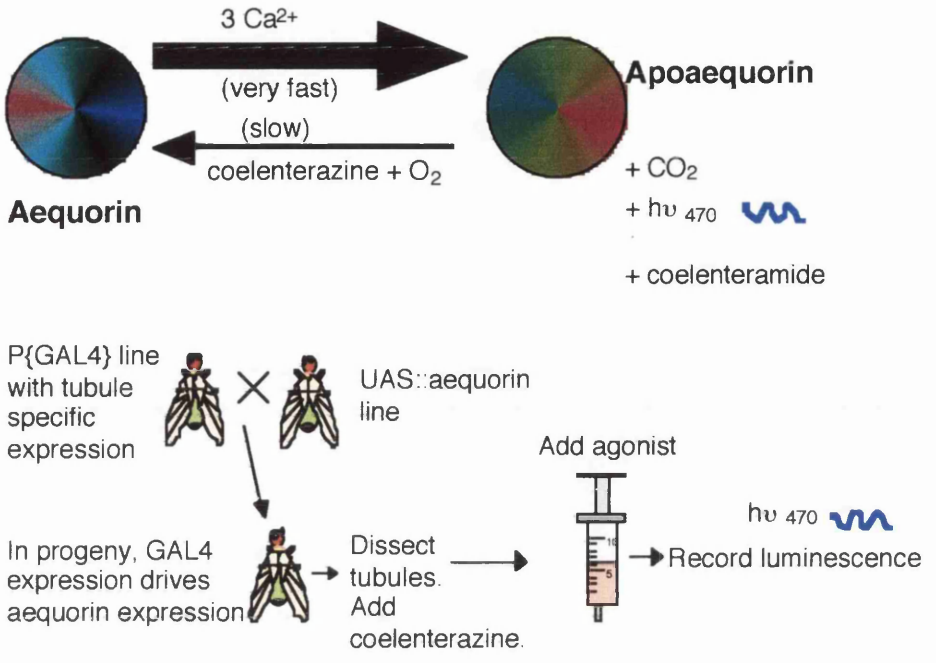

Figure 1.3: Aequorin expression in the Malpighian tubule.

Figure shows how transgenic expression of aequorin can be used to measure intracellular calcium.

Using such a method it was found that CAP_{2b} caused a rapid, dose-dependent rise in $[Ca^{2+}]_i$ exclusively in the main segment principal cells (Rosay *et al*, 1997). Although initially the CAP_{2b} calcium signal was viewed as a single peak dependent on the influx of extracellular calcium, more recent experiments revealed a secondary component, consisting of a more sustained rise in $[Ca^{2+}]_i$ (Kean *et al*, submitted). This rise was also due to the influx of extracellular calcium, as when external calcium was removed no increase in $[Ca^{2+}]_i$ was observed. Furthermore, CAP_{2b}-stimulated fluid transport is also dependent on extracellular calcium, suggesting that CAP_{2b}-stimulation of fluid secretion occurs via this calcium signal. It was also found that the neuropeptide leukokinin, stimulated a rise in $[Ca^{2+}]_i$ exclusively in the main segment stellate cells. More recently the *Drosophila* leukokinin, or 'Drosokinin' has been shown to elicit a biphasic rise in $[Ca^{2+}]_i$ of the stellate cells (Terhaz *et al*, 1999), similar to that induced by CAP_{2b} in principal cells.

Stellate and principal cells have been shown to have differing calcium cycling mechanisms, evident when the effects of the Ca^{2+}-ATPase inhibitor, thapsigargin are examined (Rosay *et al*, 1997). Thapsigargin blocks a calcium ATPase that actively pumps calcium into the endoplasmic reticulum (ER), thus causing a rise in the cytoplasmic calcium concentration. Depletion of calcium from internal stores can stimulate an influx of external calcium to refill the depleted stores (for review see Berridge, 1993). This is termed capacitative calcium entry (CCE), and will be discussed later in this chapter. In the absence of external calcium, thapsigargin stimulates a rise in $[Ca^{2+}]_i$ only in the stellate cells. However, this does not neccessarily negate a role for internal stores in the principal cells and it is possible that any internal store calcium release induced by thapsigargin is too small to be detected. An overview of signalling pathways in the principal cell is shown in Figure 1.4.

The aim of this project is to examine the production of cell-specific calcium signals in the tubule, in response to different neuropeptide and second

messenger stimuli. The different signalling molecules and calcium channels involved, and the role such molecules may play in epithelial fluid transport will be examined.

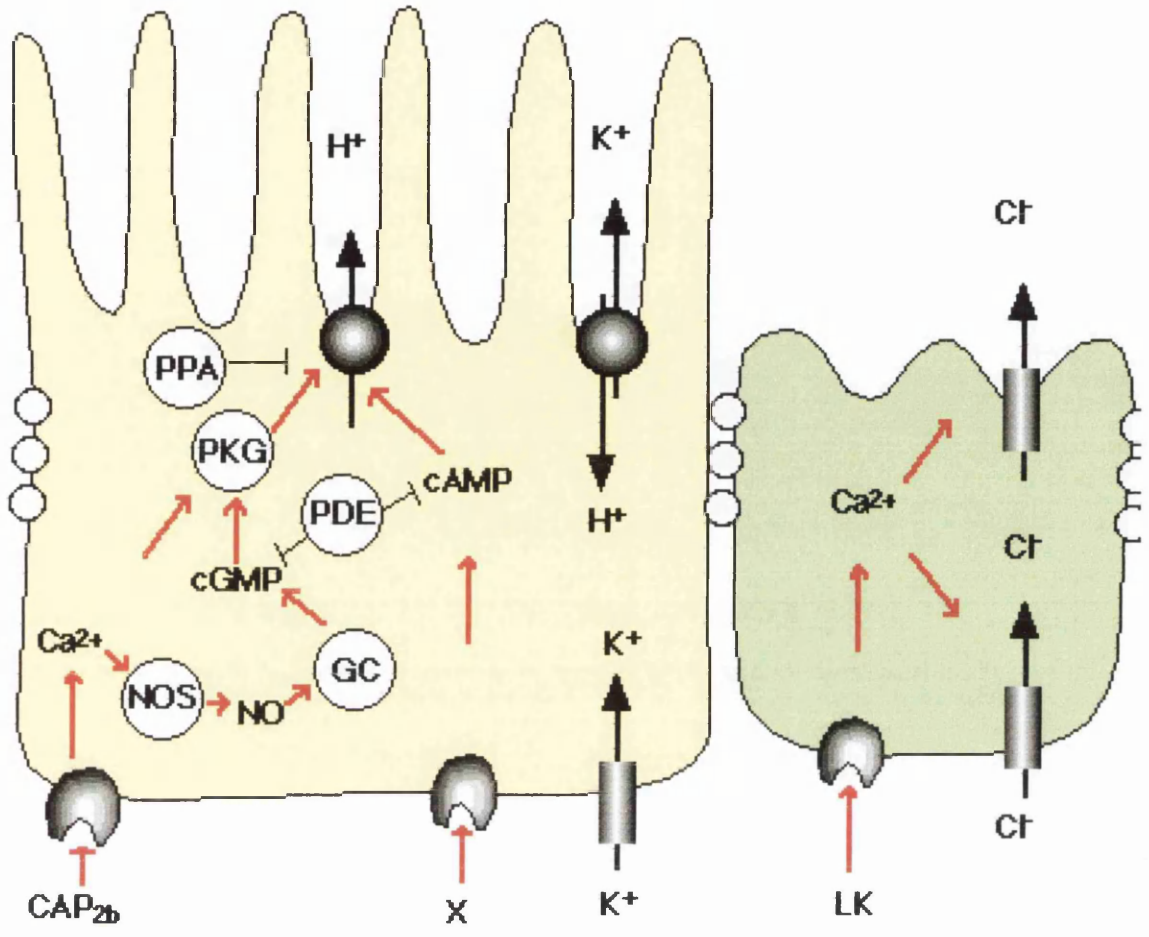

Figure 1.4: Summary of cell signalling pathways in the cells of the Malpighian tubule.

CAP_{2b} binds to a receptor on the basolateral membrane of the principal cell (left), and stimulates a rise in $[Ca^{2+}]_i$. This rise activates DNOS, producing NO, which activates soluble guanylate cyclase to produce cGMP. The rise in cGMP results in increased activity of the V-ATPase and an increase in fluid transport. Leukokinin stimulates a rise in $[Ca^{2+}]_i$ exclusively in the stellate cells (right), which increases chloride shunt conductance, which in turn increases fluid secretion. [Figure is taken from Terhaz, O'Connell, Pollock, Kean, Davies, Veenstra, Dow. 1999. Isolation and Characterisation of a Leucokinin-like peptide of *Drosophila melanogaster*. *J. Exp. Biol.* 202, 3667-3676]

1.2 The study of Calcium Signalling.

1.2.1 Background.

Calcium is a ubiquitous second messenger involved in a multitude of cellular responses, such as fertilisation, muscle contraction, proliferation and differentiation (Galione *et al*, 1991; Ebashi and Endo, 1968; Dolmetsch *et al*, 1997; Gu and Spitzer, 1995). In 1968, Ebashi and Endo showed that the concentration of intracellular calcium in smooth muscle cells controlled muscle contraction by allowing the interaction of actin and myosin fibres. Since this time, the role of calcium in many other cellular responses has been (for reviews see Peterson, 1996; Berridge, 1997; Peterson *et al*, 1999).

In order for calcium to be used as a second messenger, the intracellular concentration of calcium, ($[Ca^{2+}]_i$,) must be tightly controlled. In most cells the resting ($[Ca^{2+}]_i$) is around 100 nm. This is relatively low compared to the extracellular concentration of calcium, ($[Ca^{2+}]_e$), which varies depending on the location of the cell, but tends to be in the millimolar range. Calcium is stored within intracellular organelles, such as the endoplasmic reticulum (ER), where $[Ca^{2+}]$ is approximately 0.1-0.3 mM. With such high concentrations of extracellular calcium and of calcium in the internal stores the cell continually and actively transports calcium out of the cytoplasm, using Ca^{2+}-ATPases on the plasma membrane and the ER, to maintain the substantially lower cytoplasmic $[Ca^{2+}]_i$. This gives the cell two sources of calcium by which to modulate $[Ca^{2+}]_i$. Calcium either enters from outside the cell, via the opening of plasma membrane calcium channels, or is released from internal stores through inositol 1,4,5-trisphosphate receptor ($InsP_3R$) channels or ryanodine receptor (RyR) channels (Figure 1.5). How then does calcium control such a diversity of cell functions? The answer lies in the lack of diffusibility of calcium within the cell, due to calcium buffering and calcium removal processes. With such restriction of internal calcium movements, different

modes of spatial or temporal rises in $[Ca^{2+}]$ can be used to control various cellular functions.

1.2.2 The control of diverse cellular functions by calcium signals.

Different types of calcium signalling events can be used to control different functions within the same cell. This is best demonstrated by the situation in smooth muscle cells. Here high $[Ca^{2+}]_i$ induces contraction of the cell (Ebashi and Endo, 1968), whereas local releases of calcium from the sarcoplasmic reticulum via ryanodine receptor channels induces relaxation. The local increases in $[Ca^{2+}]_i$, termed Ca^{2+} sparks, activate Ca^{2+}-dependent potassium channels, causing hyperpolarisation and relaxation of the cell, without any overall increase in $[Ca^{2+}]_i$, which would otherwise induce cell contraction (Nelson *et al*, 1995).

Variations in the amplitude or frequency of the calcium signal can also be used to control cell function (Berridge, 1997). It has been shown that the fluid secretion rate of *Calliphora erythrocephala* salivary glands is controlled by the frequency of transepithelial potential oscillations (Rapp and Berridge, 1981). The frequency of calcium transients has also been demonstrated to control neuronal differentiation and neurite extension in *Xenopus* embryonic neurons (Gu *et al*, 1995). It was found that the frequencies of calcium signal used to control neurotransmitter expression, channel maturation and neurite extension were critical and could not be changed without losing control of these particular events. Furthermore, the amplitude of calcium signals has been demonstrated to control the differential activation of transcription factors in B-lymphocytes (Dolmetsch *et al*, 1997). When naive B-lymphocytes are challenged with an antigen that has not been encountered previously, a large Ca^{2+} signal is produced, (Healy *et al*, 1997) stimulating cell proliferation and positive selection through the activation of the transcriptional factors NF-κB (nuclear factor) and the oncogene c-Jun. However, B-cells tolerant to the

antigen produce a small Ca^{2+} signal which blocks plasma cell differentiation and antibody secretion through the activation of the transcription factor NFAT (nuclear factor of activated T-cells).

Calcium signals can also occur in different compartments of the cell. For instance, gene expression in neuronal cells can be differentially controlled by nuclear and cytoplasmic calcium signals (Hardingham *et al*, 1997). It has been demonstrated that increases in nuclear $[Ca^{2+}]$ control gene expression mediated by the cyclic-AMP-response element (CRE), whereas increases in cytoplasmic $[Ca^{2+}]$ activate transcription through the serum response element (SRE). Studies in pancreatic acinar cells show that $[Ca^{2+}]_i$ rises induced by agonist stimulation cause the release of calcium from distinct Ca^{2+}pools in specific localisations within the cell (Tortorici *et al*, 1994). Thus, compartmentalisation and localisation of Ca^{2+} signals can add to the variations of control that this enigmatic second messenger can exert (review by Thorn, 1996)

It is clear that the frequency, amplitude and localisation of calcium signals can give rise to a multitude of outcomes. What, though, are the mechanisms underlying the production of such diverse signals?

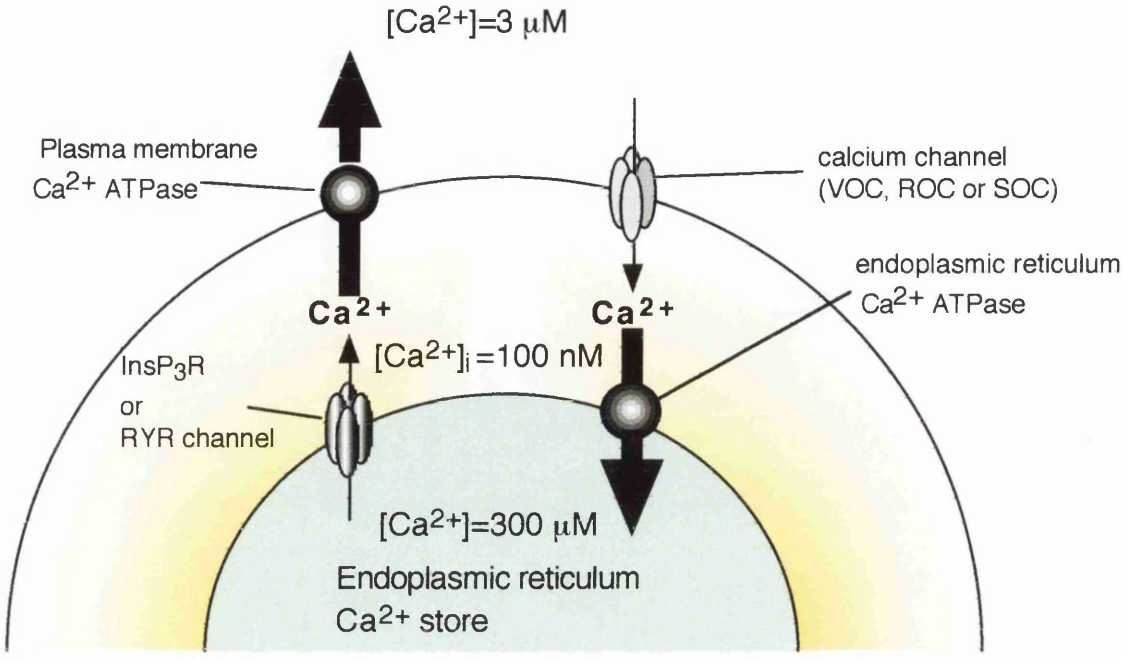

Figure 1.5: Control of $[Ca^{2+}]_i$ in the cell cytoplasm.

Figure 1 shows how the resting cytoplasmic $[Ca^{2+}]$ is kept between 80 and 100 nM. Ca^{2+}-ATPases on the plasma membrane and the endoplasmic reticulum (ER) pump Ca^{2+} out of the cell and into the ER respectively, to maintain a low cytoplasmic $[Ca^{2+}]$. Also shown are the channels through which Ca^{2+} enters the cytoplasm, either from the external medium or from internal stores which are also shown. (VOC=Voltage-Operated Channels; ROC=Receptor-Operated Channels; SOC=Store-Operated Channels; $InsP_3R$=Inositol 1,4,5-trisphosphate receptor channels; RyR=Ryanodine receptor channels.)

1.2.3 Mechanisms of calcium signalling.

As previously described, Ca^{2+} signals arise due to calcium influx from either outside the cell or from intracellular stores. Release from intracellular stores occurs through either $InsP_3R$ channels or RYR channels. It is the combination of the diffusible second messenger inositol 1,4,5-trisphosphate ($InsP_3$) and the relatively non-diffusible Ca^{2+} ions that permit such tight local control of $[Ca^{2+}]_i$ within the cell. $InsP_3$ is produced when a hormone/peptide/neurotransmitter ligand (such as acetylcholine or carbachol) binds to a receptor on the plasma membrane. This induces a conformational change in the receptor thus activating a heterotrimeric G-protein, which then goes on to activate phospholipase C (PLC). PLC catalyses the hydrolysis of phosphatidylinositol 4,5-bisphosphate ($PtdIns(4,5)P_2$) to diacylglycerol (DAG) and $InsP_3$. $InsP_3$ then binds to $InsP_3R$ channels on the endoplasmic reticulum, causing release of Ca^{2+} into the cytoplasm (for review see Berridge, 1993, also see Figure 1.8). This causes the depletion of calcium from intracellular stores and in turn leads to an influx of external calcium necessary for the refilling of these stores (McDonald *et al*, 1993; Hoth and Penner, 1992). The process by which this store depletion activates calcium entry has been termed capacitative calcium entry (CCE) (Putney, 1986) or store operated calcium entry (SOCE), and has been reviewed extensively (Berridge, 1995; Peterson, 1996). The signal which induces calcium influx upon store depletion is thought to occur either via a small diffusible messenger (Randriamampita *et al*, 1993; Parekh *et al*, 1993), or through a functional interaction between the $InsP_3R$ channels and SOC's (Kiselyov *et al*, 1998), but could conceivably occur through both. However, release of calcium from intracellular stores does not always result in calcium influx from outside the cell. Functionally distinct stores controlling Ca^{2+} release and influx have been demonstrated in rat basophilic leukemia cells (Parekh *et al*, 1997).

1.2.4 Inositol trisphosphate and the production of calcium signalling events.

$InsP_3$ has been shown to activate calcium entry in pancreatic acinar cells (Bird *et al*, 1991), and many studies to discern calcium signalling mechanisms have utilised this cell type. Pancreatic acinar cells are polarised cells, with an apical pole where there is a high concentration of secretory granules (zymogen granules). The nucleus lies at the basal end of the cell surrounded by a network of ER. This network is extensive in the basolateral region but only fine terminals extend up into the apical region.

When stimulated with acetylcholine a rise in $[Ca^{2+}]_i$ originating from the apical pole is produced, and is thought to be due to release of calcium from intracellular stores present in this region. Indeed, the type 3 $InsP_3$ receptor was found to be present at high concentrations in this region by immunocytochemistry (Nathanson *et al*, 1994), and release of Ca^{2+} here induces a global rise in $[Ca^{2+}]_i$. This is thought to occur through a process of calcium induced calcium release (CICR). This process depends on the sensitivity of $InsP_3$ receptors to Ca^{2+} itself. Low concentrations of calcium are known to activate $InsP_3$ receptors whereas high $[Ca^{2+}]$ has an inhibitory effect. Using confocal microscopy to visualise the calcium concentration in different regions of the cell, Bootman *et al*, 1997, were able to view the processes that make up such global calcium signals in HeLa cells (Figure 1.6). Here the signalling could be divided into three different categories (for review see Berridge, 1997):

1) Fundamental events caused by the opening of a single calcium release channel (on the ER) were seen as a 'blip' of brief localised $[Ca^{2+}]$ rise.

2) Elementary events were caused by the opening of a group of channels on the ER and gave rise to a 'puff' of localised $[Ca^{2+}]$ rise.

3) Global events were caused when a puff arose inducing the opening of nearby channels, which release calcium to activate other nearby channels. This continued until a rise in [Ca^{2+}] was propagated throughout the cell.

It is thought that, in pancreatic acinar cells, the high concentration of $InsP_3$ receptors at the apical pole facilitate the production of such global events originating from this region. Some of the calcium channels that control the influx of extracellular calcium to produce calcium signalling will be discussed in the following section.

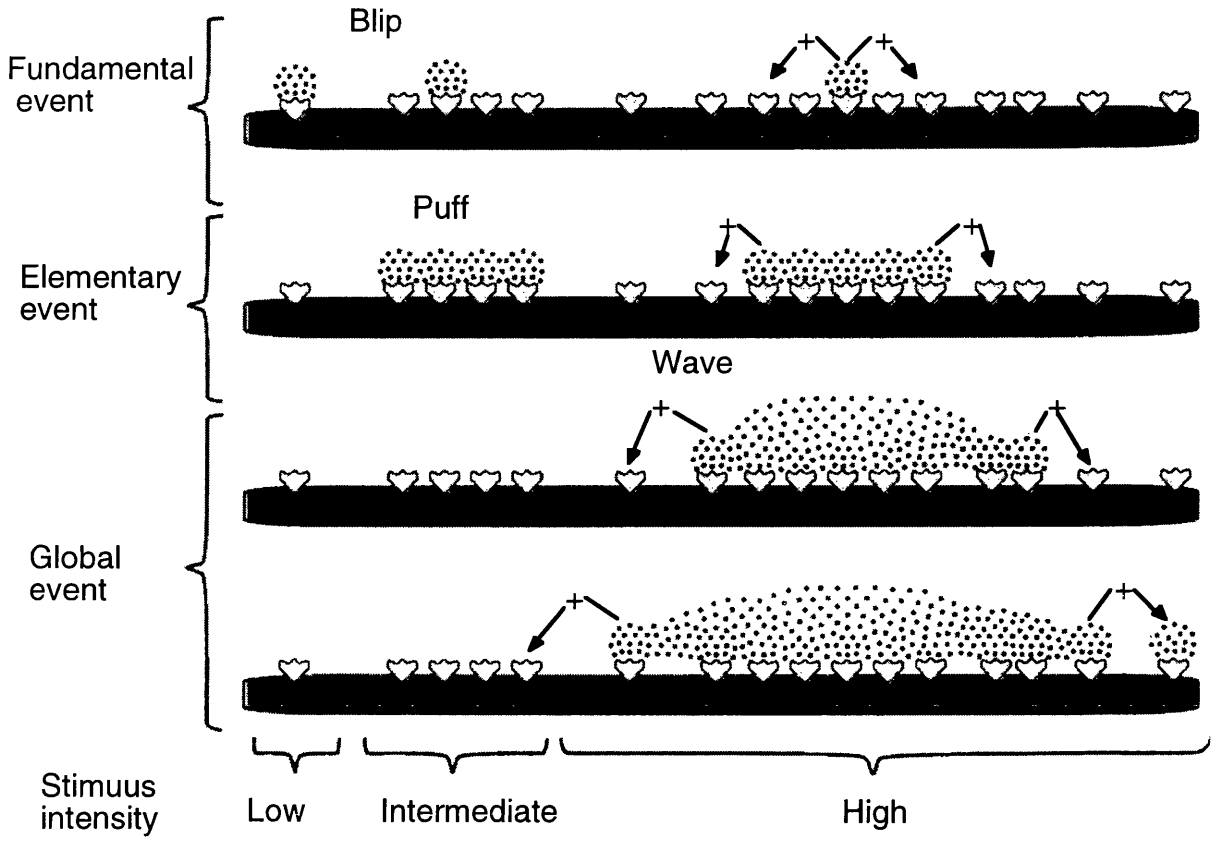

Figure 1.6: A hierarchical organisation of intracellular calcium signalling.

The stimulus intensity seems to determine which events are elicited. Fundamental events are the consequence of opening single intracellular channels to give blips. Elementary events, represented by puffs, result from the concerted opening of small groups of $InsP_3R$'s. These elementary events appear to be the building blocks of the global events, which develop as a wave resulting from the progressive recruitment of neighbouring receptors through a process of CICR. [Figure is taken from Berridge, M. J. 1997. Elementary and global aspects of calcium signalling: *Journal of Physiology* (1997),499.2, 291-306].

1.3 Voltage-gated Calcium channels.

1.3.1 Background.

Voltage-gated calcium channels are generally located and studied in neural or innervated muscle tissues, although this is not always the case. They are involved in many physiological processes including muscular contraction, neurotransmitter release and dendritic cell function (McCleskey *et al*, 1994, Dunlap *et al*, 1995, Zocchi *et al*, 1998). They have been implicated in disorders such as absence epilepsy and hypokalemic periodic paralysis (Fletcher *et al*, 1996; Ptacek *et al*, 1994). Studies in vertebrates have been able to split up such channels into six different classes (A, B, C, D, E and S) based on sequence similarities, tissue distribution and electrophysiological and pharmacological characteristics (Hofmann *et al*, 1994). These classes can be divided into two sets also: the dihydropyridine-insensitive calcium channel classes A, B and E; and the dihydropyridine-sensitive calcium channels C, D and S (called L-type channels when grouped together).

All these channels are composed of up to five subunits $\alpha 1$, $\alpha 2$, β, γ, and δ with the $\alpha 1$ subunit forming the calcium conducting pore of the channel. The other subunits are thought to play a regulatory role and it has been demonstrated that the binding of β subunits to the $\alpha 1$ subunit results in significant increases in transmembrane current and changes in the kinetics of this current (Pragnell *et al*, 1994). Channel diversity is acheived by multiple genes encoding each calcium subunit (to date there are two $\alpha 1$ subunit genes known in *Drosophila, dmca1A* and *dmca1D* with the possibility of a third (see later)). Further diversity can arise from alternative splicing (Snutch *et al*, 1991, Peixoto *et al*, 1997, Smith *et al*, 1996), RNA editing (Peixoto *et al*, 1997, Smith *et al*, 1998), and post-translational modification (Nunoki *et al*, 1989).

1.3.1 Structure of voltage-gated calcium channels.

The α1 subunit consists of four homologous domains or repeats; each composed of six putative α-helical transmembrane domains. The four repeat domains fold into a calcium channel with the link between the fifth and sixth transmembrane domains in each repeat forming the pore of the channel (see figure 1.7). Within the fourth transmembrane domain of each repeat there are positively charged residues every three amino acids thought to be involved in the sensing in changes of voltage (Tanabe *et al*, 1987). L-type calcium channels are characterised by their sensitivity to dihydropyridines. It has been shown that this sensitivity is conveyed by segments IIIS5, IIIS6 and IVS6 (Grabner *et al*, 1996) and that nine amino acids in these regions are critical for dihydropyridine sensitivity (Sinnegyer *et al*, 1997). This was demonstrated by transfer of DHP-sensitivity, through translocation of these amino acids to the DHP-insensitive neuronal α1A subunit, by site-directed mutagenesis.

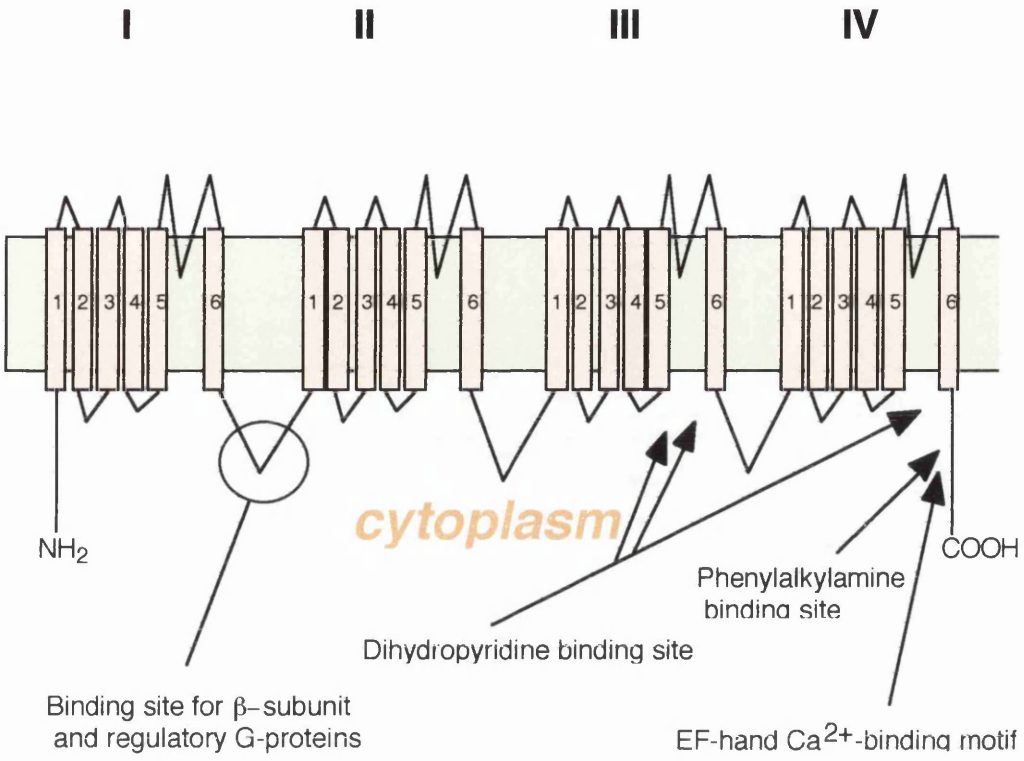

Figure 1.7: Structure of typical voltage gated channel.

The voltage-gated channel shown is composed of four repeat domains, each consisting of six transmembrane segments. The cytoplasmic linker region between repeats I and II contains the binding site for both regulatory G-proteins and β-subunits. The binding sites for DHP's, PAA's and calcium are also indicated. When the domains are all folded together the loops between the fifth and sixth transmembrane regions of each repeat form the pore of the calcium channel. Voltage sensitivity is conveyed by the fourth transmembrane segments in each repeat, where there are positively charged residues every third amino acid.

1.3.3 Control of channels by β-subunits and G-proteins.

As was stated previously the binding of β subunits to the α1 subunits significantly increased transmembrane current and changed the kinetics of the channel (Pragnell *et al*, 1994). This study also demonstrated that in dihydropyridine-sensitive (i.e. L-type) α1 subunits from skeletal, cardiac and neuronal muscle, the β subunit bound to the cytoplasmic linker region between repeats I and II. Mutations in this region reduced the increases in transmembrane current apon β subunit binding. Further to this, it has been suggested that voltage-gated calcium channels are, to a degree, controlled by the competitive binding of inhibitory G-proteins and β subunits to the same region of the α1 subunit (Zhang *et al*, 1996). This study also showed that structural elements in the C-terminus of the α1 subunits were important for G-protein inhibition. However, De Waard *et al*, 1997, showed that in neuronal α1A subunits expressed in Xenopus oocytes, a direct interaction between the G-protein βγ complex and the α1 subunit mediated G-protein inhibition, and that the βγ complex binding site was distinct from that of the β subunit binding site. However, this interaction was not present in α1S and α1C channels (L-type). Contrary to this, G-protein regulation of an L-type calcium channel current in canine jejunal circular smooth muscle cells has been demonstrated (Farrugia *et al*, 1997). These experiments used GTP-αS and GTP to stimulate inward currents which were inhibited by nifedipine. This suggested rather than proved a direct G-protein modulation of the nifedipine sensitive current.

1.3.4 The effects of calcium on voltage-gated calcium channels.

In order to control influx of calcium into cells many calcium channels are sensitive to calcium itself, providing a negative feedback mechanism preventing a constant self-stimulatory influx of calcium. Studies on α1C (cardiac L-type channels), demonstrated that a consensus Ca^{2+} binding motif (an EF-hand), located in the C-terminus of α1C was required for Ca^{2+}

inactivation of these channels (De Leon *et al*, 1995). Furthermore, it was demonstrated that calmodulin is the actual calcium sensor for inactivation of these calcium channels (Peterson *et al*, 1999). Here, overexpression of Ca^{2+}-insensitive calmodulin in mammalian HEK 293 cells ablated Ca^{2+}-dependent inactivation of α1C channels in a dominant-negative manner. As well as demonstrating the calcium sensing properties of calmodulin it suggested that it was tethered to the channel complex. Voltage-gated channels have been demonstrated to be affected by related calcium signalling events. For example, direct interaction between ryanodine receptors and dihydropyridine sensitive channels has been shown in skeletal muscle (Leong and MacLennon, 1998). It is clear that the different isoforms of voltage-gated calcium channel have many differences between them probably due to their distinct functions in different cell types.

1.3.5 Voltage-gated calcium channels in *Drosophila*.

In 1989 Greenberg *et al* showed that membranes isolated from *Drosophila* heads had binding sites for phenylalkylamine (PAA)-sensitive calcium channel blockers. Further to this, Pelzer *et al*, 1989, revealed the presence of eight biochemically distinct Ca^{2+} channels in reconstituted *Drosophila* head membranes. The most frequently observed channel type in these experiments was extremely sensitive to PAA's but insensitive to dihydropyridines (DHP's). However there were distinct channels that were sensitive to DHP's also, indicating the presence of differing isoforms of voltage-gated calcium channels in *Drosophila*.

To date, α1 and β subunits have been cloned from the housefly (Grabner *et al*, 1994; Grabner *et al*, 1994), and two *Drosophila* α1 subunit genes, *Dmca1A* and *Dmca1D* (Smith *et al*, 1996; Zheng *et al*, 1995).

Dmca1D

Dmca1D encodes an α1 calcium channel subunit 2516 amino acids in length

with 78% similarity to the rat brain type D α1 subunit isoform, hence its name. Dmca1D differed from the vertebrate homologues, in that it has unusually long initial amino and terminal carboxy tails, the significance of which, if any, is unknown. The PAA binding site situated in transmembrane segment IVS6 is highly conserved suggesting that this channel is PAA-sensitive. However, the domains involved in DHP binding show numerous changes. This is confusing as this suggests that Dmca1D is insensitive to DHP's, whilst being 78.3% similar to the DHP-sensitive class of α1 subunits in rat. However, It has been reported that mutation in *Dmca1D* was associated with the loss of a DHP-sensitive current in *Drosophila* larval muscle (Ren *et al*, 1998), suggesting the sensitivity of this channel to DHP's.

Northern analysis showed three classes of mRNA in head (9.5, 10.2, and 12.5 kb) and two in the body (9.5 and 12.5 kb), although the 10.2 kb mRNA may be due to non-specific binding to the *Dmca1A* transcript. Alternative splicing in at least two regions (Zheng *et al*, 1995) generated further diversity in Dmca1D. It appears that Dmca1D plays an important role in the developing nervous system as *in situ* hybridisation experiments show it to be highly expressed here as well as showing a temporal expression peak at late pupal stages (Eberl *et al* 1998). However, studies in mutants at the *Dmca1D* locus did not show any nervous system abnormalities. Most of these mutants died before hatching or at the late pupal stage where *Dmca1D* has its expression peaks. Late embryonic lethality observed in *Dmca1D* mutants, was attributable to defects in muscle contraction involved in vigorous hatching movements and the gas filling of trachea, although neuronal defects in the modulation of such contractions could not be ruled out.

Dmca1A

Dmca1A encodes an α1 calcium channel subunit of 1851 amino acids showing most similarity to the A, B and E isoforms (non L-type) of voltage-gated calcium channels (Smith *et al*, 1996). Like Dmca1D, the PAA binding site is

completely conserved whilst the DHP binding site is poorly conserved giving a channel predicted to be PAA-sensitive and DHP-insensitive.

Dmca1A consists of 34 exons spread over 45 kb of genomic sequence. Although Northern blot analysis reveals only one size of transcript (10.5 kb), there is, however, diversity in the transcripts produced as revealed by PCR analysis (Peixoto *et al*, 1997). Alternative exons are found at the linking region between repeats I and II (I/IIa and I/IIb), and at the transmembrane segment IS4 (IS4a and IS4b). The alternative exons for the region coding the linking region between repeats I and II is particularly interesting as this is where β-subunit G-protein βγ binding is postulated to occur. I/IIb encodes a sequence conserving both these regulatory sites whereas I/IIa has poor conservation of the β-subunit binding site and lacks the Gβγ interaction motif altogether (Smith *et al*, 1998). It is suggested that the alternative exons may be for differential regulation by different β-subunits Smith *et al*, 1996).

Dmca1A maps to the locus of the *cacophony*, *nightblind-A* and *lethal L(1)L13* mutations and is indeed the gene product responsible for these genetic phenotypes (Peixoto *et al*, 1997). The *cacophony* mutation results in defects in male courtship song and *nightblind-A* mutations result in visually defective mutants, whilst mutant alleles of *L(1)L13* cause late embryonic lethality consistent with the first expression peak of *Dmca1A*. Both the cacophony and night-blind mutations have been demonstrated to have pleiotropic effects on vision and courtship song, as well as temperature-sensitive convulsions (a phenotype associated with mutations in ion channel genes) (Peixoto *et al*, 1997). These pleiotropic effects might be expected for such a widely expressed gene and as we will be looking at the functions of such genes in the Malpighian tubules this is encouraging.

1.4 Transient receptor Potential Calcium channels.

1.4.1 Store Operated Calcium Entry.

Store operated calcium entry (SOCE) is a widely studied phenomenon in both vertebrates and invertebrates. It describes the influx of calcium into the cell, through store operated channels (SOC), following the release or depletion of Ca^{2+} from intracellular calcium stores (for reviews see Berridge, 1995; Mackrill, 1999; Petersen, 1996), and is also termed capacitative calcium entry (CCE) (Putney, 1986). In *in vitro* studies, store operated entry is induced by application of thapsigargin. This causes store depletion through the inhibition of the endoplasmic reticulum (ER) Ca^{2+}-ATPase, which pumps calcium into the ER (Figure 1.8).

In the mammalian field much attention has been devoted to the study of calcium-release-activated calcium current (I_{CRAC}) which flows through CCE channels. It is probable that more than one class of channel is responsible for I_{CRAC} generation, although these have yet to be identified at the molecular level. However, it is thought the current may be made up from a family of Ca^{2+} channels with homology to the *Drosophila* TRP channel, a putative SOC.

In 1969 Cosens and Manning discovered a visually defective *Drosophila* mutant that lacked a sustained response to bright light, by measuring electrical activity in the eye, expressed as an electroretinogram (ERG). They termed the mutation transient receptor potential (*trp*) (Figure 1.9). The *trp* gene was then identified by the rescue of the phenotype by germline transformation (Montell *et al*, 1985). More recently, two other genes encoding proteins with homology to the TRP protein, *trpl* and *trpγ*, have been identified in *Drosophila*.

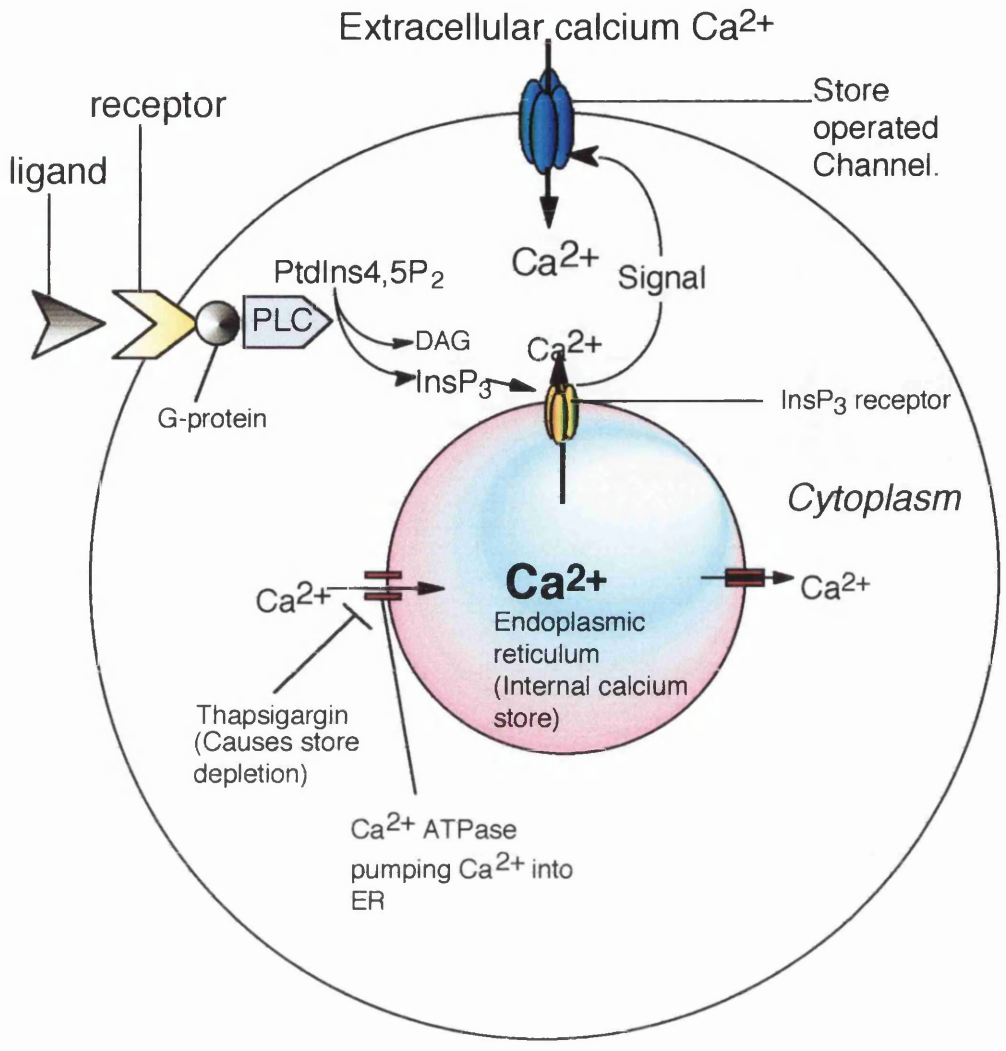

Figure 1.8: Store operated calcium entry.

The binding of ligand to G-protein coupled receptor results in the activation of phospholipase C (PLC). This produces diacyl glycerol (DAG) and Inositol 1,4,5 trisphosphate ($InsP_3$) which stimulates the release of calcium from the endoplasmic reticulum (ER) through $InsP_3$ receptor channels. This leads to an influx of extracellular calcium through store-operated channels.

Since the discovery of TRP in *Drosophila,* several TRP homologues have been found in mammals. Seven human homologues, TRPC1-7, have been identified that function similarly to TRP and TRPL in *Drosophila* (for review see Harteneck, 2000). Other calcium channels, with less homology to TRP, such as the Vanilloid receptor (VR1) and Vanilloid receptor-like protein 1 (VRL1) (Caterina *et al*, 1997; Caterina *et al*, 1999) involved in the transduction of painful stimuli, are thought to be part of a large diverse family of TRP-like proteins. TRP homologues have been identified in *C. elegans*, and a recent study of these has allowed the division of the TRP-related channel family into three different subfamilies. These are the short, long (both named due to protein length) and osm subfamily, so-called due to their similarity to the Osm-9 protein of *C. elegans* (Colbert *et al*, 1997). The short family, all around 900 amino acids in length, are activated in response to stimulation of receptors linked to different forms of phospholipase C (PLC), and include *Drosophila* TRP, TRPL and TRPγ as well as the mammalian homologues TRPC1-7. Despite their similarities at the amino acid level, the channels in this subfamily are highly variable with regards to conductivity, selectivity, and activity.

The TRP channels in the long family are around 1600 amino acids long and to date, little is known about them. Two of the long TRP family found in *C. elegans* can be linked with known gene loci, *ced-11* and *gon-2*. These genes are involved in the timing of cell death and gonadal cell division respectively. From this and other data, it is thought that members of the long TRP subfamily are involved in cell growth, death and differentiation.

The TRP channels of the osm subfamily are all around 900 amino acids in length and are activated by physical or chemical stimuli. This family includes the aforementioned VR1 and VRL1 channels as well as the Osm-9 protein of *C.elegans*, from which the family takes its name.

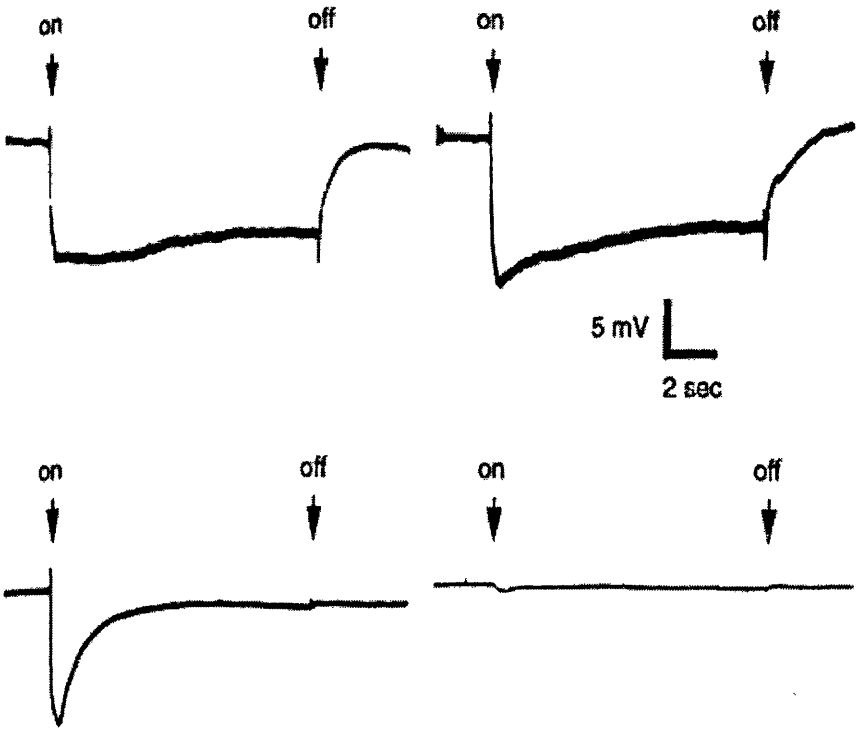

Figure 1.9: The *trp* ERG phenotype.

Wild-type (top) and trp^{cm} (bottom) flies were exposed to white light. The flies were dark adapted for either 2 min (left) or 5 sec (right). The initiation (on) and cessation (off) of the light stimulus, signal amplitude, and time scale are indicated. [Figure is taken from Montell, Jones, Hafen, and Rubin. 1985. Rescue of the *Drosophila* mutation *trp* by germline transformation. *Science* 230, 1040-1043.]

1.4.2 TRP channels in *Drosophila*.

The *trp* gene was identified by the rescue of the *Drosophila* phototransduction mutation by germline transformation (Montell *et al*, 1985). It was found to be expressed in late pupal development and in the adult fly. *In situ* hybridisations to tissue sections showed *trp* to be expressed predominantly in the retinula cells of the eye.

The *trpl* gene was originally cloned in a screen for calmodulin-binding proteins and encodes a calcium channel with 40% identity to the TRP protein, and is also expressed predominantly in the retinula cells (Philips *et al*, 1992).

More recently, *trpγ* was cloned using a low stringency screen for genomic clones homologous to the *slowpoke (slo)* Ca^{2+}-activated K^+ channel, followed by screening of a *Drosophila* head cDNA library (Xu *et al*, 2000). It encodes a protein of 1128 residues, 54% identical to TRP or TRPL over an 800 aa segment. It is expressed in late pupae and adult heads, and is highly enriched in the rhabdomeres of *Drosophila* photoreceptors. Unlike TRP or TRPL, though, it is also found in fly bodies by Northern analysis.

The TRP proteins (consisting of six transmembrane domains) are structurally homologous to known sodium, potassium and voltage-gated channels and are assumed to form tetrameric calcium channels. All the proteins contain ankyrin-binding domains, while TRPL also has two calmodulin binding sites. The pore forming region, conferring the channel selectivity, resides between the fifth and sixth transmembrane segment (see Figure 1.6).

Cell expression studies showed that *trp* encodes a cation channel selective for Ca^{2+} over Na^{2+}, that can be activated by depletion of internal stores by thapsigargin (Vaca *et al* 1994). The thapsigargin-induced current in TRP-expressing cell lines is blocked with lanthanides, such as lanthanum or gadolinium, which suggests sensitivity of TRP channels to these trivalent cations. *trpl*, on the other hand encodes a cation channel that is constutively

active, relatively non-selective with respect to Ca^{2+}, Ba^{2+} and Na^{2+}, unaffected by thapsigargin, and insensitive to lanthanides (Vaca *et al*, 1994; Hu *et al*, 1994; Hu *et al*, 1995; Dong *et al*, 1995). TRPL has been shown, however, to be stimulated indirectly by thapsigargin (Yagodin *et al*, 1998; Estacion *et al*, 1999). Expression of TRPγ in cell lines results in a constitutively active current similar to that seen for TRPL. It is also insensitive to thapsigargin and lanthanides, as well as to activation via PLC or the G-protein, Gq/11 (Xu *et al*, 2000).

TRP differs from TRPL and TRPγ in that it has a long carboxy-terminal region absent in TRPL and TRPγ (Figure 1.10). Using chimeric proteins where the COOH-terminal domains of TRP and TRPL were exchanged, and the resulting proteins expressed in Sf9 cells, it was discovered that thapsigargin sensitivity is conferred by the COOH-terminal domain of TRP while constitutive activity is conferred by the COOH-terminal domain of TRPL (Sinkins *et al*, 1996). In this experiment the selectivity of the two channels remained unchanged. These channels have been studied in a variety of cell lines, but until now, all *in vivo* studies have been carried out in *Drosophila* photoreceptors.

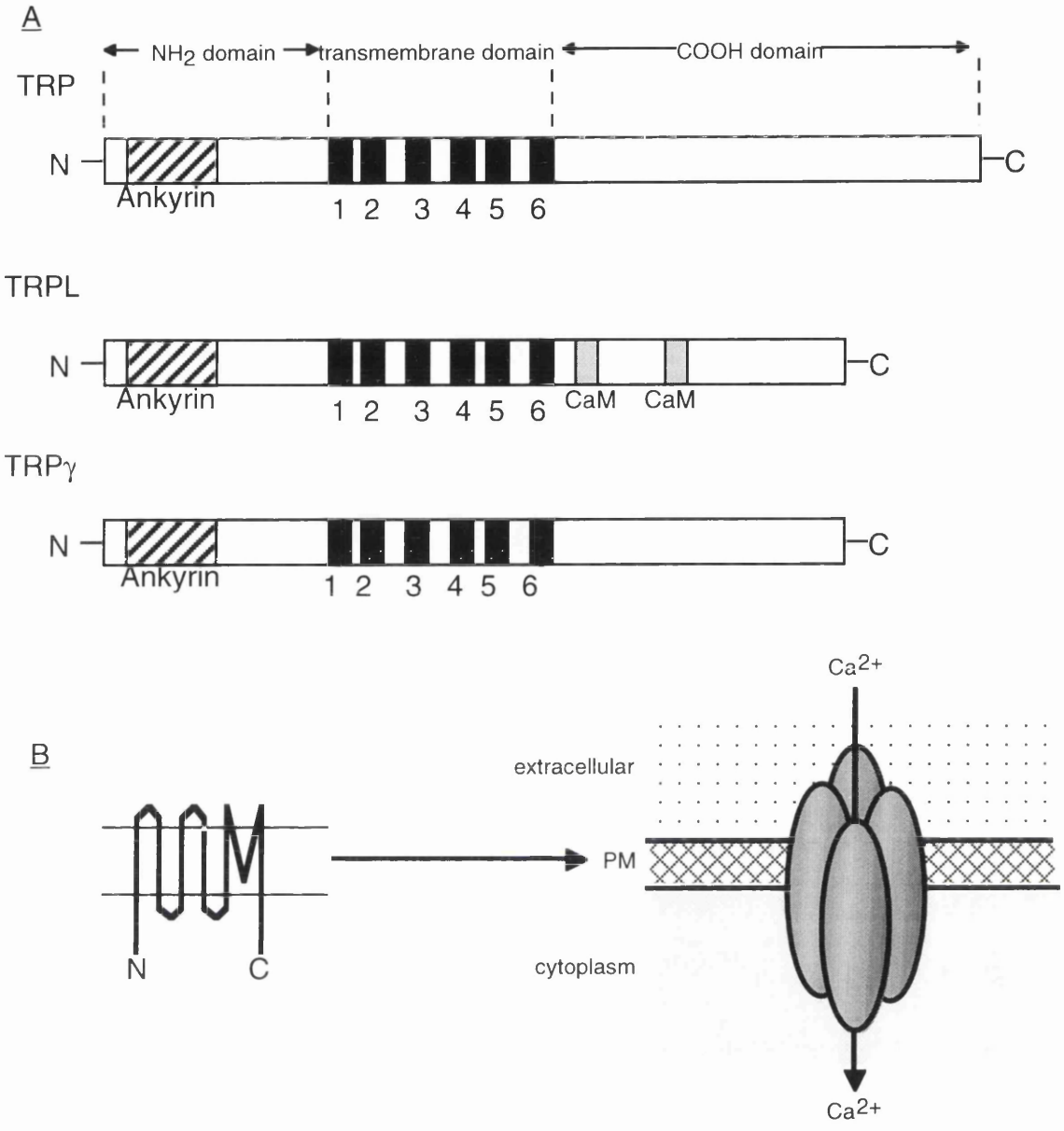

Figure 1.10: Structure of TRP, TRPL and TRPγ.

(A) Diagram showing the domain structures of TRP, TRPL, and TRPγ. Ankyrin repeat regions (Ankyrin), transmembrane domains (1-6) and calmodulin binding sites (CaM) are all shown.

(B) Diagram of TRP channel in plasma membrane (PM). The pore is formed from the region between the fifth and sixth transmembrane domains, and the channels form as tetramers.

1.4.3 TRP and TRPL in phototransduction

During phototransduction, light-activated rhodopsin stimulates a heterotrimeric G-protein, activating PLC which hydrolyses $PtdIns(4,5)P_2$ to DAG and $InsP_3$. This results in the influx of external calcium through TRP, TRPL (Niemeyer *et al,* 1996), and possibly TRPγ heteromultimers. The activation of TRP and TRPL channels has been the focus of much study and will be discussed later.

It is known that light-activated conductance in *Drosophila* photoreceptors requires both TRP and TRPL function (Neimeyer *et al,* 1996). In whole-cell patch clamp recordings of photoreceptor responses to flashes of bright light, mutations in the *trp* gene resulted in a depolarisation of reduced amplitude compared to wild-type. Since TRP and TRPL serve overlapping functions, any effect of mutations in *trpl* may be masked, by functioning TRP channels. As such, flies with mutations in the *trpl* gene were found by screening for the loss of TRPL antigen. The $trpl^{302}$ mutation has an amber stop codon at position 302 leading to the premature termination of the TRPL polypeptide resulting in flies which are completely null for TRPL. Experiments on $trpl^{302}$ photoreceptors showed a photoresponse not significantly different from that of wild-type photoreceptors. However in a $trpl;trp^{301}$ double mutant there was a greater than 10,000 fold reduction in sensitivity (Figure 1.11). In the double mutant there was still a small, but significant response that could be abolished by La^{3+} (a blocker of TRP channels) and was therefore attributed to a residual expression of TRP in the mutants. This explanation was confirmed by the measurement of light activated current in photoreceptor cells of a $trpl;trp^{cm}$ double mutant (Reuss *et al*, 1997). Here the light activated current was completely abolished demonstrating that this current could be attributed solely to TRP and TRPL. Recently, a TRPL phenotype has been observed during prolonged light stimuli and shows a reduced sustained component in ERG's, oscillations superimposed

on the response, a poststimulus hyperpolarisation and altered adaptation properties to dim background light (Leung *et al*, 2000).

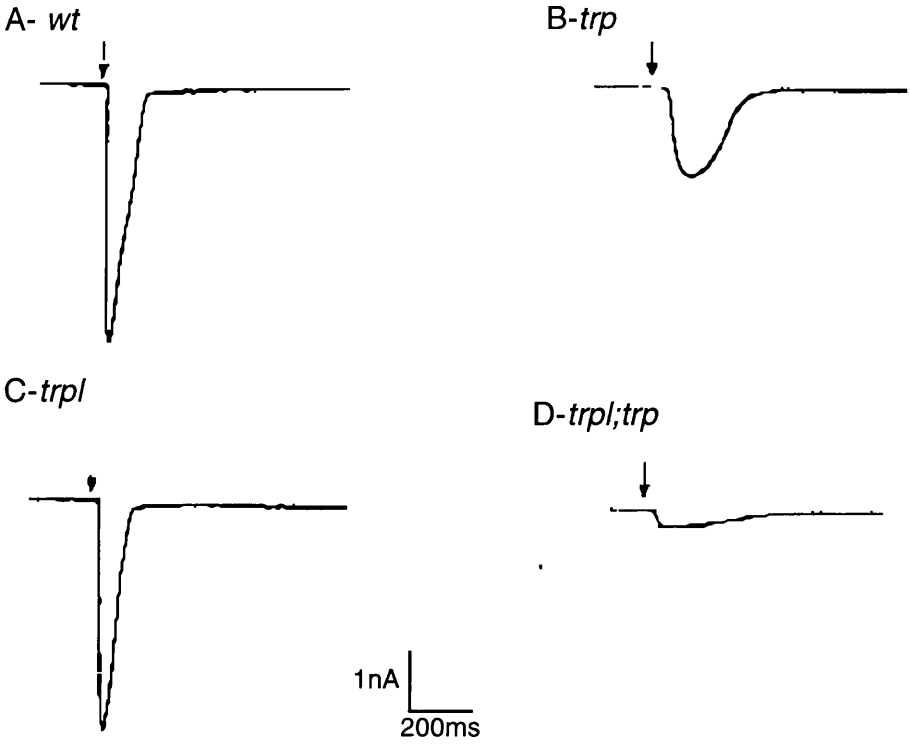

Figure 1.11: Photoreceptor Cell Function in *trp* and *trpl* Mutants

Shown are representative whole-cell, voltage-clamped recordings of light-activated currents from A) wild-type controls, b) *trp*, c) *trpl*, and d) *trpl;trp* photoreceptors. Cells were stimulated with 10ms flashes of 580nm light at a holding potential of -60mV at the time indicated by the arrow. Note the dramatic loss of responsiveness in the double mutant. [Figure is taken from Neimeyer, Suzuki, Scott, Jalink, Zuker. 1996. The *Drosophila* light-activated conductance is composed of the two channels TRP and TRPL. *Cell* 85: 651-659.]

1.4.4 Dmca1A in Phototransduction

It is interesting to note at this stage that although TRP and TRPL have been shown to be responsible for the light activated conductance, mutations in another calcium channel gene, *Dmca1A,* causes visually defective mutants with abnormal ERGs (Smith *et al*, 1998). The abnormal ERGs for three of these alleles are shown in figure 1.12, namely *H18*, *P73* and *EE171*. Both *H18* and *EE171* show lower amplitude of depolarisation in response to sustained light stimuli, with *EE171* also showing an initial reversal of potential. *P73* shows slower kinetics of response than wild-type. With no other electrophysiological experiments performed in these mutants, it is unclear whether these defects occur pre- or post synaptically. Interestingly, the *H18* allele is only defective in vision and contains a mutation that abolishes expression of an alternative eye-specific transcript containing the I/IIa exon. We would hope that further studies in phototransduction and indeed on Malpighian tubule function with such mutants would shed light on the interaction of these channels to produce calcium signals. Also it is interesting to speculate on the possible pleiotropic effects of TRP and TRPL mutations on, for example, *Drosophila* courtship song.

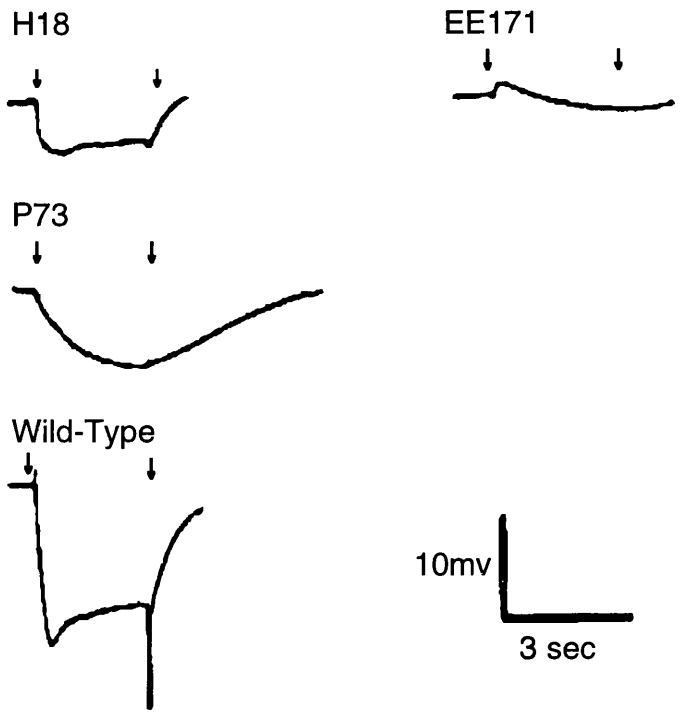

Figure 1.12: Electroretinogram phenotypes of flies expressing various *cac* alleles. Such alleles are indicated by superscripts only. ERG's were obtained by extracellular recordings from eyes of the indicated types; positive is up. Positive -going lights -on and negative lights-off transients are caused by synaptic activity in the outer optic ganglia of the brain and are indicated in the wild-type by arrows. [Figure is taken from Smith, Alexandre, Peixoto, Elena, Kramer, Villella, and Hall. 1998. Courtship and Visual Defects of *cacophony* Mutants Reveal Functional Complexity of a Calcium-Channel α1 Subunit in *Drosophila Genetics* 149, 1407-1426].

1.4.5 Interaction of TRP, TRPL and TRPγ subunits.

TRP, TRPL and TRPγ have been shown to form both homo- and heteromultimers when expressed in cell lines (Vaca *et al*, 1994; Hu *et al*, 1994; Xu *et al*, 1997; Xu *et al*, 2000). TRPγ however, preferentially forms heteromultimers with TRPL. In all cases it was found that when the different subunits did interact, the heteromultimeric channel thus formed possessed distinct properties from homomultimers of the individual components. TRP and TRPL were coimmunoprecipitated from photoreceptors, indicating an interaction between these channels in these cells. However, from fly head extracts, TRPγ coimmunoprecipitates with both TRP and TRPL but preferentially with TRPL. Using a yeast two-hybrid scheme, it was found that TRPγ has six-fold the affinity with TRPL, than with TRP (Xu *et al*, 2000).

Expression of TRP and TRPL in 293T cells results in formation of TRP/TRPL heteromultimers that are thapsigargin-sensitive (like TRP) and displayed a large outward rectification (like TRPL). However, when TRPL/TRPγ hetreomultimers were tested in 293T cells they lack constitutive activity (unlike either of the subunits alone), are sensitive to thapsigargin and seem to be stimulated via phospholipase C.

Although earlier work suggested that the *Drosophila* light-activated conductance was composed of only two channels, TRP and TRPL, recent evidence suggests that TRPγ may also be involved *in vivo* (Xu *et al*, 2000). This was shown by expression of the N-terminal 318 residues of TRPγ, in trp^{343} (a mutation that abolishes TRP expression) flies by germline transformation. The interaction of TRPγ with TRPL is mediated through the TRPγ N-terminal region and so interaction of TRPL with the truncated TRPγ would result in a dysfunctional channel. By expression of the TRPγ N-terminal region, the remaining light-activated current in the trp^{343} flies is abolished, showing an interaction of TRPL with TRPγ and also the involvement of TRPγ in the production of light-activated current.

It thus appears that all combinations of TRP/TRPL/TRPγ homo- or heteromultimers may form *in vivo*. This results in at least six separate channels with different properties, and may explain some of the conflicting results that have been obtained from studies of these channels. Further heterogeneity of channels may result from expression of splice variants or RNA editing, especially as RNA editing has been documented as occurring in the generation of ion channel diversity (Smith *et al*, 1996; Eberl *et al*, 1997).

1.4.6 The Multimolecular signalling complex

The regulation of channel activity is complex and is achieved by direct interaction of channels with regulatory signalling molecules. Mutations in genes coding for the signalling molecules *inaD*, *inaC* (encoding PKC), and *norpA* (encoding PLC) result in abnormal photoresponses in *Drosophila*. PLC has been shown to be involved in activation and deactivation of the light-activated current, through the reduced amplitude and slow kinetics of response in *norpA* mutants (Pearn *et al*, 1996). Mutants in PKC show slower deactivation kinetics, implicating the enzyme in this process (Smith *et al*, 1991). Through similar mutation studies the *inaD* gene product has been shown to play a central role in the interaction of the molecules involved in the photoresponse. INAD is a photoreceptor-specific poypeptide of 674 residues, none of which are long hydrophobic residues; this indicates that it is not an integral membrane protein (Sheih *et al*, 1995). However, it contains five PDZ (post-synaptic density protein-95, discs-large, ZO-1) domains that mediate protein-protein interactions. PDZ domains are about 90 amino acids in length and form a 'cradle' of β-barrels with a conserved hydrophobic pocket with a buried arginine. INAD has been shown to interact with PLC, PKC, rhodopsin, TRP and TRPL, as well as itself, through these PDZ domains (Shieh *et al*, 1997; Huizen *et al*, 1998; Adamski *et al*, 1998; Xu *et al*, 1998). Mutations in the *inaD* gene that abolish specific interactions, produce phenotypes similar to

those produced by mutations in the genes encoding proteins to which the interactions occur. This shows the importance of these protein-protein interactions and the central role of INAD in this. INAD is thought to coordinate all the signalling molecules into a multimolecular signalling complex, consisting of INAD, TRP, TRPL, PLC, PKC, rhodopsin and calmodulin, allowing close interaction of the signalling molecules (Xu *et al*, 1998) (Figure 1.13). It has been suggested that the purpose of this complex is to facilitate the speed of the photoresponse, the fastest signal transduction cascade known in biology. Another proposed function of this complex is to gather various signalling molecules into a single unit, which would then be expected to give a 'unitary' response. In photoreceptor cells small spontaneous currents, called quantum bumps, thought to result from the stimulation of a single rhodopsin molecule with a single photon, can be elicited in conditions of dim light. In calmodulin mutant flies (*cam*), the activation of a single rhodopsin molecule results in the production of many quantum bumps. This occurs because calmodulin is required for rhodopsin shut-off by the regulation of arrestin function. The quantum bumps produced by stimulation with a single photon in this case had the same amplitude of response every time, demonstrating the association of the rhodopsin molecule with a single 'unit' (Scott and Zuker, 1998). It has also been recently suggested that the purpose of the INAD/TRP interaction is to retain the precise localisation to the rhabdomeres of the 'signalplex' (Li *et al*, 2000). Here, it was demonstrated that mutations in either *inaD* or *trp* as well as those disrupting their interaction together caused the mislocalisation of the other signalling molecules PKC and PLC. This mislocalisation was age dependent, as in wild-type and mutant flies the proteins postulated to be involved in the 'signalplex', were localised to the rhabdomeres initially but then became mislocalised with age in the mutant flies. In flies where the TRP/INAD interaction had been disrupted the photoresponse was normal in young flies but deteriorated with age. This

suggested that the lack of interaction between TRP and INAD did not affect the kinetics of the response to light as long as the molecules were localised at the membrane. Therefore, even if signalplex molecules are not directly associating with each other their proximity is enough to facilitate correct phototransduction.

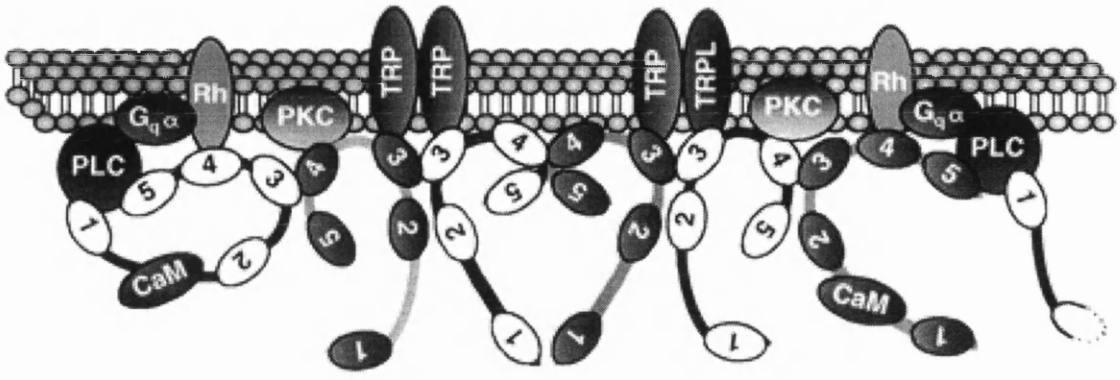

Figure 1.13: The multimolecular signalling complex.

INAD homomultimerizes through PDZ3 and PDZ4. Rhodopsin, PKC, and TRPL bind to either PDZ3 or PDZ4. Calmodulin binds to the linker region between PDZ1 and PDZ2. TRP binds to PDZ3 and PLC to PDZ1 and PDZ5. The individual PDZ domains (1-5) in each INAD monomer are indicated by the ovals. Figure is taken from Xu, Choudhury, Li, Montell. 1998. Coordination of an array of signaling proteins through Homo- and Heteromeric Interactions Between PDZ Domains and Target Proteins The *J. Cell Biol.* 142, 545-555.]

1.4.7 Regulation of the TRP and TRPL channels

Although it is known that many signalling molecules are involved in the control of TRP and TRPL channels, it is still relatively unclear as to how the channels are gated *in vivo*. Conflicting results seem to arise where different systems of cell expression are used, possibly due to the presence of different endogenous signalling molecules that can interact with the molecules expressed through transfection. However, much can be discerned from studies of the control of TRP and TRPL activity. Less is known about TRPγ regulation, due to its recent discovery.

TRP

TRP is a putative store-operated channel whose activation by the depletion of internal stores through the activity of thapsigargin has been demonstrated (Hu *et al*, 1994). The depletion of internal stores may result in the gating of Ca^{2+} channels by one of three processes: 1) Through the action of a messenger molecule released upon store depletion; 2) By direct coupling of plasma membrane channels to $InsP_3$ receptor channels on the endoplasmic reticulum; 3) By indirect coupling of $InsP_3R$ to plasma membrane channels mediated by the cells cytoskeleton. The mammalian TRP homologue hTRP3 has been shown to be functionally coupled to $InsP_3R$ (Kiselyov *et al*, 1998), and $InsP_3$ itself has been shown to stimulate whole cell Ca^{2+} current in mast cells and human T cells (McDonald *et al*, 1993; Hoth and Penner, 1992). However, mutations in the $InsP_3R$ gene in *Drosophila* have no discernible effect on the functioning of the TRP channel (Raghu *et al*, 2000). Furthermore, caged $InsP_3$ released by flash photolysis, failed to activate any light-sensitive channels *in situ* in *Drosophila* photoreceptors (Hardie *et al*, 1998). This does not necessarily rule out an involvement of $InsP_3$, but indicates that $InsP_3$ on its own is not sufficient for activation of these channels. It has been demonstrated that Ca^{2+} influx and Ca^{2+} release can be dissociated and may be controlled by distinct Ca^{2+} stores activated at differing levels of $InsP_3$ (Parekh

et al, 1997). Thus, the lack of $InsP_3$-activated Ca^{2+} influx in photoreceptors may be due to a lack of specificity regarding location and concentration of $InsP_3R$'s upon light stimulation.

When activated, PLC not only generates $InsP_3$ but diacylglycerol (DAG). It has been demonstrated that polyunsaturated fatty acids (PUFA's) (to which DAG is a precursor) activate TRP and TRPL channels independently of the activation of PKC, PLC or G-proteins through PUFA's (Chyb *et al*, 1999). Furthermore the human homologues TRPC6 and TRPC3 have been shown to be directly activated by DAG (Hoffman *et al*, 1999). Activation and inactivation of TRP and TRPL has also been shown to be sensitive to calcium. Experiments using whole-cell recordings of the light-activated current in dissociated photoreceptors (Hardie *et al*, 1991) showed that as external $[Ca^{2+}]$ was increased, the kinetics of response to flashes of light were accelerated. This demonstrated both positive and negative feedback of the transduction cascade mediated by the action of Ca^{2+} influx on the light-sensitive channels. Inactivation of the light activated channels may also occur through the action of PKC, which is known to be stimulated by DAG and Ca^{2+} (Smith *et al*, 1991). However, Hardie and Minke, 1994, showed that Ca^{2+}-dependent inactivation was suppressed by an internal calcium chelator. This suppression of inactivation was unaffected by mutations in the *inaC* gene (encoding PKC). Thus, this may represent two control levels of inactivation of the light-activated channels. Certainly, regulation of TRP channels by PKC-induced phosphorylation of TRP and INAD has been demonstrated in photoreceptor cells (Liu *et al*, 2000), suggesting that PKC-regulation of TRP may occur *in vivo*.

TRPL

The heterologous expression of TRPL has shown that it is activated and regulated in a complex manner. Interestingly, upon expression of TRPL in *Drosophila* S2 cells, Yagodin *et al*, 1998, found that TRPL was not constitutively active and was activated by thapsigargin; this does not occur when TRPL is

expressed in other cell types, demonstrating the importance of cellular context in TRPL regulation. TRPL contains two calmodulin-binding sites, one thought to be involved in activation and the other in inactivation of the channel (Lan *et al*, 1998). Heterologous expression of TRPL in Sf9 cells showed that calcium can activate TRPL (Estacion *et al*, 1999). In this study TRPL was shown to be activated by the rise in intracellular calcium that occured through thapsigargin-stimulated endogenous CCE pathway. It has also been demonstrated to be activated by agonists of G-protein-coupled receptors or directly by Gα11 subunits (Harteneck *et al*, 1995; Obukhov *et al*, 1996). Other studies found that TRPL currents were inhibited by $[Ca^{2+}]_i$ with an IC_{50} of 2.3 μM (Obukhov *et al*, 1998) without the requirement of calmodulin in Sf9 cells, and inhibited at concentrations between 200 and 500 nM when expressed in S2 cells (Hardie *et al*, 1998). This could reflect a self-inhibitory mechanism of TRPL when critical intracellular $[Ca^{2+}]_i$ is reached via calcium influx through TRPL channels.

There is much evidence implicating many different factors in the control of TRP and TRPL channels. However, much of this evidence comes from *in vitro* studies and may not reflect regulation within *Drosophila*. In cell expression systems, it is possible that interaction with endogenous cellular proteins occurs upon heterologous expression of non-native channels. Also, upon expression of proteins that form complexes, any differences in expression levels will result in a mixture of interacting and non-interacting proteins within the transfected cell. This is demonstrated by the study of TRPL/TRPγ interactions when expressed in 293T cells (Xu *et al*, 2000). When these channels were coexpressed, 30 out of 35 cells showed constitutive activity of the Ca^{2+}-channels formed. In the remaining five cells no constitutive activity was observed, but the channels were responsive to ATP-like agonists. It was thought that this smaller group represented the formation of true heteromultimers, whereas the other cells constitutive activity observed in 30

cells was due to the presence of TRPL or TRPγ homomultimers. To solve this problem, a TRPγ-TRPL heterodimer was created, by linking the coding regions of the two genes via a polyglycine linker. Upon expression of this heterodimer in 293T cells, the TRPγ-TRPL heterodimer was not constitutively active, but was activated by agonists that stimulated receptors coupled to PLC. The recent findings concerning TRPγ shed new light on previous studies. It seems that the light-activated conductance may occur via a variety of homo- and heteromultimeric calcium channels affected by a plethora of signalling molecules. Until now, studies in *Drosophila* have addressed the involvement of TRP channels in phototransduction; with one exception: a study by Stortkluhl *et al*, 1999, which looked at the involvement of TRP in olfactory adaptation. Our own studies have looked at the possible involvement of TRP channels in calcium signalling in epithelial transport, and hope to shed new light on the *in vivo* function of these channels.

2.1 *Drosophila melanogaster*

2.1.1 *Drosophila* stocks

Listed below are the *Drosophila* lines utilised in this study, their phenotypes and application.

Strain	Genotype	Purpose
Oregon R	Wild type	Control for fluid secretion assays. Immunocytochemistry. Histochemical staining. Binding studies of fluorescent calcium channel antagonists. Western and Northern analyses. cDNA production.
c42 aeq	aeq/aeq; +/+; c42/c42	Measurement of $[Ca^{2+}]_i$ in main segment principal cells. (Rosay *et al*, 1997)
hsGAL4 aeq	aeq/aeq; hsGAL4/hsGAL4; +/+	Measurement of $[Ca^{2+}]_i$ in whole tubule. (Rosay *et al*, 1997)
trp^{cm}. Kind gift of R.C. Hardie, Cambridge.	w^-; +/+; trp^{cm}/trp^{cm}	Temperature-sensitive mutation in *trp* gene. Mutant phenotype apparent when reared at 25 °C.

trp^{301} Kind gift of R.C. Hardie, Cambridge.	w$^-$; +/+; trp^{301}/trp^{301}	Mutation in the *trp* gene.
$trpl^{302}$ Kind gift of R.C. Hardie, Cambridge.	w$^-$; $trpl^{302}/trpl^{302}$; +/+	Mutation in the *trpl* gene.
$trpl^{302};trp^{cm}$ Kind gift of R.C. Hardie, Cambridge.	w$^-$; $trpl^{302}/trpl^{302}$; trp^{cm}/trp^{cm}	Double mutation, *trp* and *trpl* genes.
see genotype	w-/w-; Bl/CyO; TM2e^- /TM6Tb^-Hup^-	Fly crosses.
see genotype	aeq/aeq; +/+; +/+	Fly crosses. Aequorin gene under control of UAS_G promoter.
see genotype	w-; hsGAL4/hsGAL4; +/+	Fly crosses. GAL4 gene under control of heat shock promoter on second chromosome.
see genotype	w-; +/+; hsGAL4/hsGAL4	Fly crosses. GAL4 gene under control of heat shock promoter on third chromosome.
see genotype	aeq/aeq; Bl/CyO; TM2e$^-$ /TM6Tb^-Hup^-	Fly crosses. See appendix.

see genotype	w-/w-; hsGAL4/hsGAL4; TM2e^{-} /TM6$Tb^{-}Hup^{-}$	Fly crosses. See appendix.
see genotype	w-/w-; Bl/CyO; hsGAL4/hsGAL4	Fly crosses. See appendix.
see genotype	aeq/aeq; hsGAL4/hsGAL4; trp^{cm}/trp^{cm}	Measurement of $[Ca^{2+}]_i$ in tubules with mutation in *trp* gene.
see genotype	aeq/aeq; hsGAL4/hsGAL4; trp^{301}/trp^{301}	Measurement of $[Ca^{2+}]_i$ in tubules with mutation in *trp* gene.
see genotype	aeq/aeq; $trpl^{302}/trpl^{302}$; hsGAL4/hsGAL4	Measurement of $[Ca^{2+}]_i$ in tubules with mutation in *trpl* gene.
dN1-1B. Kind gift of M. Regulski, Cold Spring Harbour.	hs*dNOS*/hs*dNOS*; +/+; +/+	Contains full length dNOS gene under control of heat shock promoter, on first chromosome.
dN1-3. Kind gift of M. Regulski, Cold Spring Harbour.	w-/w-; +/+; hs*dNOS*/hs*dNOS*	Contains full-length dNOS gene under control of heat shock promoter, on first chromosome.

dN1-2A. Kind gift of M. Regulski, Cold Spring Harbour.	w-/w-; hs*dNOS*/hs*dNOS*; +/+	Contains full-length dNOS gene under control of heat shock promoter, on second chromosome.
dN2-2A. Kind gift of M. Regulski, Cold Spring Harbour.	w-/w-; hs*dNOST*/hs*dNOST*; +/+	Contains truncated dNOS gene under control of heat shock promoter, on second chromosome.
dN2-3A. Kind gift of M. Regulski, Cold Spring Harbour.	w-/w-; +/+; hs*dNOST*/hs*dNOST*	Contains truncated dNOS gene under control of heat shock promoter, on third chromosome.

Table 2.1 ***Drosophila melanogaster*** **genotypes used in this study.**

2.1.2 *Drosophila* rearing

Flies were reared in vials on standard *Drosophila* medium at 25°C (appendix 2). If large quantities of flies were required, rearing was in large bottles on standard medium.

2.2 *Escherichia coli*

2.2.1 *E. coli* strains and plasmids

Strain	Genotype
TOP10 competent cells (Invitrogen).	(F^- *mcr*A, Δ(*mrr-hsd*RMS-*mcr*BC), ϕ80*lacZ* ΔM15, Δ*lac*X74, *rec*A1, *deo*R, *ara*D139, Δ(*ara-leu*)7697, *gal*U, *gal*K, *rps*L, (Str^R), *end*A1, *nup*G).

Table 2.2 ***E. coli* strains used in this study.**

Plasmid	Purpose
pCR®2.1TOPO	For cloning of PCR products according to the TOPO TA cloning kit protocol (Invitrogen).

Table 2.3 **Plasmids utilised in this study.**

2.2.2 Storage of bacterial cultures

0.5 ml of bacterial culture was added to 1 ml of a 2% peptone, 40% glycerol solution (in H_2O) before being frozen under liquid nitrogen. Frozen stocks were stored at -70°C.

2.3 Nucleic Acid Isolation and Quantification

2.3.1 Plasmid DNA isolation

Small scale plasmid DNA preparation was performed with the Qiaprep Spin Miniprep Kit (Qiagen) following manufacturer's instructions.

2.3.2 Single fly Genomic DNA preparation

Single fly genomic DNA preparations for utilisation in PCR reactions were performed according to Gloor and Engels, 1991. Briefly, an anaesthetised single fly was placed in a 0.5 ml Eppendorf tube. 50 µl of 'squishing buffer' (10 mM Tris-HCl (pH 8.3), 1 mM EDTA, 25 mM NaCl, 200 µg/ml proteinase K) was drawn up into the pipette tip and the fly squashed by the tip, without expelling the liquid.

Once the fly was suitably squashed, the liquid was expelled and the reaction incubated for 30 min at 37°C. The proteinase K was inactivated by heating the reaction for 1.5 min at 95°C. 1 µl of the reaction was then utilised for PCR. DNA from squashed flies could be maintained for several months at -20°C.

2.3.3 Preparation of total RNA

Prior to RNA isolation all solutions were made RNase free with a 0.1% (v/v) DEPC solution where required. Solutions were then autoclaved for 15 minutes at 15 lb/sq. in. on liquid cycle to remove traces of DEPC. Fresh plasticware and pipette tips were used and gloves worn at all times. The homogeniser was

washed thoroughly with ethanol and rinsed in RNAzol B (Biogenesis) before use.

For large scale total RNA extraction 500 flies were frozen in liquid nitrogen in a Sterilin tube and homogenised with a Polytron homogeniser in 2 ml RNAzol B (Biogenesis), then transferred to fresh Eppendorf tubes. For extraction from heads, bodies, and tubules flies were dissected by hand before homogenisation as above. For each isolation 500 heads, 500 bodies or 3500 tubules were used.

0.1x volumes of chloroform was added to fly homogenate and the samples were shaken for 15 s then left on ice for 5 min.

The samples were centrifuged for 15 min at 12 000 g (4°C). The aqueous phase was removed to a fresh tube to which isopropanol of an equal volume was added before leaving for 15 min on ice.

The samples were centrifuged as before and the supernatant carefully removed from the RNA pellet. The pellet was washed with 75% ethanol, vortexed, then centrifuged at 8 000 g for 8 min (4°C).

The pellet was left to air dry then dissolved in an appropriate volume of 0.5% SDS (initially 200 µl then more added if necessary).

2.3.4 Quantification of nucleic acids

Nucleic acid concentrations were estimated by spectrophotometry at $A_{260/280}$, where an OD of 1 at 260 nm corresponds to 50 µg/ml of double-stranded DNA and 40 µg/ml of single-stranded DNA and RNA. Readings were standardised with the solution in which the samples had been diluted. The ratio of $A_{260/280}$ provided an estimation of nucleic acid purity. Values of 1.8 for DNA and 2.0 for RNA indicated pure preparations.

Where amounts of DNA were extremely small the DNA concentration was estimated by spotting 1 µl onto a 1% agarose (w/v in H_2O) plate containing 0.5 µg/ml ethidium bromide (EtBr), allowing it to dry and comparing its intensity to that of a series of known standards under UV illumination.

2.4 Restriction Digests and Electrophoresis

2.4.1 Restriction digests

DNAs were restricted in single strength REact® buffer appropriate to the restriction enzyme being used (all Gibco BRL).
Typical amounts of DNA in a restriction digest were 1 µg of plasmid DNA and 5 µg of genomic DNA.

2.4.2 Agarose gel electrophoresis of DNA

DNAs were separated in 1% agarose in 1x TBE (90 mM Tris, 90 mM boric acid (pH 8.3), 2 mM EDTA) containing 0.1 µg/ml EtBr, as described in Sambrook *et al*, 1989, using 1x TBE as the electrophoresis buffer. Sizes were compared to a 1 kb ladder (Gibco BRL). Prior to loading 3 µl of loading dye (0.25% (w/v) bromophenol blue, 0.25% (w/v) xylene cyanol, 30% (v/v) glycerol in water) was added to the samples.

2.4.3 Electrophoresis of RNA

40 µg RNA (per lane) was denatured by the addition of;

3.5 µl formaldehyde

10 µl formamide

2 µl 5x MOPS (0.1 M MOPS (pH 7), 40 mM sodium acetate, 5 mM EDTA (pH 8))

Samples were denatured by heating to 70°C for 10 min, then snap-chilling on ice prior to the addition of 2.5 µl loading dye (as above).

The RNA was electrophoresed overnight in a denaturing gel (20% (v/v) 5x MOPS, 18% (v/v) formaldehyde, 1% agarose in DEPC-treated water) in 1x MOPS, containing 0.01 µg/ml EtBr, as the electrophoresis buffer. Sizes were compared to the Gibco BRL 0.24-9.5 kb RNA ladder and gels were photographed with a ruler.

2.4.4 Polyacrylamide gel electrophoresis for DNA sequencing

Denaturing polyacrylamide gel electrophoresis was used to separate the products of sequencing reactions. Sequencing gels were composed of 6% (w/v) acrylamide/bis (acrylamide:N, N'-methylenebisacrylamide, 19:1), 7 M urea in 1x TBE (provided as a complete solution by Anachem). Gels were polymerised via the addition of 1 ml 10% (w/v in H_2O) APS (ammonium persulphate) and 50 µl TEMED in a Bio-Rad sequencing apparatus. Gels were allowed to set for at least half an hour before use and pre-run to reach the desired temperature (50°C). The samples to be electrophoresed were denatured for 5 min at 90°C and snap-chilled on ice before loading. Gels were run for two to four hours (in 1x TBE) at 50°C depending on the size of DNA to be resolved before drying down onto Whatman 3MM paper under vacuum.

2.5 Labelling of Nucleic Acids

2.5.1 Labelling of DNA with ^{32}P

Radioactive probes were generated by the random priming method modified from Feinberg and Vogelstein, 1983.

30-50 ng of gel-purified DNA or linearised plasmid in 30 µl of water was denatured at 90°C for 5 min and snap-chilled on ice before the addition of;

2 µl of BSA (1 mg/ml in H_2O)

10 µl 5x OLB (oligo labelling buffer (appendix 3))

3 µl of [α-^{32}P] dCTP (30 µCi: 3 000 Ci/mM (ICN))

5 µl of Klenow DNA polymerase (Boehringer Mannheim)

The mix was incubated at 37°C for 1-3 hr. Before adding to filters, the probes were boiled for 5 min and snap-chilled on ice.

2.6 Nucleic Acid Hybridisation

2.6.1 Northern blotting

Gels were treated for 20 min in 0.05 N NaOH then soaked in 20x SSC for 40 min, prior to capillary blotting to a nylon membrane (Hybond-N, Amersham) with 20x SSC buffer. After overnight transfer the RNA was fixed to the membrane by UV crosslinking as above.

2.6.2 Northern hybridisation

Filters were prehybridised for several hours in Church buffer (appendix 3) containing formamide (2:1 buffer:formamide) at 42°C. The denatured probe was added and hybridised overnight. Filters were washed as follows;

2x SSC, 0.1% SDS for 20 min at 25°C

0.2x SSC, 0.1% SDS for 30 min at 65°C

Size was determined with respect to the Gibco BRL 0.24-9.5 kb RNA ladder.

2.6.3 Autoradiography

Filters hybridised to radioactive probes were wrapped in Saran wrap and exposed to Fuji X-ray film for a sufficient number of days at -70°C (between intensifying screens) to produce a clear signal.

2.6.4 Re-screening filters

When filters were required to be re-screened with a different probe they were first soaked in boiling 0.1% SDS for 10 min to remove the previous probe. They were pre-hybridised again for several hours before the addition of the new probe and repetition of the hybridisation procedure.

2.7 Oligonucleotides

2.7.1 Oligonucleotide synthesis

Oligonucleotides were synthesised by the Gibco BRL custom primer service and were provided deprotected at 50 nmol. These were resuspended in TE buffer to a concentration of 100 µM. All primers were stored at -20°C. A list of primers used in this study and not included in the text are provided in appendix 4. Primer concentrations were determined by UV spectrophotometry if required.

2.8 Polymerase Chain Reaction

2.8.1 Standard PCR

Standard PCR protocols were used in the everyday amplification of DNAs. Amounts of template DNA varied, with 0.5 µg genomic template DNA used per reaction and 0.1 µg or less of plasmid template. For reactions using Boehringer Mannheim *Taq* polymerase, dNTPs (Boehringer Mannheim) were added at 0.125 mM each to single strength PCR buffer, left and right primers at a concentration of 0.5 µM with 1 u of *Taq* polymerase. When Applied Biosystems Reddy Load Mix *Taq* was used, only template and primers at the same concentrations as above were added to the pre-aliquoted mix.

Cycling was performed in thin walled PCR tubes in a Hybaid OmnE or Hybaid PCR Sprint machine.

Cycling procedures were typically:

94°C for 1-2 min to ensure denaturation of template.

Then 20-30 cycles of;

denature at 94°C, 30 sec

anneal at 48-60°C, 30 sec

extend at 72°C, 1 min

then a final 2 min extension step of 72°C.

Annealing temperatures depended on the primers used.

2.8.2 Reverse transcriptase PCR

PolyA$^+$ RNA was obtained using the magnetic Dynabeads mRNA DIRECT kit (Dynal®) according to manufacturers instructions. Heads (5) or tubules (20), were used in the extraction. Tissues were ground in Treff tubes with matching homogeniser.

Once the mRNA was extracted a reverse transcriptase reaction was set up.

This reaction contained;

0.2 mM of each dNTP

40 u RNAsin (Promega)

10 mM dithiothreitol (DTT)

1x first strand buffer,

and H_2O in a volume of 18 µl.

2 µl Superscript™ II RNase H$^-$ Reverse Transcriptase (Gibco BRL) was then added to start the reaction.

Reactions were incubated at 42°C for >30 min, with occasional tapping to resuspend the beads. The beads were then collected using the Dynal MPC magnet, washed and suspended in 20 µl TE buffer, the suspension being stored at -20°C. 1 µl of the Dynabead solution was sufficient template for a standard PCR reaction.

2.8.3 Cloning of PCR products

PCR products were cloned using the Invitrogen TA cloning or TOPO TA cloning kits into pCR®2.1 or pCR®2.1 TOPO according to manufacturers instructions and transformed into TOP10 competent cells.

pCR®2.1 transformations were accomplished by first adding 2 µl of β-mercaptoethanol to 50 µl of competent TOP10 cells then gently stirring in 1 µl of ligated product on ice. (Ligations were performed according to manufacturers instructions).

The cells were left on ice for 30 min then heat shocked at 42°C for 30 s. The cells were put back on ice for 2 min before adding 250 µl SOC medium (appendix 2) then transformations were shaken on their side for 30 min at 37°C.

100 µl of the transformation was spread onto L-agar plates containing 100 µg/ml ampicillin and incubated overnight at 37°C. These plates also contained X-gal (see below). White transformants were removed as single colonies and were grown overnight (with shaking) at 37°C in 10 ml L-broth (appendix 2) containing 100 µg/ml ampicillin.

2.9 DNA Sequencing

2.9.1 Manual

Double-stranded DNA sequencing was carried out using the T7 Sequenase version 2.0 DNA sequencing kit (Amersham) or the T7 Sequenase quick denature plasmid sequencing kit (Amersham) using the methods described by

the manufacturer. Both employ the dideoxy chain termination method of DNA sequencing using ^{35}S-α-dATP (ICN).

2.9.2 Automated

A single stranded PCR was performed with template and primers supplied at 1 μg and 3.2 pmol respectively, with a PCR mix containing fluorescently labelled dideoxynucleotides. Samples were run on an agarose gel with the nucleotides being detected on an ABI automated DNA sequencer. Automated sequencing procedures and materials were carried out by the Glasgow University Molecular Biology Support Unit. Analysis was carried out with the Applied Biosystems automated sequence analysis programme (Autoassembler 2.0).

2.10 Fluid Secretion Assays

Adult *Drosophila* tubules were dissected out into Schneiders revised *Drosophila* medium (Gibco BRL) and pairs of tubules were transferred to a 9 μl drop of a 1:1 (Schneiders:*Drosophila* saline) mix (*Drosophila* saline, 117.5 mM NaCl, 20 mM KCl, 2 mM $CaCl_2$, 8.5 mM $MgCl_2$, 10.2 mM $NaCO_3$, 4.3 mM Na_2HPO_4, 8.6 mM HEPES, pH=6.9, with 20 mM glucose added before use).

One tubule was drawn from the drop and looped around a pin, ensuring that the ureter (from where secretion issues), was out of the drop.

Every ten minutes the droplets excreted from the ureter were removed with a fine rod and their diameter measured using an eyepiece graticule. For a schematic diagram see figure 1.2

When agonists were to be added they were first diluted in Schneiders:*Drosophila* saline if required before addition of 1 μl of the

compound to the bubble. Results were analysed using Excel 5.0 (Microsoft), where secretion rate was calculated in nl/min from the volume of fluid secreted in 10 minutes.

2.11 Staining for NADPH-diaphorase activity.

Slides were treated with 1mg/ml poly-L-Lysine. Tubules were dissected and stuck down on slides in 1 X Phosphate buffered saline (PBS). The tubules were fixed for 20 minutes in 4 % paraformaldehyde in 1 x PBS at room temperature. Slides were then washed 5-7 times in 1 x PBS. The tubules were then permeabilised in 0.2 % triton X-100 in 1 x PBS for thirty minutes. For detection of NADPH-diapharose activity the tubules were placed in 0.2 % triton X-100/0.2 mM nitro blue tetrazolium (NBT). NADPH was then added to a concentration of 1 mM and the slides left in the dark for 10 -60 minutes. The reaction was stopped by washing 5-7 times in PBS.

2.12 Immunoprecipitations

Co-immunoprecipitations from *Drosophila* heads (100) and bodies (100) were performed according to the protocol described in Xu *et al*, 1998). Tissue was homogenised in ice-cold IPB buffer (phosphate-buffered saline with 500 mM NaCl, 5 mM MgCl2, 5 mM GTP, 0.2 % dodecyl-B-maltoside (pH 7.5), a protease inhibitor cocktail (Calbiochem, 500 µM AEBSF, 500 µM EDTA, 1 µM E-64, 1 µM leupeptin and 1 mg/ml Aprotinin), and centrifuged to remove debris. Antibodies (1 µl TRP or TRPL) and 50 µl of protein-A Sepharose beads were added to the extracts and rotated at 4 °C overnight. The mixture was then centrifuged for two minutes at 15000 rpm to collect beads. Supernatant was

removed and the beads washed in 0.5 ml IPB buffer. The beads were washed like this for a further three times. The bead-bound immunocomplexes were then eluted with SDS sample buffer (appendix 4), and half of the eluted volume was used for Western blotting.

2.13 Western Blot analyses

For Western analyses tissues were homogenised in 130 ml of Tris-lysis buffer (2% SDS, 70 mM Tris pH 6.8) + 1 µl protease inhibitor cocktail (Calbiochem, 500 µM AEBSF, 500 µM EDTA, 1 µM E-64, 1 ,µM leupeptin and 1 mg/ml Aprotinin) and centrifuged to remove debris.

The protein concentration of each sample was measured using the Lowry protein assay. To each 25 µl of unknown or standard protein sample 100 µl of Folin-Cocteau reagent and, 1 ml of solution X (10 µl 1% $CuSO_4$, 10 µl 2% K^+Na^+ tartate, 1ml 10% Na_2CO_3 in 0.1 M NaOH) was added. Absorbency of each sample was then measured at λ750 nM with the spectrophotometer and unknown sample concentrations estimated through comparison with known 1-5 mg/ml BSA standards. The samples were then electrophoresed on a 3-8 % Tris-acetate gel with 5 µl loading buffer (60 % glycerol, 12.5 % β-mercaptoethanol, 1 % bromophenyl blue) for 30 minutes at 200 V in running buffer (see appendix). A nitrocellulose membrane was cut to the size of the gel and soaked for 10 minutes in H_2O, then 10 minutes in Transfer buffer (appendix 4). The blot for transfer was prepared according to kit instructions (NuPage Electrophoresis system, NOVEX), and the proteins were transferred from gel to membrane by electric current (45 minutes at 190 V).

Transfer of proteins was affirmed by staining the membrane with Ponceau dye. The membrane was then washed twice in distilled water.

The membrane was then blocked in 5 % dehydrated milk powder, 0.1 % Tween in 1 X PBS for 1-2 hours. The membrane was hybridised with the appropriate primary antibody diluted in 5 % dehydrated milk powder, 0.1 % Tween in 1 X PBS overnight. After two thirty minute washes in 1 XPBS, the membrane was hybridised with the secondary antibody diluted in 1 X PBS.

2.14 Immunocytochemistry

Slides were washed with water and dried with ethanol, before a wax circle was drawn on them using a wax pen (Vector). Slides were treated with 100 µl 0.1mg/ml poly-L-lysine solution (Sigma Diagnostic Inc.). The slides were then washed with tap water and left to air dry. Tubules were dissected and stuck onto slides in 1 X PBS solution. Tubules were then fixed with 4 % paraformaldehyde in 1 XPBS for thirty minutes. They were then washed 5-7 times in 1 XPBS before permeabilisation with 0.2% (v/v) Triton X-100 in PBS for thirty minutes. Permeabilisation solution was changed every ten minutes. The tubules were then blocked for three hours in PAT (PBS containing 0.5 % (w/v) Sigma cold fraction V bovine serum albumin and 0.2 % (v/v) Triton X-100). The tubules were then hybridised overnight in a humidity chamber with the primary antibody diluted in PAT. The tubules were then washed four times in PAT over a period of two hours. They were then blocked with PAT containing 2 % (v/v) normal goat serum (Scottish Antibody Production Unit (SAPU)) for a further four hours. The tubules were then incubated overnight with the secondary antibody diluted in PAT with 2 % normal goat serum in a humidity chamber. The tubules were then washed four times over a period of two hours in PAT and twice for 10 minutes in PBS. The tubules were then mounted in Vectashield mounting medium (Vector). Slides were examined

with a Molecular dynamics Multiprobe laser scanning confocal upright microscope. The excitation (488 nm) and emission (515 nm) barrier filters used as appropriate.

2.15 Antibodies

Primary: 1) Rabbit anti-universal nitric oxide synthase polyclonal antibody (Affinity Bioreagents Inc.). Working concentration 1: 100

2) Rabbit anti TRP. Specific for residues 11-26 of the mature TRP protein. A kind gift of Charles Zuker, University of California, USA.

3) Rabbit anti TRPL. Specific for amino acids 1082-1097 of the TRPL protein. A kind gift of Craig Montell, John Hopkins University, Baltimore, USA.

2.16 Binding of fluorescently labelled calcium channel antagonists

Slides were treated with 1mg/ml poly-L-Lysine. Tubules were dissected and stuck down on slides in 1 X Phosphate buffered saline (PBS). The tubules were fixed for 20 minutes in 4 % paraformaldehyde in 1 X PBS at room temperature. Slides were then washed 5-7 times in 1 X PBS. The tubules were then incubated for 10-30 minutes in 1 X PBS with fluorescent analogues of calcium channel antagonists: DM-BODIPY-FL verapamil, BODIPY-FL phenylalkylamine, BODIPY-FL nifedipine, or BODIPY-FL vinblastine (Molecular Probes, Inc) at the concentrations described in chapter 4 (10 nM, 100 nM or 100 μM). The slides were then washed 3-4 times in 1 X PBS before mounting in PBS and examination using confocal microscopy. Slides were examined with a Molecular dynamics Multiprobe laser scanning confocal upright microscope.

The excitation (488 nm) and emission (515 nm) barrier filters used as appropriate.

2.17 $[Ca^{2+}]_i$ measurements in aequorin expressing tubules.

The method for measurement of $[Ca^{2+}]_i$ in aequorin expressing tubules is described in Rosay *et al*, 1997, and is as follows. For reconstitution of intracellular aequorin, 20-30 tubules from 3-7 day old adults were dissected in Schneider's medium and placed in 160 µl of Schneider with coelenterazine added to a final concentration of 2.5 µM. Samples were then incubated in the dark for 3-4 hours. Bioluminescence recordings were carried out using an LB9507 luminometer (Berthold Wallac). Samples were 'mock' injected with 25 µl of Schneider's before injection with neuropeptides, cyclic nucleotides or thapsigargin at the desired concentration. At the end of each recording tubules were disrupted in 350 ml lysis solution (1% (v/v) Triton X-100, 100 mM $CaCl_2$), causing discharge of the remaining aequorin and allowing estimation of the total amount of aequorin in the sample by integration of total counts. Calcium concentrations for each time point in an experiment were calculated by backward integration, using a program written in Perl, based on the method described by Button and Eidsath (1996), summarised below.

2.18 Estimation of Ca^{2+} concentration from aequorin luminescence.

To estimate the intracellular Ca^{2+} concentration from the photon signal intensity, it is necessary to calculate the fractional loss rate of aequorin luminescence, or the apparent rate constant of the luminescent (k_{app}). K_{app} is dependent on the reactions quantum yield and fractional saturation of photoprotein with Ca^{2+}. The luminescence reaction of aequorin is first order with respect to the amount of luminescent protein remaining.

Photon signal intensity (I) $= k_{app} * L$,

Where L is the amount of aequorin luminescence in the sample.

Therefore, the k_{app} for any time t during the measurement is calculated by dividing the observed photon signal intensity at time t (I_t) by the amount of luminescent photoprotein remaining in the sample at time t (L_t).

$$k_{app} = I_t/L_t$$

To calculate the luminescent photoprotein remaining at each interval of the measurement the samples total luminescence (L_{tot}) must be known, and is calculated retrospectively by integrating all the photons observed during the measurement (cell lysis and saturation of the photoprotein with Ca^{2+} is necessary for total luminescence determination (see section 2.17).

$$L_{tot} = \Sigma L_i$$

Where L*i* is the background-subtracted photon production during interval *i*.

A running sum of luminescence detected up to interval *x* ($L_{rs}(x)$) is subtracted from L_{tot} to calculate the remaining luminesence activity ($L_{rem}(x)$) at each interval *x* of the measurement.

$$L_{rem}(x)) = L_{tot} - L_{rs}(x))$$

The apparent rate constant is thus equal to the luminescence rate detected at interval *x* divided by the remaining sample luminescence at time *x*.

$$k_{app} = L_i(x))/ L_{rem}(x))$$

The apparent rate constant (k_{app}) is a function of Ca^{2+} concentration. Calibration curves, relating k_{app} to Ca^{2+} concentration, are obtained by measurement of k_{app} in aequorin-expressing tubule lysates injected with buffer (50 mM K_2-tartrate, 10 mM HEPES (pH 7.1), 1mM GSH, and 0.5 M each of EGTA,HEDTA, and NTA) containing 0-1 mM Ca^{2+}. The luminsescence of the samples is measured and the k_{app} calculated by dividing the instantaneous photon production rate by the corresponding remaining sample

luminnescence activity, as described above. A graph of k_{app} against known Ca^{2+} concentrations can then be plotted to allow estimation of Ca^{2+} from samples.

3.1 Summary

A RT-PCR strategy was adopted to examine the expression of genes thought to be involved in calcium signalling within the *Drosophila* Malpighian tubule. PCR reactions were carried out using cDNA derived from both OreR heads and tubules, as well as genomic DNA acquired from whole flies. Primer pairs specific for genes *trp, trpl, trpγ, DmcaIA, DmcaID, inaC, pkc53e, inaD, norpA* and *plc-21* were designed to flank intron/exon boundaries, giving different product sizes from genomic DNA and cDNA. PCR products corresponding to the intronless (spliced) gene were produced in most, but not all, of the reactions using tubule cDNA templates. The PCR products were cloned and sequenced to confirm their identity. This was taken as evidence of expression of the gene in the Malpighian tubule.
In this way it was found that *trp, trpl, trpγ, DmcaIA, DmcaID, inaC, pkc53e, norpA* and *plc-21* but not *inaD* are expressed in the Malpighian tubules.

3.2 Introduction

In the preceding introduction, neuropeptide-induced calcium influx in the cells of the main segment was discussed. Upon stimulation with CAP_{2b} and Drosokinin, calcium influxes were induced exclusively in the principal and stellate cells respectively. It is thought that calcium acts as a second messenger to stimulate, through other effector molecules, an increase in the fluid secretion rate (Davies *et al*, 1995; Rosay *et al*, 1997). The calcium signals produced by stimulation with these neuropeptides are complex and seem to consist of at least two separate calcium influx events in both cases. As these neuropeptides stimulate calcium influx of external calcium, it is sensible to examine the expression of plasma

membrane calcium channels. Furthermore signalling molecules involved in the regulation of such calcium channels may also be involved in the tubule.

Therefore, we initially looked for the expression of five different calcium channel genes previously found in *Drosophila*: *Dmca1A*, *Dmca1D*, *trp*, *trpl* and *trpγ*. Both *Dmca1A* and *Dmca1D* encode different isoforms of the alpha subunit of voltage gated calcium channels. Both channels are involved in the production of male courtship song, and *Dmca1A* is also involved in *Drosophila* vision, as demonstrated by mutations in these genes (Peixoto *et al*, 1998; Smith *et al*, 1998).
TRP and TRPL calcium channels have been extensively studied in *Drosophila* phototransduction and are thought to be the major route of calcium influx in this process (Neimeyer *et al*, 1996). In the *Drosophila* photoreceptors, TRP and TRPL form a multimolecular complex with Rhodopsin, PLC, PKC and INAD (Xu *et al*, 1998), which is thought to facilitate the speed and control of the phototransduction response. Therefore, the expression of genes encoding these molecules was also examined in tubules. As different isoforms of PLC and PKC have been shown to be present in other tissues, the expression of a non-eye specific phospholipase C (*plc-21*) (Shortridge *et al*, 1991) and a non-eye specific protein kinase C (*pkc53e*) (Rosenthal *et al*, 1987) was examined.
Primer pairs were designed specifically for each gene in question. In all cases they flanked a known intron. This meant that the PCR product obtained using genomic DNA would be larger than that produced from cDNA providing a control for genomic contamination in cDNA (see Figure 3.1). This strategy has been successfully adopted for transport and signalling genes in the tubule (Dow *et al*, 1994, Davies *et al*, 1997).

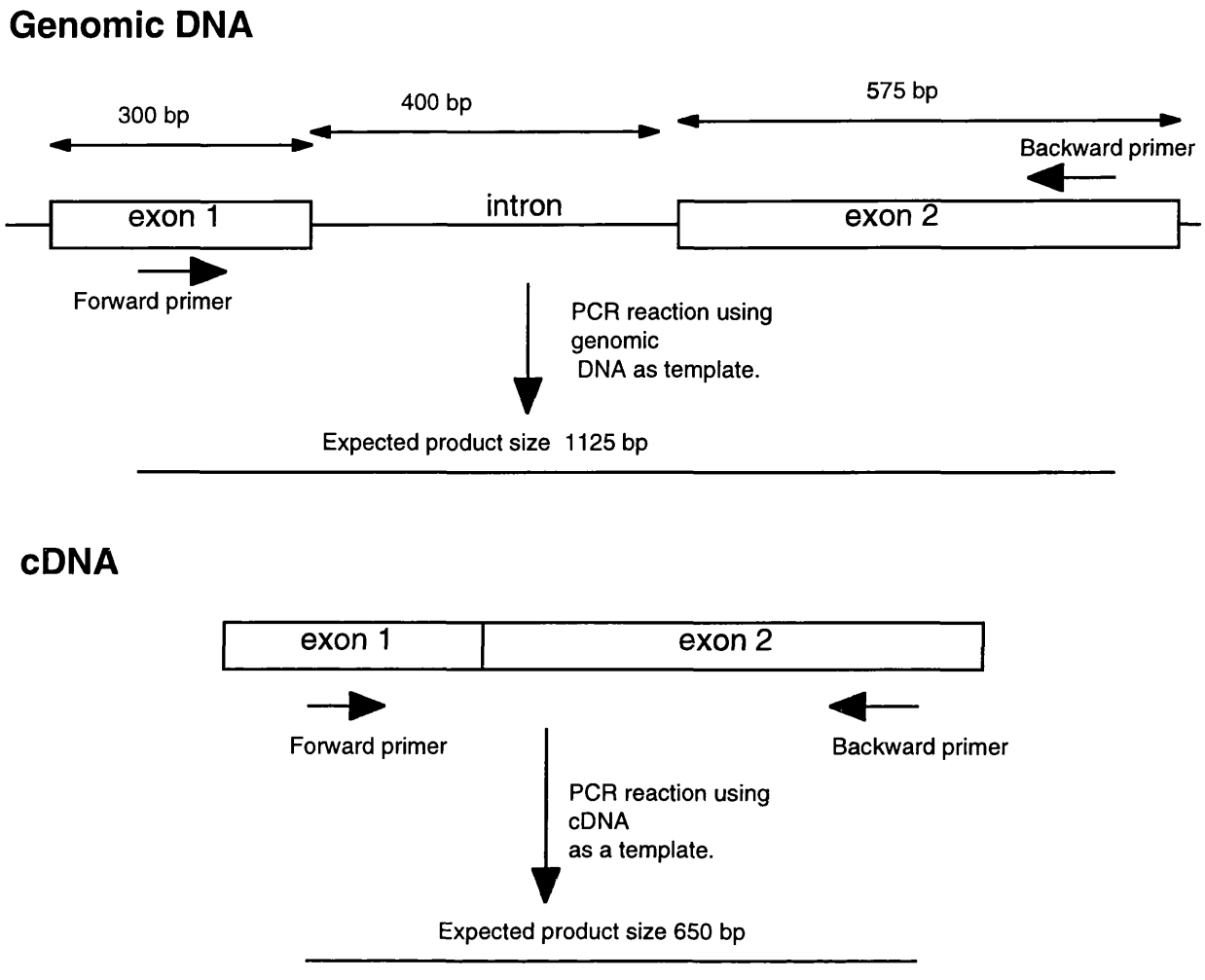

Figure 3.1: Diagram showing RT-PCR strategy to determine expression of genes in Malpighian tubules.

Primer pairs that anneal to separate exons flanking a known intron of the gene in question were designed. These primers are then used in PCR reactions using genomic, cDNA from heads and cDNA from tubules as template. If the gene is expressed in the tissue from which the cDNA is obtained, the resulting PCR product will be the size of the spliced gene lacking the intron, whereas PCR reactions with genomic DNA as a template will give a larger product (including the intron). Irrespective of any larger product caused by genomic DNA carry-over, the presence of the spliced product in the cDNA is taken as evidence of the expression of the gene in that tissue.

3.3 Expression of *Dmca1A* and *Dmca1D* in Malpighian tubules

PCR reactions were carried out using primer pairs specific for the *Dmca1A* and *Dmca1D* genes. Genomic DNA, cDNA from *Drosophila* heads, and cDNA from *Drosophila* tubules were used as templates for the reactions. The PCR products were analysed on a 1% agarose gel with 1-kb ladder (Gibco BRL).

The forward and reverse *Dmca1A* primers corresponded to bases 5829-5850 and 6327-6306 respectively of the *Dmca1A* complete coding sequence flanking an intron (Genbank #U55776; Smith *et al*, 1996). The expected genomic and cDNA template PCR product sizes were 564 and 498 bp respectively.

The forward and reverse *Dmca1D* primers corresponded to bases 5581-5602 and 6003-5982 respectively of the *Dmca1D* complete coding sequence flanking an intron (Genbank #U00690; Zheng *et al*, 1995). The expected genomic and cDNA template PCR product sizes were 541 and 422 bp respectively.

Products of the expected sizes were obtained for both genes, from head cDNA and tubule cDNA templates. For both *Dmca1A* and *Dmca1D* significant genomic contamination was observed in the tubule cDNA reactions. It is thought that this reflects a lower expression of the genes in this tissue relative to heads, and not any difference in quality of cDNA obtained from the two tissues. The PCR products from the tubule cDNA template were cloned into PCRII.1 vectors (Invitrogen) and sequenced to confirm their identity. The sequences were then compared to the published *Dmca1A* and *Dmca1D* sequences using BLAST (NCBI). There was no difference between the sequences produced by PCR of tubule cDNA and the published sequences, showing that both *Dmca1A* and *Dmca1D* are expressed in *Drosophila* Malpighian tubules.

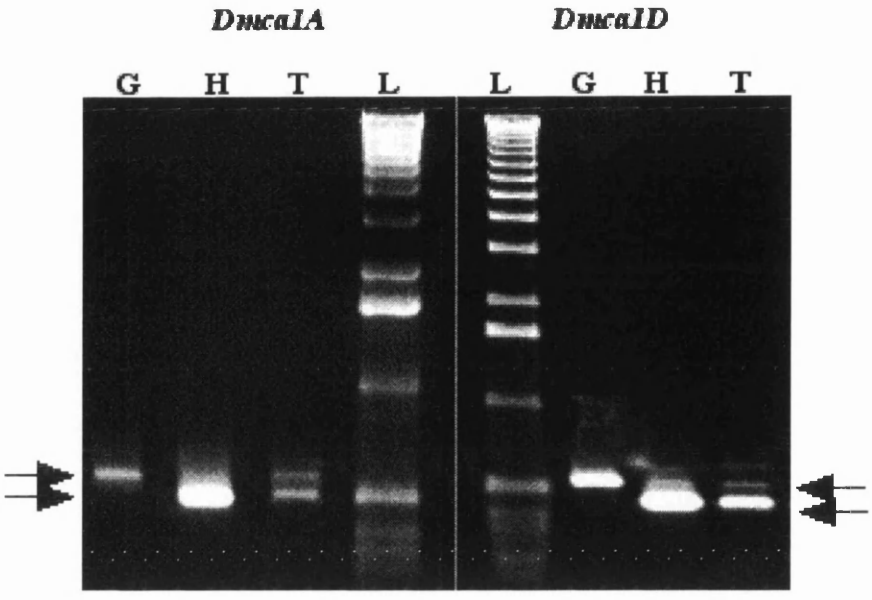

Figure 3.2: The expression of *DmcaIA* and *DmcaID* in *D. melanogaster* Malpighian tubules.

Reverse-transcription polymerase chain reaction (RT-PCR) using *D. melanogaster* genomic DNA (G), head (H) and tubule (T) template cDNA with primers directed against *DmcaIA* (left-hand panel) and *DmcaID* (right-hand panel). Upper arrow denotes PCR products obtained with genomic DNA, lower arrows denote PCR products obtained with cDNA.

DmcaIA: Lane 1, genomic DNA template results in a product of 564 bp; lane 2, product of expected 498 bp with head cDNA template; lane 3, product of expected 498 bp with tubule cDNA template; lane 4, 1-kb ladder (Gibco BRL).

DmcaID: Lane 1, 1-kb ladder (Gibco BRL); lane 2, genomic DNA template results in a product of 541 bp; lane 3, product of expected 422 bp with head cDNA template; lane 4, product of expected 422 bp with tubule cDNA template.

3.4 Expression of *trp* and *trpl* in Malpighian tubules

PCR reactions were carried out using primer pairs specific for the *trp* and *trpl* genes. Genomic DNA, cDNA obtained from *Drosophila* heads, and cDNA obtained from *Drosophila* tubules were used as templates for the reactions.

The PCR reactions were examined on a 1% agarose gel with 1-kb ladder (Gibco BRL).

The forward and reverse *trp* primers corresponded to bases 4731-4752 and 5291-5270 of the *trp* gene complete coding sequence flanking two introns at bases 4863-4921 and 5077-5136 (Genbank #M21306; Montell and Rubin, 1989). The expected product sizes from genomic DNA and cDNA templates were 560 and 443 bp respectively. The forward and reverse *trpl* primers corresponded to bases 2652-2672 and 3119-3095 respectively of the *trpl* complete coding sequence (Genbank #M88185; Philips *et al*, 1991). The expected genomic and cDNA template PCR product sizes were 524 and 467 bp respectively. Products of the expected sizes were obtained for both *trp* and *trpl* from the head and tubule cDNA templates (Figure 3.3). The tubule cDNA PCR products were then cloned into the PCRII.1 vector (Invitrogen) and sequenced to confirm their identity. Once the sequence was obtained it was compared to the known *trp* gene sequence using BLAST. No differences were found between our cloned sequences and those published for *trp* and *trpl*, indicating that both these genes were expressed in the Malpighian tubule.

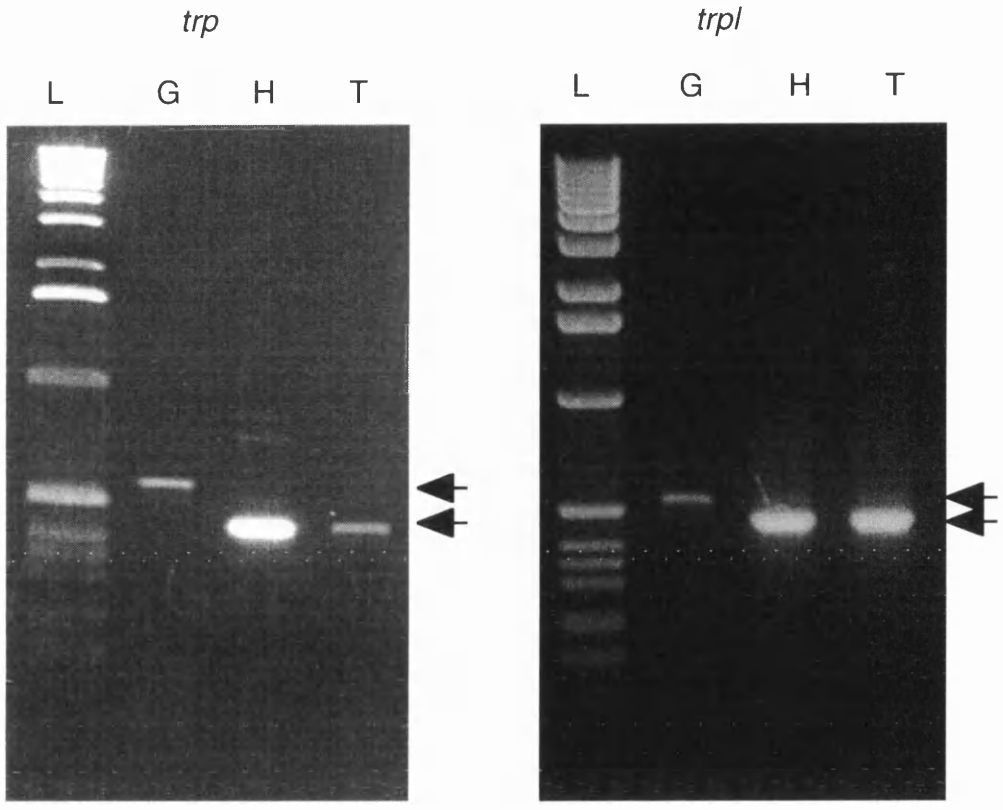

Figure 3.3: The expression of *trp* and *trpl* in *D. melanogaster* Malpighian tubules. Reverse-transcription polymerase chain reaction (RT-PCR) using *D. melanogaster* genomic DNA (G), head (H) and tubule (T) template cDNA with primers directed against *trp* (left-hand panel) and *trpl* (right-hand panel). Upper arrow denote PCR products obtained with genomic DNA, lower arrows denote PCR products obtained with cDNA.

trp: Lane 1, 1-kb ladder (Gibco BRL); lane 2, genomic DNA template results in a product of 560 bp; lane 3, product of expected 443 bp with head cDNA template; lane 4, product of expected 443 bp with tubule cDNA template.

trpl: Lane 1, 1-kb ladder (Gibco BRL); lane 2, genomic DNA template results in a product of 524 bp; lane 3, product of expected 467 bp with head cDNA template; lane 4, product of expected 467 bp with tubule cDNA template.

3.5 Expression of *trpγ* in the Malpighian tubule.

Following the recent discovery of a third *trp* related gene in *Drosophila*, *trpγ* (Xu *et al*, 2000), RT-PCR was used to look for expression of this gene in the Malpighian tubules. PCR reactions were carried out using primers specific for *trpγ*. The forward and reverse primers corresponded to bases 3256-3278 and 3776-3800 respectively of the *trpγ* encoding sequence (Genbank #AJ277967; Xu *et al*, 2000). Genomic DNA, cDNA obtained from heads and cDNA from Malpighian tubules were used as templates for this reaction. The expected genomic and cDNA PCR product sizes were 656 and 544 bp respectively. PCR products of the expected size were obtained from all the templates (Figure 3.4). There is a significant amount of the genomic sized band produced with the tubule cDNA template due to genomic contamination, suggesting a relatively low level of expression as compared to that in heads. The PCR product obtained from the tubule cDNA template was cloned into a PCRII.1 vector and sequenced. The sequence was compared to the published *trpγ* sequence using BLAST and the sequences were found to be identical, showing the expression of *trpγ* in Malpighian tubules.

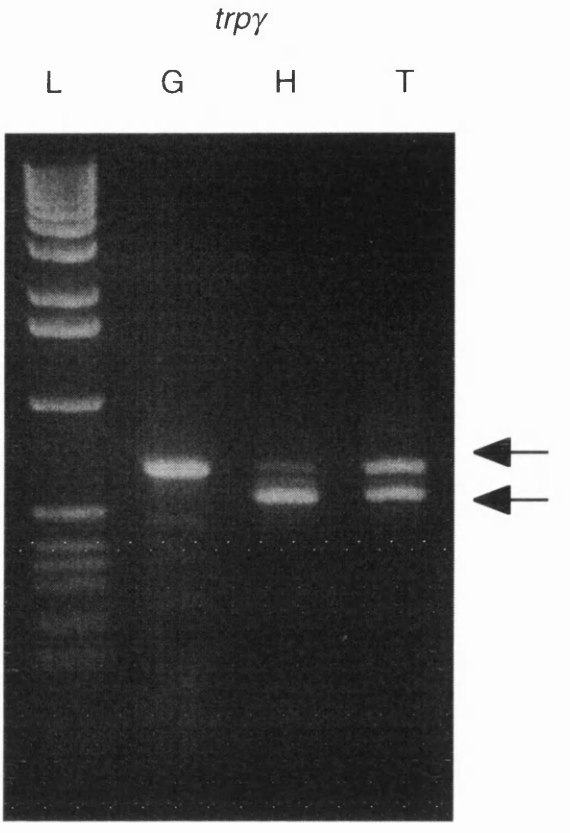

Figure 3.4: The expression of *trpγ* in *D. melanogaster* Malpighian tubules.

Reverse-transcription polymerase chain reaction (RT-PCR) using *D. melanogaster* genomic DNA (G), head (H) and tubule (T) template cDNA with primers directed against *trpγ*. Upper arrow denote PCR products obtained with genomic DNA, lower arrows denote PCR products obtained with cDNA.

trpγ: Lane 1, 1-kb ladder (Gibco BRL); lane 2, genomic DNA template results in a product of 656 bp; lane 3, product of expected 544 bp with head cDNA template; lane 4, product of expected 544 bp with tubule cDNA template.

3.6 Expression of *inaC, pkc53e, inaD, norpA,* and *plc-21* in Malpighian tubules.

Having found the expression of both *trp* and *trpl* in the tubules, it seemed likely that some of the gene products that interact with TRP and TRPL channels in phototransduction may also be expressed in the tubules. This included *inaC, inaD* and *norpA*. The expression of other signalling molecules, not specific to photoreceptors, were also examined, namely those encoding non-eye specific PKC (*pkc53e*), and non-eye-specific PLC (*plc-21*).

PCR reactions were carried out using primer pairs specific for the *inaC* (Schaeffer *et al,* 1989), *pkc53e* (Rosenthal *et al,* 1987), *inaD* (Sheih *et al*, 1995), *norpA* (Bloomquist *et al*, 1988), *and plc-21* (Shortridge *et al,* 1991) genes. Genomic DNA, cDNA obtained from *Drosophila* heads, and cDNA obtained from *Drosophila* tubules were used as templates for the reactions. The PCR products were examined on a 1% agarose gel with 1-kb ladder (Gibco BRL) to discern their size.

The forward and reverse *inaC* primers corresponded to bases 1574-1595 and 2079-2057 of the *inaC* complete coding sequence (Genbank #JO4845). The expected genomic and cDNA template PCR product sizes were 680 and 505 bp's respectively. Products of the expected sizes were obtained from head and tubule cDNA templates. The tubule cDNA PCR product was cloned into vector PCRII.1 and then sequenced. The sequence was identical to the published sequence for the *inaC* gene, showing that this gene was expressed in the tubules. Although there was a high level of genomic contamination, a weak band with tubule cDNA was discernible. Thus, it appears that the expression level of the *inaC* in the tubules is very low.

The forward and reverse *pkc53e* primers corresponded to bases 1282-1303 and 1781-1762 of the *pkc53e* complete coding sequence (Genbank #XO5283). The expected genomic and cDNA template PCR product sizes were 500 and 372 bp's

respectively. Products of the expected sizes were obtained from both head and tubule cDNA templates. The tubule cDNA template PCR product was cloned and sequenced as before. The sequence was identical to the published sequence for *pkc53e* showing the expression of this gene in the Malpighian tubules (Figure 3.5).

The forward and reverse *inaD* primers corresponded to bases 1094-1115 and 1610-1590 of the *inaD* complete coding sequence (Genbank #U15803). The expected genomic and cDNA template PCR product sizes were 696 and 516 bp's respectively. PCR products of the expected size were obtained for both head cDNA and genomic DNA templates, but not for the tubule cDNA template PCR reaction (Figure 3.5). This experiment was repeated under a variety of different conditions, using annealing temperatures ranging from 45-55 ^{o}C and up to 40 cycles, but in no instance did tubule cDNA template give the correct product size. This result indicates the absence of expression of *inaD* in the Malpighian tubules.

RT-PCR for the genes *norpA* and *plc21* were carried out by Valerie Pollock, and in both cases expression of the genes was apparent in the Malpighian tubules (results not shown).

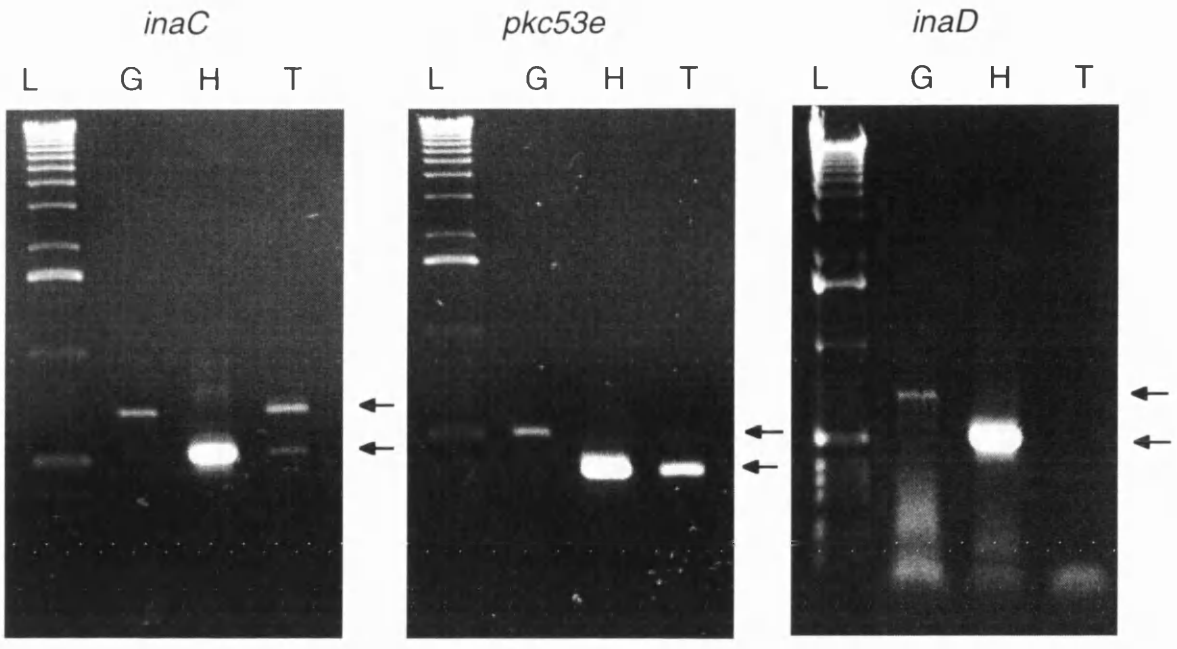

Figure 3.5: The expression of *inaC*, *pkc53e* and *inaD* in *D. melanogaster* Malpighian tubules.

Reverse-transcription polymerase chain reaction (RT-PCR) using *D. melanogaster* genomic DNA (G), head (H) and tubule (T) template cDNA with primers directed against *inaC* (left-hand panel), *pkc53e* (middle panel) and *inaD* (right-hand panel). Upper arrows denote PCR products obtained with genomic DNA; lower arrows denote PCR products obtained with cDNA.

inaC: Lane 1, 1-kb ladder (Gibco BRL); lane 2, genomic DNA template results in a product of 680 bp; lane 3, product of expected 505 bp with head cDNA template; lane 4, product of expected 505 bp with tubule cDNA template.

pkc53e: Lane 1, 1-kb ladder (Gibco BRL); lane 2, genomic DNA template results in a product of 500 bp; lane 3, product of expected 372 bp with head cDNA template; lane 4, product of expected 372 bp with tubule cDNA template.

inaD: Lane 1, 1-kb ladder (Gibco BRL); lane 2, genomic DNA template results in a product of 696 bp; lane 3, product of expected 516 bp with head cDNA template; lane 4, no PCR product with tubule cDNA template.

3.7 Discussion

The experiments described in this chapter utilize a RT-PCR strategy to gain a general picture of relevant signalling genes expressed in the Malpighian tubule, and provide a basis for further study of the specific functions of these genes. The expression of the calcium channel genes *Dmca1A*, *Dmaca1D*, *trp*, *trpl*, and *trpγ* in tubules suggests a previously undocumented role for these calcium channels in epithelial transport. Voltage-gated calcium channels, such as Dmca1A and Dmca1D, had been previously thought only to exist in excitable tissues; however, their presence has recently been demonstrated in non-excitable tissues, including epithelia (Zhang and O'Neil, 1996; Farrugia, 1997; Barry *et al*, 1998). Our results demonstrate that a role in epithelial tissues is conserved in invertebrates.

Although RT-PCR usually only shows simply either the presence or absence of transcripts in a given tissue, some semi-quantitative information regarding expression can be inferred from our experiments. Certainly it looks as though the expression level of all the calcium channels is relatively low compared to that seen in heads.

Another interesting and somewhat unexpected result was the lack of expression of *inaD* in tubules. INAD is a protein containing five PDZ domains (which mediate protein-protein interaction) that acts in *Drosophila* photoreceptors as a 'scaffold' for TRP, TRPL, PLC, PKC, Rhodopsin and calmodulin (Xu *et al*, 1997). In this context it brings together molecules involved in the control of TRP and TRPL calcium channels. However, as it is lacking in the tubules, while the other signalling molecules (with the exception of Rhodopsin) are present it seems that either the signalling molecules reside untethered within the cells of the tubule, or that another 'scaffolding' molecule, as yet unidentified, organises signalling complexes in the tubule. The apparent low expression level

of *inaC* also seems to indicate a difference in the organisation of signalling molecules in head and tubules.

It would be desirable to determine expression levels of the calcium channel genes using Northern blot analysis. However, as many of these seem to be expressed at quite low levels in the Malpighian tubule, Northern analysis would have to be highly sensitive to detect the transcripts for these genes. For example, to detect the *DmcalD* transcript in *Drosophila* head (Eberl *et al*, 1998), 20 µg/lane of Poly(A^+) RNA was necessary. To obtain this amount of Poly(A^+) RNA from Malpighian tubules would require the dissection of around 20,000 tubules. However, Northern blots were attempted using 40 µg/lane total RNA extracted from heads, bodies and 3500 tubules. Using probes specific for the calcium channel transcripts *DmcalA, DmcalD, trp and trpl* no bands could be detected. This was not surprising due to the predicted low expression levels of these genes within the tubules. With regard to the voltage-gated calcium channels DmcalA and DmcalD, Zhang *et al*, 1996 predicted that approximately two L-type Ca^{2+} channels per cell would be sufficient to significantly contribute to calcium influx during membrane depolarisation, indicating that very low expression levels of such channels need not negate a functional significance. The possibility of fault with the Northern blotting technique was tested using a probe specific for the 16 kD V-ATPase subunit encoding gene *vha16*, known to be expressed at high levels in the tubule. A transcript of 1.4 kb in size was detected in agreement with the predicted transcript size (Figure 3.6).

With the availability of more efficient RNA isolating technologies, and the resulting increased sensitivity of Northern analysis it may be possible to examine expression levels and the possibility of alternative transcripts in the tubules. Evidence for alternative exons and differential splicing has been found in both *DmcalA* and *DmcalD* (Peixoto *et al*, 1997; Zheng *et al*, 1995).

This chapter demonstrates the expression of various calcium channels and signalling molecules in the Malpighian tubules but by no means represents all the channels expressed. It may be that there is further as yet undiscovered *Drosophila* calcium channels, playing an important role in calcium signalling, expressed in Malpighian tubules. For instance in *C. elegans* the *Osm-9* gene encodes a cation channel with structural homology to the TRP channel that is involved in response to osmotic and olfactory stimuli. Using a BLAST search of the *Drosophila* peptide database with the Osm-9 gene as a probe, two gene products CG4536 and CG5842 of current unknown function with significant homology to Osm-9 (60% and 47% respectively) were found. As we are studying a transporting epithelium sensitive to changes in osmotic potential, the examination of these genes in Malpighian tubules may be an interesting avenue for further study. Searches of the *Drosophila* genome project have revealed one possible L-type related channel; gene CG1517 but no further *trp*-related genes. However, RT-PCR using primers specific for CG1517 (Figure 3.7) indicated expression of this gene in head but not in the tubules. Bands corresponding to the correct genomic (600 bp) and cDNA (500 bp) were produced using genomic and cDNA from *Drosophila* heads respectively; but only a faint band of 600 bp, caused by genomic contamination was obtained using tubule cDNA. It is evident from my initial searches of the *Drosophila* genome project, that there may be a plethora of uncharacterised calcium channel encoding genes. Suffice to say that, at present, when studying signalling within the Malpighian tubules, this should be taken into account.

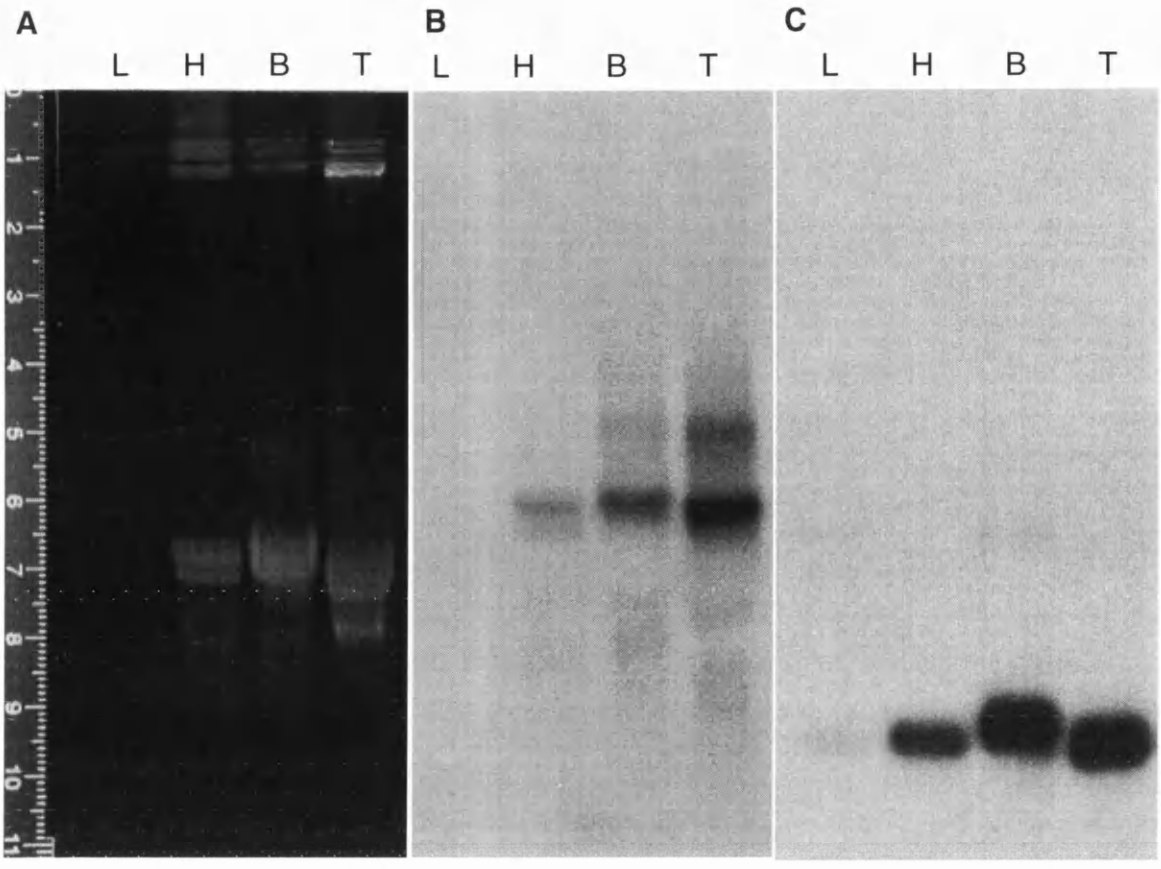

Figure 3.6: Northern blot Analysis of *vha16*.

Northern blot analysis of the *vha16* gene in malpighian tubules.

A) 40 µg/lane of total RNA extracted from *Drosophila* heads (H), bodies (B), and tubules (T).

B) RNA was transferred onto a nitrocellulose filter and hybridised with ^{32}P-labelled DNA probes for *vha16*. A transcript of around 1.4 kb is evident in heads, bodies and tubules. The lighter bands are due to non-specific binding to ribosomal RNA.

C) Hybridisation of the filter with an RP49 control specific for a ubiquitously expressed ribosomal protein. It is evident that there is slightly more tubule and body RNA present on the filter relative to head RNA.

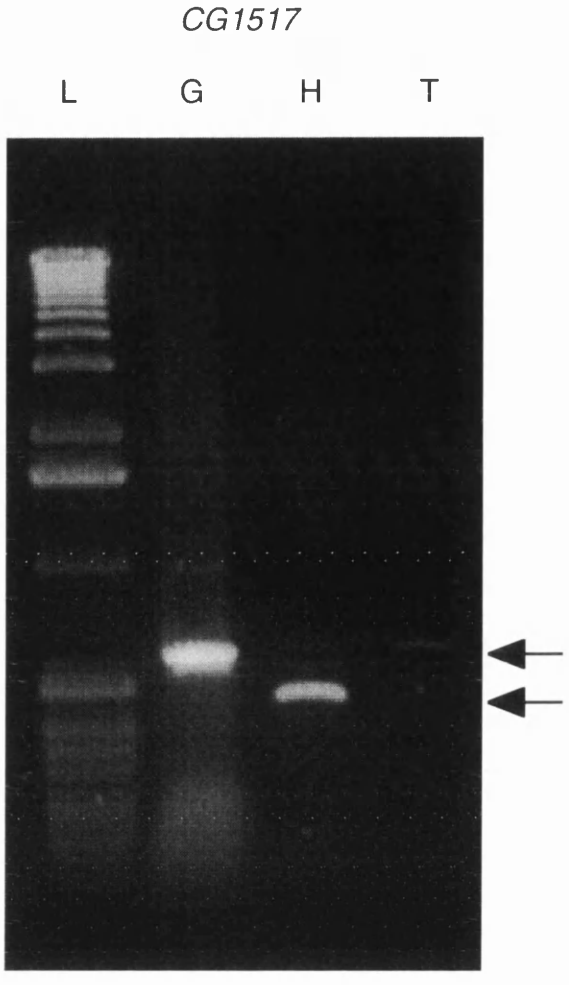

Figure 3.7: *CG1517* is not expressed in *D. melanogaster* Malpighian tubules.

Reverse-transcription polymerase chain reaction (RT-PCR) using *D. melanogaster* genomic DNA (G), head (H) and tubule (T) template cDNA with primers directed against *CG1517*. Upper arrow denotes PCR products obtained with genomic DNA, lower arrow denotes PCR products obtained with cDNA. *CG1517*: Lane 1, 1-kb ladder (Gibco BRL); lane 2, genomic DNA template results in a product of 600 bp; lane 3, product of expected 501 bp with head cDNA template; lane 4, product of 600 bp due to genomic DNA contamination of tubule cDNA template.

Chapter 4

oltage-gated calcium channels are involved in epithelial fluid transport and calcium signalling

Chapter 4

4.1 Summary

Having already demonstrated the presence of *Dmca1A* and *Dmca1D* transcripts in Malpighian tubules, this chapter investigates the involvement of these channels in fluid transport, and also in CAP_{2b}- and cGMP-induced calcium influxes in the principal cells. Results demonstrate that CAP_{2b}-stimulated fluid transport and cytosolic calcium increases ($[Ca^{2+}]_i$), are inhibited by the 'L'-type calcium channel antagonists, verapamil and nifedipine. It is also shown that cGMP induces a slow $[Ca^{2+}]_i$ increase in tubule principal cells via verapamil- and nifedipine-sensitive calcium entry. Using fluorescent calcium channel blockers (BODIPY-FL verapamil, BODIPY-FL phenylalkylamine and BODIPY-DM nifedipine) it is demonstrated that phenylalkylamines bind with differing affinities to the basolateral and apical surfaces of principal cells in the main segment and that nifedipine binds apically in the tubule initial segment. Immunocytochemical evidence suggests localisation of α1 subunits to both basolateral and apical surfaces of principal cells in the tubule main segment. Together this suggests a role for PAA- and DHP-sensitive calcium channels and cGMP-mediated calcium influx, in both calcium signalling and fluid transport mechanisms in *Drosophila*.

4.2 Introduction

The existence of voltage-gated calcium channels was first shown in *Drosophila* when Pelzer *et al*, 1989, revealed the presence of eight pharmacologically distinct Ca^{2+} channels in reconstituted *Drosophila* head membranes. Channels sensitive to both phenylalkylamines (PAA's) and dihydropyridines (DHP's) were observed, indicating the presence of different isoforms of voltage-gated calcium channels. To date, two voltage-gated α subunit

calcium channel genes have been cloned in *Drosophila*, *Dmca1D* and *Dmca1A* (Zheng *et al*, 1995; Smith *et al*, 1996). These were originally cloned from head cDNA libraries, but in the previous chapter the presence of transcripts for these channels in Malphigian tubules was demonstrated by RT-PCR. Such voltage-gated channels are not unknown in epithelial cells and have recently been found in the mouse distal convoluted tubule (Barry *et al*, 1998) and in rabbit proximal tubule cells (Zhang *et al*, 1996). These studies do not report molecular evidence for a possibly new class of epithelial L-type calcium channel but instead infer its presence by patch clamp experiments, revealing voltage-regulated dihydropyridine-sensitive calcium currents. A 388 bp fragment of an $\alpha 1$ subunit was cloned from RNA isolated from rabbit cultured proximal tubule cells, that encoded part of a protein identical to the $\alpha 1C$ subunit (cardiac L-type channel). Further to this, full-length transcripts of $\alpha 1C$ were detected in mouse distal convoluted cells (Barry *et al*, 1998).

The properties of Dmca1D and Dmca1A with regard to their sensitivities to calcium channel antagonists have been inferred by homology with vertebrate calcium channels. Both Dmca1D and Dmca1A have highly conserved PAA binding domains implying sensitivity to this calcium channel antagonist. The DHP binding site in Dmca1D shows numerous changes although the subunit is 78.3% similar to the DHP-sensitive class of $\alpha 1$ subunits. However, Ren *et al*, 1998, suggest that Dmca1D is DHP-sensitive. Dmca1A has a poorly conserved DHP binding site resulting in a channel expected to be PAA-sensitive and DHP-insensitive.

Mammalian L-type currents are blocked by three major classes of channel ligands, DHPs, PAAs and benzothiazepines. However, the efficacy of these ligands in the blocking of invertebrate Ca^{2+} currents differs from those observed in mammalian studies. For example, neuronal current components in *Drosophila* (Pelzer *et al*, 1989) and honeybee (Schafer *et al*, 1994) are more sensitive to PAAs

whilst those measured in *Drosophila* muscle are more sensitive to DHPs (Gielow *et al*, 1995; Ren *et al*, 1998). The table in appendix 6 (page 217) summarises the effects and affinities of PAAs and DHPs and cations to invertebrate calcium channels (for review see Jeziorski *et al*, 2000). Other targets of DHPs and PAAs may also be expressed in tubules. For example, Dube *et al*, 2000, measured Ca^{2+} in secreted fluid of the Malpighian tubule and found that 500 μM verapamil decreased calcium flux up to 3.3 fold. However at lower concentrations of verapamil and nifedipine (100 μM), Ca^{2+} tranport remained unaffected. In vertebrates the calcium transporter CaT2, specifically expressed in the kidney, is inhibited to 88.2±0.9 % and 96±1.8 % of normal calcium transport function, by nifedipine (DHP) and verapamil (PAA) respectively, both at 100 μM (Vennekens *et al*, 2001). It appears then, that calcium transporters are only affected at relatively high concentrations of DHPs and PAAs. Of the calcium channel classes postulated to be sensitive to DHP's and PAA's only *DmcaID* and *DmcaIA* are expressed in tubules. This means that any sensitivities of calcium influxes to PAAs and DHPs can be attributed to an effect on these two channels. However when examining fluid secretion, high concentrations of verapamil and nifedipine (above 10^{-4} M) may effect calcium transport as well as calcium signalling.

It is not clear, at present, how DmcaIA and DmcaID may be regulated in the tubule. A lack of innervation would intuitively exclude a voltage-regulated mechanism. However, it is possible that local currents created by ion-pumps such as the V-ATPases (Dow *et al*, 1999) or Na^{2+}/K^{+} exchangers produce localised potential differences across the plasma membrane that could activate such voltage-gated channels. CAP_{2b} may stimulate calcium channels indirectly through the stimulation of PLC, which results in the release of Ca^{2+} from internal stores (see section 1.1); or directly through interaction with an activating trimeric G-protein. CAP_{2b} is known to stimulate fluid secretion through calcium

mediated stimulation of *Drosophila* nitric oxide synthase (DNOS), to produce NO, which in turn stimulates soluble guanylate cyclase to produce cGMP, which acts to increase fluid secretion (Dow *et al*, 1994; Davies *et al*, 1995). Downstream elements of this pathway such as cGMP might be expected to modulate $[Ca^{2+}]_i$ to contribute to a stimulation of fluid secretion lasting much longer than the initial calcium peak. cGMP can act to produce a $[Ca^{2+}]_i$ rise either by calcium influx through cyclic nucleotide-gated channels, or by stimulation of protein kinases that in turn act on calcium channels to allow the influx of external calcium.

Experiments in this chapter also examine the binding sites of dihydropyridines, phenylalkylamines and verapamil within intact tubules, visualised with fluorescently labelled derivatives of these molecules. Fluorescently labelled DHP's and PAA's have been used to locate L-type calcium channels in skeletal muscle (Knaus *et al*, 1992), perisynaptic glial cells in frogs (Robitaille *et al*, 1996) and also in sunflower protoplasts (Vallee *et al*, 1997). Here the molecules have been labelled with either (4,4-Difluoro-5,7-dimethyl-4-bora-3a,4a-diaza)-3-(s-indacene) propionic Acid (DMBodipy), or (4,4-Difluoro-7-styryl-4-bora-3a,4a-diaza)-3-(s-indacene) propionic Acid (STBodipy) molecules. In all these cell types, binding was specific to defined regions of the cell and shown by competition with non-fluorescently labelled PAA or DHP to bind similarly to unlabelled molecules. As verapamil is a substrate for P-glycoproteins (Lelong *et al*, 1991) as well as being a calcium channel antagonist, we distinguished the binding to P-glycoproteins from that of calcium channels by examining the binding of the P-glycoprotein substrate vinblastine.

Overall these results demonstrate the importance of L-type calcium channels in stimulating calciumg influx events within the principal cells of the Malpighian tubule. Also demonstrated is the presence of calcium channels that

are activated either directly or indirectly by cGMP which produce a verapamil- and nifedipine-sensitive influx of calcium into the cell.

4.3 CAP_{2b}-stimulated tubule fluid secretion is sensitive to 'L'-type calcium channel antagonists.

[The fluid secretion assays in this section were caried out by Miss Valerie Pollock, and have been included for clarity, and for comparison with $[Ca^{2+}]_i$ measurements] Phenylalkylamines and 1,4-dihydropyridines (DHP) are selective antagonists of 'L'-type calcium channels and are known to be effective in *Drosophila* (Pelzer *et al*, 1989). Fluid secretion assays were carried out where either verapamil or nifedipine was applied to the tubules over a range of concentrations, 10 minutes prior to stimulation with CAP_{2b} (10^{-7} M). The basal rates of fluid secretion were not significantly altered upon calcium channel antagonist pre-treatments, except where verapamil was applied at 10^{-2} M, whereupon tubule secretion was completely abolished (not shown). However, both the DHP, nifedipine, and the phenylalkylamine, verapamil, inhibit CAP_{2b}-stimulated fluid secretion (Figure 4.1A and B).

The dose response curve for verapamil inhibition of the CAP_{2b}-stimulated fluid secretion response (Figure 4.1C) shows significant inhibition between 10^{-5} M and 10^{-3} M, and again at 10^{-8} M. 1 mM verapamil pre-treatment completely abolishes CAP_{2b}-stimulated fluid secretion rates. In contrast, the DHP, nifedipine, significantly inhibits CAP_{2b}-stimulated fluid secretion at all concentrations between 10^{-10} M and 10^{-7} M (Figure 4.1D), with maximal inhibition to approximately 31% of control (10^{-7} M). The complexity of the dose-response curves, with significant effects spanning wide concentration ranges, implies multiple targets of differing affinity for each drug.

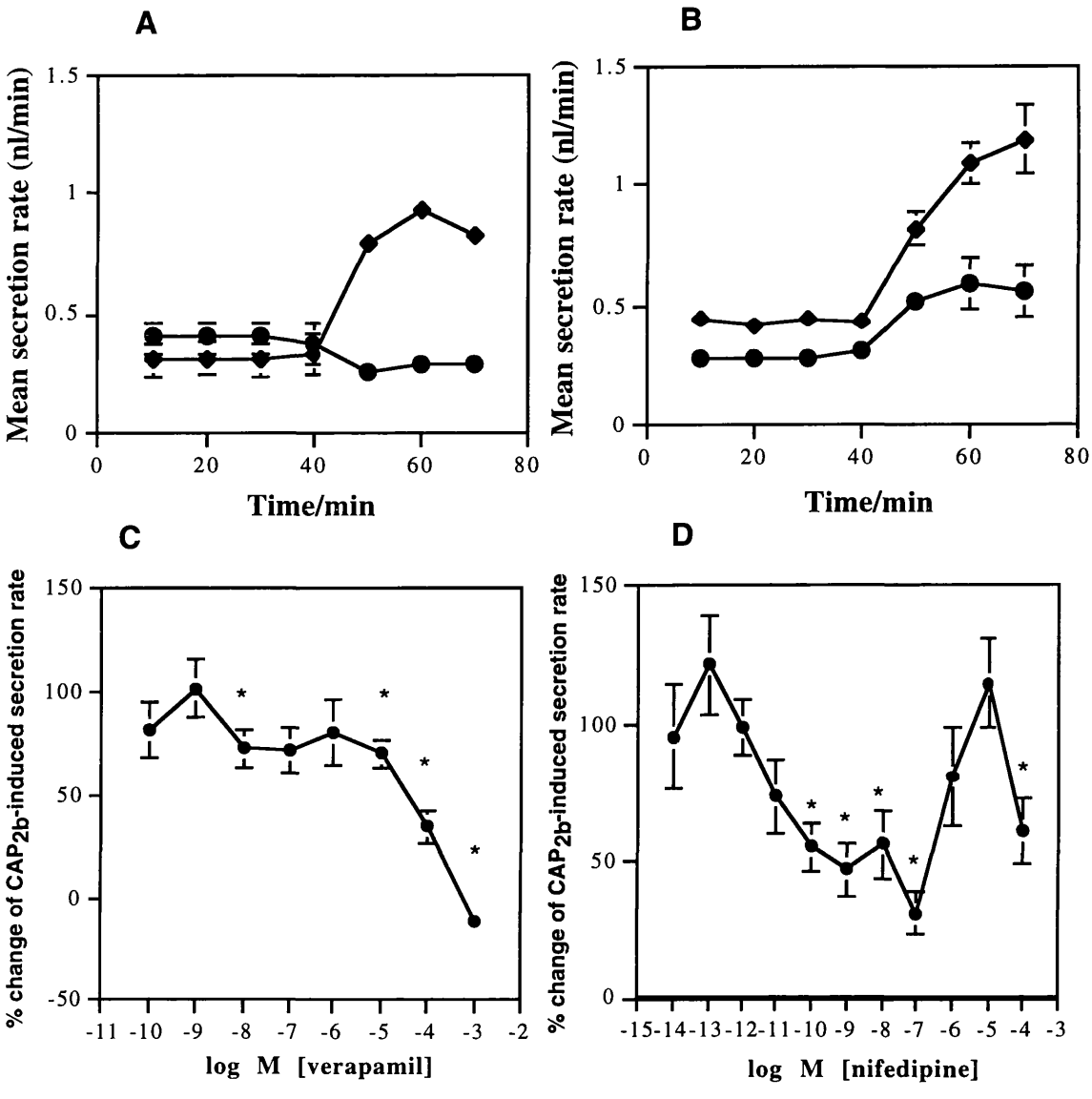

Figure 4.1: CAP_{2b}-stimulated fluid secretion is inhibited by verapamil and nifedipine.

Tubules isolated from c42-aequorin-expressing tubules were pre-treated with appropriate concentrations of verapamil or nifedipine at 30 min, prior to stimulation with CAP_{2b} (10^{-7} M) at 40 min. A) Verapamil inhibits CAP_{2b}-stimulatedfluid secretion. Control (♦); 10^{-3} M pre-treatment (•). Results are expressed as mean fluid secretion rates in nl/min ± SEM., N=8.

B) Nifedipine inhibits CAP_{2b}-stimulated fluid secretion. Control (♦); 10^{-9} M pre-treatment (•). Results are expressed as mean fluid secretion rates in nl/min ± SEM., N=8.

C) The dose response curve for verapamil between 10^{-10} M and 10^{-3} M is expressed as percentage change of CAP_{2b}-stimulated fluid secretion rates ([maximal stimulated rates of CAP_{2b}-stimulated verapamil-treated samples/ maximal stimulated rates of CAP_{2b}-stimulated control samples] x 100%). (n=9-10 tubules per concentration).

(1D) The dose-response curve of nifedipine inhibition of CAP_{2b}-stimulated secretion. Data are expressed as in 1C. (n=9-10 tubules per concentration). In both 1C and 1D significant inhibition of CAP_{2b}-stimulated fluid secretion from samples lacking prior treatment with nifedipine or verapamil is denoted by *, *P<0.05, determined with the Student's *t*-test on unpaired samples assuming unequal variances.

4.4 CAP_{2b}-stimulated increase in $[Ca^{2+}]_i$ is sensitive to 'L'-type calcium channel antagonists.

CAP_{2b} is known to act obligatorily through entry of extracellular calcium (Rosay *et al*, 1997). If 'L'-type calcium channels contributed to calcium entry, we would also expect to see reduced $[Ca^{2+}]_i$ upon CAP_{2b} stimulation in the presence of nifedipine or verapamil. Indeed, the CAP_{2b} stimulated $[Ca^{2+}]_i$ increase in principal cells of c42-aeq tubules is modulated by both verapamil and nifedipine. Although it is reported later that CAP_{2b} evokes a biphasic rise in $[Ca^{2+}]_i$ (see chapter 5), here we examined only the initial rise, as the secondary rise was not apparent at the time of these experiments. With respect to verapamil, inhibition of the CAP_{2b}-induced calcium signal mirrors that of the fluid secretion response (Figure 4.1C). Verapamil significantly reduces the CAP_{2b}-induced calcium response over a similar concentration range that inhibits fluid transport, between 10^{-5} M and 10^{-3} M, and again at 10^{-7} M. Maximal inhibition occurs at 10^{-3} M verapamil (Figure 4.2). Although the verapamil dose-response curves for fluid secretion and calcium are complex their agreement is near perfect; this implies that all the effects of verapamil on fluid secretion can be ascribed to effects on intracellular calcium signalling.

By contrast, the relationship between fluid secretion and calcium dose-response curves for nifedipine is more complex. Indeed, there was even some disagreement in the dose-response curves of nifedipine when the experiments were repeated a year apart. Originally, when these experiments were first performed (work with Claire O'Connell), the CAP_{2b}-induced $[Ca^{2+}]_i$ was inhibited at nifedipine concentrations of 10^{-7} M to 10^{-10} M with maximal inhibition at 10^{-9} M (figure 4.3A). These experiments were repeated by others at the time with similar results. However, when these experiments were repeated more recently,

nifedipine did not show the U-shaped dose-response curve previously obtained, but showed inhibition at concentrations 10^{-3} M to 10^{-4} M and again at 10^{-7} M (Figure 4.3B). In both circumstances these experiments were repeated and carried out alongside fluid secretion experiments using the same solutions of nifedipine (which continued to show the same original dose-response curve). Therefore, the difference in results can only be attributed to unknown factors. It is possible that there was a change in the Schneider's solution used or an as yet unidentified environmental factor or possibly a change in the flies themselves. Both sets of results have been shown (Figure 4.3A and B).

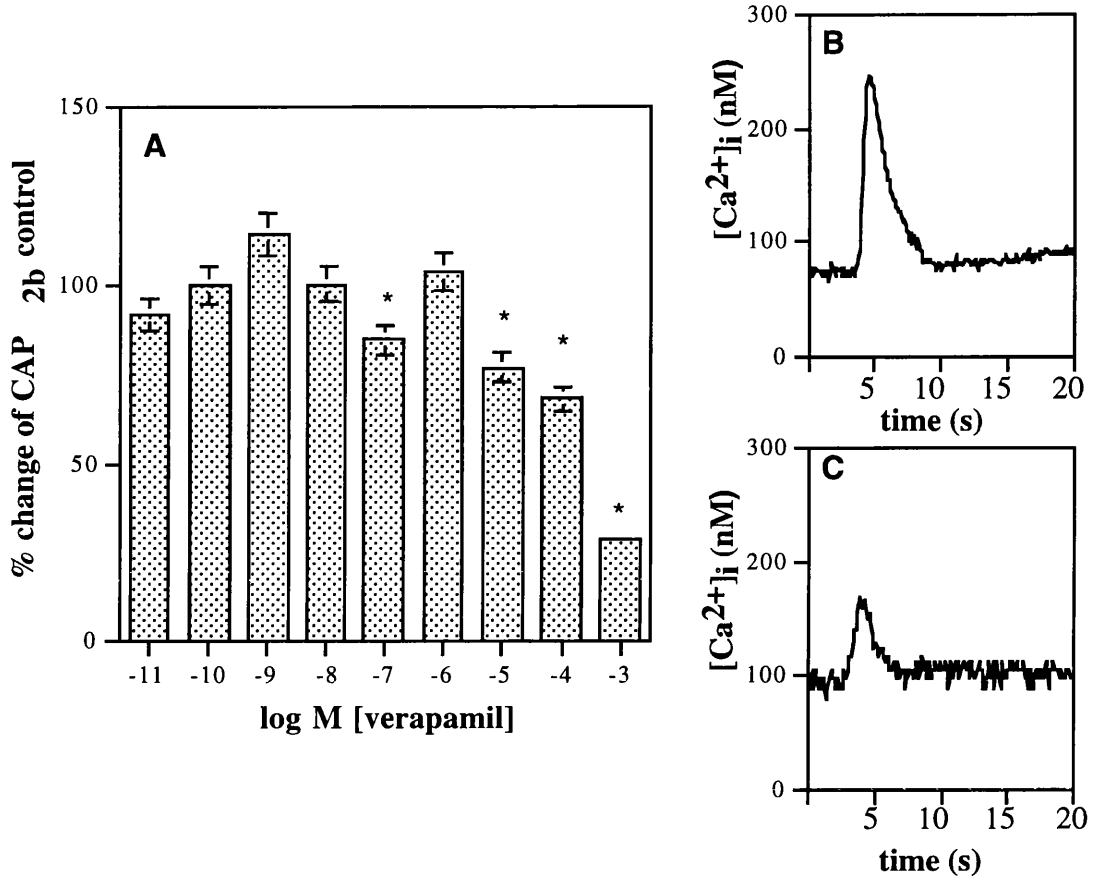

Figure 4.2: CAP_{2b}-stimulated increase in $[Ca^{2+}]_i$ in principal cells is inhibited by verapamil.

A) Dose-response curve for effects of verapamil on $[Ca^{2+}]_i$. For these aequorin experiments, $[Ca^{2+}]_i$ values were calculated as the difference in $[Ca^{2+}]_i$ (nM) between CAP_{2b}-stimulated peaks and the average resting levels over the time period before stimulation for each sample. These experiments were performed using c42-aeq tubules. Results are expressed as % ratio of these $[Ca^{2+}]_i$ (nM) values between CAP_{2b}-stimulated antagonist-treated: untreated samples (N=8 per sample). Significant inhibition of CAP_{2b}-stimulated $[Ca^{2+}]_i$ rise, from control samples lacking prior verapamil treatment is denoted by *. *P<0.05 determined with the Student's *t*-test, on unpaired samples assuming unequal variances.

B) Typical trace of $[Ca^{2+}]_i$ change in c42-aeq upon stimulation with 10^{-7} M CAP_{2b}.

C) Typical trace of $[Ca^{2+}]_i$ change in c42-aeq upon stimulation with 10^{-7} M CAP_{2b}; prior treatment with 10^{-3} M verapamil.

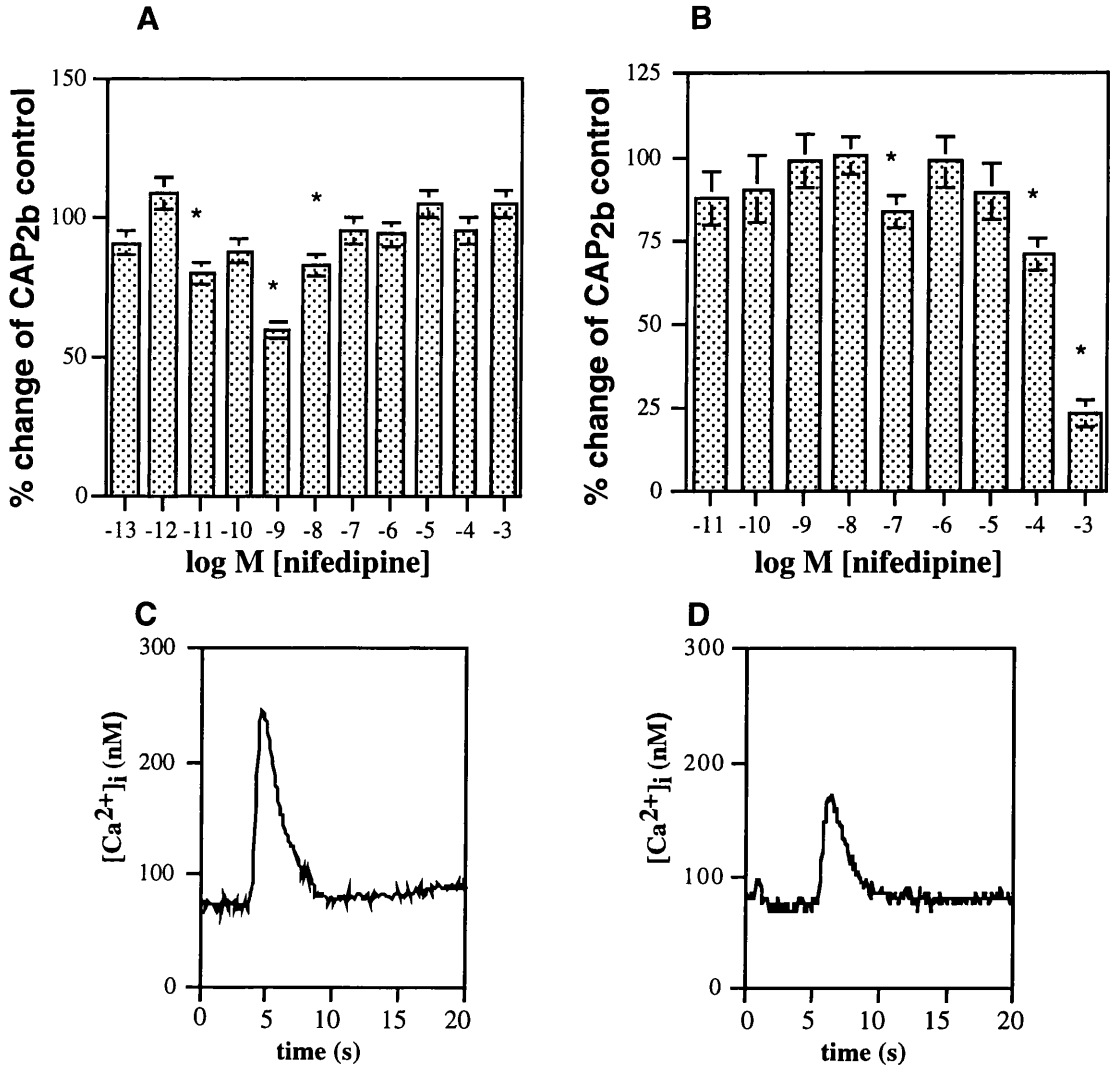

Figure 4.3: The effect of nifedipine on CAP_{2b}-stimulated rises in $[Ca^{2+}]_i$.

Dose-response curves for effect of nifedipine on $[Ca^{2+}]_i$. These experiments were performed using c42-aeq tubules. Results are expressed as in the previous figure. A and B show the results of the same set of experiments carried out at different times (N=8 for all samples). Both sets of results were duplicated at the time for verification where the observed effects were confirmed. Significant inhibition of the CAP_{2b}-stimulated calcium response from samples lacking prior nifedipine treatment is denoted by *. *P<0.05 determined with the Student's *t*-test, on unpaired samples assuming unequal variances. C shows a typical trace of $[Ca^{2+}]_i$ change upon stimulation with CAP_{2b}. D shows a typical trace of $[Ca^{2+}]_i$ change upon stimulation with CAP_{2b} following prior treatment with 10-9 M nifedipine (corresponding with the results in 4.3A).

4.5 cGMP-stimulated increase in $[Ca^{2+}]_i$ in principal cells requires calcium entry.

It has been previously demonstrated that calcium entry is essential for CAP_{2b}- and thapsigargin-stimulated $[Ca^{2+}]_i$ responses in principal cells (Rosay *et al*, 1997). Although cGMP is downstream of Ca^{2+} in the CAP_{2b} signalling cascade, it is theoretically possible that there may be cross talk between these two messengers. Although cGMP is usually thought of as cell impermeable, it has been shown to cause a rise in fluid secretion that is abolished in the presence of agents known to block organic anion transporters (OATPs) (Dow *et al*, 1994; Leah Torrie, personal communication). This, coupled with the expression of OATPs in tubules (Leah Torrie, personal communication) strongly suggests that cyclic nucleotides gain access to the cell via these transporters.

The effects of cGMP (10^{-4} M) on $[Ca^{2+}]_i$ were examined and it was found that cGMP induces a slow, sustained increase in $[Ca^{2+}]_i$ (Figure 4.4A), and that this increase is dependent on a calcium-entry process (figure 4.4B). As the cGMP-induced $[Ca^{2+}]_i$ signal is abolished in the absence of extracellular calcium, it is probable that in this cell type, release of calcium from intracellular calcium stores does not contribute to cGMP-induced $[Ca^{2+}]_i$ increases.

4.6 cGMP-mediated calcium entry occurs via verapamil and nifedipine-sensitive calcium channels.

cGMP-stimulated epithelial transport is sensitive to verapamil and nifedipine (V. Pollock, personal communication). As CAP_{2b} stimulates a linear signalling pathway, acting through $[Ca^{2+}]_i$, NOS, NO, sGC, cGMP and cGK (Dow *et al*, 1994), downstream elements of this pathway might be expected to modulate $[Ca^{2+}]_i$. This

in turn, may contribute to a stimulation of fluid secretion that lasts much longer than the initial calcium peak. Therefore, the sensitivity of the cGMP-mediated calcium entry to verapmil and nifedipine at 10^{-3} M and 10^{-9} M respectively was examined. Figure 4.5 shows that, both verapamil and nifedipine pre-treatment completely abolishes the cGMP-induced $[Ca^{2+}]_i$ signal but that cGMP-stimulated. However, fluid secretion is only partially reduced by these calcium channel antagonists (V. Pollock, personal communication), suggesting that the cGMP-induced increase in $[Ca^{2+}]_i$ is not the only contributary signal to stimulated fluid transport.

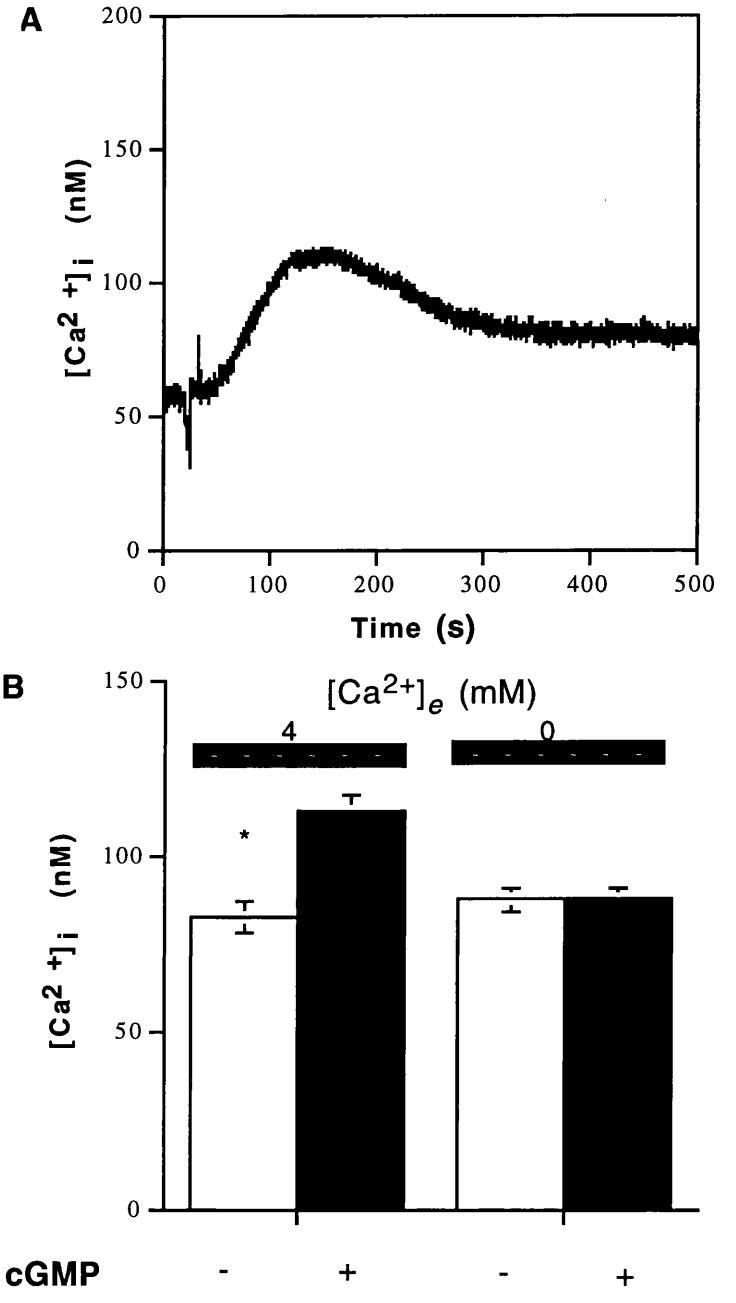

Figure 4.4: cGMP-stimulates an increase in $[Ca^{2+}]_i$ in principal cells via calcium entry.

(A) Typical trace of cGMP-induced $[Ca^{2+}]_i$ increase in tubule principal cells. These experiments were performed using c42-aeq tubules. Tubules were stimulated with 10^{-4} M cGMP and the samples were

monitored for a total of 500 s. Results shown are representative of at least 14 similar traces and are expressed as nM $[Ca^{2+}]_i$ against time.

(B) Pooled nM $[Ca^{2+}]_i$ values of cGMP-induced peaks in the presence and absence of $[Ca^{2+}]_e$ from experiments described in 5A. Tubules were washed extensively (>3x) in Ca^{2+}-free Schneider's medium, thus reducing the extracellular Ca2+ concentration ($[Ca^{2+}]_e$) from 4 mM to approximately 0 mM. Tubules were then incubated in Ca^{2+}-free Schneider's medium and stimulated with 10^{-4} M cGMP. Resting (unstimulated) levels $[Ca^{2+}]_i$ (open bars) = 83 ± 4.2 nM (n=14) in 4 mM $[Ca^{2+}]_e$; 88 ± 3.3 nM (n=9) in the absence of $[Ca^{2+}]_e$. cGMP-stimulated $[Ca^{2+}]_i$ (shaded bars) = 113 ± 4.6 nM (n=14) in 4 mM $[Ca^{2+}]_e$; 88 ± 3.2 nM (n=9) in the absence of $[Ca^{2+}]_e$. A significant rise in $[Ca^{2+}]_i$ following application of cGMP is denoted by *. *P<0.05 determined with the Student's *t*-test, on unpaired samples assuming unequal variances.

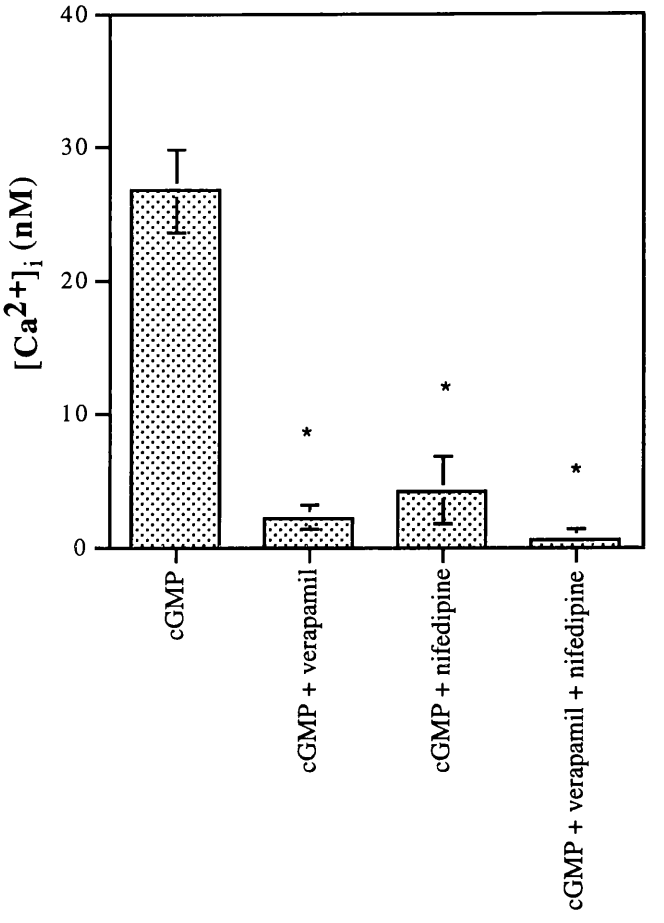

Figure 4.5: cGMP-induced $[Ca^{2+}]_i$ increase is verapamil- and nifedipine-sensitive.

c42-aeq-tubules were pre-treated with verapamil (10^{-3} M) or nifedipine (10^{-9} M) prior to stimulation by 10^{-4} M cGMP. Data are expressed in $[Ca^{2+}]_i$ (nM) ± SEM values of cGMP-induced rise in $[Ca^{2+}]_i$ minus average resting $[Ca^{2+}]_i$ for each sample (n=21, cGMP only, n=7-10 cGMP + inhibitor(s)). Significant inhibition of the cGMP-induced $[Ca^{2+}]_i$ rise by verapamil or nifedipine is denoted by *. *P<0.05 determined with the Student's *t*-test, on unpaired samples assuming unequal variances.

4.7 Co-localisation of verapamil binding and α1 subunits in the tubule; differential binding of DHP to tubule sub-regions.

To examine the sites of sensitivity to verapamil and nifedipine, fluorescent-labelled phenylalkylamine, verapamil, and dihydropyridine were applied to tubules at various concentrations used previously by others (Lelong *et al*, 1991; Knaus *et al*, 1992; Robitaille *et al*, 1996; Vallee *et al*, 1997) (Figure 4.6). Fluorescent-labelled phenylalkylamine at low concentration (10 nM) binds to the basolateral membrane in only principal cells in the main segment of the tubule (Figure 4.6A). The same concentration of verapamil also binds to the basolateral membrane of the main segment principal cells (Figure 4.6B). However, use of verapamil at a concentration which inhibits CAP_{2b}-induced increases in fluid secretion and $[Ca^{2+}]_i$ (10^{-4} M), shows punctate staining of the basolateral membrane, with diffuse, non-specific staining at the apical surface (Figure 4.6C). These data strongly suggest that there are multiple targets for verapamil in tubules. Verapamil is known to act as a substrate for P-glycoprotein and in order to discern binding of fluorescent-labelled verapmil to P-glycoprotein, the binding of a fluorescently-labelled P-glycoprotein substrate, BODIPY-vinblastine was examined. It was found that vinblastine had a distinct binding pattern from verapamil. Figure 4.6D shows that vinblastine binds only in the initial segment of the anterior tubule. It is thus reasonable to assume that verapamil is accurately labelling L-type channels in the main segment.

Immunocytochemistry using an anti-pan α1 antibody, carried out by Kate Broderick, suggest that α1 subunits are located on the basolateral surface of principal cells (Figure 4.8). Also, it can be seen that there is significant signal at the apical surface; the large globular structures may be due to membrane blebbing; this may suggest that a different class of α1 subunit may be located on

apical surface microvilli. These results correlate well with those showing the binding of fluorescent-labelled phenylalkylamine and verapamil.

The localisation of BODIPY-nifedipine was also examined. It did not correlate with either verapamil binding or α1 subunit localisation, and showed clear apical binding in the initial segment of the anterior tubule (Figure 4.7A) (similar to that observed for BODIPY-vinblastine), known to be a major calcium transporting region (Dube *et al*, 2000). BODIPY-nifedipine binding was also seen in principal cells in the main segment (Figure 4.7B), where most fluorescence was observed to be perinuclear, with some staining observed in lateral membranes. Thus, DHPs may have a role in transepithelial calcium transport in *Drosophila* tubules; however, this calcium transport process is distinct from, and does not overlap with, calcium signalling processes in the main segment induced by CAP_{2b}, or indeed, cGMP.

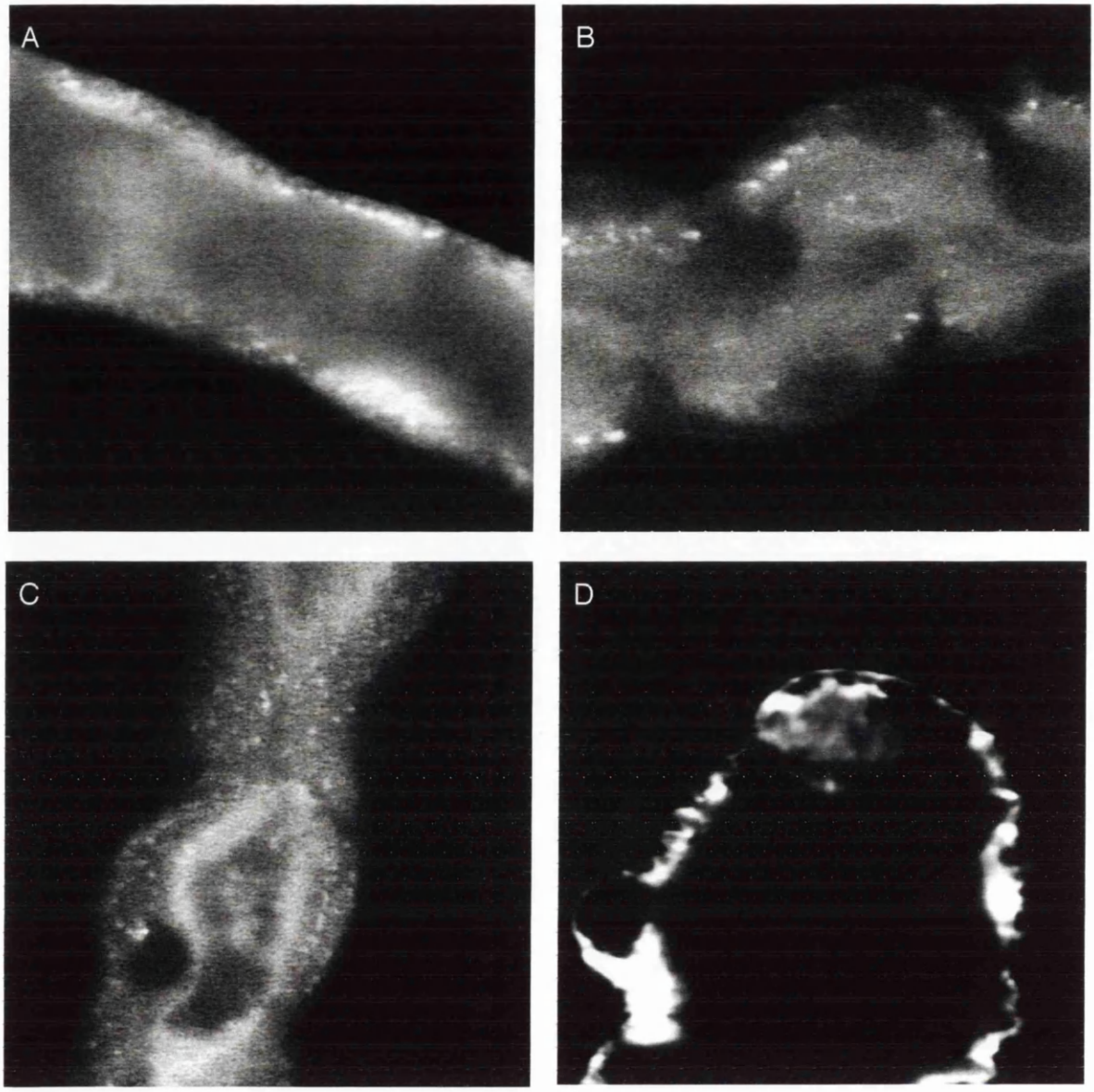

Figure 4.6: Phenylalkylamine and verapamil bind to basolateral membranes in tubule main segment.

Grren fluorescent phenylalkylamine, BODIPY-FL PAA, (Panel A) and verapamil, BODIPY-FL verapamil, (Panels B and C), binding in unfixed whole tubule preparations were observed by confocal microscopy. Panel A shows basolateral binding of phenylalkylamine (10 nM) to only principal cells in the main segment. Panel B shows 10 nM verapamil binding to basolateral membranes of main segment principal cells. When the concentration of verapamil is increased to 100 mM (Panel C), in addition to punctate basolateral staining, there is significant apical brush-border membrane staining seen. In

order to determine if verapamil binding in the tubules was due to binding to P-glycoprotein, binding of a specific P-glycoprotein substrate, vinblastine (BODIPY-FL vinblastine) was assessed. using 100 nM BODIPY-vinblastine, P-glycoprotein is localised only to the initial segment (Panel D), suggesting that BODDIPY-verapamil staining in the main segment is not due to the binding of verapamil to P-glycoprotein.

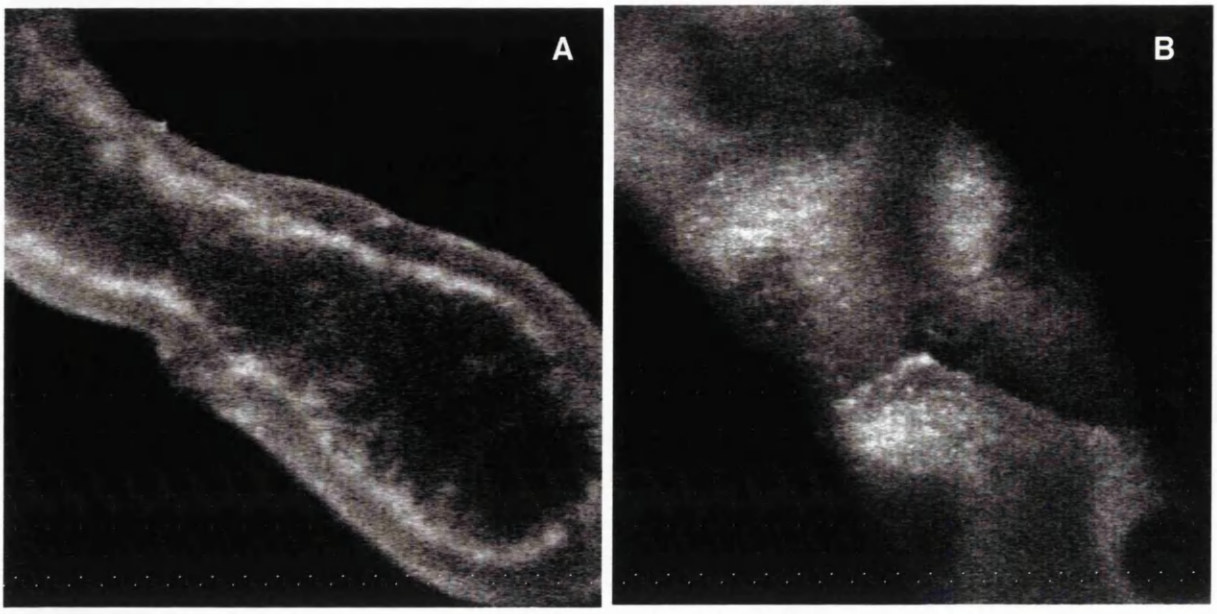

Figure 4.7: Nifedipine binds to tubule initial and main segments.

Confocal microscopy of unfixed tubule preparations, using fluorescent nifedipine (BODIPY-DHP). High affinity BODIPY-DHP was used at 100 nM (Panel A). Confocal image of anterior tubule initial segment shows clear apical localisation of DHP binding. DHP also binds to principal cells in the main segment. At 100 nM low affinity DHP (Panel B), perinuclear staining is observed; lateral staining of principal cell membranes is also seen.

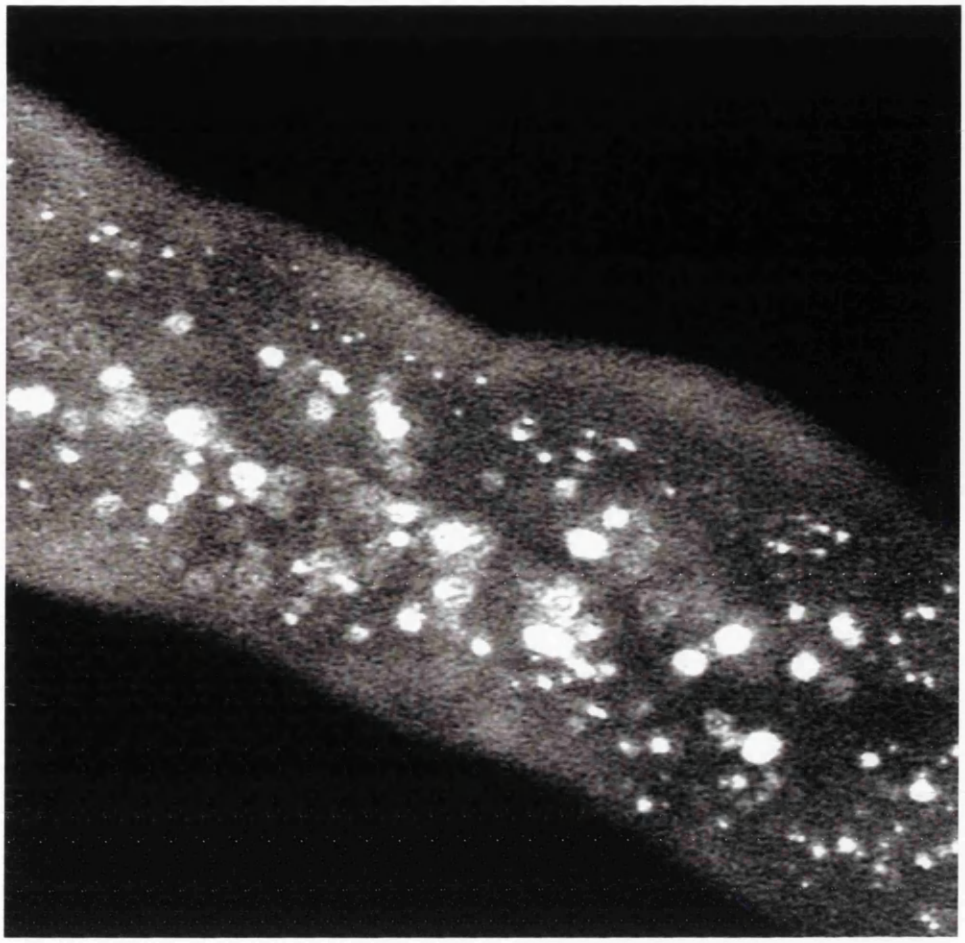

Figure 4.8: Immunocytochemical localisation of α1 subunits.

An anti-pan α1 subunit antibody (Alomone labs) was used to localise α1 subunits in tubules. This epitope, specific to all α1 subunits, is located between domain IV and the C-terminus which is conserved between all species. The peptide sequence used to raise the anti-sera [(C)DNFDYLTRDWSILGPHHLD] has 100% identity with *Dmca1D* and 89% identity with *Dmca1A.* in both *Dmca1A* and *Dmca1D.* Confocal microscopy of immuno-stained whole mount tubules reveals punctate staining in basolateral membranes of the main segment. There is also significant fluorescence observed in apical membranes; the non-distinct nature of these fluorescent patches may be due to membrane blebbing during fixation, which obscure defined localisation of α1 subunits in apical microvilli.

4.8 Discussion

The experiments presented in this chapter have demonstrated a role for phenylalkylamine- (PAA) and dihydropyridine- (DHP) sensitive calcium channels in both epithelial fluid transport and CAP_{2b} or cGMP-stimulated rises in $[Ca^{2+}]_i$. Furthermore it has been shown that cGMP stimulates an influx of external calcium through PAA- and DHP-sensitive calcium channels.

The presence of *DmcaID* and *DmcaIA* transcripts was demonstrated in tubules (chapter 3), and so using a pharmacological apprach, a possible role for these channels was investigated. The effects of the calcium channel antagonists verapamil and nifedipine were examined on both fluid secretion and calcium signalling. DmcaID has a highly conserved PAA-binding site and a mutation in the gene has been shown to be associated with the loss of a dihydropyridine-sensitive current in *Drosophila* larva muscle (Ren *et al*, 1998). Therefore it is postulated to be both sensitive to PAA's and DHP's. DmcaIA has a highly conserved PAA binding site and a poorly conserved DHP binding site and so is presumed to be PAA sensitive and DHP insensitive. Indeed the most frequently observed Ca^{2+} channel in reconstituted membranes from *Drosophila* head was extremely PAA-sensitive and DHP-insensitive and may therefore be attributable to DmcaIA. Certainly our data indicates the presence of PAA-sensitive calcium channels in the tubules. From our data it appears that both verapamil (a PAA) and nifedipine (a DHP) have a dramatic effect on fluid secretion. Indeed at 10 mM verapamil inhibits fluid secretion completely, with profound inhibition of CAP_{2b}-stimulated fluid secretion rates between 10^{-3} M and 10^{-5} M. Similar results are observed when the inhibition of CAP_{2b}-stimulated rises in $[Ca^{2+}]_i$ are examined. If one compares figures 4.1C and 4.2, the inhibition of fluid secretion matches closely with that of CAP_{2b}-sitmulated $[Ca^{2+}]_i$ rises, indicating that the effect on fluid secretion is mainly attributable to an attenuated calcium signal.

The effect on calcium signalling of these calcium channel antagonists can be, at present, ascribed to either Dmca1A and Dmca1D, as a search of the *Drosophila* genome found only one other possible voltage-gated calcium channel, CG1517. This channel was not to be expressed in tubules (chapter 3). In support of the effect of verapamil on CAP_{2b} signalling in the principal cells, binding of fluorescently labelled PAA was observed on the basolateral membranes of principal cells in the main segment (Figure 4.6A) at concentrations of both 10 nM and 1 μM. Similar staining is observed using fluorescently labelled verapamil but in addition to the punctate basolateral staining there is also significant apical brush-border staining. Immunocytocemical staining indicates the presence of α1 calcium channel subunits in apical membranes of principal cells. Taken together, this suggests the presence of PAA-sensitive channels, on both the apical and basolateral membranes of the main segment principal cells, that contribute to CAP_{2b}-induced calcium influxes. The presence of PAA-sensitive binding sites in the tubule is supported by a study by Dube *et al*, 2000, where verapamil at 10^{-3} M retarded transepithelial Ca^{2+} transport.

The results concerning the inhibition of fluid secretion and CAP_{2b}-induced calcium influx by nifedipine do not match each other quite as well. Like verapamil, nifedipine causes major inhibition of stimulated fluid secretion albeit at concentrations between 10^{-7} and 10^{-10} M. However, the inhibition of the CAP_{2b} signal in figure 4.3A is at best 66% of normal at 10^{-9} M, and the more recent results shown in figure 4.3B only show significant inhibition at 10^{-3}, 10^{-4}, and 10^{-7} M. From these results it appears that the effect of nifedipine on fluid secretion is not wholly attributable to the attenuated CAP_{2b}-induced calcium signals. It appears that there is further inhibition of stimulated fluid secretion through another route. Certainly the staining of fluorescently labelled nifedipine is not confined to the membranes of the main segment principal

cells, but includes perinuclear staining in these cells and also apical membrane staining in the initial segment of anterior tubules. The presence of DHP binding sites in the initial segment is important as this tubule region is the main site of calcium storage in *Drosophila* and is the major calcium transporting region (Dube *et al*, 2000; Dube *et al*, 2000a). It may be that the attenuation in fluid secretion and CAP_{2b}-stimulated $[Ca^{2+}]_i$ rises is due to the blockade of calcium secretion into the lumen of the tubule and so reduces influx through calcium channels on the apical membrane.

Experiments described here also demonstrate the presence of a cGMP-stimulated calcium influx pathway. CAP_{2b} is known to stimulate an increase in cGMP levels through the stimulation of DNOS by an increase in $[Ca^{2+}]_i$. Therefore it was thought that cGMP may have a feedback effect on calcium signalling events. Here cGMP stimulates a long slow rise in $[Ca^{2+}]_i$ (Figure 4.4A) due to the influx of external calcium. As the immunocytochemical staining of $\alpha 1$ calcium channel subunits and nifedipine differs, the difference of nifedipine staining in the principal cells (lateral membrane and perinuclear staining) could be attributed to cyclic nucleotide channels, which have been shown to be expressed in the tubules (MacPherson *et al*, 2001). It has been demonstrated in B lymphocytes that cGMP mediates calcium entry through dihydropyridine-sensitive channels (Sadighi Akha *et al*, 1996). Another possibility is the stimulation of cGMP-dependent kinases that effect calcium channels. The presence of such protein kinases has been demonstrated in the tubules (Dow *et al*, 1994) and is currently being further investigated in our lab. The postulated cellular locations of these channels and associated pharmacological sensitivities in the tubule principal cell are shown in figure 4.9.

Further work studying voltage-gated calcium channel in the tubule would include a thorough investigation of mutants in both *Dmca1D* and *Dmca1A*.

Mutants are available for these genes (Eberl *et al*, 1998; Peixoto *et al*, 1997), however, most *Dmca1D* mutants are embryonic lethal and so studies of tubule function would be impossible. *Dmca1A*, on the other hand, has several viable mutants available for study. Although studies of fluid secretion would be as straightforward as for any other mutants, calcium signalling studies would be complicated by *Dmca1A*'s location on the X-chromosome. Another method of looking at the gene disruption of these two genes would be to use antisense oligonucleotides complementary to the *Dmca1D* and *Dmca1A* sequences. Such a method has been used effectively in mouse distal convoluted cells (Barry *et al*, 1998) where the antisense oligonucleotides complementary to the α1C calcium channel subunit inhibited the rises in $[Ca^{2+}]_i$ induced by thiazide diuretic. Also, the effects of the L-type calcium channel agonist, BAYK 8644 (which increases the open probability of L-type channels) could be examined. Indeed an effect of this agonist has already been shown in epithelial cells in rabbit proximal tubules (Zhang *et al*, 1996).

Overall, results described in this chapter demonstrate the involvement of PAA- and DHP-sensitive calcium channels in epithelial fluid transport and CAP_{2b} stimulated $[Ca^{2+}]_i$ rises. It also shows that cGMP stimulates a prolonged rise in $[Ca^{2+}]_i$ via influx of external calcium, through nifedipine- and verapamil-sensitive channels in main segment principal cells. Together with the following chapters, investigating the functioning of TRP and TRPL channels, these studies aim to define the role of plasma-membrane calcium channels in stimulated Ca^{2+} signalling and fluid transport.

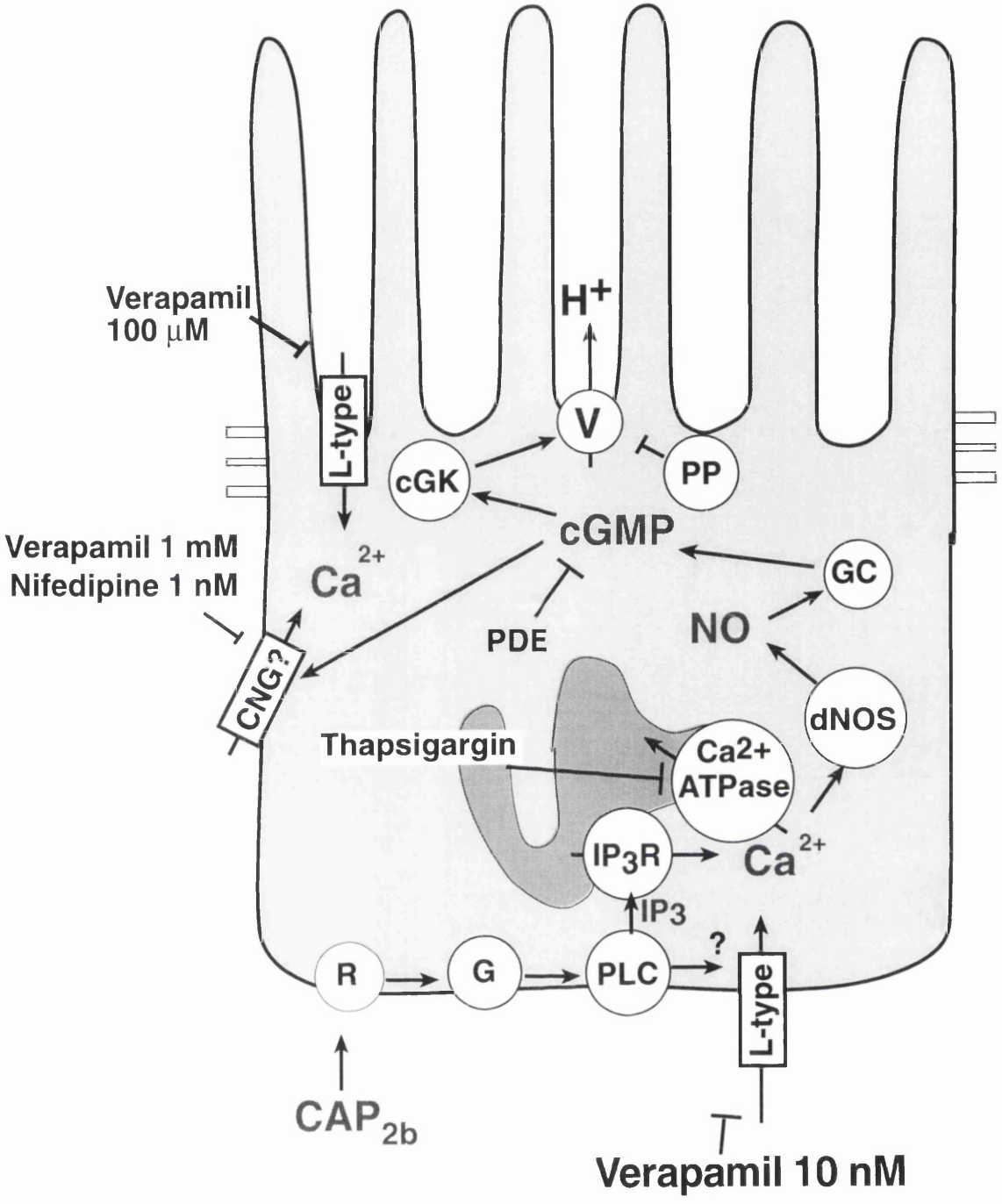

Figure legend overleaf

Figure 4.9: Working model for calcium signalling pathyways in the tubule principal cell and postulated position of L-type and CNG calcium channels.

In principal cells CAP_{2b} acts on a G-protein coupled receptor (inferred) to activate PLC; $InsP_3$ receptor, and hence IP3, are known to be necessary for CAP_{2b} action (Pollock, Davies, Hasan and Dow, in preparation). Release from internal stores is too small to measure under calcium-free conditions implying that Ca^{2+} entry is essential. Basolateral, verapamil-sensitive channels (possibly *DmcalA*) contribute to this calcium entry. Calcium is returned to store by a thapsigargin-sensitive Ca^{2+}-ATPase. Downstream, the CAP_{2b}-induced $[Ca^{2+}]_i$ signal activates DNOS, raising NO and acting on guanylate cyclase to raise cGMP. cGMP acts on cGK to activate an apical V-ATPase. cGMP also acts on a plasma-membrane nifedipine and verapamil-sensitive channel (CNG?) to raise intracellular calcium in the longer term so providing feedback modulation. [Figure taken from MacPherson, Pollock, Broderick, Kean, O'Connell, Dow and Davies. 2001. L-type calcium channels regulate epithelial fluid transport in *Drosophila melanogaster*. *Am. J. Physiol. Cell. Physiol.* 280.]

Chapter 5

Analysis of trp and trpl mutations in Malpighian tubules

Chapter 5

5.1 Summary

This chapter examines the function of TRP and TRPL calcium channels in Ca^{2+} signalling mechanisms and epithelial transport. As previously discussed, CAP_{2b} elicits a biphasic rise in $[Ca^{2+}]_i$, exclusively in principal cells. This response is dependent on extracellular calcium. Thapsigargin also stimulates an increase in $[Ca^{2+}]_i$ in principal cells, via the influx of extracellular calcium (see introduction). Following the discovery of *trp* and *trpl* expression in tubules (section 3.4), four different mutant lines (trp^{cm}, trp^{301}, $trpl^{302}$, and $trpl^{302};trp^{cm}$.) were examined for a transport phenotype in the tubule.

CAP_{2b}-stimulated fluid secretion was examined in the different mutants, where it was demonstrated that mutations in either *trp* or *trpl* attenuate the CAP_{2b} response. Immunocytochemistry with TRP and TRPL antibodies localised TRP to the principal cells of the main segment, and TRPL throughout the tubule. Western blot analysis of both wild type and mutant tubules showed no discernible difference in levels of TRP or TRPL expression. To examine the effect of *trp* and *trpl* mutations on CAP_{2b}- and thapsigargin-elicited rises in $[Ca^{2+}]_i$, a complex three-way cross was devised to unite the desired mutation with UAS:aequorin on the first chromosome and a hsGAL4 construct on either the second or third chromosome (see introduction). Expression of aequorin in the Malpighian tubule was activated following heat-shocking of the flies at 37°C for thirty minutes, thus allowing measurement of $[Ca^{2+}]_i$ in a mutant background.

Results from such experiments show that both trp^{cm} and $trpl^{302}$ mutations caused an attenuation of the CAP_{2b}-induced $[Ca^{2+}]_i$ rise. In contrast, the trp^{301} mutation caused a potentiation of the CAP_{2b}-induced $[Ca^{2+}]_i$ rise. The thapsigargin-induced $[Ca^{2+}]_i$ rise was not significantly different in either the trp^{cm} or $trpl^{302}$ tubules, but was potentiated in the trp^{301} tubules. Lanthanum is known to block

TRP channels *in vivo* at micromolar concentrations (Neimeyer *et al*, 1996). Therefore, to investigate the calcium channel components that contribute to calcium influx in wild type and *trp* or *trpl* tubules, the sensitivities to lanthanum of the CAP_{2b} calcium signal in the tubule principal cells were examined. The CAP_{2b}-induced $[Ca^{2+}]_i$ rises in trp^{301} and $trpl^{302}$ were found to be sensitive to lanthanum at 50 μM. However, both wild type and trp^{cm} were not significantly affected by lanthanum.

The effect of pharmocological blockade of TRPL using the lipoxygenase inhibitor, cinnamyl-3,4-dihydroxy-α-cyanocinnamate (CDC), upon fluid transport was investigated. At 50 μM, CDC activates a calcium influx through TRP and TRPL channels in photoreceptors and S2 cells (Chyb *et al*, 1999). Application of CDC at this concentration to wild-type tubules, resulted in the cessation of fluid secretion. Furthermore, 50 μM CDC elicited a prolonged increase in $[Ca^{2+}]_i$. However, at 5 μM, a concentration known to block TRPL channels (Chyb *et al*, 1999), there was no effect on either $[Ca^{2+}]_i$ or fluid secretion in wild-type tubules. The effects of 5μM CDC on fluid secretion in trp^{cm}, trp^{301}, $trpl^{302}$, and $trpl^{302};trp^{cm}$ tubules was examined. In trp^{cm} tubules 5 μM CDC caused a cessation of fluid secretion within thirty minutes of application. A similar effect was observed in the trp^{301} tubules, albeit to a lesser extent. There was no effect of 5 μM CDC when applied to $trpl^{302}$ and $trpl^{302};trp^{cm}$ tubules as might be expected if these mutants do not contain functional TRPL channels (to which CDC is an agonist).

Overall, this chapter demonstrates a role for TRP and TRPL calcium channels in calcium signalling and fluid transport, and suggests that a major role is played by the TRPL channel.

5.2 Introduction

The transient receptor potential (*trp*) gene was first discovered in a screen for mutations that led abnormal electroretinograms in *Drosophila* photoreceptors (Cosens and Manning, 1969). The original *trp* mutation resulted in visually defective flies whose photoreceptors could not sustain a response to bright light. The *trp* gene codes for a calcium channel consisting of six transmembrane domains and a long carboxy terminal region thought to confer store-operated sensitivity (Sinkins *et al*, 1996). It was also found to be sensitive to micromolar concentrations of lanthanides. *trpl* was originally cloned due to its calmodulin-binding properties, and encodes a calcium channel with 40% identity to the TRP protein (Philips *et al*, 1992), but lacks the long carboxy terminal domain present in TRP. It is insensitive to lanthanides at micromolar concentrations.

In *Drosophila* photoreceptors these two channels make up the light-activated conductance (Niemeyer *et al*, 1996) with the possible involvement of the recently discovered TRPγ channel (Xu *et al*, 2000). As was shown in the previous chapter *trp, trpl,* and *trpγ* are all expressed in *Drosophila* tubules; thus we set out to investigate the involvement of these channels in agonist-stimulated calcium responses in the tubule using trp^{cm}, trp^{301}, $trpl^{302}$ mutant flies. trp^{cm} is a temperature-sensitive mutation where flies reared at 18°C have wild-type TRP expression levels and behave as wild-type; when reared at 25 °C they are visually defective and express TRP at less than 5% of normal levels (Minke, 1983). trp^{301} is a mutation that reduces TRP expression to less than 5 % of wild type levels (Neimeyer *et al*, 1996). The mutations in both these alleles lie outside the open reading frame but neither of these mutations have been molecularly characterised. The $trpl^{302}$ allele has an amber nonsense codon at amino acid 302, resulting in premature termination of the polypeptide chain before the first

transmembrane segment, and represents a complete null allele (Neimeyer *et al*, 1996).

Cardioaccelatory peptide 2b (CAP_{2b}), is one of a family of neuropeptides so named due to its effect on *Manduca sexta* heart (Tublitz *et al*, 1992). It elicits a biphasic rise in $[Ca^{2+}]_i$ exclusively in the principal cell of the Malpighian tubule via calcium entry (Kean *et al*, submitted; Rosay *et al*, 1997), and increases fluid secretion rates via activation of the nitric oxide/cGMP signalling pathway (Davies *et al*, 1995; Davies *et al*, 1997). One of the aims of the work described in this chapter is to examine the role of TRP and TRPL channels in CAP_{2b}-stimulated influxes of calcium and increases in fluid secretion rate.

Thapsigargin is known to directly activate TRP channels and indirectly activate TRPL channels in cell expression studies (see introduction) (Vaca *et al*, 1994; Estacion *et al*, 1999). Direct activation by thapsigargin-induced calcium store depletion of TRP channels suggests that they may be putative store-operated channels (SOCs). Thapsigargin has been demonstrated to induce a prolonged rise in $[Ca^{2+}]_i$ in the principal cells of Malpighian tubules via the influx of extracellular calcium (Rosay, *et al*, 1997). Here, through the use of mutants and pharmacological intervention we investigate the involvement of TRP and TRPL channels in the thapsigargin-induced calcium influx in main segment principal cells.

The effects of CDC on $[Ca^{2+}]_i$ and fluid secretion were examined. CDC is a lipoxygenase inhibitor which when applied to cells leads to the build up of polyunsaturated fatty acids (PUFA's) in human aortic endothelial cells (Honda *et al*, 1999). PUFA's are produced in normal cell metabolism through the breakdown of diacyl glycerol (DAG). Therefore, in effect, CDC causes modulation of the DAG signalling pathway. However, CDC has also been shown to block TRPL channels at micromolar concentrations (Chyb *et al*, 2000). We examined both the effect of CDC

at concentrations known to stimulate the DAG signalling pathway (50 μM) and also at concentrations known to inhibit TRPL channel activity (5 μM).

5.3 The effect of mutations in the *trp* and *trpl* genes on CAP_{2b}-stimulated fluid secretion.

[This work was carried out by Miss Valerie Pollock, and has been included to describe the epithelial phenotype in these mutants. These results are comparable with those in figure 5.7, where similar experiments were performed with aequorin expressing *trp* and *trpl* mutants.]

The CAP_{2b}-stimulated rise in fluid secretion was examined in trp^{cm}, trp^{301}, $trpl^{302}$, and $trpl^{302}$;trp^{cm} mutants. The fluid secretion rate was measured for thirty minutes before CAP_{2b}, to a final concentration of 10^{-7}M, was added to the bathing solution, and the fluid secretion rate measured for a further thirty minutes. Figure 5.1 shows the results of fluid secretion assays on trp^{cm}, trp^{301}, $trpl^{302}$, $trpl^{302}$; trp^{cm} with appropriate OreR controls. Due to variance in the basal fluid secretion rates of Malpighian tubules, the percentage rise in fluid secretion rate compared to basal was taken as the most fitting and consistent measurement of the efficacy of CAP_{2b}. This value was calculated as shown below.

Percentage change=max. stimulated rate/average basal rate x 100.

Where max. stimulated rate is the maximum fluid secretion rate recorded post-CAP_{2b} stimulation and average basal rate is an average of the measurements taken prior to CAP_{2b} stimulation (Figure 5.1).

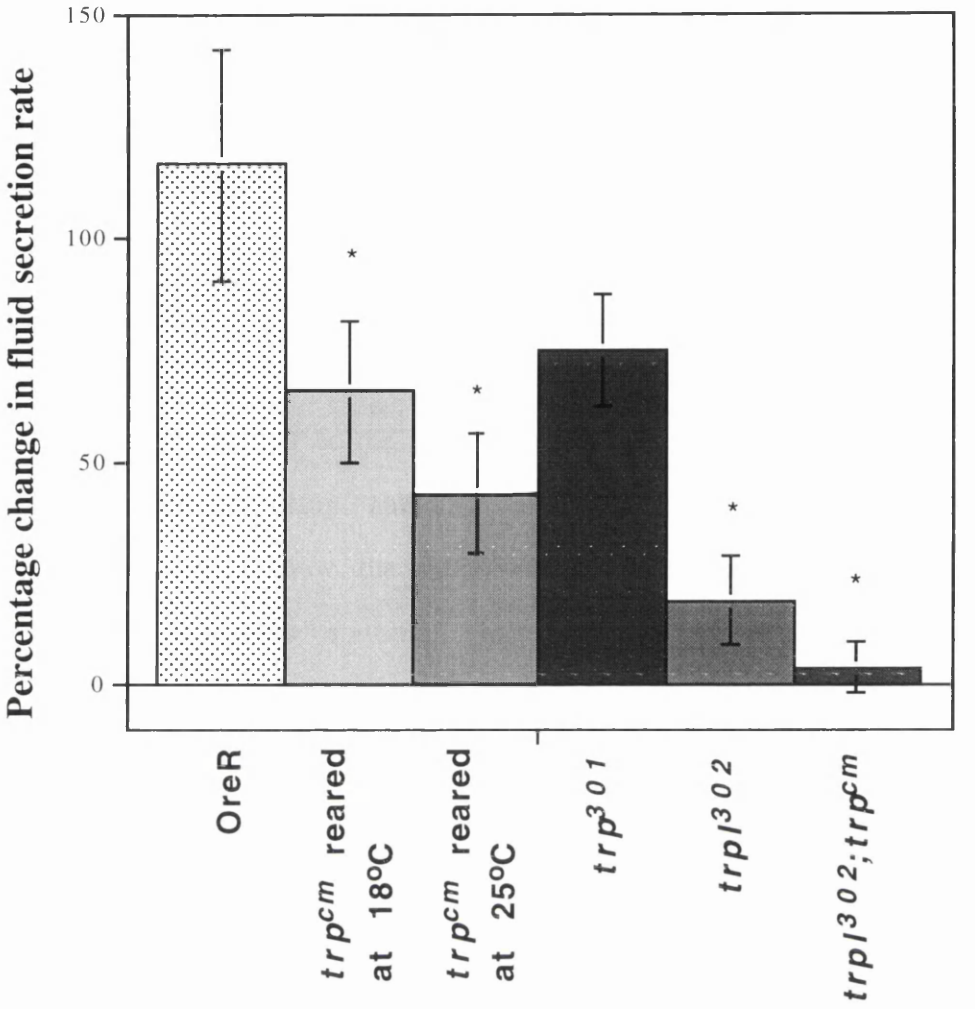

Figure 5.1: CAP_{2b}-stimulated fluid secretion is attenuated in *trp* and *trpl* mutants.

Basal rates of fluid secretion were measured for 30 minutes before stimulation with CAP_{2b} (10^{-7} M). Fluid secretion rates were then measured for a further 30 minutes.

Data are expressed as mean ± SEM., N=8. Percentage change of fluid secretion rate is as defined in the text. Significant difference of the CAP2b-stimulated rise in fluid secretion rate from that observed in OreR tubules is denoted by *. *P<0.05 determined with the Student's *t*-test, on unpaired samples assuming unequal variances.

5.4 Localisation of TRP and TRPL in Malpighian tubules.

Using antibodies specific for TRP and TRPL the cellular distribution of both TRP and TRPL proteins was examined in tubules. The anti-TRP antibody was a kind gift from Charles Zucker, University of California, USA, and the anti-TRPL antibody was a kind gift from Craig Montell, The John Hopkins University Baltimore, USA. Results obtained using the anti-TRP antibody are shown in figure 5.2 and show the localisation of TRP to the principal cells of the main segment. These results were also obtained using anti-TRP antibody (gift from R.C.Hardie, Cambridge). Figures 5.2A and B show the main/initial and main/lower segment boundaries respectively, and show staining exclusively in the main segment of the tubule. Figure 5.2C shows the localisation of TRP to the principal cells and demonstrates lack of staining the stellate cells in the main segment. The results obtained using the anti-TRPL antibody are shown in figure 5.3. Here, staining was observed throughout the tubule. Figures A, B and C show the main, initial, and lower segments of the tubule respectively. As can be seen most clearly in 5.3A the staining is confined to the principal cells, and furthermore to both the apical and basolateral membranes. There is also some staining within both the nucleus and cytoplasm as well as around the nuclear membrane. It is not known if some of this is due to non-specific binding of the TRPL antibody. Non-specific binding of the secondary antibody can be ruled out as controls lacking primary antibody showed no signal at all.

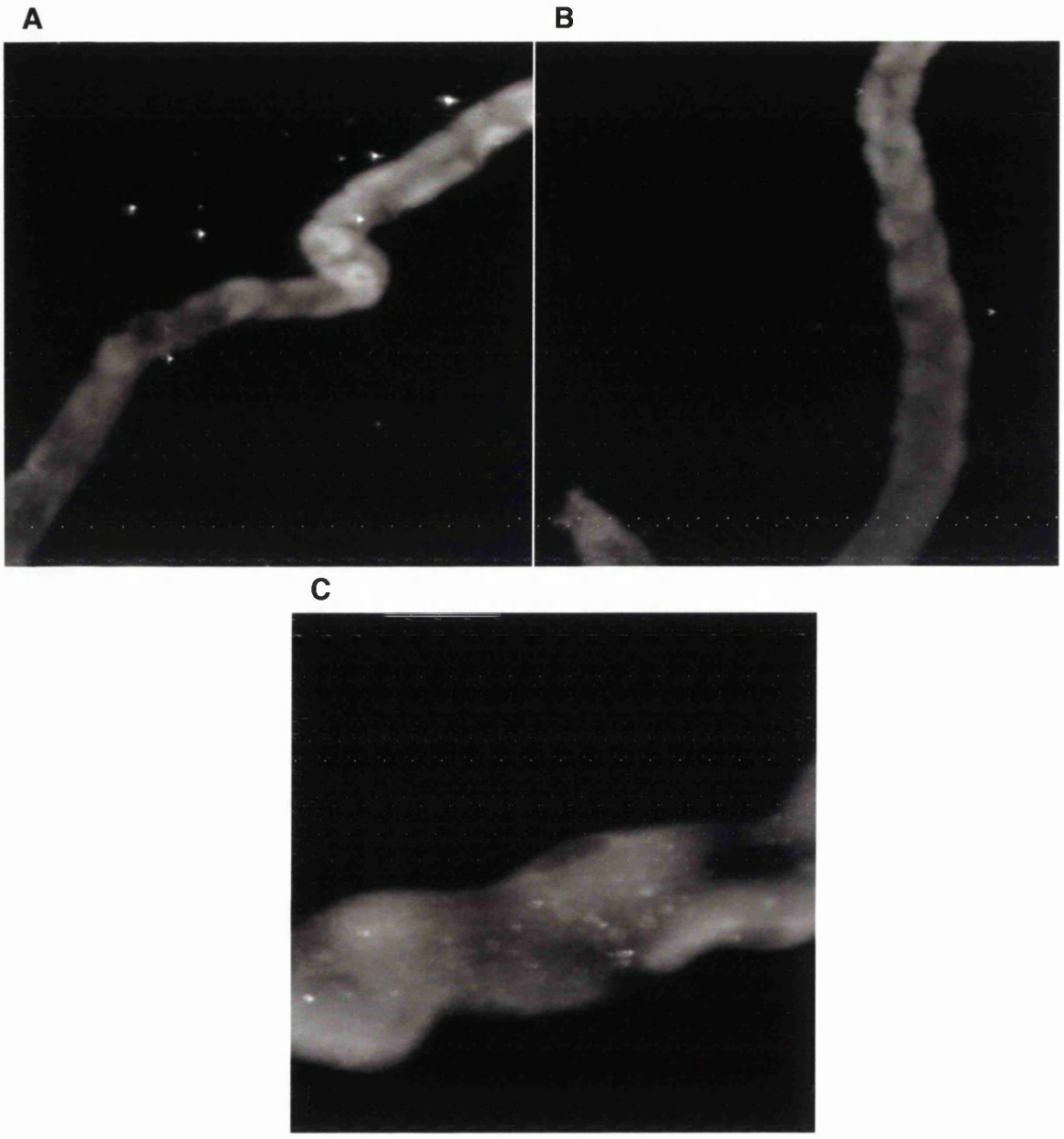

Figure 5.2: Localisation of TRP using immunocytochemistry.

Immunocytochemicl staining was carried out on whole-mount tubules using an antibody specific for TRP, and photographs were taken using a confocal microscope. The antibody was specific for residues 11-26 of the mature TRP protein (KALGSRLDYDLMMAEE). A) shows the main/initial segment boundary at x20 magnification. B) shows the main/lower segment boundary at x20 magnification. C) shows the principal and stellate cells of the main segment at x40 magnification.

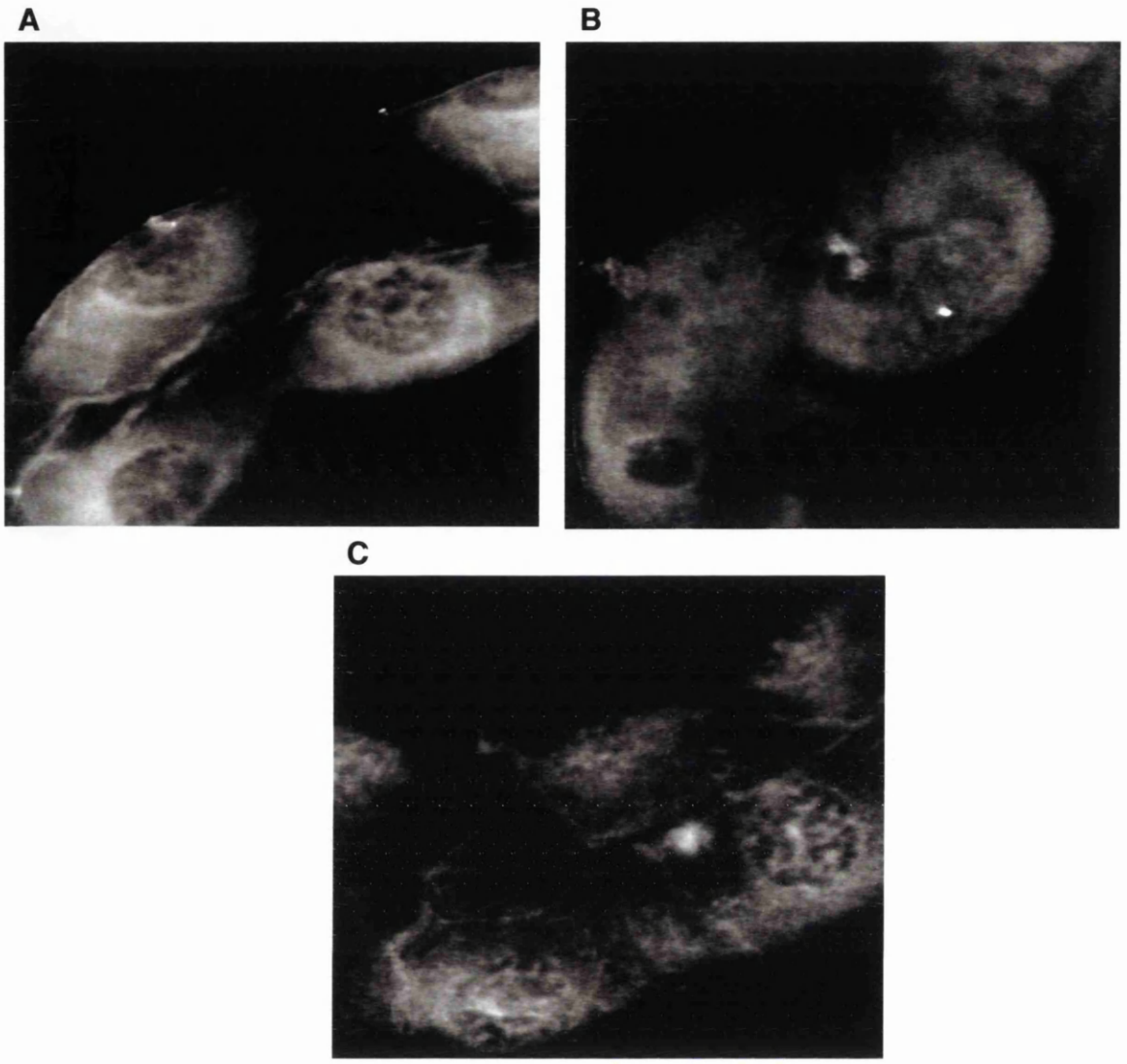

Figure 5.3: Localisation of TRPL using immunocytochemistry.

Immunocytochemical staining was carried out on whole-mount tubules using an antibody specific for TRPL, and photographs were taken using a confocal microscope. The anti-TRPL antibody was a polyclonal antibody raised against a C-terminal portion of TRPL (residues 667-1124). Panels A), B), C) show the cells in the main, initial and lower segment respectively.

5.5 Western analysis of TRP and TRPL in Malpighian tubules.

[These experiments were carried out with the assistance of Miss Valerie Pollock.] Using western blot analysis the expression levels of both TRP and TRPL proteins were examined in trp^{cm}, trp^{301}, $trpl^{302}$, $trpl^{302};trp^{cm}$ as well as OreR (wild-type) tubules. Using standard Western procedures multiple bands were obtained and it was hard to distinguish the expected TRP and TRPL bands, which are 145 kD for TRP, and 129 kDa for TRPL. As such, a method similar to that used in immunoprecipitation experiments was adopted (Xu *et al*, 2000, Chapter 2), where the same antibody used for immunoprecipitation was used to probe the proteins immunoprecipitated. Initially, the expression levels in bodies were used as an indicator of the levels in tubules. The results of immunoprecipitation followed by Western blot analysis with the TRP-specific antibody are shown in Figure 5.4. A prominent band of 145 kDa, corresponding to the predicted size of TRP, is observed as well as a fainter band of around 75 kDa in size, in both head and bodies. In bodies, an additional band of around 90 kDa is detected. No discernible difference in expression can be seen in any of the head or body samples. It is possible that the low expression of TRP observed in trp^{301}, trp^{cm}, and $trpl^{302};trp^{cm}$ mutants (Minke, 1983; Neimeyer *et al*, 1996), is enough to detect in these experiments due to its highly sensitive nature. i.e. at low levels of TRP protein our immunoprecipitation TRP-specific antibody becomes saturated, showing no differences in TRP expression between mutants and wild-type.

The results of immunoprecipitation followed by Western analysis using a TRPL specific antibody are shown in Figure 5.5. Here, several bands were detected at 200 kDa, 140 kDa, 130 kDa, 115 kDa and 100 kDa. The bands at 140 and 130 kDa were the most prominent, and that at 130 kDa corresponds to the predicted TRPL protein size (129 kDa). Although one might expect one single band at 129 kDa, the

detection of five bands is not alarming: using an antibody specific to residues 1082-1097 (DNSNFDIHVVDLDEK) of TRPL, Neimeyer *et al*, 1996, detected five bands, of similar relative density and size to ours, in Western analysis of wild-type flies. However, whereas in Neimeyer *et al*, 1996, no proteins were detected by Western analysis in $trpl^{302}$ mutants, we detect the same protein bands as in wild type.

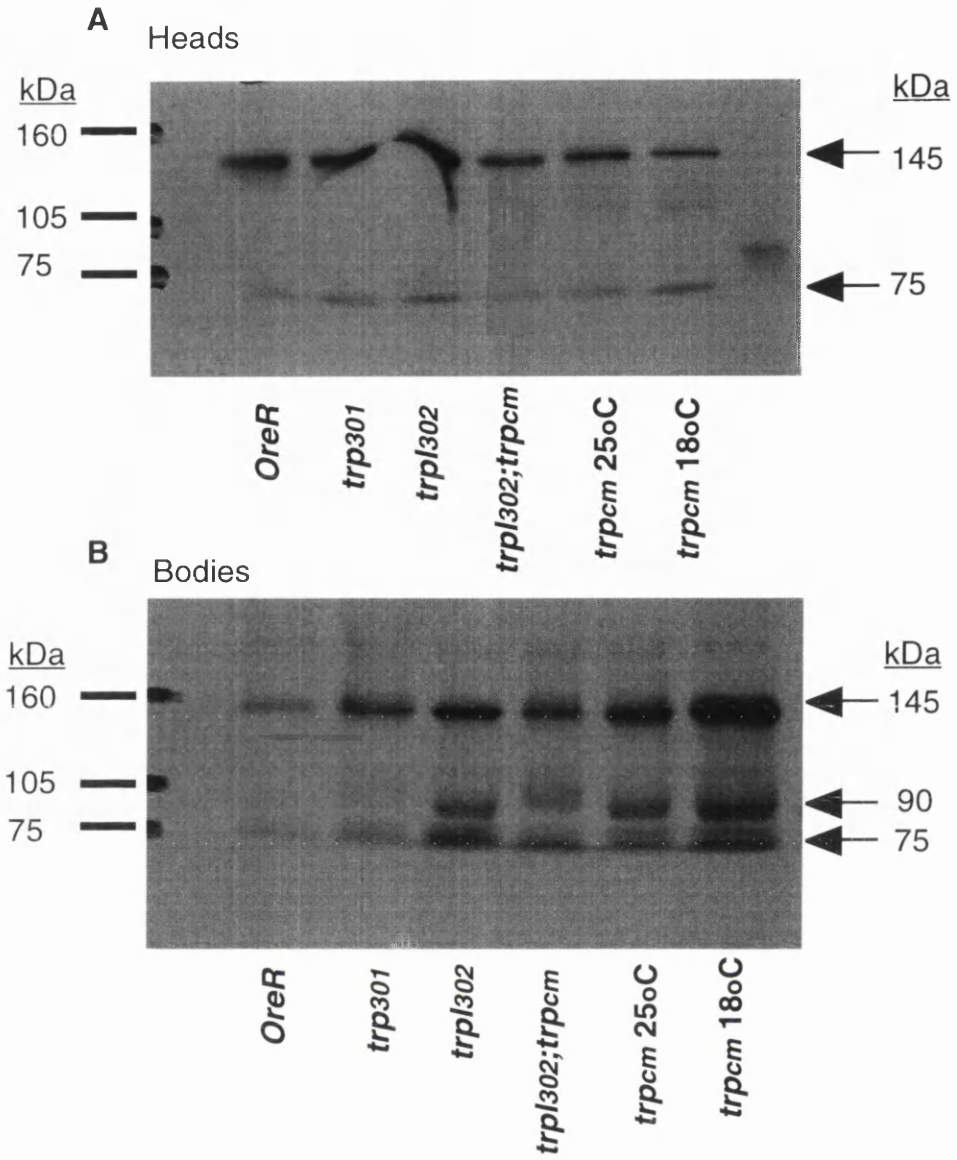

Figure 5.4: Immunoprecipitation, followed by Western analysis with TRP specific antibody.

Protein samples were prepared as described in Materials and Methods. Following immunoprecipitation with the TRP-specific antibody, precipitated protein samples were separated on a 3-8% Tris-acetate gel. Western blot analysis was carried out as normal with the TRP-specific antibody. Protein Markers are indicated to the left of the figures, whilst the sizes of the detected bands are indicated by the arrows on the right in kDa.

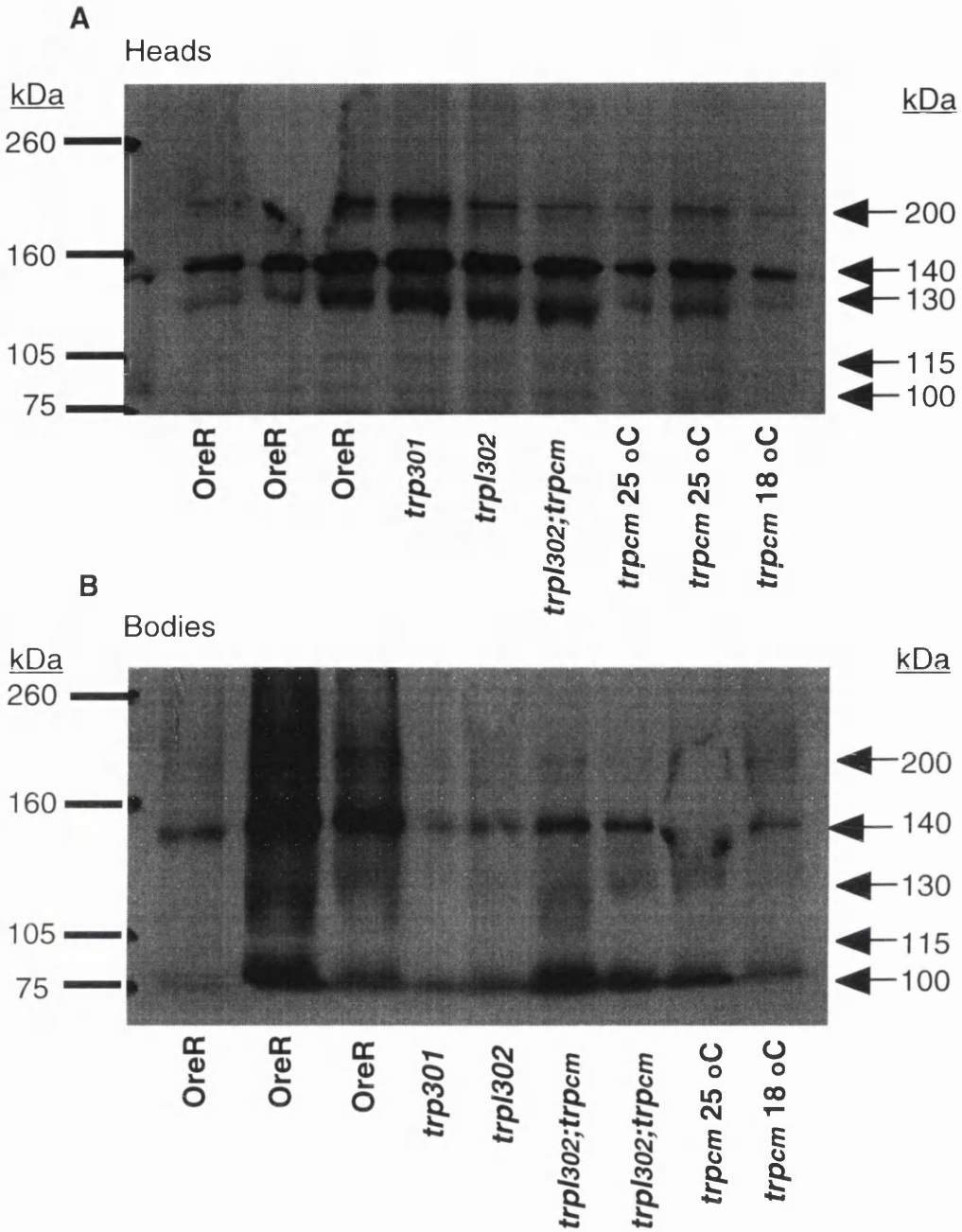

Figure legend overleaf

Figure 5.5: Immunoprecipitation, followed by Western analysis with TRPL specific antibody.

Protein samples were prepared as described in Materials and Methods. Following immunoprecipitation with the TRPL-specific antibody, precipitated protein samples were separated on a 3-8% Tris-acetate gel. Western blot analysis was carried out as normal with the TRPL-specific antibody.

Protein Markers are indicated to the left of the figures, whilst the sizes of the detected bands are indicated by the arrows on the right in kDa.

5.6 Measurement of $[Ca^{2+}]_i$ in *trp* and *trpl* mutants.

To make direct and non-invasive $[Ca^{2+}]_i$ measurements in *trp* and *trpl* tubules the mutations must be placed in an aequorin expressing background. To do this a complex three-way cross was carried out to unite specific mutations with the aequorin binary expression system, with hsGAL4 construct driving expression of aequorin under control of a UAS promoter (Figure 5.6). The cross shown, is that to achieve aequorin expression in a trp^{cm} background but the cross can be adapted to unite any three alleles assuming they are on different chromosomes. The crossing scheme for trp^{301} and $trpl^{302}$ are shown in the appendix. Before dissection of the tubules for $[Ca^{2+}]_i$ measurement the flies are heat-shocked at 37°C for thirty minutes and left to recover for one hour. Various lengths of heat-shock and recovery time were tried to obtain the best aequorin expression. It was found that heat-shocks of more than thirty minutes did not improve aequorin expression. Also, recovery of less than one hour resulted in poor aequorin expression, whereas if left to recover for longer than one hour there was no worthwhile increase in aequorin expression.

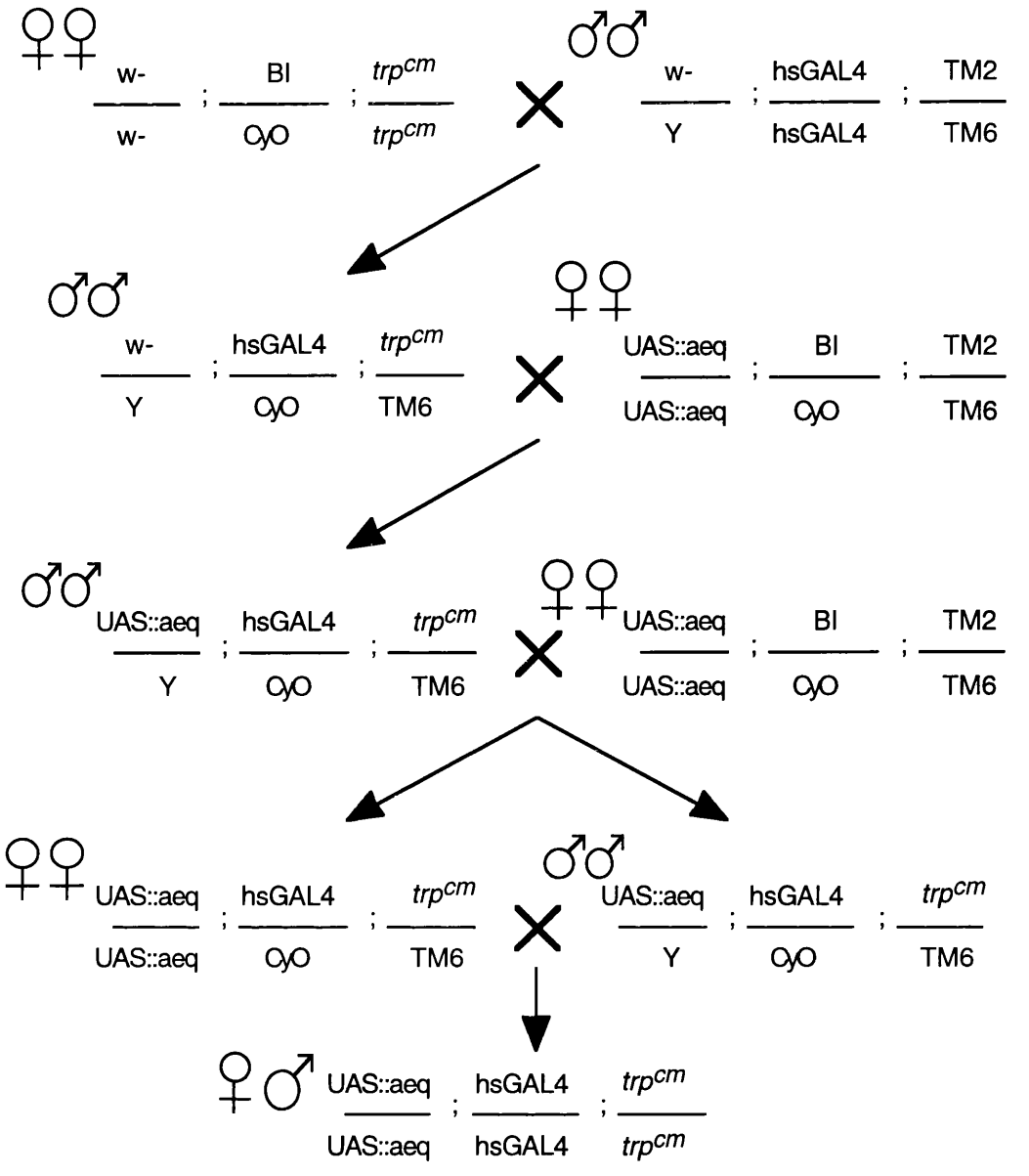

Figure 5.6: Three-way crossing scheme to unite the *trp*^{cm} mutation with hsGAL4 and UAS::aequorin constructs.

5.7 Confirmation of mutant phenotypes in an aequorin expressing background

To confirm the presence of the trp^{301}, trp^{cm} and $trpl^{302}$ mutations in the flies resulting from the three-way crosses, the response to CAP_{2b} in fluid secretion experiments was measured. The results are shown in figure 5.7. An attenuation of the response to CAP_{2b} has been demonstrated confirming the presence of the trp^{cm}, and $trpl^{302}$ alleles in our aequorin expressing lines, corresponding well with the previous secretion assay measurements on non aequorin expressing trp^{cm} and $trpl^{302}$ mutants. However, there does appear to be a greater attenuation of CAP2b-stimulated fluid secretion in the aequorin expressing trp^{301} tubules as compared to the original trp^{301} tubules. The original assays on trp^{301} tubules were performed several times and the results in figure 5.1 represent several separate assays. The assays presented here represent a single assay to confirm the mutant phenotype, hence the discrepancy between figures 5.1 and 5.7. To check for the abnormal responses to light seen in *trp* and *trpl* mutants whole-cell recordings of photoreceptor cells from aeq;hsGAL4;trp^{cm}, aeq;hsGAL4;trp^{301}, and aeq;$trpl^{302}$;hsGAL4 flies were taken by R.C.Hardie, Cambridge. It was found that the abnormal responses to light had been retained in the aequorin expressing background (R. Hardie, personal communication). Therefore, although Western analysis of *trp* and *trpl* mutants showed no discernible difference from wild-type, the mutant phenotype is retained.

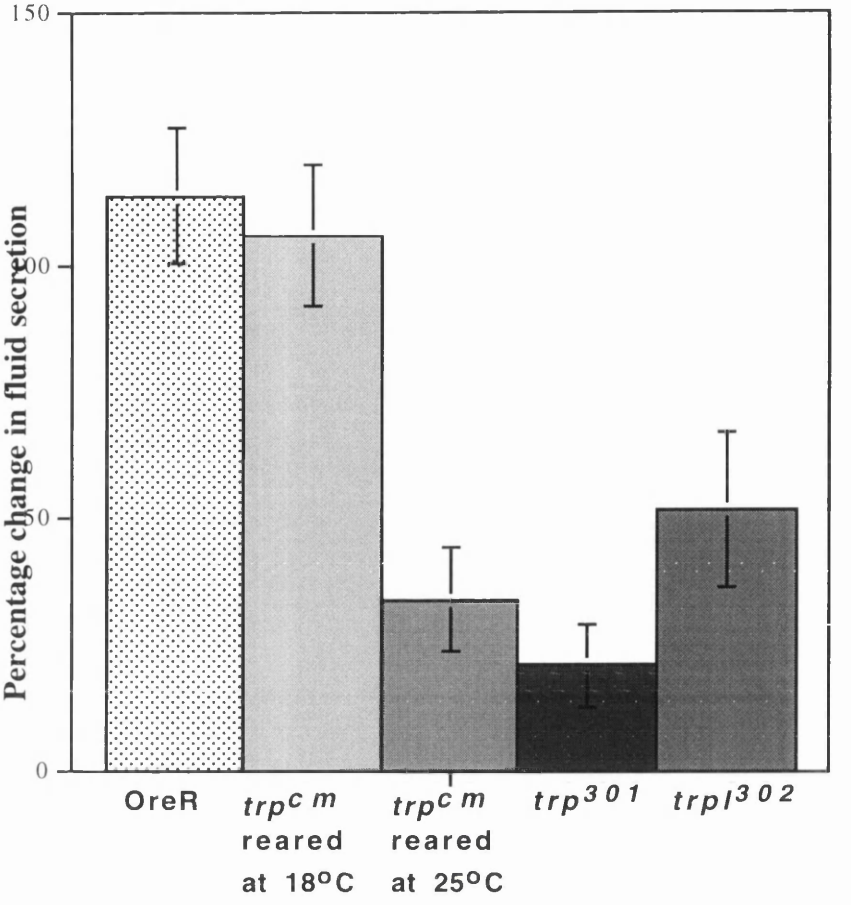

Figure 5.7: CAP_{2b}-stimulated fluid secretion is attenuated in aequorin expressing *trp* and *trpl* mutants.

Basal rates of fluid secretion were measured for 30 minutes before stimulation with CAP_{2b} (10^{-7} M) in heat-shocked lines. Fluid secretion rates were then measured for a further 30 minutes.

Data are expressed as n=8 ± SEM. Percentage change of fluid secretion rate =max rate/mean basal rate x 100

Where max rate is the maximum rate recorded after CAP_{2b} stimulation and the basal unstimulated rate is an average of the three readings taken before stimulation with CAP_{2b}.

5.8 The effect of mutations in *trp* and *trpl* on the CAP_{2b}-induced $[Ca^{2+}]_i$ rise.

Measurements of cytosolic calcium levels ($[Ca^{2+}]_i$) were made for each of the trp^{cm}, trp^{301}, and $trpl^{302}$ mutations, as well a wild-type control. After a mock injection with Schneider's solution the tubules were injected with at 10^{-7}M and the luminescence recorded for a further three minutes. Figure 5.8 shows a typical $[Ca^{2+}]_i$ before, during, and after, CAP_{2b} stimulation for the mutants as well as a wild type control. It has been demonstrated that CAP_{2b} elicits a biphasic rise in $[Ca^{2+}]_i$, where the secondary rise is dependent on an unknown component of Schneider's which is absent in *Drosophila* saline (Kean, personal communication). As the TRP and TRPL channels have been postulated to be involved in store-refilling or transient receptor potential abnormalities, it was thought that both parts of the CAP_{2b} elicited response be examined. Therefore, the tubules were incubated in Schneider's solution at all times. Figure 5.9 shows a summary of results obtained over a number of experiments. The primary stimulation is taken as the value of the initial $[Ca^{2+}]_i$ peak stimulated by CAP_{2b} whereas the best quantification of the secondary response was taken as the average $[Ca^{2+}]_i$ for four minutes post CAP_{2b}-stimulation.

Results show that the initial responses of the $trpl^{302}$, and trp^{cm} to be severely attenuated to 40% and 50% of control responses respectively. The secondary response was also significantly lower in these mutants. The primary response in trp^{301} tubules, however, was found to be significantly potentiated, 125% of control response. The secondary response in trp^{301} tubules was not significantly different from that seen in wild type. The conspicuous double 'bump' observed in the 'representative' aeq;hsGAL4;trp^{301} trace is not necessarily characteristic of trp^{301} and similar anomalies were seen in other tubule samples.

It does, however, demonstrate the diversity of shape of secondary rise (see discussion). These results suggest that both TRP and TRPL channels are involved in the CAP_{2b}-induced $[Ca^{2+}]_i$ rises, and also demonstrates a difference in calcium signalling phenotype between trp^{301} and trp^{cm}. This is in contrast to the fluid transport and electroretinogram phenotypes, where there is no difference observed between these two mutant types. This suggests that one or both of these alleles have calcium signalling specific effect in the principal cells.

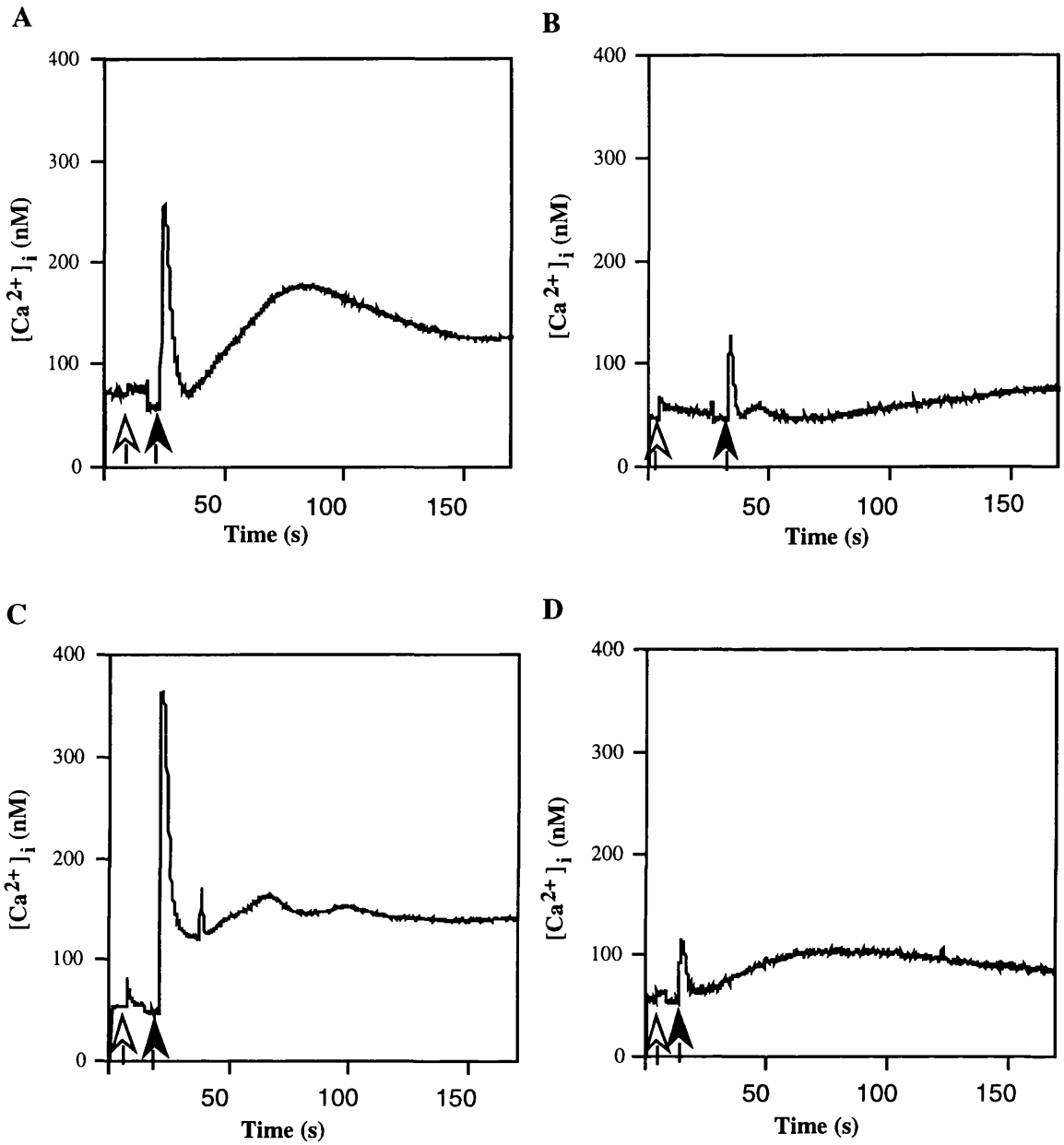

Figure 5.8: CAP_{2b}-induced $[Ca^{2+}]_i$ rises in *trp* and *trpl* mutants- representative traces.

Typical traces of changes in $[Ca^{2+}]_i$ in tubule cells when stimulated by 10^{-7} M CAP_{2b} (black arrows)in different fly lines, (A) aeq;hsGAL4, (B) aeq;$trpl^{302}$;hsGAL4, (C) aeq;hsGAL4;trp^{301}, (D) aeq;hsGAL4;trp^{cm}. The small peaks prior to the main rises in $[Ca^{2+}]_i$ are caused by the mock injection of Schneider's (clear arrows).

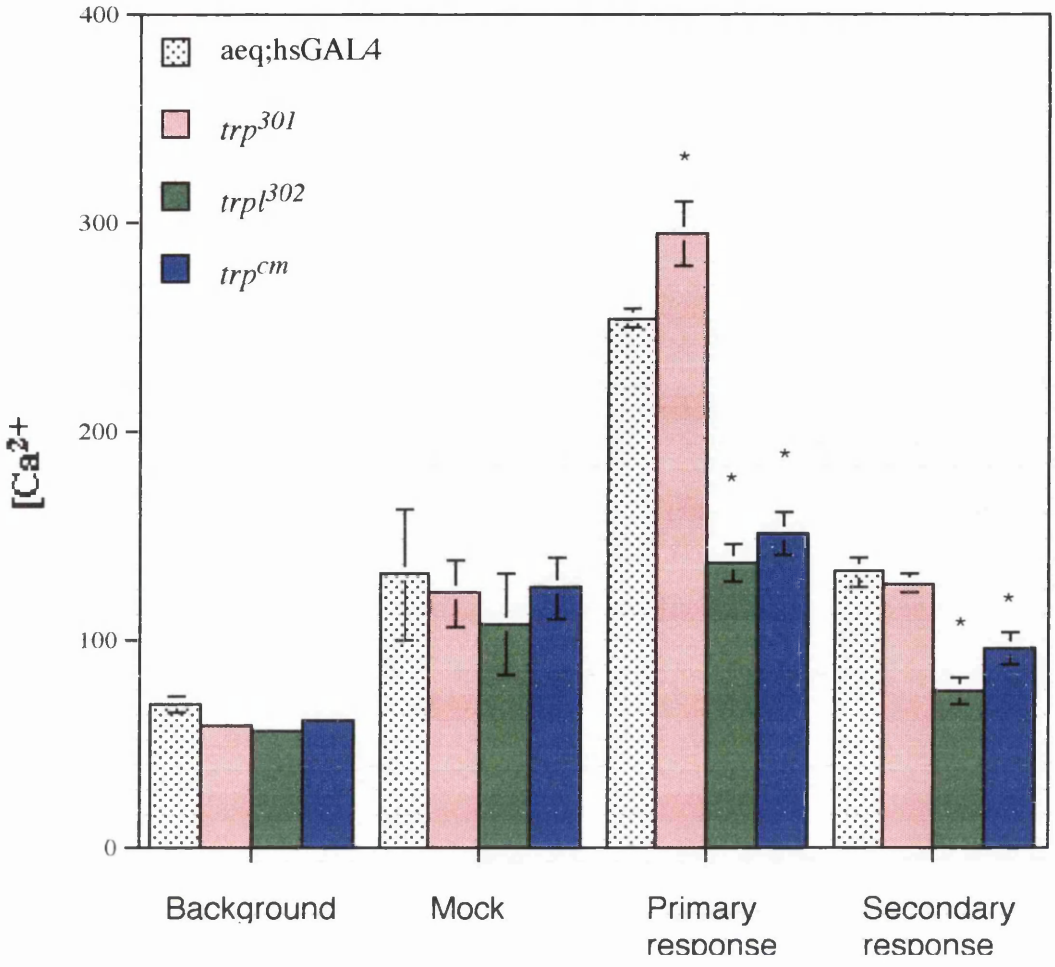

Figure 5.9: CAP_{2b}-induced $[Ca^{2+}]_i$ rises in *trp* and *trpl* mutants-pooled results.

Shown are the pooled results of changes in $[Ca^{2+}]_i$ in *trp* and *trpl* mutants in response to 10^{-7} M CAP_{2b}. Results are expressed as mean ± SEM., N=8 for unstimulated background $[Ca^{2+}]_i$, primary response $[Ca^{2+}]_i$ and secondary response $[Ca^{2+}]_i$. $[Ca^{2+}]_i$ significantly different from those in aeq; hsGAL4 tubules are denoted by *. *P<0.05 determined with the Student's *t*-test, on unpaired samples assuming unequal variances.

5.9 The effect of mutations in *trp* and *trpl* on the thapsigargin-induced $[Ca^{2+}]_i$ rise.

The calcium influx induced by thapsigargin was examined in wild type and in trp^{cm}, trp^{301}, and $trpl^{302}$ tubules. After a mock injection with Schneider's solution the tubules were injected with thapsigargin at 2.5 μM and the luminescence recorded for a further four minutes. Figure 5.10 shows typical $[Ca^{2+}]_i$ measurements for wild type (aeq;hsGAL4) and trp^{cm}, trp^{301}, and $trpl^{302}$ tubules.

Results show that thapsigargin induces a prolonged rise in $[Ca^{2+}]_i$. The initial peaks occurring at the moment of injection are caused by the ethanol in which the thapsigargin is dissolved. For each set of tubules the maximum $[Ca^{2+}]_i$ (nM) and average $[Ca^{2+}]_i$ (nM) post-thapsigargin stimulation was recorded. A summary of these results is presented in figure 5.11.

Results demonstrate no significant difference in the trp^{cm} tubule response to thapsigargin, as compared to that of wild type. The response in $trpl^{302}$ tubules although not statistically significant, was lower than that seen in wild-type tubules. However, both the maximum and average post thapsigargin $[Ca^{2+}]_i$ were significantly higher in trp^{301} tubules than in wild type. Together with the CAP_{2b} stimulated responses observed in the trp^{301} tubules, these results suggest that there is a higher calcium conductance in the trp^{301} tubule principal cells (both CAP_{2b} and thapsigargin responses are potentiated. It does not appear that the TRP channel is a 'CCE' channel. However, it does seem as though TRPL may be involved in the thapsigargin-induced calcium influx.

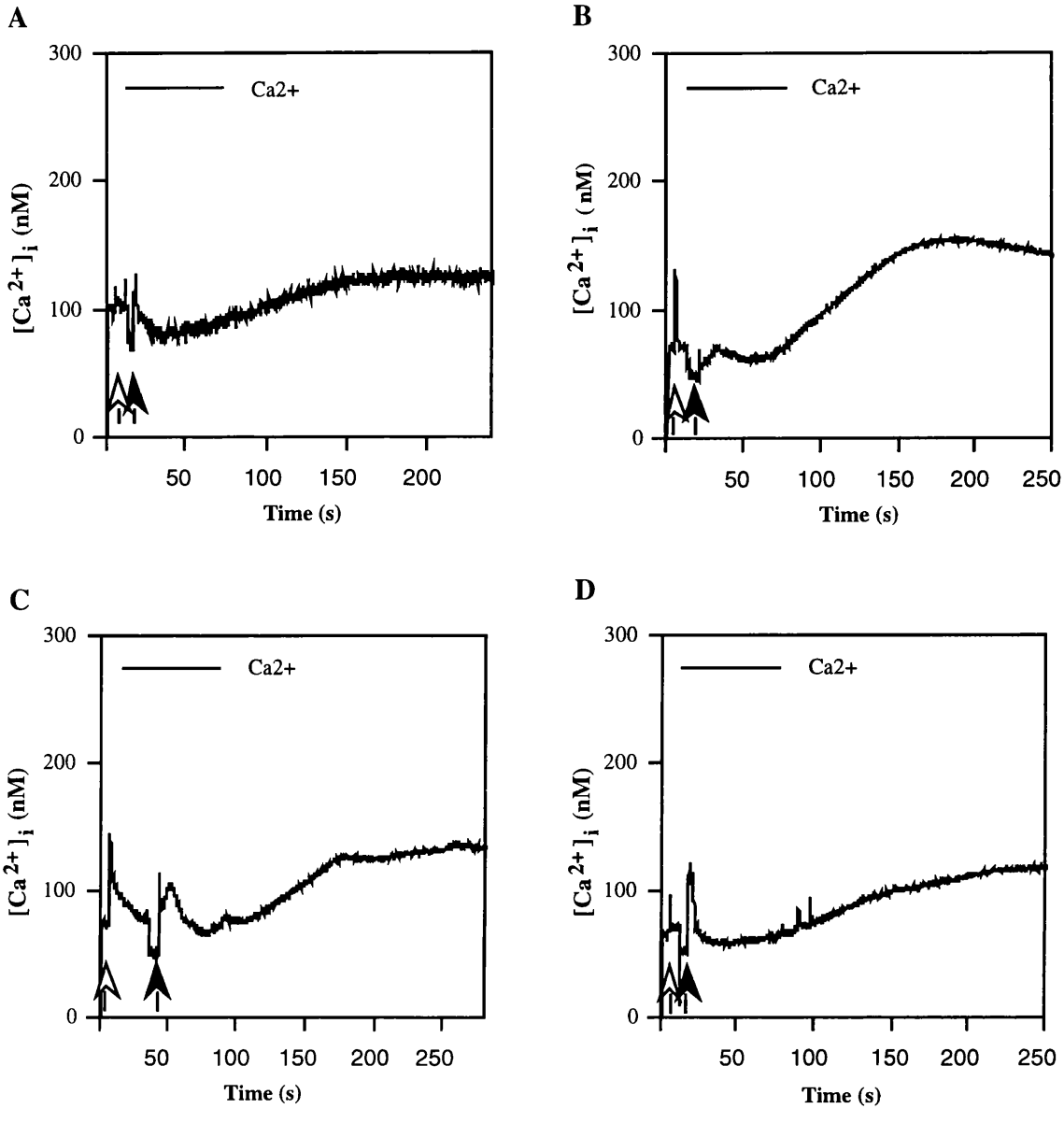

Figure 5.10: Thapsigargin-induced $[Ca^{2+}]_i$ rise in *trp* and *trpl* mutants- representative traces.

Typical traces of changes in $[Ca^{2+}]_i$ in tubule cells when stimulated by 2.5 μM thapsigargin (black arrows), in different fly lines: (A) aeq;hsGAL4, (B) aeq;hsGAL4;trp^{301}, (C) aeq;$trpl^{302}$;hsGAL4, (D) aeq;hsGAL4;trp^{cm}. Initial rises in $[Ca^{2+}]_i$ seen upon thapsigargin application are due to the ethanol in which the thapsigargin is dissolved, and do not effect the subsequent response. Clear arrows indicate mock injections of Schneider's.

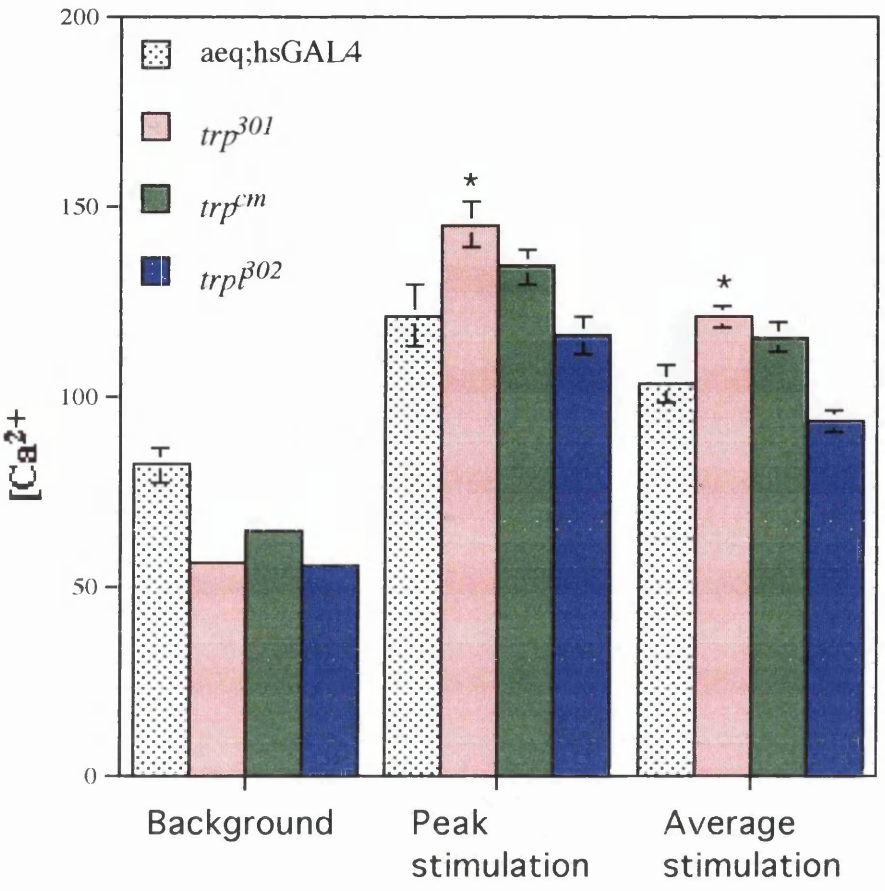

Figure 5.11: Thapsigargin-induced $[Ca^{2+}]_i$ rises in *trp* and *trpl* mutants-pooled results.

Pooled results of changes in $[Ca^{2+}]_i$ in *trp* and *trpl* mutants in response to 2.5 μM thapsigargin are shown. Results are expressed as mean ± SEM., N=8. The peak stimulation represents the highest $[Ca^{2+}]_i$ reached post stimulation and the average stimulation is the average $[Ca^{2+}]_i$ measured over four minutes post-stimulation. $[Ca^{2+}]_i$ significantly different from those in aeq; hsGAL4 tubules are denoted by *. *P<0.05 determined with the Student's *t*-test, on unpaired samples assuming unequal variances.

5.10 The effect of lanthanides on CAP_{2b}- and thapsigargin-induced $[Ca^{2+}]_i$ rises.

TRP channels are known to be sensitive to lanthanides, such as lanthanum or gadolinium, at micromolar concentrations (Vaca *et al*, 1994).

The effect of lanthanides on the CAP_{2b}-stimulated rise in $[Ca^{2+}]_i$ was examined. As TRP was shown to be localised to the main segment principal cells, wild-type flies which express aequorin in principal cells (c42/c42; aeq, see appendix) were used to monitor $[Ca^{2+}]_i$. Lanthanum (La^{3+}) or gadolinium (Gd^{3+}) (50 μM) were added to samples five minutes prior to CAP_{2b} stimulation (10^{-7} M). Samples were also given a mock injection with 25 μl Schneiders solution prior to an injection of CAP_{2b} at 10^{-7} M. The $[Ca^{2+}]_i$ was recorded for a further four minutes. Figure 5.12A shows that CAP_{2b}-induced $[Ca^{2+}]_i$ in principal cells is not inhibited by either La^{3+} or Gd^{3+}. The primary response refers to the sharp initial rise in $[Ca^{2+}]_i$ following stimulation with CAP_{2b} and is calculated as the peak $[Ca^{2+}]_i$ reached - pre-stimulation average $[Ca^{2+}]_i$ = delta $[Ca^{2+}]_i$.

The effect of the application of La^{3+} (50 μM) 5 minutes prior to stimulation of the tubules with thapsigargin was also examined. For each set of tubules the maximum $[Ca^{2+}]_i$ post-thapsigargin stimulation was recorded. The results are summarised in figure 5.1_{2b}. There was no significant effect of 50 μM La^{3+} or Gd^{3+} on the thapsigargin induced $[Ca^{2+}]_i$ rise. These results suggest that either La^{3+} does not inhibit TRP in tubules or that La^{3+}-inhibited TRP channels do not affect either the CAP_{2b} or thapsigargin response. It seems that either La^{3+} does not block TRP/TRP homomultimers in wild-type flies or that such homomultimers do not significantly contribute to either the CAP_{2b} or thapsigargin-induced $[Ca^{2+}]_i$ rises in wild-type tubules.

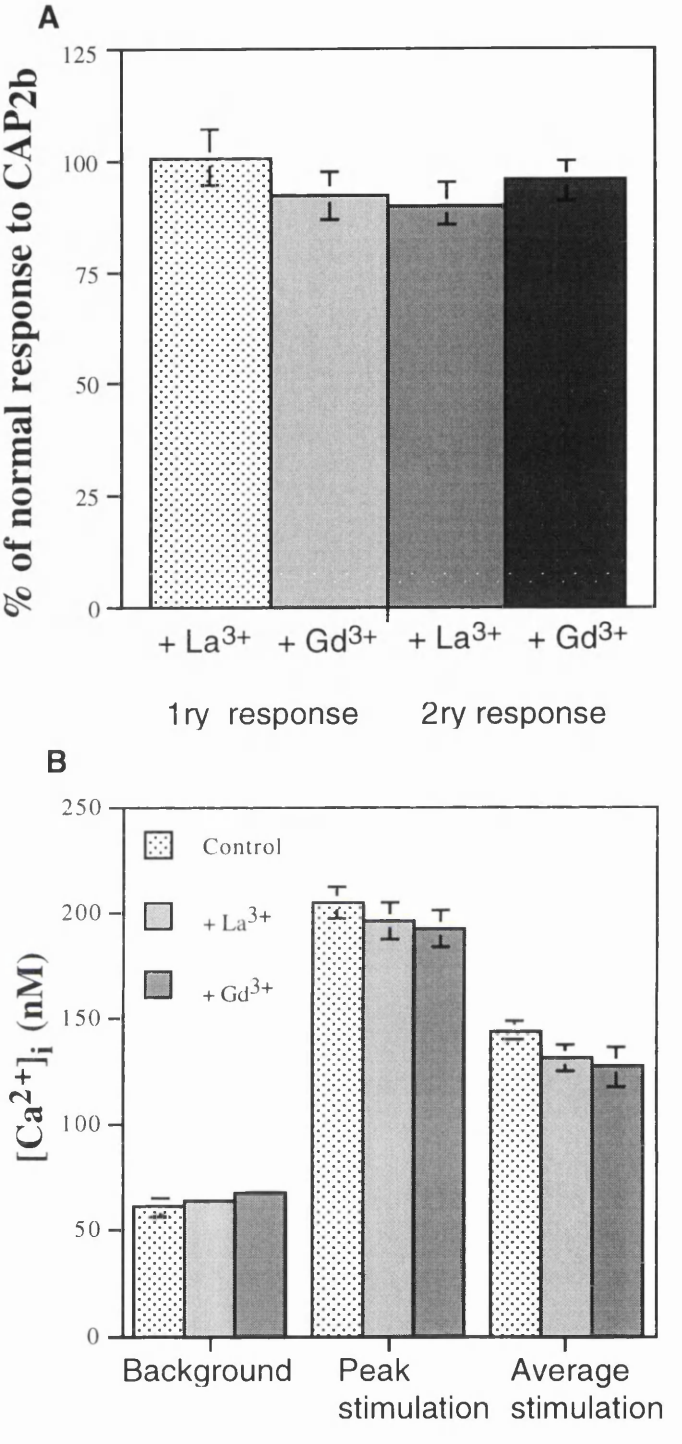

Figure legend overleaf

Figure 5.12: The effect of lanthanides on CAP_{2b} and thapsigargin stimulated $[Ca^{2+}]_i$ rises.

Results are expressed as mean ± SEM., N=12.

A) The effects of 50 μM La^{3+} and Gd^{3+} on CAP_{2b} induced primary responses. The percentage of normal response to CAP_{2b} is calculated as the experimental delta $[Ca^{2+}]_i$ / control delta $[Ca^{2+}]_i$ x 100, where delta $[Ca^{2+}]_i$ is the peak$[Ca^{2+}]_i$ pre-stimulation average $[Ca^{2+}]_i$. Results are expressed as mean ± SEM., N=12.

B) The effect of 50 μM La^{3+} and Gd^{3+} on thapsigargin induced $[Ca^{2+}]_i$ rises. Due to the prolonged thapsigargin response, $[Ca^{2+}]_i$ values were expressed for background, peak stimulation and average stimulation. Results are expressed as mean ± SEM., N=12. There is no significant difference between the responses in samples with prior treatment wih La^{3+} or Gd^{3+}.

5.11 The effect of Lanthanum on CAP_{2b}-stimulated $[Ca^{2+}]_i$ rise in *trp* and *trpl* mutants.

As it was shown that La^{3+} does not affect CAP_{2b}-stimulated $[Ca^{2+}]_i$ in wild-type tubules the effect of La^{3+} on CAP_{2b}-stimulated $[Ca^{2+}]_i$ rise in *trp* and *trpl* tubules was examined. The effects of La^{3+} at 50 μM are summarised in figure 5.13. The responses to CAP_{2b} shown in figure 5.9 suggest that, compared to mock injections, the CAP_{2b}-induced calcium response is virtually abolished in trp^{cm} and $trpl^{302}$ tubules. However, in subsequent experiments a response to CAP_{2b} was evident, possibly due to higher concentrations in separate CAP_{2b} aliquots, as well as lower mock-stimulated $[Ca^{2+}]_i$ peaks. Therefore, when examining the effect of La^{3+} (50 μM) in these mutant tubules, the differences between CAP_{2b}- and mock-stimulated $[Ca^{2+}]_i$ peaks was calculated. Figure 5.13 shows the effect of La^{3+} (50 μM) on CAP_{2b}-stimulated $[Ca^{2+}]_i$ rises. It is apparent that there is a significant reduction of CAP_{2b} stimulation with prior application of La^{3+}, in both trp^{301} and $trpl^{302}$ tubules, and no effect on trp^{cm} tubules. La^{3+} almost completely abolishes the CAP_{2b}-response in $trpl^{302}$ tubules. This may be due to the blocking of remaining TRP channels in these tubules, similar to the light-activated calcium current in $trpl^{302}$ photoreceptors (Neimeyer *et al*, 1996). This suggests that the CAP_{2b}-induced initial calcium influx is entirely due to TRP and TRPL channels. However, the attenuation of CAP_{2b}-stimulated $[Ca^{2+}]_i$ rises by nifedipine and verapamil (chapter 4), suggests the involvement of voltage-gated calcium channels also. It appears that both voltage-gated and TRP and TRPL calcium channels may interact to produce the CAP_{2b}-stimulated calcium influx.

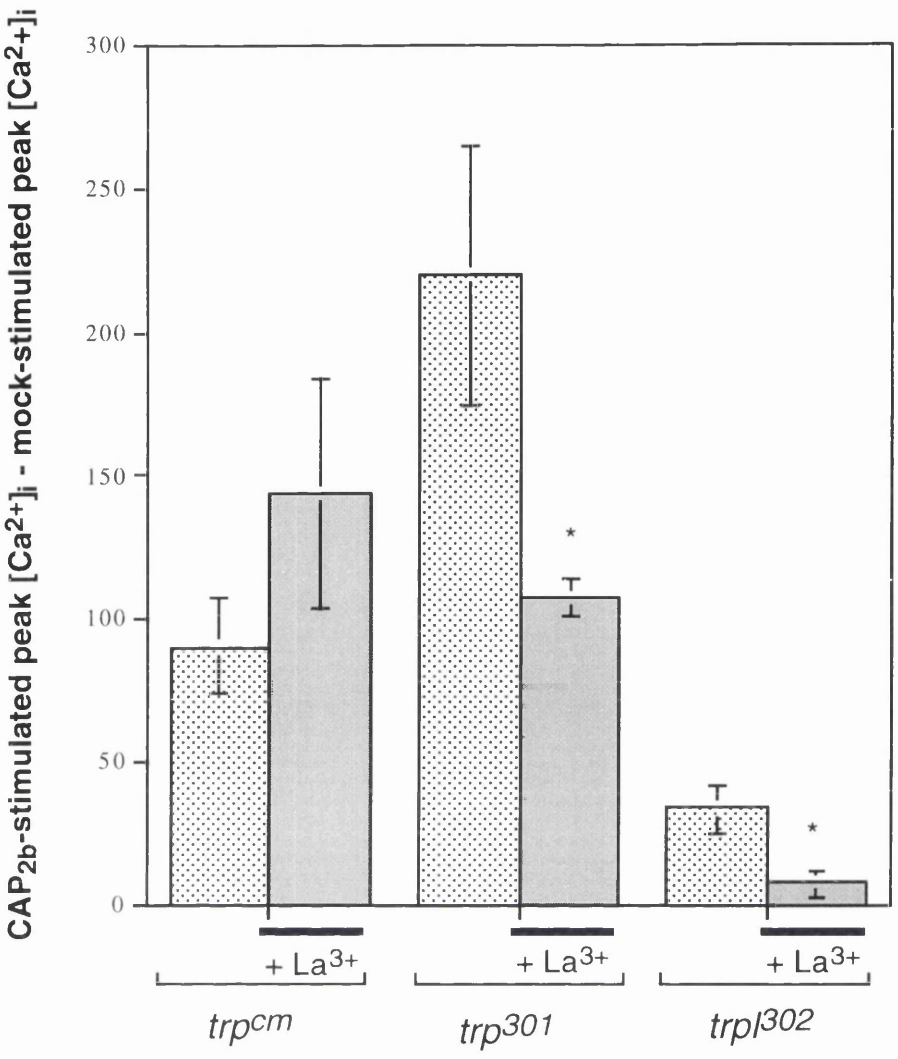

Figure 5.13: The effect of Lanthanum on CAP_{2b}-stimulated $[Ca^{2+}]_i$.

Prior to mock injections and stimulation with CAP_{2b} 10^{-7} M, samples were either left untreated or La3+ at 50 µM applied. $[Ca^{2+}]_i$ was measured for 4 minutes post-CAP_{2b} stimulation, in trp^{cm} (n=9), trp^{301} (n=4) and $trpl^{302}$ (n=9). The peak $[Ca^{2+}]_i$ reached following mock injection was subtracted from the peak $[Ca^{2+}]_i$ reached following stimulation with CAP_{2b}. Results where the CAP_{2b} calcium response is significantly different following prior treatment with La^{3+} (50 µM) are denoted by *. *P<0.05 determined with the Student's *t*-test, on unpaired samples assuming unequal variances.

5.12 The effects of the TRPL inhibitor, CDC, on fluid secretion and $[Ca^{2+}]_i$.

Cinnamyl 1-3,4-dihydroxy-α-cyanocinnanate (CDC) is a lipoxygenase inhibitor that was first used to elucidate the role of lipoxygenase metabolites in endothelial cells (Honda *et al*, 1999). The inhibition of lipoxygenases might be expected to lead to the build up of endogenous fatty acids normally produced by the breakdown of diacyl-glycerol (DAG). Experiments in photoreceptors demonstrated that CDC activated the normally light-activated current carried by the TRP and TRPL channels at concentrations of 10 μM (Chyb *et al*, 1999). It was demonstrated that CDC blocked the response to light in *trp* mutants but not in wild-type or *trpl* mutant flies; and also that it inhibits TRPL channels expressed in S2 cells with a half maximal inhibitory concentration of 1 μM. The effects of CDC on fluid secretion and calcium signalling in wild-type tubules at concentrations of 5 μM and 50 μM were tested. Results demonstrate that at 50 μM, CDC produced a prolonged rise in $[Ca^{2+}]_i$ very much like that elicited by thapsigargin but over a longer time period (Figure 5.14A). However, when 50 μM CDC was applied to secreting tubules, fluid secretion ceased after 30 minutes (Figure 5.14C). At 5 μM CDC had no effect on either $[Ca^{2+}]_i$ or fluid secretion (Figure 5.14 B and D).

5.13 The effect of CDC on fluid secretion in *trp* and *trpl* mutants.

The effects of CDC on fluid secretion in trp^{cm}, trp^{301}, $trpl^{302}$, and $trpl^{302};trp^{cm}$ were examined. At 50 μM CDC, tubules from all these lines ceased to secrete, as do wild type tubules. However, when CDC was applied to the tubules at 5 μM, there was only an effect in the trp^{cm} tubules reared at 25 °C (Figure 5.15). The fluid secretion rate in the tubules was reduced to almost zero over a thirty minute

period. As these tubules are postulated to lack functioning TRP channels, this would leave an abundance of TRPL homomultimers. These results suggest that these remaining TRPL/TRPL homomultimers are major contributors to fluid transport mechanisms and that the absence of effect of 5 μM CDC in $trpl^{302}$ and $trpl^{302};trp^{cm}$ tubules is due to the absence of TRPL homomultimers.

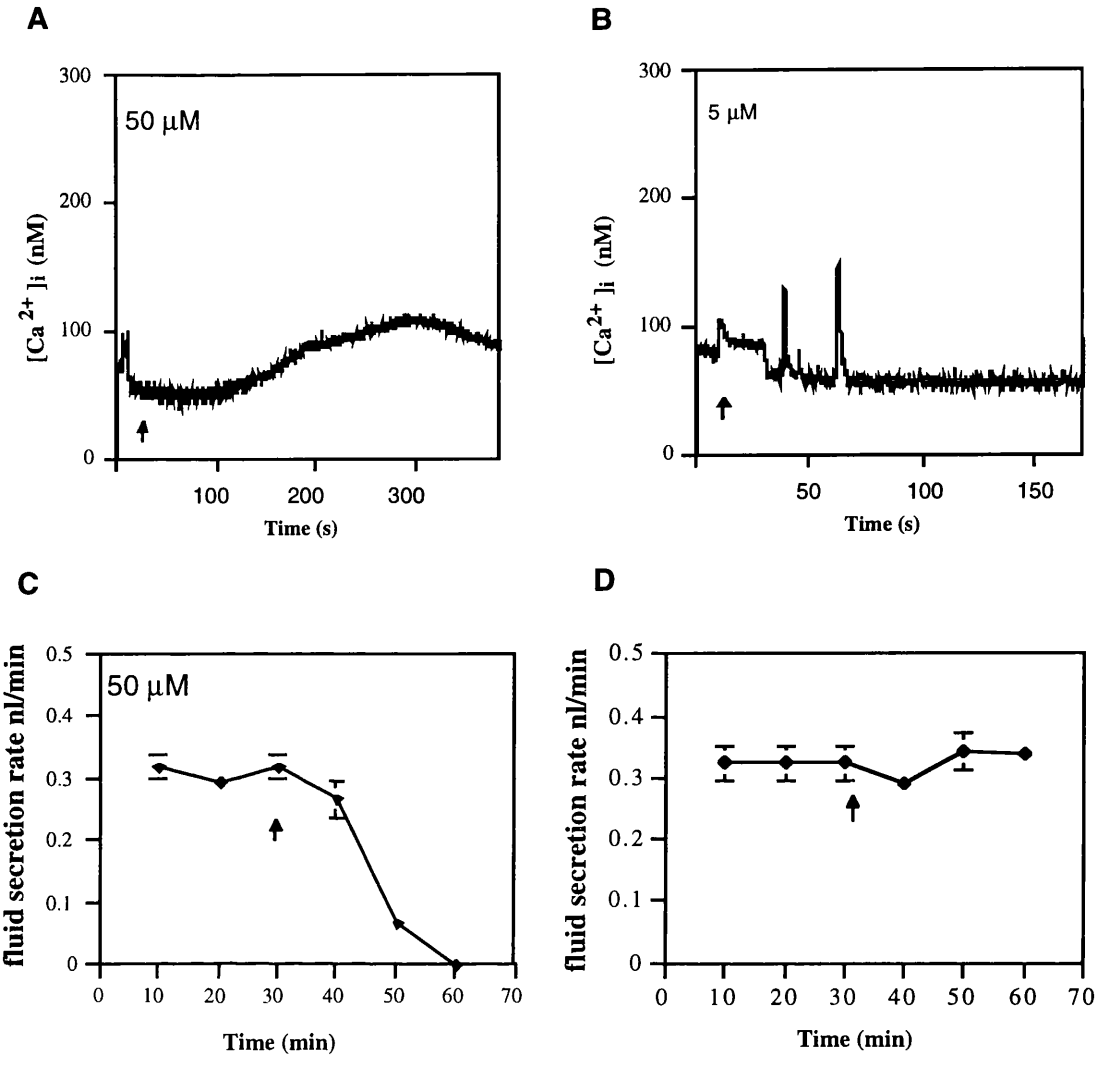

Figure 5.14: The effects of CDC on $[Ca^{2+}]_i$ and fluid secretion.

A) and B) show the effect of 50 µM and 5 µM CDC on $[Ca^{2+}]_i$ respectively. The traces shown are representative of a sample of six. The extra peaks present in B) may represent spontaneous random activation events but were only present in two of six traces.

C) and D) show the effect of 50 µM and 5 µM CDC respectively on fluid secretion rates. Tubules were allowed to secrete normally for thirty minutes before the application of CDC at either 50 µM (C) or 5 µM (D). The fluid secretion rate was then recorded for a further 30 minutes. Results are expressed as mean fluid secretion rate ± SEM., N=7-10.

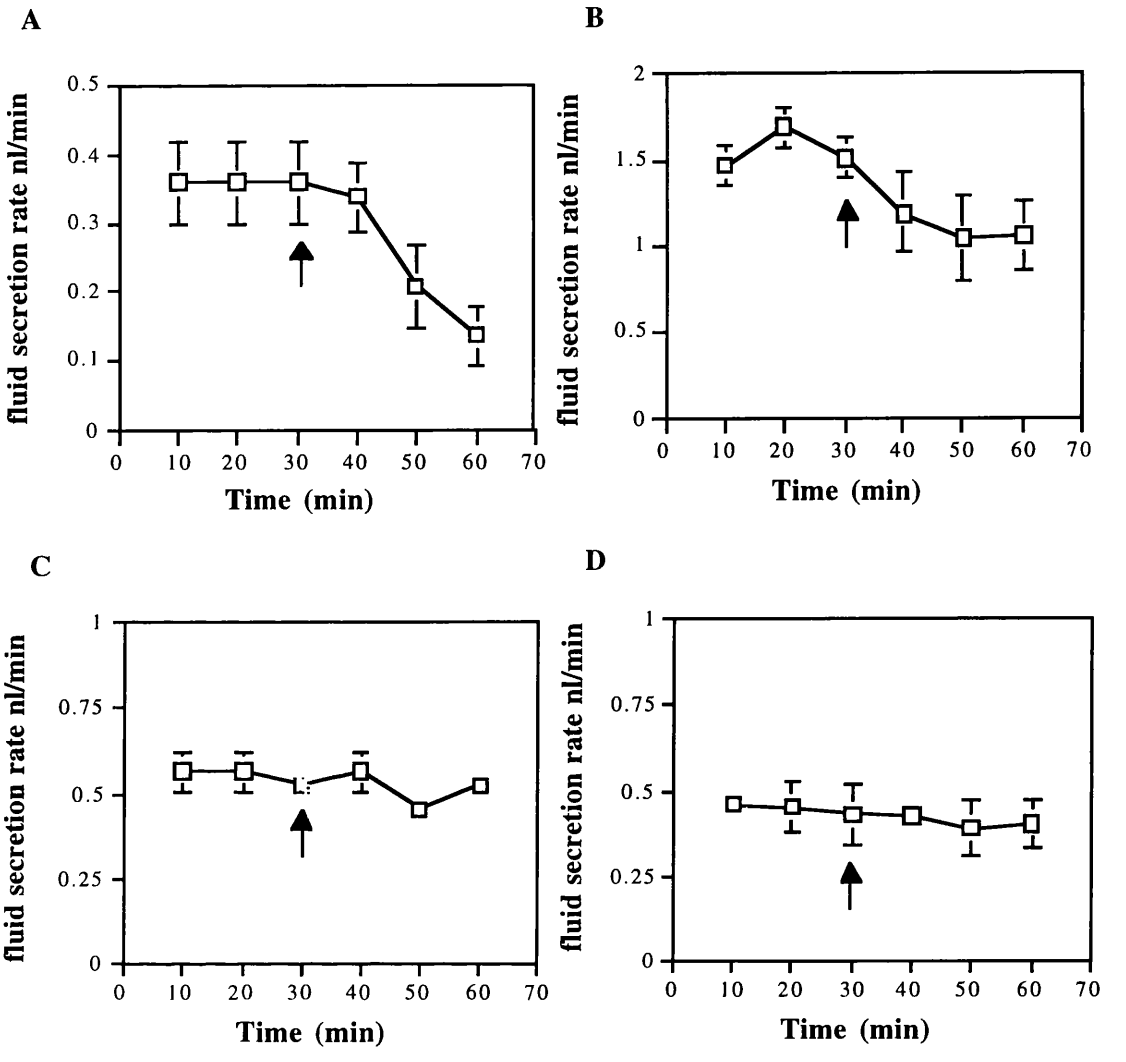

Figure 5.15: The effects of CDC on fluid secretion in *trp* and *trpl* tubules.

Basal rates of fluid secretion were recorded for thirty minutes prior to addition of 5 μM CDC to trp^{cm} reared at 25°C (A), trp^{301} (B), $trpl^{302}$ (C) and $trpl^{302};trp^{cm}$ (D). Fluid secretion rates were then recorded for a further 30 minutes. Results are expressed as mean fluid secretion rate ± SEM., N=6-10.

5.14 Discussion

Experiments described in this chapter, work carried out in order to investigate the function of TRP and TRPL calcium channels in *Drosophila* tubules. Previous to this, *in vivo* studies were carried out solely on *Drosophila* photoreceptor cells, and so many of our experimental cues have come from this field. However, there are important differences between photoreceptor and Malpighian tubule cells. First of all, TRP and TRPL channels are stimulated by light-activated rhodopsin in photoreceptors, whereas in tubules, the stimulus comes from a variety of sources, for example, the neuropeptides, such as CAP_{2b}, or *Drosophila* Leukokinin. There may be significant differences in the Ca^{2+} signalling mechanisms utilized in these different cell types in response to very different stimuli. Also in tubules the cells form a polarised epithelia involved in the transport of, amongst other things, calcium. Seen in this light, tubules are more akin to pancreatic acinar cells, where an abundance of studies of calcium signalling exist. Therefore when interpreting our results we must be careful not to associate too closely the mechanism of calcium signalling in tubule cells with that in photoreceptor cells.

For example, results in the previous chapter show a lack of expression of inaD, suggesting that signalling molecules present in the tubule associate differently from those present in the multimolecular signalling complex found in photoreceptor cells. An association of INAD and TRP has been found to be critical to the retention of signalling molecules (PKC and PLC) at the tips of the rhabdomere (Li *et al*, 2000). It may be possible that in tubules TRP could interact with another INAD-like molecule to provide a 'scaffold' for other signalling molecules. However, in the principal cells of the tubule we can only speculate on how calcium channels and their regulators are associated.

Fluid secretion assays were carried out on trp^{cm}, trp^{301}, $trpl^{302}$, and $trpl^{302};trp^{cm}$ tubules. It was found that all of the single mutations (trp^{cm}, trp^{301}, $trpl^{302}$) caused an attenuation of fluid secretion in response to CAP_{2b}. This implied a role for both TRP and TRPL channels in the CAP_{2b} signal transduction cascade. This role was supported by the localisation of TRP to the principal cells of the main segment, and TRPL in principal cells throughout the tubule, by immunocytochemistry. CAP_{2b} had been previously shown to stimulate fluid secretion through a pathway involving cGMP and *Drosophila* nitric oxide synthase (dNOS) (Davies *et al*, 1997). DNOS is a calcium/calmodulin sensitive enzyme and so the involvement of calcium channels in this pathway was not surprising. Further to this, it was found that the $trpl^{302};trp^{cm}$ double mutant was almost completely unresponsive to CAP_{2b} and had a reduced basal fluid secretion rate (V. Pollock, personal communication). This suggested a complementary role for TRP and TRPL in normal tubule function and possibly calcium transport, as single mutations did not reduce basal rates of fluid secretion. The reduced basal rate could also reflect a tubule developmental retardation caused by the double mutation but this possibility was not further investigated.

Western blot analysis of trp^{cm}, trp^{301}, $trpl^{302}$, and $trpl^{302};trp^{cm}$ heads and bodies showed no discernible difference of levels of expression of TRP or TRPL, in our experiments. Also multiple bands were detected using both anti-TRP and anti-TRPL antibodies. However, these bands were comparable to those detected by others (Neimeyer *et al*, 1996; Hardie *et al*, personal communication), using different antibodies. As we detect both bands postulated to be due to TRP and TRPL in all our mutants, the identity of the proteins we have detected remains in question. However, only protein sequencing of bands isolated directly from our gels will identify these proteins. The five bands detected with our TRPL antibody

are particularly interesting as these have been detected before (Neimeyer, *et al*, 1996), and shown to be dependent on TRPL expression. As the antibodies used both in our and Neimeyer's experiments are specific for the C-terminal end of TRPL, it is possible that these bands are translated from shorter *trpl* transcripts that contain the C-terminal region of TRPL. Such shorter TRPL proteins may be involved in post-translational regulation of TRPL channels.

The cytosolic calcium signals in response to CAP_{2b} were measured in the different mutant lines by aequorin expression using the GAL4/UAS binary expression system. The crossing scheme involved in creating such fly lines, was necessarily complex with much room for potential error. Therefore the phenotypes for both photoreception and fluid secretion were verified before further experiments were attempted. With regard to the fluid secretion phenotypes, although the percentage increases of the aequorin expressing lines differ slightly with those of the original *trp* and *trpl* mutant lines, it is clear that there is attenuation of the CAP_{2b} response. The discrepancy, especially in trp^{301}, is probably due to a degree of experimental error when measuring such an attenuated response. The aequorin-expressing flies were sent to Roger Hardie, Cambridge, who verified the trp^{cm}, trp^{301}, and $trpl^{302}$ phenotypes in the photoreceptor assay. The effects of *trp* and *trpl* mutations on the CAP_{2b}-stimulated $[Ca^{2+}]_i$ rise were then examined. We found that the primary responses to CAP_{2b} were attenuated in both the trp^{cm} and $trpl^{302}$ tubules, and potentiated in trp^{301} tubules. The attenuation in $trpl^{302}$ tubules indicates a major role for TRPL channels in producing the primary CAP_{2b} induced calcium influx. However the opposing effect caused by the different *trp* mutations negates a simple explanation for the role of TRP channels. It may be that TRP channels play an equally important role to that of TRPL as demonstrated by the attenuation of CAP_{2b} response in trp^{cm} tubules, and that the potentiation in

trp^{301} tubules is caused by some, as yet unknown effect of this mutation. As the existence of overlapping reading frames in the *trp* gene has been reported (Wong *et al*, 1987), it may be possible that the *trp*^{cm} and *trp*^{301} mutations effect the transcription or function of other genes, involved in calcium signalling. Interestingly, the gene encoding CAP_{2b} is situated just downstream of *trp* (Kean *et al*, submitted), which suggests that any mutations in either of these genes may effect the transcription of the other.

However, assuming a major role for TRPL in epithelial function based on results presented here it is possible to venture a hypothesis of TRP and TRPL function in the tubule from these results. First of all, in the wild-type fly principal cell, plasma membranes are peppered with both homo- and heteromultimers formed from TRP, TRPL and TRPγ channel subunits (see Figure 5.16 A). The overall conductance of these channels, combined with their specific inhibitory sensitivity to calcium is what controls the size of calcium influx in response to CAP_{2b} (Hardie *et al*, 1991; Obukhov *et al*, 1998; Hardie *et al*, 1998). As there is no observable sensitivity to 50 μM La^{3+}, it suggests a lack of contributory TRP/TRP homomultimers in the CAP_{2b}-induced calcium influx.

In the *trp*^{301} mutant there is a lack of expression of functional TRP channel subunits. Therefore there is an abundance of the more conductive, yet less selective, homo and heteromultimers produced from TRPL and TRPγ. This leads to a larger overall calcium conductance and subsequently larger response to CAP_{2b} (Figure 5.16 B). As one might intuitively think that a larger calcium signal would lead to a larger CAP_{2b}-induced increase in fluid secretion rate, this result seems at first a little strange. It is plausible that the poor selectivity of channels in some way disrupts the normal processes involved in calcium transport, which in turn has disrupted stimulated fluid transport, or that the influx of other bivalent cations has disrupted proper calcium signalling.

Another explanation could be that high $[Ca^{2+}]_i$ levels have an inhibitory effect on enzymes further down the CAP_{2b} signal transduction cascade. Interestingly, the potentiated CAP_{2b} calcium signal in *trp*^{301} tubules shows sensitivity to 50 μM La^{3+}, and suggests that in these tubules there are TRP homomultimers contributing to the calcium signal. However, the n-numbers in this experiment were quite low (n=4), and so the results may be misleading.

In the *trpl*^{302} tubules there is a lack of expression of TRPL channel subunits which leaves an abundance of TRP and TRPγ homo- and hetero-multimers. This leads to a lower overall calcium conductance and subsequently to a smaller CAP_{2b}-induced calcium influx (Figure 5.16 C). Here a statistically significant sensitivity to 50 μM La^{3+} is also apparent, which must be due to the presence of TRP/TRP homomultimers. Here the signal appears to be almost completely abolished and would suggest that the CAP_{2b}-stimulated calcium influx is via TRP and TRPL channels only. However, the attenuation of CAP_{2b}-stimulated $[Ca^{2+}]_i$ rises by nifedipine and verapamil (chapter 4), suggests the involvement of voltage-gated calcium channels also. It appears that both voltage-gated and TRP and TRPL calcium channels may interact to produce the CAP_{2b}-stimulated calcium influx (see chapter 7, for further discussion).

In the *trp*^{cm} tubules an attenuated calcium response to CAP_{2b} is observed, which due to the explanation given for potentiation in the *trp*^{301} mutants, cannot be explained by a lack of TRP subunits. Here one can only speculate the cause of this attenuation. It may be that *trp*^{cm} mutation causes the expression of dysfunctional TRP subunits that still interact with TRPL and TRPγ channel subunits, disrupting their function, and leading to a reduction in functional channels at the plasma membrane (Figure 5.16 D). Another explanation could be that *trp*^{cm} disrupts somehow an important signalling molecule encode by a nearby or overlapping transcript (see above and Wong *et al*, 1987), and it is the

dysfunction of this molecule that attenuates the CAP_{2b} response. It is clear though that, without clear molecular knowledge of the mutations in trp^{301} and trp^{cm}, the results here are hard to explain.

A similar situation can be seen when the response of the different mutants to thapsigargin is examined. Again the calcium signal in trp^{301} tubules is significantly potentiated reflecting the predicted higher overall channel conductivity. The thapsigargin-induced calcium response in trp^{cm} and $trpl^{302}$ tubules is not significantly different from wild type. However, the thapsigargin-induced signal is relatively small compared to the peaks induced by CAP_{2b} and any small differences from the wild type would be hard to detect. It does appear that the response in $trpl^{302}$ tubules is reduced though this is not statistically significant. From our results, it appears that neither TRP nor TRPL are activated by thapsigargin induced internal Ca^{2+} store depletion. However, it is possible that one or both may be activated in trans by calcium influx through channels activated by ER calcium release. This is evidenced by the increased calcium influx observed in the trp^{301} tubules.

One of the problems encountered in these experiments was a reduction in aequorin expression in subsequent generations of hsGAL4 containing lines. This is thought to be due to the acquisition of genetic modifiers that reduce the inducible GAL4 expression. Although the quantification of $[Ca^{2+}]_i$ takes the total amount of aequorin expressed into account, there is a level of aequorin below which the readings become unreliable. Also, because aequorin expression in a mutant background requires three separate components (UAS:aeq, hsGAL4, *trp*) the lengthy crossing scheme required to unite these three alleles becomes a constraint when doing these experiments.

The effects of the lipoxygenase inhibitor and TRPL channel antagonist CDC, on fluid secretion and $[Ca^{2+}]_i$ were examined. At 50 μM, a concentration

known to lead to the build up of PUFA's, there is the activation of a long and steady calcium influx. Whether this is due to entry through TRP or TRPL channels, can not be discerned without experiments on aequorin expressing *trp* and *trpl* mutants. Unfortunately, due to the problems outlined earlier, we are unable to carry out these experiments at present. To further speculate, CDC-induced calcium influx could be due to another effect of downstream elements of the diacylglycerol signalling pathway. The cessation of fluid secretion caused at 5 μM, a concentration known to inhibit TRPL channel conductance, in the trp^{cm} and trp^{301} tubules suggests a major role for TRPL channels in fluid transport and agrees well with previous results. Also, the lack of effect on $trpl^{302}$ and $trpl^{302};trp^{cm}$, both of which lack TRPL channel subunits appears to confirm the status of CDC as a specific TRPL channel antagonist. To clarify the effects of CDC, further experiments, investigating the direct effects of PUFA's, such as linoeic acid and arachidonic acid, could be carried out.

Overall the experiments described in this chapter have shown a role for TRP and TRPL channels in fluid transport and CAP_{2b}-stimulated calcium influx, as well as suggesting that TRPL is the main component in both these processes. However, the contribution of the recently discovered *trpγ* has still to be examined and may have profound implications on the speculated roles of these channels both in photoreceptors and in the Malpighian tubule. An overview of what might be happening in each of the *trp* and *trpl* mutants is shown in Figure 5.16, and represents accumulated results from the experiments described in this chapter.

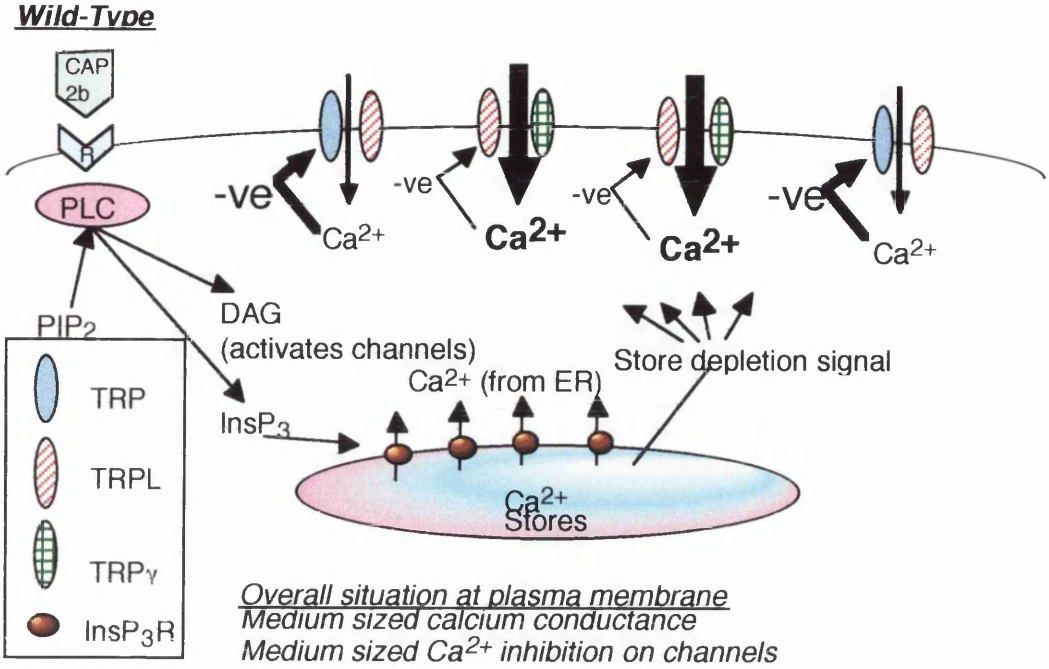
Wild-Type
CAP 2b
R
PLC
-ve
Ca2+
-ve
Ca2+
-ve
Ca2+
-ve
Ca2+
PIP2
DAG
(activates channels)
Ca2+ (from ER)
Store depletion signal
InsP3
TRP
TRPL
TRPγ
InsP3R
Ca2+ Stores
Overall situation at plasma membrane
Medium sized calcium conductance
Medium sized Ca2+ inhibition on channels

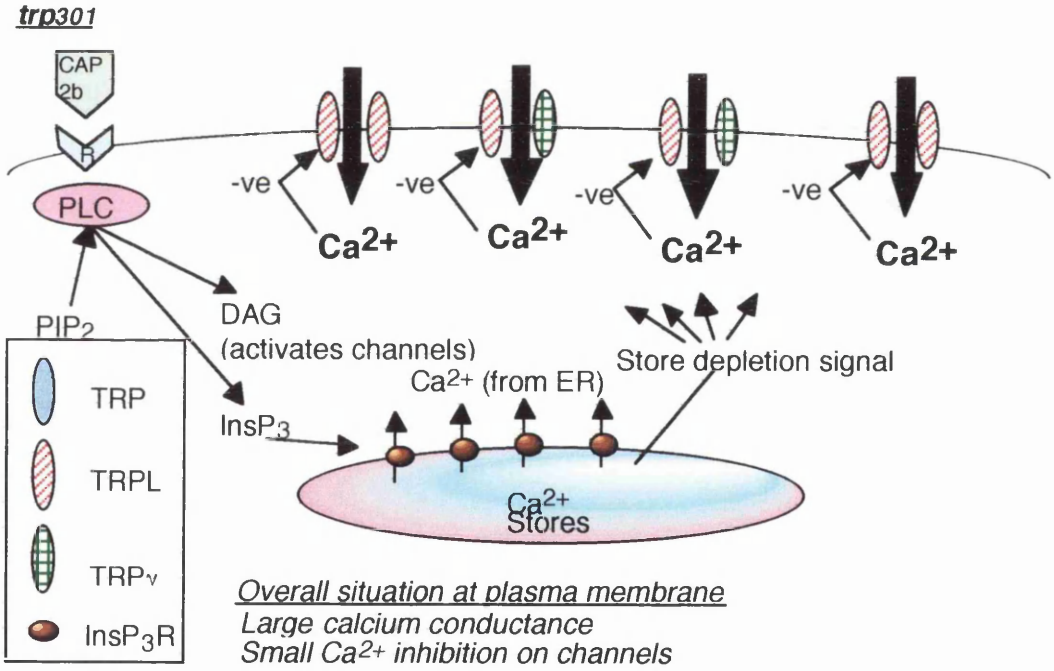
trp301
CAP 2b
R
PLC
-ve
Ca2+
-ve
Ca2+
-ve
Ca2+
-ve
Ca2+
PIP2
DAG
(activates channels)
Ca2+ (from ER)
Store depletion signal
InsP3
TRP
TRPL
TRPγ
InsP3R
Ca2+ Stores
Overall situation at plasma membrane
Large calcium conductance
Small Ca2+ inhibition on channels

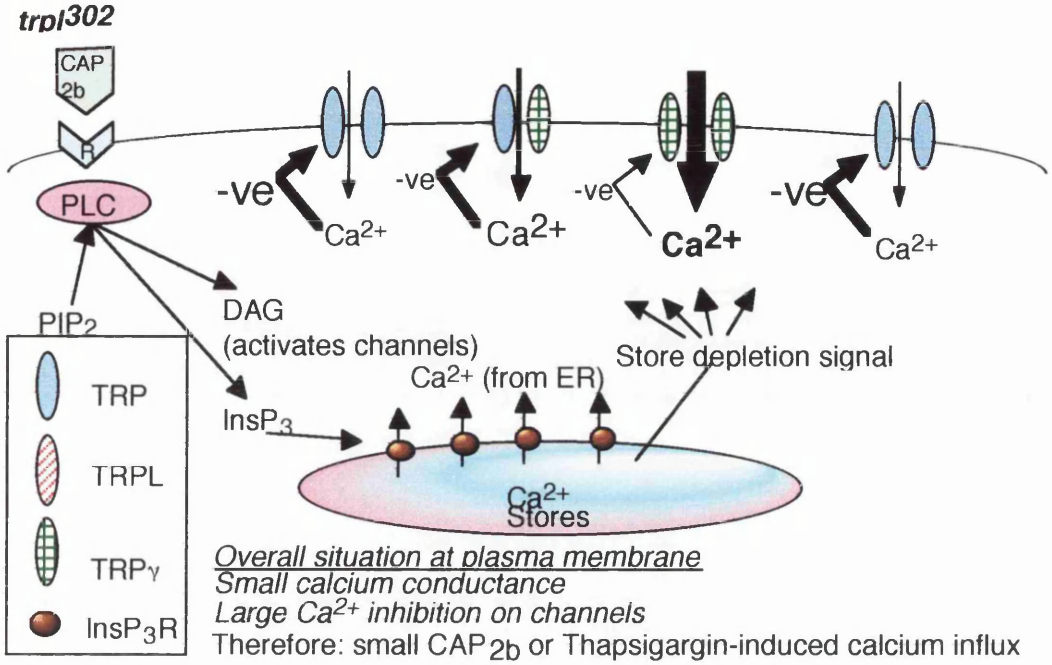

Overall situation at plasma membrane
Small calcium conductance
Large Ca^{2+} inhibition on channels
Therefore: small CAP_{2b} or Thapsigargin-induced calcium influx

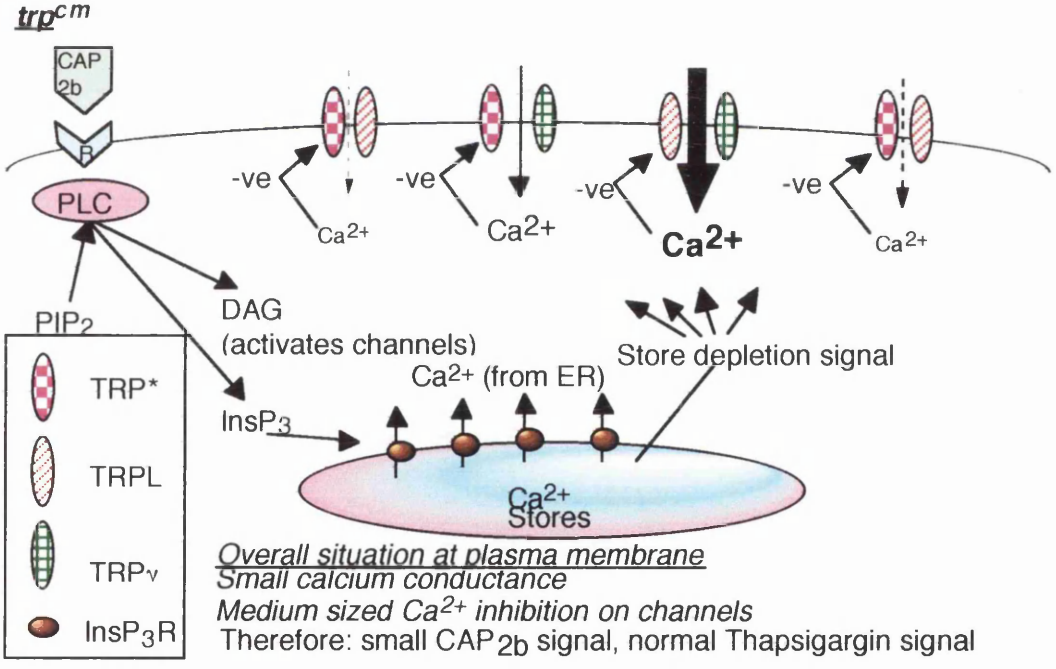

Overall situation at plasma membrane
Small calcium conductance
Medium sized Ca^{2+} inhibition on channels
Therefore: small CAP_{2b} signal, normal Thapsigargin signal

Figure 5.17: Hypothesis of calcium conductance in *trp* and *trpl* mutant tubules. Shown is a model for the situation following CAP_{2b} stimulation in wild-type *trp301*, $trpl^{302}$ and trp^{cm} tubules as indicated above. Channel conductance is indicated by the thickness of the arrows as is the inhibitory effect of Ca^{2+}. The TRP* in the trp^{cm} panel indicates a dysfunctional TRP channel subunit. For further information see text.

Chapter 6

Nitric Oxide signalling in the Malpighian tubule

Chapter 6

6.1 Summary

The experiments in this chapter examine the effects of heat shock-induced ectopic expression of *Drosophila* nitric oxide synthase. Firstly, the effect of heat shock induced expression of either the full-length *dNOS* transcript (Fly lines dN1-1B, dN1-3, and dN1-2A) or the shortened transcript (fly lines dN2-2A and dN2-3A), on unstimulated fluid secretion was examined. It was found that in dN1-2A tubules basal levels of fluid secretion were increased upon heat shock-induced expression of the full-length transcript. In dN2-2A tubules basal fluid secretion rates were decreased upon heat shock-induced expression of the shortened *dNOS* transcript. The heat shock-induced expression of DNOS was then examined in dN1-2A tubules using Western blotting and measurement of NADPH-diaphorase activity. No detectable increase in the amount of DNOS expressed was observed in dN1-2A tubules following heat shock using Western blot analysis. However, heat shocking did increase NADPH-diaphorase activity, suggesting an increase in DNOS activity. Stimulated fluid secretion was then examined in dN1-2A tubules, with cGMP, cAMP and CAP_{2b}. It was found that cGMP had no stimulatory effect on heat shocked dN1-2A tubules suggesting that this part of the signalling pathway had already been saturated by heat shock-induced DNOS expression. Both CAP_{2b} and cAMP increased the rates of fluid secretion in dN1-2A tubules. Although basal secretion rates were reduced upon heat shock in dN2-2A tubules their response to cGMP was similar to wild type. The rises in $[Ca^{2+}]_i$, induced by cGMP and CAP_{2b}, were examined in dN1-2A tubules and it was found that there was no significant difference from those produced in wild-type flies.

6.2 Introduction

Nitric oxide (NO) has been found to be both an inter- and intracellular second messenger. It was suspected to be responsible for the smooth muscle relaxation of endothelium derived relaxing factor (EDRF). Indeed, EDRF was shown to possess very similar biological properties to NO and thus deemed to be NO (Ignarro *et al*, 1987). However, Myers *et al*, 1990, found that EDRF was more similar in effect to S-nitrosocysteine, a compound that contains NO within its structure which it releases following a one-electron reduction. This suggested that NO could be complexed within a nitrosylated compound, thus facilitating its transport and durability as a second messenger. In cellular signalling, NO is produced from the oxidation of L-arginine to L-citrulline. This reaction was found to be dependent on the presence of NADPH and is catalysed by the Nitric oxide synthase enzymes (Bredt *et al*, 1990).

Nitric oxide synthases (NOS) are encoded by a large multigene family and can be divided into two general types: constitutively active, dependent on exogenous Ca^{2+}/calmodulin and inducible, independent of exogenous Ca^{2+}/calmodulin. Three different classes have been identified in vertebrates, namely neuronal, endothelial and inducible (Bredt *et al*, 1991; Lamay *et al*, 1992; Sessa *et al*, 1992; Xie *et al*, 1992), so called due to their location and effect.

In 1995 Regulski and Tully described a NOS enzyme in *Drosophila melanogaster*. This enzyme had 43% amino acid identity with rat neuronal NOS (Bredt *et al*, 1991), and like the mammalian NOS's contained binding sites for flavin adenine dinucleotide (FAD), flavin mononucleotide (FMN) and nicotinamide adenine dinucleotide phosphate (NADP). DNOS (*Drosophila* nitric oxide synthase) was found to be Ca^{2+}/calmodulin dependent when expressed in human 293 embryonic kidney cells. It is suggested that the *dNOS* gene encodes a NOS enzyme that is regulated by transient changes in intracellular calcium. This study also

found a shortened *dNOS* transcript, which would encode a protein with a 105-amino acid in-frame deletion. It is speculated that this shortened transcript may play a regulatory role in DNOS expression.

A NO/cGMP pathway was shown to be active in *Drosophila* Malpighian tubules (Dow *et al*, 1994), and the neuropeptide CAP_{2b} has been shown to stimulate fluid secretion through a rise in intracellular cGMP levels via stimulation of the DNOS enzyme (Davies *et al*, 1995). Here CAP_{2b} was shown to cause an increase in DNOS activity, measured by the conversion of [^{3}H]-L-arginine to [^{3}H]-L-citrulline, and this increase in DNOS activity was accompanied by an increase in intracellular cGMP levels. As discussed in the introduction, CAP_{2b} stimulates a rise in $[Ca^{2+}]_i$ exclusively in the main segment principal cells, and it is this rise that is thought to control DNOS activity (Rosay *et al*, 1997). Furthermore, DNOS has been localised to main segment principal cells in tubule (Davies, 2000) and suggests that this pathway is compartmentalised to this cell type. This chapter aims to further investigate the functioning of DNOS within the Malpighian tubule, and the effect of induced ectopic expression of DNOS on calcium signalling. To do this, flies containing the *dNOS* gene under control of a heat shock promoter were used. These flies were obtained from Mike Regulski, Cold Spring Harbour Laboratory, USA. Fly lines contained either the full-length *dNOS* transcript (dN1-1B, dN1-3, dN1-2A), or the truncated *dNOS* transcript (dN2-2A, dN2-3A) (M. Regulski, personal communication). Before experiments, expression of the dNOS gene was induced by heat shocking the flies at 37 ^{o}C for 30 minutes. The dN1-2A line has been used previously, to show an involvement of NO in *Drosophila* eye development (Kuzin *et al*, 2000); this line, at least has thus been validated with NOS overexpression Expression of DNOS was analysed in tubules by Western blotting and also by measurement of NADPH-diaphorase activity. This activity is a histochemical activity that reduces tetrazolium dyes, such as Nitro Blue Tetrazolium (NBT) in the presence

of NADPH. NADPH-diaphorase activity has been shown to be due to NOS (Dawson *et al*, 1991; Hope *et al*, 1991), and Huang *et al*, 1993, demonstrated a lack of NADPH-diaphorase staining in mice lacking neuronal NOS. Fluid secretion was analysed in the mutant flies following heat shock; and, although results were inconsistent, it was suggested that heat shock-induced expression of DNOS activated the cGMP signalling pathway. The effect of heat shock-induced expression of DNOS on calcium signalling was also examined, as one might speculate that a feedback regulatory mechanism occurs via components of the CAP_{2b} signalling pathway further downstream of the initially induced calcium signal.

6.3 Analysis of the transport phenotype in tubules from flies overexpressing DNOS.

Fluid secretion assays were performed on different transgenic lines containing either the *dNOS* transcript encoding the full-length transcript or that encoding the truncated DNOS protein under control of a heat shock activated promoter. Three lines contained the full-length transcript either on the first (dN1-1B), second (dN1-2A), or third chromosomes (dN1-3). Another two contained the truncated DNOS transcript found to be expressed in *Drosophila* (Regulski and Tully, 1995). It was speculated that overexpression of DNOS within the Malpighian tubule may increase fluid secretion rate by subsequent activation of soluble guanylate cyclase to increase the intracellular levels of cGMP (Figure 1.4). The basal fluid secretion rates of each fly line were measured, where one group of flies were heat shocked at 37 ^{o}C for 30 minutes and left to recover for 2-3 hours before dissection for the fluid secretion assay; and the other group left non-heat shocked. Figure 6.1 shows the average basal secretion rates for each set of flies both heat shocked and non-heat shocked. It was found that dN1-2A tubules showed a significant increase in unstimulated

fluid secretion rate following heat shock. These tubules also appeared to have a relatively high basal secretion rate without heat shock. Further to this the dN2-2A tubules showed a significant reduction in unstimulated secretion rate following heat shock. dN1-1B, dN1-3 and dN2-3A tubules showed no difference in basal secretion rates after heat shocking.

These results indicated that overexpression of the full-length *dNOS* transcript resulted in an increase in fluid secretion rate (in the case of dN1-2A), and also that overexpression of the truncated *dNOS* transcript reduced the rate of fluid secretion.

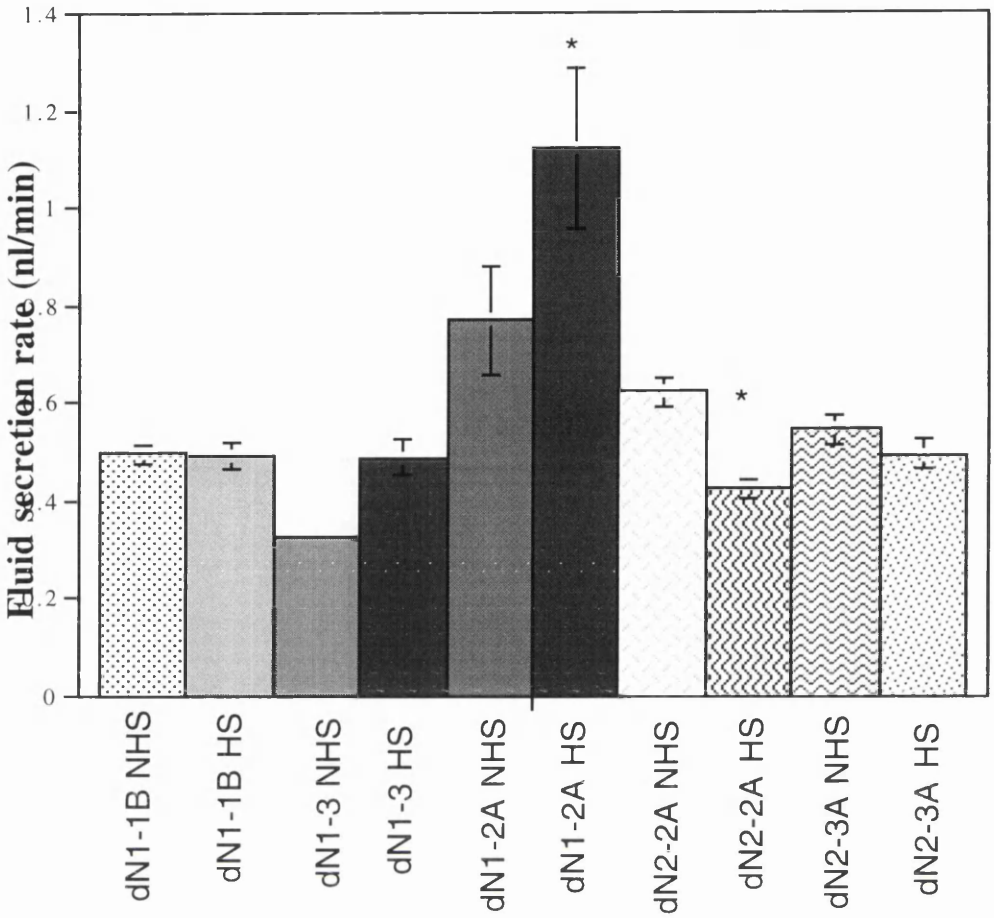

Figure 6.1: Basal fluid secretion rates in tubules overexpressing either the full length or truncated DNOS protein.

Unstimulated fluid secretion rates in dN1-1B, dN1-3, dN1-2A, dN2-2A, dN2-3A, non-heat shocked (NHS) and heat shocked (HS) tubules. The fluid secretion rates given are an average for those obtained in between two and five separate experiments, and are expressed as mean fluid secretion rate ± SEM. N=40 for dN1-1B, dN1-3, and dN1-2A. N=16 for dN2-2A and N=24 for dN2-3A. A significant change in unstimulated fluid secretion rate in tubules dissected from heat shocked flies, from those dissected from un heat shocked flies is denoted by *. *P<0.05, determined with the Srudent's *t*-test, on unpaired samples assuming unequal variances.

6.4 DNOS expression in Oregon R and dN1-2A tubules.

As dN1-2A flies were the only flies to show an obvious fluid secretion phenotype (Figure 6.1) and have been used successfully in other studies (Kuzin *et al*, 2000), further experiments concentrated on these flies. To examine the heat shock-induced expression of DNOS in tubules, Western blot analysis was performed on both OreR and dN1-2A tubules that had either been untreated or heat shocked as described previously. The effect on expression of DNOS of rearing at 18°C and 25°C was also examined. Figure 6.2 shows the expression levels of DNOS in OreR and dN1-2A tubules. Protein samples were prepared from dissected tubules and 0.5 μg per lane were separated on a 0.1 % agarose gel by electrophoresis. The protein was then transferred to a Hybond-C (nitrocellulose) membrane. The membrane was probed using a universal anti-NOS antibody (Affinity Bioreagents Inc.) specific to residues 1113-1122 of murine iNOS and nNOS (DQKRYHEDIFG). In all cases a band of around 150 kDa was obtained corresponding to the predicted size of DNOS (152 kDa) (Regulski and Tully, 1995). There did not appear to be any detectable difference in the levels of expression of DNOS between non-heat shocked and heat shocked tubules. This paradoxical finding contradicts subsequent data and is discussed later.

6.5 NADPH-Diaphorase activity in dN1-2A tubules.

The DNOS enzyme has binding sites for, NADPH, and NADPH-diaphorase activity has long been utilised as an indicator of NOS activity in vertebrates (Dawson *et al*, 1991; Hope *et al*, 1991), and insects (Muller *et al*, 1993). Therefore NADPH-diaphorase activity was examined in both non-heat shocked and heat shocked dN1-2A tubules, using a simple histochemical stain. It was found that NADPH-diaphorase activity

was significantly higher in tubules dissected from heat shocked dN1-2A flies (Figure 6.3). Together with the western data, these results seem to indicate that paradoxically, although there is no increase in the DNOS enzyme detected by Western blotting in heat shocked tubules, there is an increase in enzymatic activity.

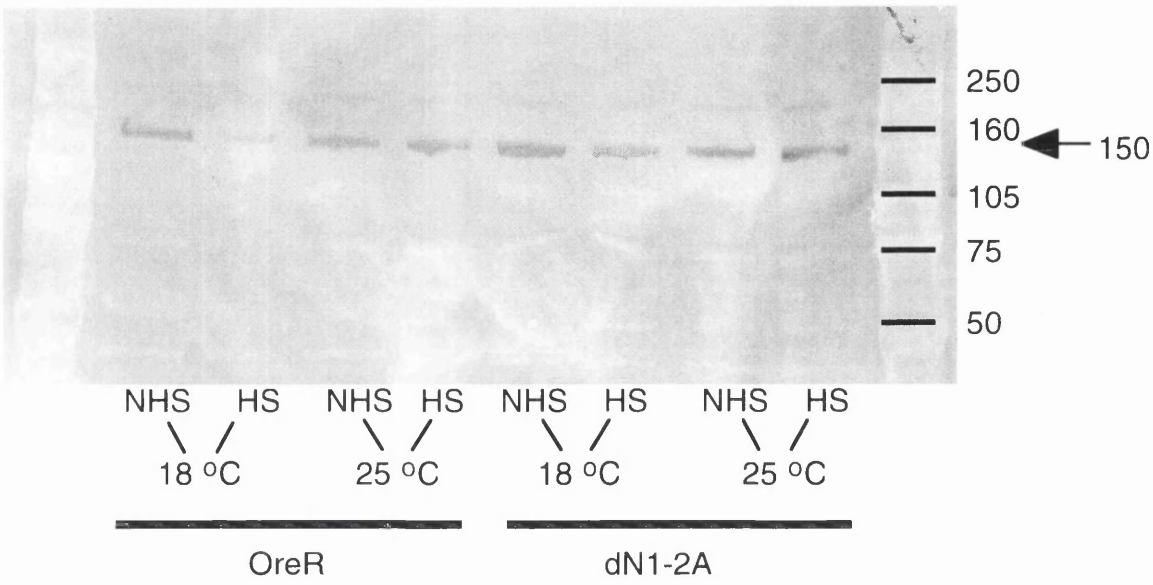

Figure 6.2: Western analysis of DNOS expression in tubules.

Results of western blot analysis using a universal anti-NOS antibody (Affinity Inc). Tubules were dissected from OreR and dN1-2A flies that had been reared at either 18 or 25 ^{o}C and then either heat shocked (HS) as described previously or not (NHS). Protein samples were prepared from the dissected tubules and then separated on a 0.1 % agarose gel (0.5 µg/lane). The proteins were then transferred to a nitrocellulose membrane (Hybond-C, Amersham), before probing using the DNOS specific antibody. One prominent band corresponding to DNOS (150 kDa) was observed.

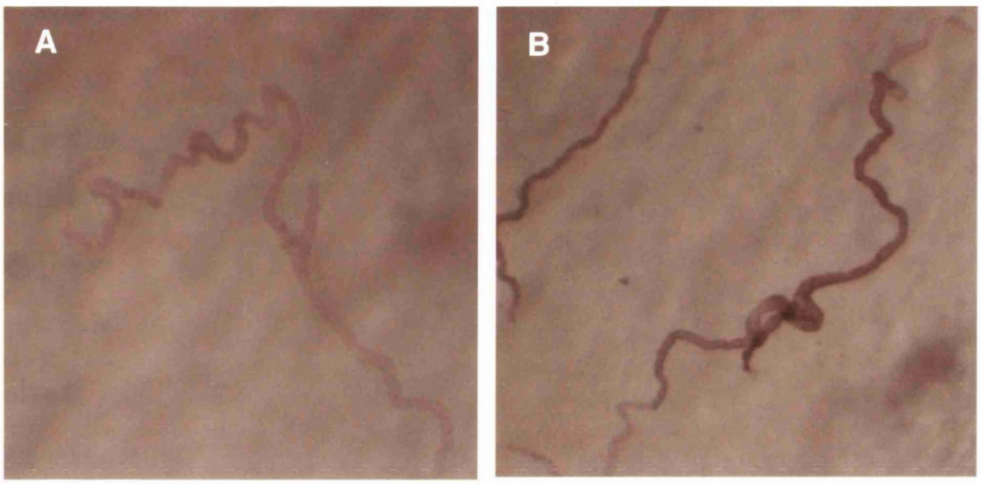

Figure 6.3: NADPH-Diaphorase activity in dN1-2A tubules.

Tubules were dissected from either heat shocked or non-heat shocked dN1-2A flies and stuck onto microscope slides coated in poly-L-lysine. The activity of NADPH diaphorase was assayed using the technique described in chapter 2.

A) NADPH-Diaphorase activity in tubules from a non-heat shocked dN1-2A fly.

B) NADPH-Diaphorase activity in tubules from a heat shocked dN1-2A fly.

The tubules shown are representative of between 6 and 10 tubules assayed on two separate occasions. There is an obvious increase of staining in heat shocked tubules (B).

6.6 Stimulated fluid secretion in dN1-2A tubules.

Fluid secretion assays were performed where the response of dN1-2A tubules to stimulation with the neuropeptide CAP_{2b}, and the cyclic nucleotides cAMP and cGMP, was measured. Secretion rates were measured for 30 minutes before stimulation with either CAP_{2b} 10^{-7}M, cAMP (1 mM) or cGMP (1 mM). As NOS was involved in the same signal transduction pathway as both CAP_{2b} and cGMP, one might expect an effect on the tubule response to either of these in dN1-2A flies. cAMP causes an increase in fluid secretion rate through a mechanism distinct from cGMP (Davies *et al*, 1995), and its concentration is not altered by CAP_{2b} stimulation. Therefore, any effect of NOS overexpression on cAMP-stimulated fluid secretion would suggest an interaction between these two signalling pathways. It became apparent during these experiments that the response to heat shock was inconsistent. Initially the unstimulated rates were generally but not always increased by heat shock. Figure 6.4 A and B provide an example of this inconsistency. Both show the response to CAP_{2b} 10^{-7}M stimulation at 30 minutes. In Figure 6.4A the basal secretion rate shows an increase following heat shock whilst there is no apparent difference in the heat shocked tubules in 6.4B. Where there was no change in basal secretion rate induced by heat shock, there was no difference in the response to CAP_{2b}, cAMP or cGMP. However, where there was an increased secretion rate there was no stimulatory effect of cGMP at 1 mM (Figure 6.4C). Both CAP_{2b} (10-7 M) and cAMP (1 mM) stimulated both heat shocked and non-heat shocked tubules equally (Figure 6.4 A and D). These results indicated that overexpression of the full length DNOS protein stimulated the cGMP pathway whilst cAMP signalling is unaffected by DNOS.

6.7 Stimulated fluid secretion in dN2-2A tubules.

Fluid secretion assays were performed on dN2-2A tubules. The basal secretion rate was measured for 30 minutes prior to stimulation with cGMP 1 mM. Unfortunately this line was lost due to fly-care inexperience, before further assays using different stimuli could be performed. However, it was observed that the basal secretion rates were significantly lower in tubules from heat shocked flies. There was no difference in the response to cGMP 1 mM in heat shocked flies.

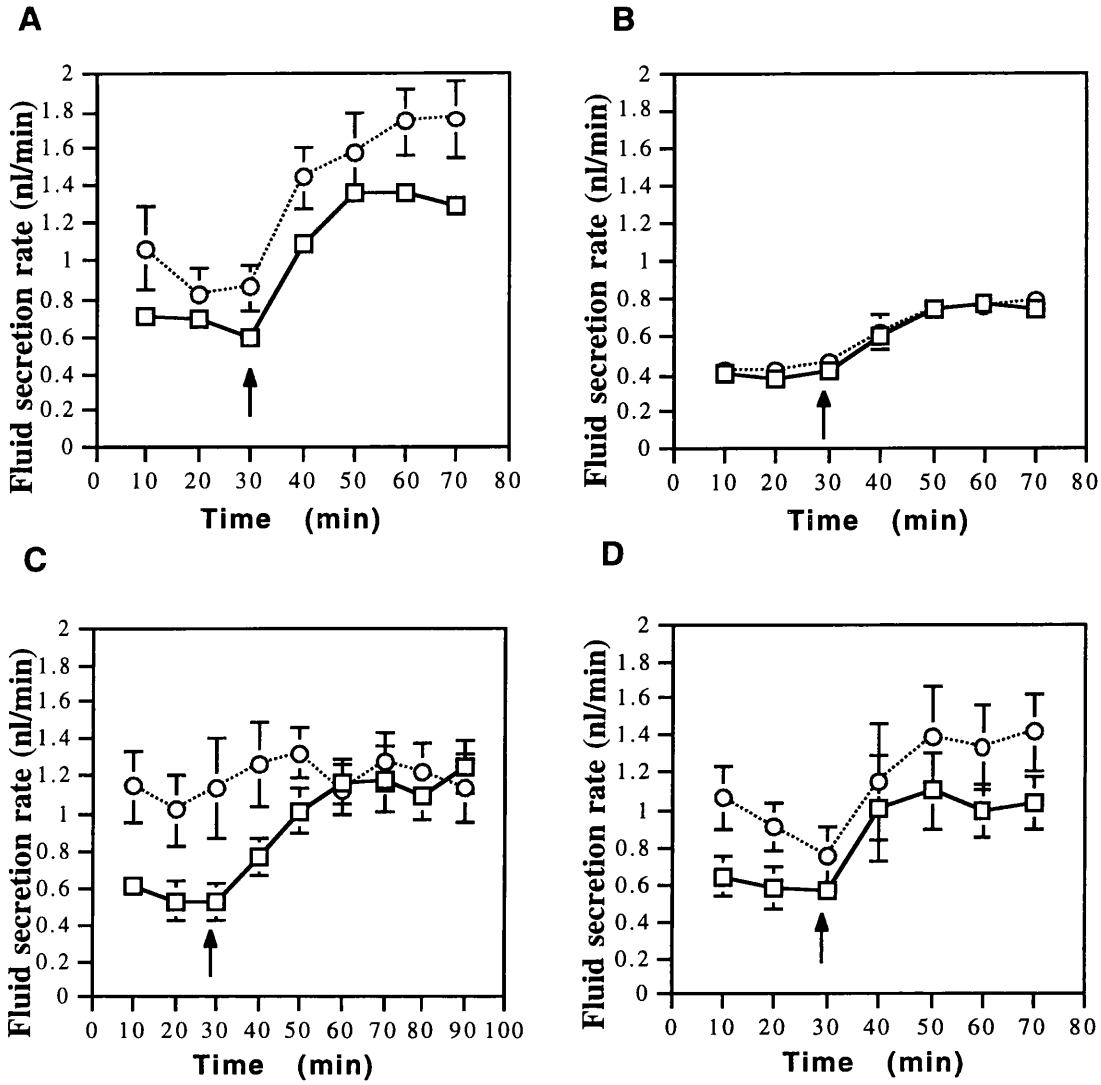

Figure 6.4: Stimulated fluid secretion in dN1-2A tubules.

Fluid secretion assays were performed on tubules dissected from dN1-2A tubules. Basal rates of secretion were measured for 30 minutes prior to stimulation with either CAP_{2b} (10^{-7} M) (A and B), cGMP (1 mM) (C) or cAMP (1 mM) (D). Prior to dissection flies were either left untreated (squares) or heat shocked at 37 ^{o}C for 30 minutes and left to recover for 2-3 hours. Results are expressed as mean fluid secretion rate ± SEM., N=6-10.

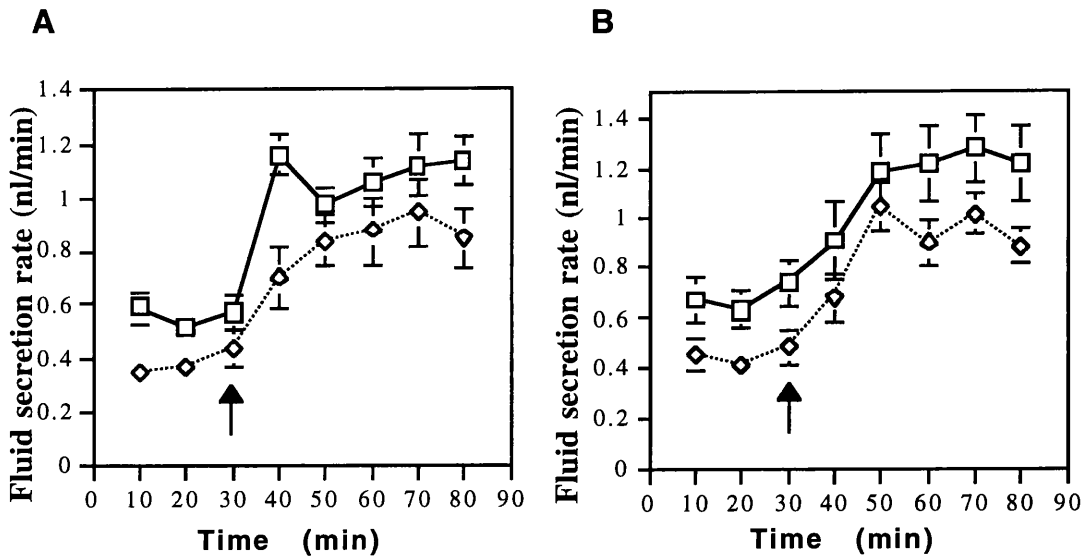

Figure 6.5: The effect of cGMP in heat shocked dN2-2A tubules.

Fluid secretion assays were performed on tubules dissected from dN2-2A tubules. Basal rates of secretion were measured for 30 minutes prior to stimulation with cGMP (1 mM). A) and B) shows cGMP stimulation on two separate occasions. Prior to dissection flies were either left untreated (squares) or heat shocked at 37 ^{o}C for 30 minutes and left to recover for 2-3 hours. Results are expressed as mean fluid secretion rate (n=6-10) ± SEM.

6.8 The effect of DNOS overexppression on cGMP induced $[Ca^{2+}]_i$ rises.

cGMP has been demonstrated to induce a prolonged $[Ca^{2+}]_i$ rise in main segment principal cells of the Malpighian tubule (MacPherson *et al*, 2001), and DNOS stimulation results in an increase in intracellular cGMP through the action of soluble guanylate cyclase (Dow *et al*, 1994). Therefore, the effect of cGMP on $[Ca^{2+}]_i$ was examined in aequorin expressing dN1-2A flies. To acquire these flies a complex crossing scheme was carried out, and is illustrated in the appendix.

Since aequorin expression in dN1-2A flies was dependent on heat shock, it was impossible to use non-heat shocked flies as our control in this crossing scheme. Furthermore, the wild type aeq;hsGAL4 flies normally used as controls were expressing aequorin at such low levels that this made $[Ca^{2+}]_i$ measurements unreliable, possibly due to the acquisition of genetic modifiers that reduced aequorin expression. Therefore c42;aeq flies which express aequorin exclusively in the main segment principal cells (Rosay *et al*, 1997), were used as a control. Results from these experiments showed that there is no significant difference between the cGMP-stimulated $[Ca^{2+}]_i$ rise in control and dN1-2A tubules (Figure 6.6).

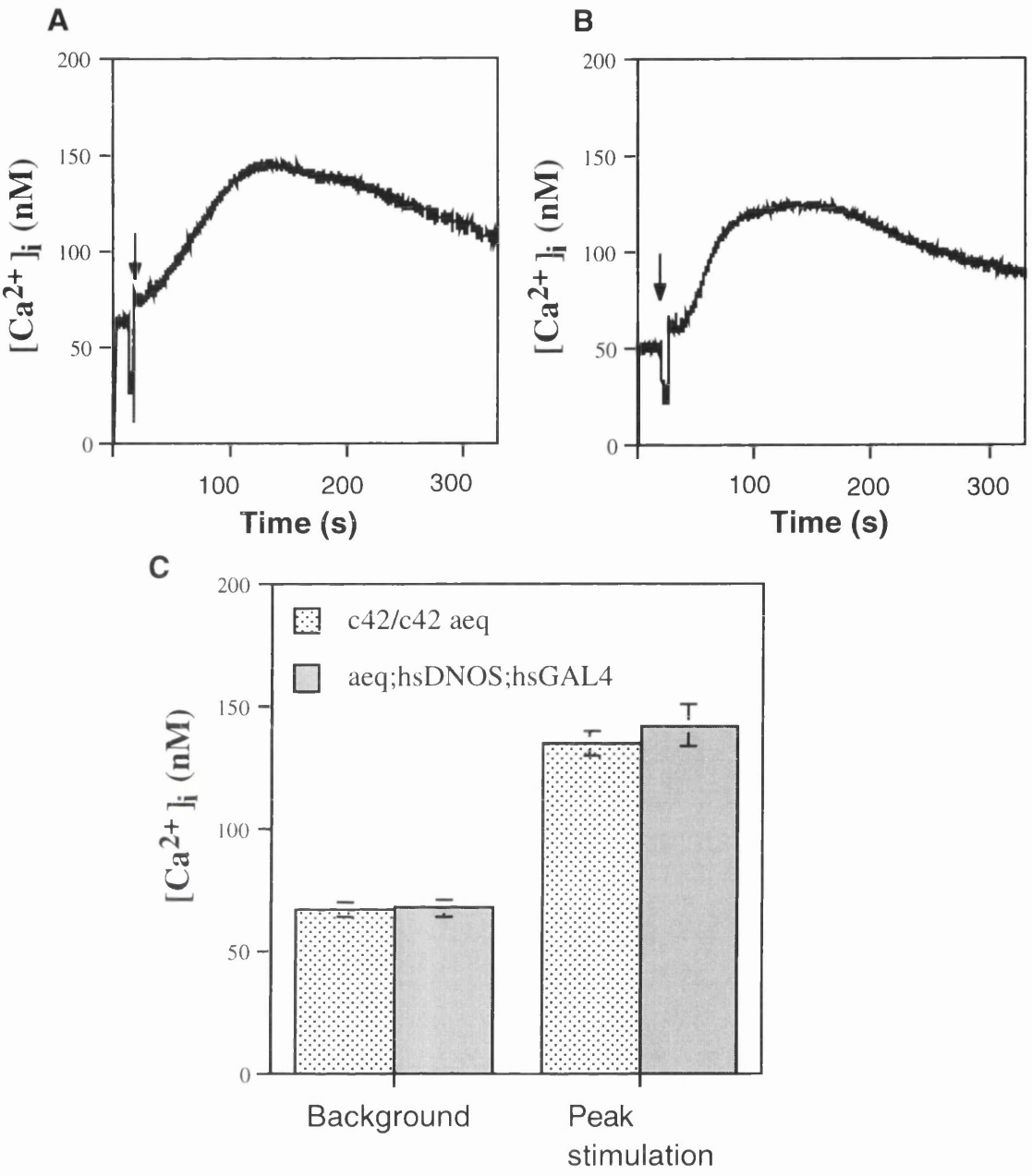

Figure 6.6: cGMP-induced $[Ca^{2+}]_i$ rises in dN1-2A tubules.

Typical traces of $[Ca^{2+}]_i$ change in c42;aeq (A) and aeq;hsDNOS;hsGAL4 (B), tubule cells upon stimulation with 1 mM cGMP.

C) Pooled results of cGMP-induced $[Ca^{2+}]_i$ rises in c42;aeq and aeq;hsDNOS;hsGAL4 tubules. Results are expressed as mean $[Ca^{2+}]_i$ (nM) ± SEM for background and peak stimulation. There was no significant difference between c42/c42 aeq cGMP-induced [Ca2+]I rise and that in aeq;hsDNOS;hsGAL4.

6.9 The effect of DNOS overexpression on CAP_{2b}-stimulated $[Ca^{2+}]_i$ rise.

CAP_{2b} is known to induce a biphasic $[Ca^{2+}]_i$ rise exclusively in main segment principal cells of the Malpighian tubule. It is also known to stimulate fluid secretion through a cGMP/DNOS pathway (Dow *et al*, 1994; Davies *et al*, 1995). Therefore, the effects of CAP_{2b} on $[Ca^{2+}]_i$ were examined in dN1-2A tubules. c42;aeq tubules were used as a control, for reasons explained in the previous section. The results are shown in Figure 6.7. There was no significant difference in the CAP_{2b}-induced $[Ca^{2+}]_i$ rises observed in dN1-2A tubules.

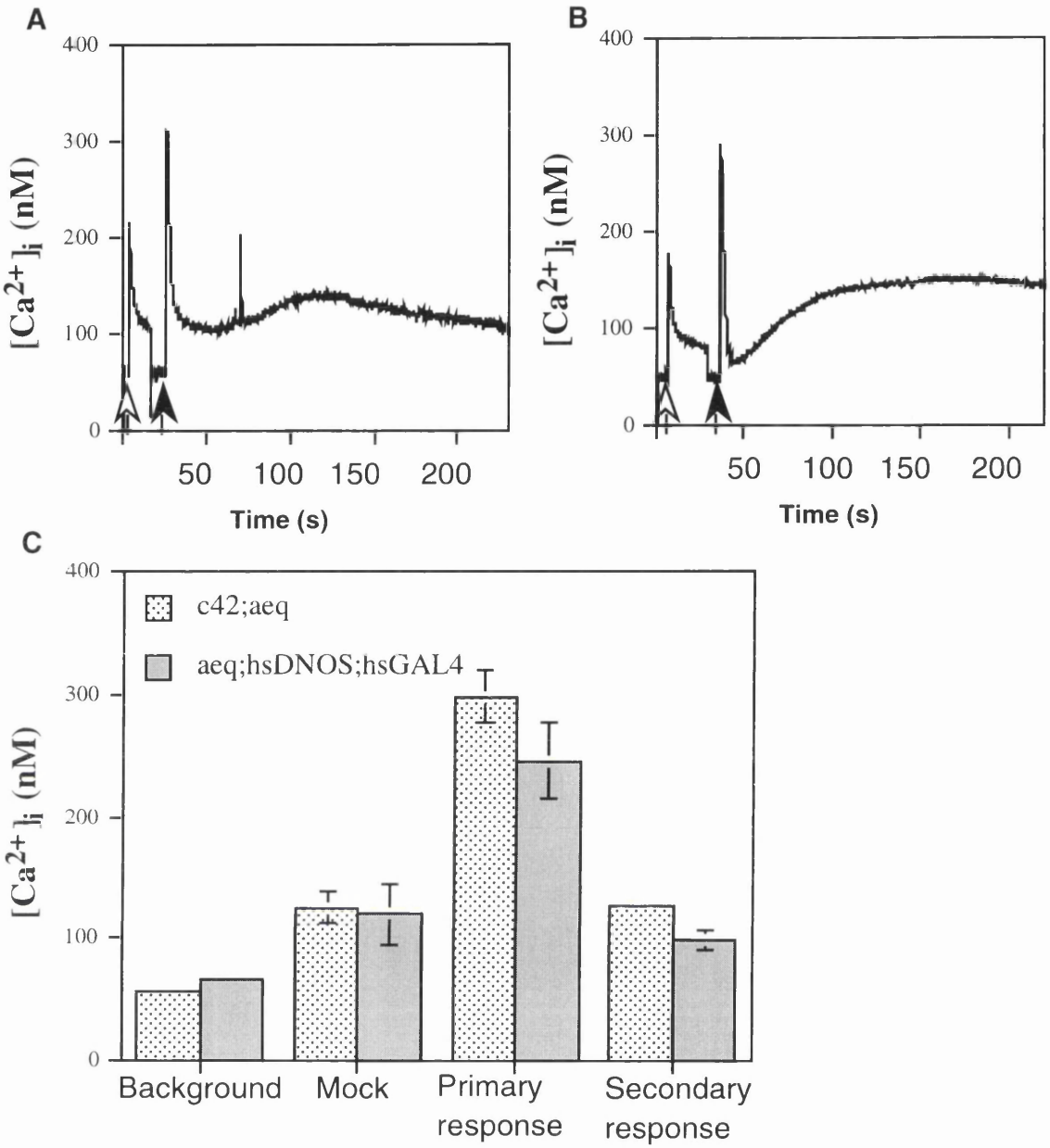

Figure 6.7: CAP_{2b}-induced $[Ca^{2+}]_i$ rise in dN1-2A tubules.

Typical traces of $[Ca^{2+}]_i$ change in c42;aeq (A) and aeq;hsDNOS;hsGAL4 (B), tubule cells upon stimulation with CAP_{2b} 10^{-7} M.

C) Pooled results of cGMP-induced $[Ca^{2+}]_i$ rises in c42;aeq and aeq;hsDNOS;hsGAL4 tubules. Results are expressed as mean $[Ca^{2+}]_i$ (nM) ± SEM., N=8 for background, mock injection, primary response and secondary response. There was no significant difference between the CAP_{2b} calcium response in aeq;hsDNOS;hsGAL4 from that in c42;aeq.

6.10 Discussion

The experiments described in this chapter aimed to examine the effects of DNOS in tubule principal cells. DNOS was already known to be expressed in this tissue (Davies *et al*, 1995) and to be involved in the principal cell response to the neuropeptide CAP_{2b}. Here, transgenic lines were utilised that contained either the full length or shortened form of the *dNOS* transcript under control of a heat shock promoter. Initial experiments with these flies involved heat-shocking flies at 37 °C for 30 minutes prior to recovery for one hour and subsequent experimentation. However, results obtained were inconsistent (see Figure 6.4), and a variety of heat shock methods were tried, including repetitive daily heat shocks and varying times of shock and recovery. It was found that there was no improvement in the consistency of results. Further to this lines were reared under different environmental conditions; indeed, when dN1-2A flies were kept at 18°C, they showed a significant rise in basal fluid secretion rates: from 0.4 ± 0.1 nl/min (flies reared at 25°C) to 2.0 ±0.2 nl/min (flies reared at 18 °C). However, these results could not be verified, and so the original heat shock conditions were used. The heat shock-induced expression of DNOS in dN1-2A tubules was examined using Western blotting and NADPH-diaphorase staining. No detectable difference in DNOS expression was observed following heat shock using Western blot analysis. However, a universal anti-NOS antibody was used to detect the DNOS protein and this may have compromised accurate quantification of DNOS expression. However, a significant increase in NADPH-diaphorase activity was observed in dN1-2A tubules following heat shock; as such, these results suggest that DNOS activity was increased following heat shock in dN1-2A tubules.

Over a series of experiments dN1-2A tubules were found to have an increased basal fluid secretion rate. This may be caused by an increase in DNOS

activity. It was also found that cGMP had no extra stimulatory effect on heat shocked dN1-2A tubules. This suggested that the intracellular cGMP had been increased in these tubules. This is supported by data from experiments that demonstrated an increase in intracellular cGMP levels in dN1-2A tubules following heat shock (S.A. Davies, personal communication). As CAP_{2b} lies upstream of DNOS in this signalling pathway, one might expect its effect to be attenuated in heat shocked dN1-2A tubules if it works solely through NOS to stimulate cGMP increases. However, it may be that the stimulatory effect of CAP_{2b} is set by the Ca^{2+} signal, and would be unaffected by DNOS overexpression. It was found that the effect of CAP_{2b} remained the same in heat shocked tubules. It seems as though CAP_{2b} may increase fluid secretion rate through other signalling mechanisms, activated by calcium, as well as through an increase in intracellular cGMP.

In dN2-2A tubules a reduction in basal fluid secretion rates was observed following heat shock. As the truncated *dNOS* transcript has been speculated to play a regulatory role in *dNOS* expression (Regulski and Tully, 1995), it appears that the truncated transcript may be reducing the level of DNOS activity. This may result in lower cGMP levels and thus a reduction in fluid secretion. As this line was lost this hypothesis cannot be confirmed. There was no difference in response to cGMP observed in dN2-2A tubules following heat shock. This might be expected as in the DNOS/cGMP signalling pathway, cGMP lies downstream of DNOS, and any speculated reduction in DNOS activity would be bypassed by adding cGMP normally produced by DNOS activation.

No difference was observed in the CAP_{2b}-or cGMP-induced calcium signals in dN1-2A tubules. Due to possible feedback mechanisms affecting calcium signalling caused by signalling molecules downstream of CAP_{2b} in the pathway, attenuation in CAP_{2b} signalling may be expected. However, due to the central

position of DNOS in the signalling pathway, one may speculate that any change in activity may be immediately compensated for under the experimental conditions. This could also be the reason for the inconsistent results obtained for the dN1-2A tubules in fluid secretion experiments. It may be that an obvious and consistent phenotype in these tubules may only be uncovered under different conditions. Indeed, recent experiments, by Kate Broderick, have examined the effects of the phosphodiesterase (PDE) inhibitor, Zaprinast, on CAP_{2b}- stimulated fluid secretion in dN1-2A flies. Phosphodiesterase is an enzyme that breaks down cAMP and cGMP to their non-cyclic derivatives. Initial results have shown a significant increase in basal and CAP_{2b}-stimulated fluid secretion, in heat shocked flies following Zaprinast application. Thus, the transport phenotype seen in the dN1-2A line may hinge on the state of the cGMP-dependent PDE, suggesting the central importance of cGMP in maintaining fluid transport in *Drosophila* tubules following heat shock and Zaprinast application. It seems that in further experiments using these flies, a more complex manipulation of signalling mechanisms involving DNOS may tell us more about the functioning of this enzyme.

hapter 7

Chapter 7

7.1 Discussion and conclusions.

In the preceding chapters the function and contribution of various calcium channels to signalling mechanisms in Malpighian tubules has been examined. This has involved physiological and molecular approaches to examine the effect of mutations in calcium channel genes (as in chapter 5), or the effect of calcium channel antagonists (chapters 4 and 5). Further to this, the regulatory effects of signalling molecules further downstream of initial calcium signal production, for example DNOS and cGMP, have been examined (chapters 4 and 6). To simplify the integration of results, conclusions on the functioning of DNOS have been confined to chapter 6 and are not discussed further here.

The aim of these studies was firstly to develop further the Malpighian tubule as a model epithelial in which to study cell specific signalling events using signalling mutants, and also to examine these signalling events with respect to fluid transport. Although the results from this work have already been discussed within the relevant Results chapters, described below is a more comprehensive overview of how coordinated signalling mechanisms may occur in tubules.

Many of the cell signalling events which contribute to fluid transport by the tubule have been well characterised (Davies *et al*, 1995; Davies *et al*, 1997; Rosay *et al*, 1997; Davies, 2000). This has been discussed fully in chapter 1, and is illustrated in figure 1.4. Here, the calcium channel components of this CAP_{2b}-stimulated $[Ca^{2+}]_i$ rise and the interactions between these channels which results in such a calcium signal have been discussed.

To simplify the results regarding calcium signalling, described in chapters 3-5, a summary of results and their implications (**in bold**) follows.

1: *Dmca1D* and *Dmca1A* are expressed in the tubule, α1 subunits appear to be located on both the apical and basolateral membranes of the main segment principal cells. Also, stimulated fluid secretion is inhibited by verapamil and nifedipine, which are known L-type calcium channel antagonists.

1. Dmca1A and Dmca1D are involved in principal cell-specific calcium signalling events and epithelial fluid transport.

2: The CAP_{2b}-stimulated $[Ca^{2+}]_i$ rise is sensitive to inhibition by verapamil and nifedipine.

2.The influx of extracellular calcium stimulated by CAP_{2b} occurs in some part via PAA- and DHP-sensitive channels possibly Dmca1A and Dmca1D.

3: cGMP stimulates the influx of calcium into the main segment principal cells via verapamil- and nifedipine-sensitive calcium channels.

3.a) A cyclic nucleotide-gated (CNG) calcium channel is present in principal cells and involved in verapamil- and nifedipine-sensitive calcium influx (MacPherson *et al*, 2001).

or

b) Dmca1D or Dmca1A is stimulated by a cGMP-dependent protein kinase to allow influx of external calcium.

or

c) Dmca1A and Dmca1D are *trans* stimulated by calcium entering via the CNG mentioned in 3a) and are responsible for the detectable cGMP-stimulated rise in $[Ca^{2+}]_i$ but not its initiation.

4: Thapsigargin induces an influx of calcium in main segment principal cells through, in part, a verapamil-sensitive calcium channel (MacPherson *et al*, 2001).

4.a) The depletion of calcium from internal stores stimulates the influx of extracellular calcium through Dmca1A, or other verapamil-sensitive calcium channels.

or

b) The depletion of calcium from internal stores stimulates an endogenous capacitative calcium entry channel, which stimulates the influx of calcium through Dmca1A, or other verapamil-sensitive channels.

5: *trp*, *trpl* and *trpγ* are all expressed in *Drosophila* tubules. TRP is located exclusively in the main segment principal cells; TRPL appears to be present throughout the tubule on the apical, basolateral and nuclear membranes.

5.TRP, TRPL and TRPγ are involved in Malpighian tubule function.

6: The CAP_{2b}-induced $[Ca^{2+}]_i$ rise in $trpl^{302}$ tubules is attenuated to 35% of normal levels and is sensitive to micromolar concentrations of lanthanum, which is known to block TRP. There is no effect of 5 μM CDC on unstimulated fluid transport rates in the mutant.

6.The TRPL channels play a major role in the CAP_{2b}-induced influx of calcium. In these mutants there is an inferred presence of TRP/TRP homomultimers.

7: The CAP_{2b}-induced $[Ca^{2+}]_i$ rise in trp^{301} tubules is potentiated to 135% of normal and is sensitive to lanthanum. In this mutant, basal fluid transport is inhibited by 5 μM CDC, a concentration known to inhibit TRPL function.

7.a) The potentiated CAP_{2b} calcium signal may be caused by an abundance of more conductive TRPL channels in these mutants, where the less conductive TRP channels are absent.

or

b) The potentiated CAP_{2b} signal could be caused by a mislocalisation of regulatory signalling molecules, such as PLC and PKC, thus allowing misregulation of membrane located TRPL channels.

and

c) The importance of TRPL channels in epithelial fluid transport is demonstrated by the inhibitory effect of CDC.

8: The CAP_{2b}-induced $[Ca^{2+}]_i$ rise in trp^{cm} tubules is attenuated to 49% of normal and is insensitive to lanthanum. 5 μM CDC, a concentration known to inhibit TRPL channels, inhibits unstimulated fluid transport rates in this mutant.

8.a) The attenuation of signal could arise from the disruption of normal channel function by dysfunctional TRP subunits.

or

b) Alternatively, the mutation in TRP could result in the mislocalisation of other signalling molecules, such as PLC and PKC important in the regulation of calcium channels.

and

c) As in trp^{301} mutants, the importance and presence of TRPL channels is shown by the inhibitory effect of 5 μM CDC.

9: *norpA*, *plc-21*, both encoding phospholipase C's, *pkc53e* and *inaC*, both encoding protein kinase C's, are expressed in the *Drosophila* Malpighian tubule. *inaD* (encoding the INAD protein) is not expressed in tubules.

9.- The expression of genes encoding PLC's suggests that CAP_{2b} may activate calcium entry through the G-protein activation of PLC's, that induce calcium release from internal stores, resulting

in calcium influx. The expression of genes encoding PKC's suggests that these may be involved in the regulation of calcium influx channels, such as is observed in *Drosophila* photoreceptors. The absence of expression of *inaD* demonstrates a difference in photoreceptors and tubules.

From our results it is apparent that at least TRP, TRPL, Dmca1D and Dmca1A and possibly others are involved in the production of CAP_{2b}- or thapsigargin-stimulated calcium signals in the tubule principal cell. How then do these channels interact to produce such signals? The involvement of several channels in the cellular response to a stimulus is not unusual. A good example of this process occurs in *Drosophila* phototransduction. It was in the *Drosophila* retina that the *trp* mutant phenotype was first discovered (Cosens and Manning, 1969). TRPL was also required to work together with TRP to produce the light-activated conductance in photoreceptor cells (Neimeyer *et al*, 1996). More recently, the involvement of other calcium channels in the *Drosophila* photoresponse was shown by Smith *et al*, 1998, who demonstrated abnormal ERG's in flies with mutations in the *Dmca1A* gene (see Figure 1.8). Another interesting aspect of this study was the diversity of ERG phenotype in the different *Dmca1A* mutants. This could be due to the mutations lying within differently spliced exons of genes with differing calcium signalling regulatory importance in the photoreceptor. This demonstrates the diversity of phenotypes from mutations in the same gene and is similar to the situation in tubules, where different phenotypes of trp^{301} and trp^{cm} are observed. It has been suggested (Smith *et al*, 1998) that Dmca1A and possibly other ion channels may be involved in the calcium-mediated light-activated current, subsequent to the light-dependent initiation of retinal depolarization, which is mediated by TRP, TRPL and possibly TRPγ currents (Neimeyer *et al*, 1996; Xu *et al*, 2000). A similar

situation can be envisioned with the principal cell response to CAP_{2b}, in that several types of channels or calcium signalling events produce the cell's calcium response. Certainly both nifedipine-sensitive and verapamil-sensitive calcium channels, as well as TRP and TRPL calcium channels seem to be involved in the CAP_{2b}-induced $[Ca^{2+}]_i$ rise. It seems possible that mutations in calcium channel genes that reduce their expression have an indirect effect on the expression of other calcium channels. Using this argument, mutations that reduce *trp* expression may lead to an increase in the expression of *trpl* or *Dmca1A*. This theory correlates well with our results, as in the trp^{301} flies the potentiated CAP_{2b} response could be explained by increased expression of TRPL and Dmca1A channels. TRPL channels have been shown to be ten times as conductive as TRP channels (Vaca *et al*, 1994), and so increased expression of TRPL may increase the total calcium conductance of the plasma membrane. As Dmca1A appears to be involved in the CAP_{2b} response (by the sensitivity of the CAP_{2b} signal to verapamil) an increase in expression of this channel in the principal cell may also be theorised to increase the calcium signal in response to CAP_{2b}. Another possibility is that the calcium signal is produced by the sequential activation of different channels. A similar mode of calcium channel activation has been proposed by Barry *et al*, 1998. Here, stimulation of mouse distal convoluted cells with chlorothiazide activates an $\alpha 1C\beta 3$ calcium channel. This results in membrane hyperpolarisation, and, it is suggested, the activation of another, as yet unidentified voltage-gated calcium channels.

The sequential stimulation of calcium channels is difficult to examine in tubules. This is because expression of transgenic aequorin in the cytosol, gives us an average measure of calcium concentration, and so any small localised calcium signalling events, such as can be visualised in individual

cells using calcium fluorescent dyes (Bootman *et al*, 1997), cannot be detected.

It is also possible that the defect in calcium signalling in the *trp* and *trpl* mutants may be due to the mislocalisation of TRP or TRPL. Such a situation has been observed in photoreceptors where it was found that the interaction between TRP and INAD was critical in the retention of PKC and PLC in the rhabdomeres (a part of the photoreceptor cell). It has been suggested that the main purpose of INAD and TRP is to retain the correct localisation of signalling molecules. It was found that in young *inaD* mutant flies, where the interaction between INAD and TRP was disrupted, signalling molecules were correctly located and the photoresponse unaffected (Li *et al*, 2000). As the flies grew older, PKC and PLC dispersed around the cell and the *inaD* mutant phenotype became apparent. In this study it was also found that TRPL did not require an interaction with either INAD or TRP for it's correct localisation to the tips of the Rhabdomeres. As we are speculating a major role for both the TRPL and L-type calcium channels a mutation in TRP should not affect the CAP_{2b} signal. However, as we see an attenuation of response in the trp^{cm} tubules, one can speculate that this mutation has somehow disrupted the interaction of TRP with an 'anchoring' protein other than INAD (*inaD* is not expressed in tubules), thus failing to tether the required signalling molecules for correct calcium signalling in this case.

It is apparent that many questions concerning the mechanisms of calcium signalling in the tubule have still to be resolved. However, the work presented here has added to that previously known about calcium signalling in the tubule, as well as demonstrating the amenability of this model epithelia for such studies.

Appendix 1

Primers used in this thesis

Primer Name	Sequence
Trp Forward	5'-AGAATACTTTCGCCTCCGATCC-3'
Trp Reverse	5'-CCTGGTTTCTTGTCATCCGTTG-3'
Trpl Forward	5'-GCTACTCAACCAAATCAGTGCTGAA-3'
Trpl Reverse	5'-TGGCAATGGAGCTAATGTCGG-3'
Trp gamma Forward	5'-AGTCGGAAACGTGAGCAAAATG-3'
Trp gamma Reverse	5'-TGGAGTTCACTGACGTATTTGGATG-3'
Dmca1A Forward	5'-TAGGGATCGGGATCGTGATAGG-3'
Dmca1A Reverse	5'-TTGTCGTTGGTTTTGGGTTAGG-3'
Dmca1D Forward	5'-TCCTTCCAGGCACTGCCCTACG-3'
Dmca1D Reverse	5'-GCGAATAAACTCGTCCAAGTGG-3'
CG1517 Forward	5'-CCATTATGAGAGCACCAAGACCC-3'
CG1517 Reverse	5'-ATGAACACCCAACCCTCCTGTG-3'
InaC Forward	5'-TGGTGAGGGGCATGTAAAGCTG-3'
InaC Reverse	5'-TGGGAGTTAAGTCCGTCTTCTCC-3'
Pkc53e Forward	5'-AGACCACAAAGACTTTCTGCGG-3'
Pkc53e Reverse	5'-GGCTTAAATGGCGGTTGCAC-3'
InaD Forward	5'-CGTCAAGCCCATCAAAAAGTTC-3'
InaD Reverse	5'-CGTGACATGGTTGTTCTTGCC-3'

Appendix 2

Drosophila and *E.coli* media

Drosphila media

Standard growth media per litre of water

- 10 g agar
- 15 g sucrose
- 30 g glucose
- 35 g dried yeast
- 15 g maize meal
- 10 g wheat germ
- 30 g treacle
- 10 g soya flour

Escherichia coli growth media

L-broth per litre of water

- 10 g Bacto-tryptone
- 5 g yeast extract
- 10 g NaCl

L-agar per litre of water

- 10 g Bacto-tryptone
- 5 g yeast extract
- 10 g NaCl
- 15 g Bacto-agar

SOC broth

- 2% tryptone
- 0.5% yeast extract
- 10 mM NaCl
- 2.5 mM KCl
- 10 mM $MgCl_2$
- 10 mM $MgSO_4$
- 20 mM glucose

Appendix 3

Solutions for use in Northern blotting

Oligo Labelling Buffer

5x OLB

To a tube of Pharmacia (50 OD units) hexamers add:

550 ml TE

917 ml 2 M HEPES (pH 6.6)

350 ml Solution _*

6.6 ml b-mercaptoethanol

1.85 ml of 100 mM stock of dATP, dGTP, dTTP

Store in 100 ml aliquots at -20°C.

*Solution _

1.25 mM Tris (pH 8)

0.125 mM $MgCl_2$

Church's Buffer

0.25 M Na_2HPO_4

7 % SDS

1 % BSA

1 mM EDTA

pH 7.2

Appendix 4

Solutions for use in Western blotting

Running Buffer

1 M Glycine

1 M Tris base

10 % SDS

Transfer Buffer

1 M Glycine

1 M Tris base

20 % methanol

Appendix 5 *Drosophila* crossing Schemes.

Marking chromosomes in *trp* an *trpl* flies

a) Scheme for trp^{cm}

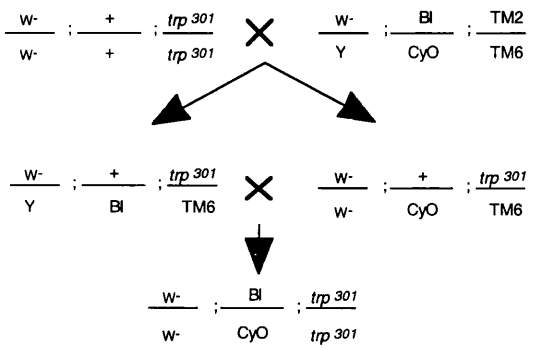

b) Scheme for trp^{301}

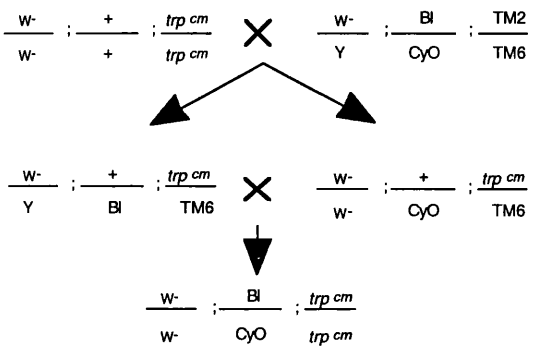

c) Scheme for $trpl^{302}$

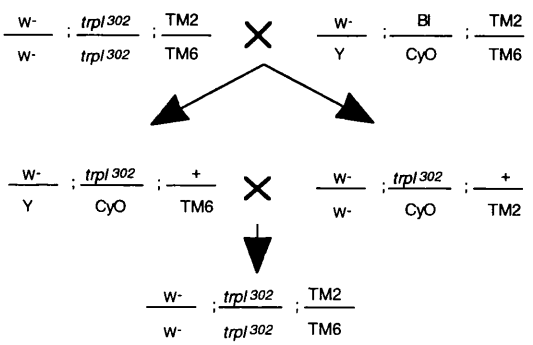

Cross for aequorin-expressing *trp^{cm}*.

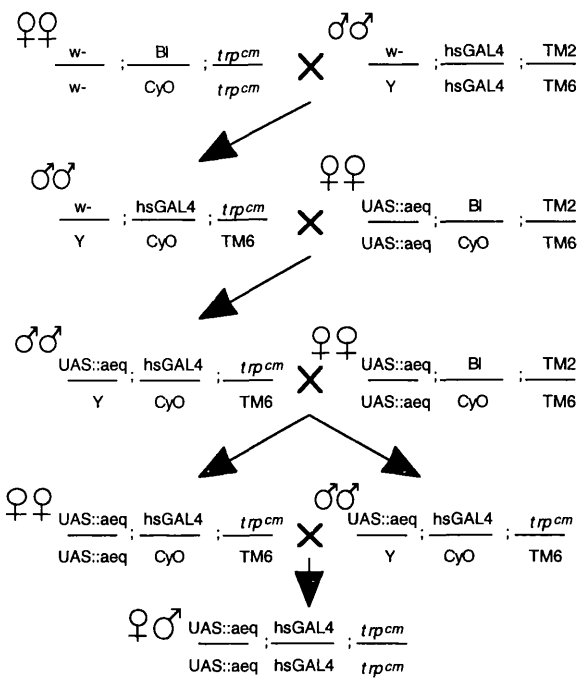

Cross for aequorin-expressing *trp^{301}*.

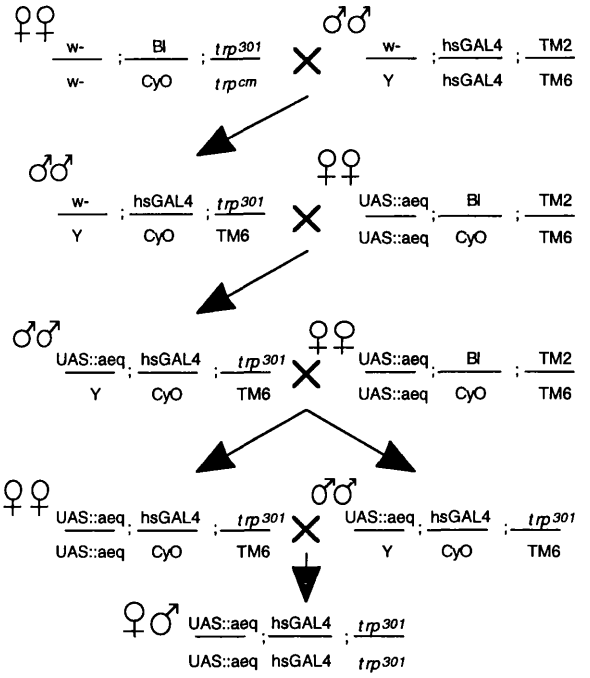

Crossing Scheme for aequorin-expressing *trpl^{302}*.

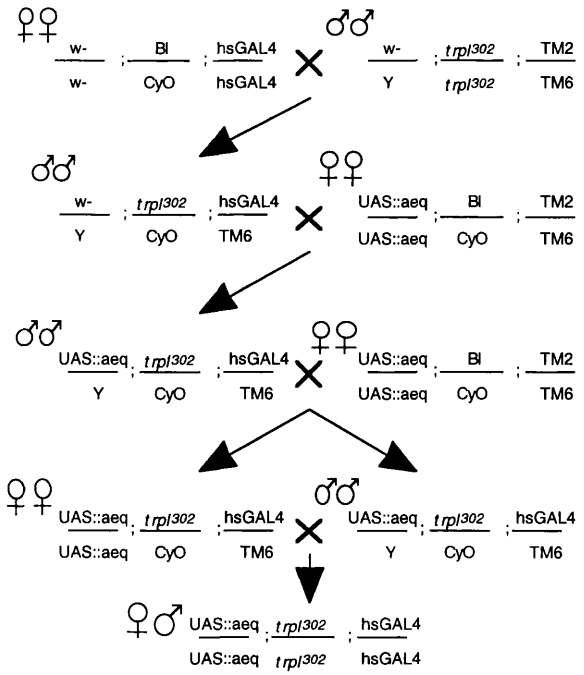

Crossing Scheme for aequorin expressing dN1-2A.

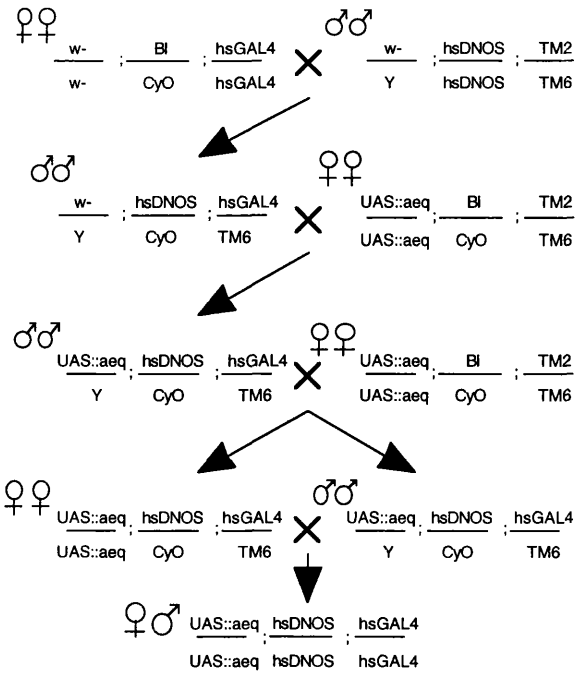

Ca^{2+} current	Organism/ tissue	DHP sens	Conc.	PAA sens	Conc.	Cation sensitivity	References
Pelzer 8pS	Drosophila head	-	Tested at $4*10^{-6}$ M	+	10^{-9} M	blocked by 10^{-2} M Co^{2+}	Pelzer *et al*, 1989
Pelzer 12pS	Drosophila head	-	Tested at $4*10^{-6}$ M	+	10^{-9} M	blocked by 10^{-2} M Co^{2+}	Pelzer *et al*, 1989
Pelzer 20pS	Drosophila head	+	10^{-8} M	-	tested at $2*10^{-5}$ M	blocked by 10^{-2} M Co^{2+}	Pelzer *et al*, 1989
Pelzer 32pS	Drosophila head	+	10^{-8} M	-	tested at $2*10^{-5}$ M	blocked by 10^{-2} M Co^{2+}	Pelzer *et al*, 1989
Pelzer 40pS	Drosophila head	-	Tested at $4*10^{-6}$ M	+	10^{-9} M	blocked by 10^{-2} M Co^{2+}	Pelzer *et al*, 1989
Pelzer 52pS	Drosophila head	-	Tested at $4*10^{-6}$ M	+	10^{-9} M	blocked by 10^{-2} M Co^{2+}	Pelzer *et al*, 1989
Pelzer 66pS	Drosophila head	-	Tested at $4*10^{-6}$ M	+	10^{-9} M	blocked by 10^{-2} M Co^{2+}	Pelzer *et al*, 1989
Pelzer 84pS	Drosophila head	-	Tested at $4*10^{-6}$ M	+	10^{-9} M	blocked by 10^{-2} M Co^{2+}	Pelzer *et al*, 1989
Morales A	Drosophila peptodergic terminals	+	$IC_{50}=2*10^{-4}$ M	+	$IC_{50}=3*10^{-5}$ M	blocked by $2*10^{-4}$ M Cd^{2+}	Morales *et al*, 1999
Morales B	Drosophila muscle membranes	+	$IC_{50}=3*10^{-6}$ M	+	$IC_{50}=2*10^{-4}$ M	blocked by $2*10^{-4}$ M Cd^{2+}	Morales *et al*, 1999
Gielow	Drosophila larval muscle	+	$IC_{50}=1\text{-}5*10^{-6}$ M	+	$IC_{50}=10^{-4}$ M	blocked by 10^{-4} M Cd^{2+}	Gielow *et al*, 1995
Nerbonne	Aplysia californica Bay cell neurons	+	$IC_{50}=1.4*10^{-6}$ M	NI		NI	Nerbonne and Garney, 1987
Brezina	Aplysia Accessory Radula	+	10^{-8} M	NI		blocked by 10^{-4} M Cd^{2+}	Brezina *et al*, 1994
Fieber	Aplysia Bag cells	+	10^{-5} M	NI		blocked by 10^{-4} M Cd^{2+}	Fieber *et al*, 1998
Schafer	Honeybee kenyon cells	+	10^{-4} M	+	10^{-4} M	blocked by $5*10^{-5}$ M Cd^{2+}	Schafer *et al*, 1994
Mills	Periplaneta americana coxal depression motor neuron	+		+	$5*10^{-5}$ M	blocked by 10^{-3} M Cd^{2+}	Mills and Pitman, 1997
Wicher	Periplaneta dorsal neurons	-		+	10^{-5} M	blocked by $5*10^{-6}$ M Cd^{2+}	Wicher and Penzlin, 1997
Dreijer	Lymnaea stagnalis neuroendocrine cells	+	10^{-5} M	+	10^{-4} M	NI	Dreijer and Kits, 1995
Yeoman	Lymnaea verntricular muscle cells	+	$IC_{50}=10^{-5}$ M	NI		Blocked by Cd^{2+} and La^{3+} at 10^{-3} M	Yeomann *et al*, 1999

Appendix 6: Table of invertebrate calcium currents: The DHP and PAA sensitivity figures are those reported to have had a significant effect which ranged from 10-50 % blockage. Half-maximal inhibition where measured has been included. NI denotes no information within the referred paper. In all the references, with the exception of Pelzer *et al*, 1989, results were obtained using whole-cell voltage clamp measurements. Pelzer *et al*, 1989 used voltage patch clamp to measure single channel Ca^{2+} currents.

References

Adamski, F. M., Zhu, M. Y., Bahiraei, F. and Shieh, B. H. (1998). Interaction of eye protein kinase C and INAD in Drosophila. Localization of binding domains and electrophysiological characterization of a loss of association in transgenic flies. *J Biol Chem.* **273**, 17713-9.

Barry, E. L., Gesek, F. A., Yu, A. S. L., Lytton, J. and Friedman, P. A. (1998). Distinct calcium channel isoforms mediate parathyroid hormone and chlorothiazide-stimulated calcium entry in transporting epithelial cells. *J Membr Biol.* **161**, 55-64.

Berridge, M. J. (1993). Inositol trisphosphate and calcium signalling. *Nature* **361**, 315-325.

Berridge, M. J. (1995). Capacitative calcium entry. *Biochem J* **312**, 1-11.

Berridge, M. J. (1997a). The AM and FM of calcium signalling. *Nature* **386**, 759-60.

Berridge, M. J. (1997b). Elementary and global aspects of calcium signalling. *J Physiol* **499**, 291-306.

Bird, G. S., Rossier, M. F., Hughes, A. R., Shears, S. B., Armstrong, D. L. and Putney, J. W. J. (1991). Activation of Ca2+ entry into acinar cells by a non-phosphorylatable inositol trisphosphate. *Nature* **352**, 162-165.

Bootman, M., Niggli, E., Berridge, M. J. and Lipp, P. (1997). Imaging the hierarchical Ca2+ signalling system in HeLa cells. *J Physiol* **499**, 307-314.

Brand, A. H. and Perrimon, N. (1993). Targetted gene expression as a means of altering cell fates and generating dominant phenotypes. *Development* **118**, 401-415.

Bredt, D. S., Glatt, C. E., Hwang, P. M., Fotuhi, M., Dawson, T. M. and Snyder, S. H. (1991). Nitric oxide synthase protein and mRNA are discretely localized in neuronal populations of the mammalian CNS together with NADPH diaphorase. *Neuron.* **7**, 615-24.

Bredt, D. S., Hwang, P. M. and Snyder, S. H. (1990). Localization of nitric oxide synthase indicating a neural role for nitric oxide. *Nature.* **347**, 768-70.

Brezina, V., Evans, C. G. and Weiss, K. R. (1994) Characterization of the membrane ion currents of a model mulluscan muscle, the accessory radula closer muscle of *Aplysia californica*. III. Depolarisation-activated Ca current. *J. Neurophysiol.* **71**, 2126-2138

Brini, M., Marsault, R., Bastianutto, C., Alvarez, J., Pozzan, T. and Rizzuto, R. (1995). Transfected aequorin in the measurement of cytosolic Ca2+ concentration ([Ca2+]c). A critical evaluation. *J Biol Chem.* **270**, 9896-903.

Button, D. and Eidsath, A. (1996), Aequorin targeted to the endoplasmic reticulum reveals heterogeneity in luminal Ca2+ concentration and reports agonist- or IP3-induced release of Ca2+. *Mol biol Cell.* **7**, 419-434.

Catterall, W. A., Seagar, M. J., Takahashi, M. and Nunoki, K. (1989). Molecular properties of voltage-sensitive calcium channels. *Adv Exp Med Biol.* **255**, 101-9.

Chyb, S., Raghu, P. and Hardie, R. C. (1999). Polyunsaturated fatty acids activate the Drosophila light-sensitive channels TRP and TRPL. *Nature.* **397**, 255-9.

Colbert, H. A., Smith, T. L. and Bargmann, C. I. (1997). OSM-9, a novel protein with structural similarity to channels, is required for olfaction, mechanosensation, and olfactory adaptation in Caenorhabditis elegans. *J Neurosci* **17**, 8259-69.

Cosens, D. J. and Manning, A. (1969). Abnormal electroretinogram from a Drosophila mutant. *Nature.* **224**, 285-7.

Davies, S. A. (2000). Nitric oxide signalling in insects. *Insect Biochemistry and Molecular Biology* **30**, 1123-1138.

Davies, S. A., Goodwin, S. F., Kelly, D. C., Wang, Z., Sozen, M. A., Kaiser, K. and Dow, J. A. T. (1996). Analysis and inactivation of vha55, the gene encoding the vacuolar ATPase B-subunit in Drosophila melanogaster reveals a larval lethal phenotype. *J Biol Chem.* **271**, 30677-84.

Davies, S. A., Huesmann, G. R., Maddrell, S. H. P., O'Donnell, M. J., Skaer, N. J. V., Dow, J. A. T. and Tublitz, N. J. (1995). CAP2b, a cardioacceleratory peptide, is present in Drosophila and stimulates tubule fluid secretion via cGMP. *Am J Physiol.* **269**, R1321-6.

Davies, S. A., Stewart, E. J., Huesmann, G. R., Skaer, N. J., Maddrell, S. H., Tublitz, N. J. and Dow, J. A. T. (1997). Neuropeptide stimulation of the nitric oxide signaling pathway in Drosophila melanogaster Malpighian tubules. *Am J Physiol.* **273**, R823-7.

Dawson, T. M., Bredt, D. S., Fotuhi, M., Hwang, P. M. and Snyder, S. H. (1991). Nitric oxide synthase and neuronal NADPH diaphorase are identical in brain and peripheral tissues. *Proc Natl Acad Sci U S A.* **88**, 7797-801.

De Leon, M., Wang, Y., Jones, L., Perez-Reyes, E., Wei, X., Soong, T. W., Snutch, T. P. and Yue, D. T. (1995). Essential Ca(2+)-binding motif for Ca(2+)-sensitive inactivation of L-type Ca2+ channels. *Science.* **270**, 1502-6.

De Waard, M., Liu, H., Walker, D., Scott, V. E., Gurnett, C. A. and Campbell, K. P. (1997). Direct binding of G-protein betagamma complex to voltage-dependent calcium channels. *Nature.* **385**, 446-50.

De Waard, M., Pragnell, M. and Campbell, K. P. (1994). Ca2+ channel regulation by a conserved beta subunit domain. *Neuron.* **13**, 495-503.

Dolmetsch, R. E., Lewis, R. S., Goodnow, C. C. and Healy, J. I. (1997). Differential activation of transcription factors induced by Ca2+ response amplitude and duration. *Nature* **386**, 855-858.

Dong, Y., Kunze, D. L., Vaca, L. and Schilling, W. P. (1995). Ins(1,4,5)P3 activates Drosophila cation channel Trpl in recombinant baculovirus-infected Sf9 insect cells. *Am J Physiol.* **269**, C1332-9.

Dow, J. A. T. (1999). The multifunctional Drosophila melanogaster V-ATPase is encoded by a multigene family. *J Bioenerg Biomembr.* **31**, 75-83.

Dow, J. A. T. and Davies, S. A. (2001). The *Drosophila melanogaster* Malpighian tubule. *Advances in Insect Physiology.*

Dow, J. A. T., Davies, S. A. and Sözen, M. A. (1998). Fluid secretion by the *Drosophila melanogaster* Malpighian tubule. *Amer. Zool.* **38**, 450-460.

Dow, J. A. T., Maddrell, S. H., Davies, S. A., Skaer, N. J. and Kaiser, K. (1994a). A novel role for the nitric oxide-cGMP signaling pathway: the control of epithelial function in Drosophila. *Am J Physiol.* **266**, R1716-9.

Dow, J. A. T., Maddrell, S. H., Gortz, A., Skaer, N. J., Brogan, S. and Kaiser, K. (1994b). The malpighian tubules of Drosophila melanogaster: a novel phenotype for studies of fluid secretion and its control. *J Exp Biol.* **197**, 197.

Dreijer, A. M. and Kits, K. S. (1995). Multiple second messenger routes enhance two high-voltage-activated calcium currents in molluscan neuroendocrine cells. *Neuroscience* **64**, 787-800.

Dube, K., McDonald, D. G. and O'Donnell, M. J. (2000). Calcium transport by isolated anterior and posterior Malpighian tubules of Drosophila melanogaster: roles of sequestration and secretion. *J Insect Physiol.* **46**, 1449-1460.

Dube, K. A., McDonald, D. G. and O'Donnell, M. J. (2000a). Calcium homeostasis in larval and adult *Drosophila melanogaster. Arch Insect Biochem Physiol* **44**, 27-39.

Dunlap, K., Luebke, J. I. and Turner, T. J. (1995). Exocytotic Ca2+ channels in mammalian central neurons. *Trends Neurosci.* **18**, 89-98.

Ebashi, S. and Endo, M. (1968). Calcium ion and muscle contraction. *Prog Biophys Mol Biol.* **18**, 123-183.

Eberl, D. F., Ren, D., Feng, G., Lorenz, L. J., Van Vactor, D. and Hall, L. M. (1998). Genetic and developmental characterization of Dmca1D, a calcium channel alpha1 subunit gene in Drosophila melanogaster. *Genetics.* **148**, 1159-69.

Estacion, M., Sinkins, W. G. and Schilling, W. P. (1999). Stimulation of Drosophila TrpL by capacitative Ca2+ entry. *Biochem J.* **341**, 41-9.

Farrugia, G. (1997). G-protein regulation of an L-type calcium channel current in canine jejunal circular smooth muscle. *J Membr Biol.* **160**, 39-46.

Feiber, L. A. (1998). Characterization of Na+ and Ca+ currents in bag cells of sexually immature *Aplysia californica. J. Exp. Biol.* **201**, 745-754.

Feinberg, A. P. and Vogelstein, B. (1983). A technique for labelling DNA restriction endonuclease fragments to high specific activity. *Annal. Biochem.* **137**, 266-267.

Fletcher, C. F., Lutz, C. M., O'Sullivan, T. N., Shaughnessy, J. D. J., Hawkes, R., W.N., F., Copeland, N. G. and Jenkins, N. A. (1996). Absence epilepsy in tottering mutant mice is associated with calcium channel defects. *Cell.* **87**, 607-17.

Galione, A., Lee, H. C. and Busa, W. B. (1991). Ca(2+)-induced Ca2+ release in sea urchin egg homogenates: modulation by cyclic ADP-ribose. *Science.* **253**, 1143-1146.

Gielow, M., Gu, G. G. and Singh, S. (1995). Resolution and pharmacological analysis of the voltage-dependent calcium channels of *Drosophila* larval muscles. *J. Neurosci.* **15**, 6085-6093.

Gloor, G. and Engels, W. (1991). Single-Fly preps for PCR. *D.I.S.* **71**, 148-149.

Grabner, M., Bachmann, A., Rosenthal, F., Striessnig, J., Schultz, C., Tautz, D. and Glossmann, H. (1994a). Insect calcium channels. Molecular cloning of an alpha 1-subunit from housefly (Musca domestica) muscle. *FEBS Lett.* **339**, 189-94.

Grabner, M., Wang, Z., Hering, S., Striessnig, J. and Glossmann, H. (1996). Transfer of 1,4-dihydropyridine sensitivity from L-type to class A (BI) calcium channels. *Neuron.* **16**, 207-18.

Grabner, M., Wang, Z., Mitterdorfer, J., Rosenthal, F., Charnet, P., Savchenko, A., Hering, S., Ren, D., Hall, L. M. and Glossmann, H. (1994b). Cloning and functional expression of a neuronal calcium channel beta subunit from house fly (Musca domestica). *J Biol Chem.* **269**, 23668-74.

Gu, X. and Spitzer, N. C. (1995). Distinct aspects of neuronal differentiation encoded by frequency of spontaneous Ca2+ transients. *Nature.* **375**, 784-787.

Hardie, R. C. and Minke, B. (1994). Calcium-dependent inactivation of light-sensitive channels in Drosophila photoreceptors. *J Gen Physiol.* **103**, 409-27.

Hardie, R. C. and Raghu, P. (1998). Activation of heterologously expressed Drosophila TRPL channels: Ca2+ is not required and InsP3 is not sufficient. *Cell Calcium.* **24**, 153-63.

Hardingham, G. E., Chawla, S., Johnson, C. M. and H., B. (1997). Distinct functions of nuclear and cytoplasmic calcium in the control of gene expression. *Nature* **385**, 260-265.

Harteneck, C., Obukhov, A. G., Zobel, A., F., K. and Schultz, G. (1995). The Drosophila cation channel trpl expressed in insect Sf9 cells is stimulated by agonists of G-protein-coupled receptors. *FEBS Lett.* **358**, 297-300.

Harteneck, C., Plant, T. D. and Schultz, G. (2000). From worm to man: three subfamilies of TRP channels. *Trends Neurosci.* **23**, 159-66.

Healy, J. I., Dolmetsch, R. E., Timmerman, L. A., Cyster, J. G., Thomas, M. L., Crabtree, G. R., Lewis, R. S. and Goodnow, C. C. (1997). Different nuclear signals are activated by the B cell receptor during positive versus negative signaling. *Immunity.* **6**, 419-428.

Hofmann, F., Biel, M. and Flockerzi, V. (1994). Molecular basis for calcium channel diversity. *Ann. Rev. Neurosci.* **17**, 399-418.

Hofmann, T., Obukhov, A. G., Schaefer, M., Harteneck, C., Gudermann, T. and Schultz, G. (1999). Direct activation of human TRPC6 and TRPC3 channels by diacylglycerol. *Nature.* **397**, 259-63.

Honda, H. M., Leitinger, N., Frankel, M., Goldhaber, J. I., Natarajan, R., Nadler, J. L., Weiss, J. N. and Berliner, J. A. (1999). Induction of monocyte binding to endothelial cells by MM-LDL: role of lipoxygenase metabolites. *Arterioscler Thromb Vasc Biol.* **19**, 680-6.

Hope, B. T., Michael, G. J., Knigge, K. M. and Vincent, S. R. (1991). Neuronal NADPH diaphorase is a nitric oxide synthase. *Proc Natl Acad Sci U S A.* **88**, 2811-4.

Hoth, M. and Penner, R. (1992). Depletion of intracellular calcium stores activates a calcium current in mast cells. *Nature* **355**, 353-356.

Hu, Y., Vaca, L., Zhu, X., Birnbaumer, L., Kunze, D. L. and Schilling, W. P. (1994). Appearance of a novel Ca2+ influx pathway in Sf9 insect cells following expression of the transient receptor potential-like (trpl) protein of Drosophila. *Biochem Biophys Res Commun.* **201**, 1050-6.

Huang, P. L., Dawson, T. M., Bredt, D. S., Snyder, S. H. and Fishman, M. C. (1993). Targeted disruption of the neuronal nitric oxide synthase gene. *Cell.* **75**, 1273-86.

Huber, A., Sander, P., Gobert, A., Bahner, M., Hermann, R. and Paulsen, R. (1996). The transient receptor potential protein (Trp), a putative store-operated Ca2+ channel essential for phosphoinositide-mediated photoreception, forms a signaling complex with NorpA, InaC and InaD. *EMBO J.* **15**, 7036-45.

Huesmann, G. R., Cheung, C. C., Loi, P. K., Lee, T. D., Swiderek, K. M. and Tublitz, N. J. (1995). Amino acid sequence of CAP2b, an insect cardioacceleratory peptide from the tobacco hawkmoth Manduca sexta. *FEBS Lett.* **371**, 311-4.

Ignarro, L. J., Buga, G. M., Wood, K. S., Byrns, R. E. and Chaudhuri, G. (1987). Endothelium-derived relaxing factor produced and released from artery and vein is nitric oxide. *Proc Natl Acad Sci U S A.* **84**, 9265-9.

Kaiser, K. (1993). Transgenic *Drosophila* - second generation enhancer traps. *Current Biology* **3**, 560-562.

Kim, S., McKay, R. R., Miller, K. and Shortridge, R. D. (1995). Multiple subtypes of phospholipase C are encoded by the norpA gene of Drosophila melanogaster. *J Biol Chem.* **270**, 14376-82.

Kiselyov, K., Xu, X., Mozhayeva, G., Kuo, T., Pessah, I., Mignery, G., Zhu, X., Birnbaumer, L. and Muallem, S. (1998). Functional interaction between InsP3 receptors and store-operated Htrp3 channels. *Nature* **396**, 478-482.

Knaus, H. G., Moshammer, T., Kang, H. C., Haugland, R. P. and Glossmann, H. (1992). A unique fluorescent phenylalkylamine probe for L-type Ca2+ channels. Coupling of phenylalkylamine receptors to Ca2+ and dihydropyridine binding sites. *J Biol Chem.* **267**, 2179-89.

Knight, M. R., Campbell, A. K., Smith, S. M. and Trewavas, A. J. (1991). Transgenic plant aequorin reports the effects of touch and cold-shock and elicitors on cytoplasmic calcium. *Nature.* **352**, 524-6.

Kuzin, B., Regulski, M., Stasiv, Y., Scheinker, V., Tully, T. and Enikolopov, G. (2000). Nitric oxide interacts with the retinoblastoma pathway to control eye development in Drosophila. *Curr Biol.* **10**, 459-62.

Lan, L., Bawden, M. J., Auld, A. M. and Barritt, G. J. (1996). Expression of Drosophila trpl cRNA in Xenopus laevis oocytes leads to the appearance of a Ca2+ channel activated by Ca2+ and calmodulin, and by guanosine 5'[gamma-thio]triphosphate. *Biochem J.* **316**, 793-803.

Lan, L., Brereton, H. and Barritt, G. J. (1998). The role of calmodulin-binding sites in the regulation of the Drosophila TRPL cation channel expressed in Xenopus laevis oocytes by ca2+, inositol 1,4,5-trisphosphate and GTP-binding proteins. *Biochem J.* **330**, 1149-58.

Lelong, I. H., Guzikowski, A. P., Haugland, R. P., Pastan, I., Gottesman, M. M. and Willingham, M. C. (1991). Fluorescent verapamil derivative for monitoring activity of the multidrug transporter. *Mol Pharmacol.* **40**, 490-4.

Leong, P. and MacLennan, D. H. (1998). The cytoplasmic loops between domains II and III and domains III and IV in the skeletal muscle dihydropyridine receptor bind to a contiguous site in the skeletal muscle ryanodine receptor. *J Biol Chem.* **273**, 29958-64.

Leung, H. T., Geng, C. and Pak, W. L. (2000). Phenotypes of trpl mutants and interactions between the transient receptor potential (TRP) and TRP-like channels in Drosophila. *J Neurosci.* **20**, 6797-803.

Li, H. S. and Montell, C. (2000). TRP and the PDZ protein, INAD, form the core complex required for retention of the signalplex in Drosophila photoreceptor cells. *J Cell Biol.* **150**, 1411-22.

Li, X. J., Xu, R. H., Guggino, W. B. and Snyder, S. H. (1995). Alternatively spliced forms of the alpha subunit of the epithelial sodium channel: distinct sites for amiloride binding and channel pore. *Mol Pharmacol.* **47**, 1133-40.

Liu, M., Parker, L. L., Wadzinski, B. E. and Shieh, B. H. (2000). Reversible phosphorylation of the signal transduction complex in Drosophila photoreceptors. *J Biol Chem.* **275**, 12194-9.

MacPherson, M. R., Pollock, V. P., Broderick, K. E., Kean, L., O'Connell, F. C., Dow, J. A. T. and Davies, S. A. (2001). Model Organisms: New Insights into Ion Channel and Transporter Function. L-type calcium channels regulate epithelial fluid transport in *Drosophila melanogaster*. *Am. j. Physiol. Cell. Physiol.* **280**, C000-C000.

Maddrell, S. H. P. (1981). The functional design of the insect excretory system. *Journal of Experimental Biology* **90**, 1-15.

Maddrell, S. H. P. (1991). The fastest fluid-secreting cell known: the upper Malpighian tubule cell of *Rhodnius*. *BioEssays* **13**, 357-362.

Maddrell, S. H. P. and O'Donnell, M. J. (1992). Insect Malpighian tubules: V-ATPase action in ion and fluid transport. *J. exp. Biol.* **172**, 417-429.

Marletta, M. A. (1994). Nitric oxide synthase: aspects concerning structure and catalysis. *Cell.* **78**, 927-30.

McCleskey, E. W. (1994). Calcium channels: cellular roles and molecular mechanisms. *Curr Opin Neurobiol.* **4**, 304-12.

McDonald, T. V., Premack, B. A. and Gardner, P. (1993). Flash photolysis of caged inositol 1,4,5-trisphosphate activates plasma membrane calcium current in human T cells. *J Biol Chem.* **268**, 3889-3896.

Mills, J. D. and Pitman, R. M. (1997). Electrical properties of a cockroach motor neuron soma depend on different characteristics of individual Ca components. *J. Neurophysiol.* **78**, 2455-2466.

Montell, C. (1997). New light on TRP and TRPL. *Mol Pharmacol.* **52**, 755-63.

Montell, C., Jones, K., Hafen, E. and Rubin, G. (1985). Rescue of the Drosophila phototransduction mutation trp by germline transformation. *Science.* **230**, 1040-3.

Morales, M., Ferrus, A. and Martinez-Padron, M. (1999). Presynaptic calcium-channelcurrents in normal and *csp* mutant *Drosophila* peptidergic terminals. *Eur..Neurosci.* **11**, 1818-1826.

Muller, U. and Buchner, E. (1993). Histochemical localization of NADPH-diaphorase in the adult Drosophila brain. Is nitric oxide a neuronal messenger also in insects? *Naturwissenschaften.* **80**, 524-6.

Myers, P. R., Minor, R. L. J., Guerra, R. J., Bates, J. N. and Harrison, D. G. (1990). Vasorelaxant properties of the endothelium-derived relaxing factor more closely resemble S-nitrosocysteine than nitric oxide. *Nature.* **345**, 161-3.

Nathanson, M. H., Fallon, M. B., Padfield, P. J. and Maranto, A. R. (1994). Localization of the type 3 inositol 1,4,5-trisphosphate receptor in the Ca2+ wave trigger zone of pancreatic acinar cells. *J Biol Chem.* **18**, 4693-4696.

Nelson, M. T., Cheng, H., Rubart, M., Santana, L. F., Bonev, A. D., Knot, H. J. and Lederer, W. J. (1995). Relaxation of arterial smooth muscle by calcium sparks. *Science* **270**, 633-637.

Nerbonne, J. M. and Gurney, A. M. (1987). Blockade of Ca2+ and K+ currents in bag cell neurons of *Aplysia californica* by dihydropyridine Ca2+ antagonists. *J. Neurosci.* **7**, 882-893.

Niemeyer, B. A., Suzuki, E., Scott, K., Jalink, K. and Zuker, C. S. (1996). The Drosophila light-activated conductance is composed of the two channels TRP and TRPL. *Cell.* **85**, 651-9.

Nunoki, K., Florio, V. and Catterall, W. A. (1989). Activation of purified calcium channels by stoichiometric protein phosphorylation. *Proc Natl Acad Sci U S A.* **86**, 6816-20.

O'Donnell, M. J., Dow, J. A. T., Huesmann, G. R., Tublitz, N. J. and Maddrell, S. H. (1996). Separate control of anion and cation transport in malpighian tubules of Drosophila Melanogaster. *J Exp Biol.* **199**, 1163-75.

O'Donnell, M. J. and Maddrell, S. H. (1995). Fluid reabsorption and ion transport by the lower Malpighian tubules of adult female Drosophila. *J Exp Biol.* **198**, 1647-53.

O'Donnell, M. J., Rheault, M. R., Davies, S. A., Rosay, P., Harvey, B. J., Maddrell, S. H., Kaiser, K. and Dow, J. A. T. (1998). Hormonally controlled chloride movement across Drosophila tubules is via ion channels in stellate cells. *Am J Physiol.* **274**, R1039-49.

Obukhov, A. G., Harteneck, C., Zobel, A., Harhammer, R., Kalkbrenner, F., Leopoldt, D., Luckhoff, A., Nurnberg, B. and Schultz, G. (1996). Direct activation of trpl cation channels by G alpha11 subunits. *EMBO J.* **15**, 5833-8.

Obukhov, A. G., Schultz, G. and Luckhoff, A. (1998). Regulation of heterologously expressed transient receptor potential-like channels by calcium ions. *Neuroscience.* **85**, 487-95.

Parekh, A. B., Fleig, A. and Penner, R. (1997). The store-operated calcium current I(CRAC): nonlinear activation by InsP3 and dissociation from calcium release. *Cell.* **89**, 973-80.

Parekh, A. B., Terlau, H. and Stuhmer, W. (1993). Depletion of InsP3 stores activates a Ca2+ and K+ current by means of a phosphatase and a diffusible messenger. *Nature* **364**, 814-818.

Pearn, M. T., Randall, L. L., Shortridge, R. D., Burg, M. G. and Pak, W. L. (1996). Molecular, biochemical, and electrophysiological characterization of Drosophila norpA mutants. *J Biol Chem.* **271**, 4937-45.

Peixoto, A. A. and Hall, J. C. (1998). Analysis of temperature-sensitive mutants reveals new genes involved in the courtship song of Drosophila. *Genetics.* **148**, 827-38.

Peixoto, A. A., Smith, L. A. and Hall, J. C. (1997). Genomic organization and evolution of alternative exons in a Drosophila calcium channel gene. *Genetics.* **145**, 1003-13.

Pelzer, S., Barhanin, J., Pauron, D., Trautwein, W., Lazdunski, M. and Pelzer, D. (1989). Diversity and novel pharmacological properties of Ca2+ channels in Drosophila brain membranes. *EMBO J.* **8**, 2365-71.

Petersen, C. C. H. (1996). Store operated calcium entry. *Seminars in the neurosciences* **8**, 293-300.

Petersen, O. H., Burdakov, D. and Tepikin, A. V. (1999). Polarity in intracellular calcium signaling. *Bioessays.* **21**, 851-860.

Peterson, B. Z., DeMaria, C. D., Adelman, J. P. and Yue, D. T. (1999). Calmodulin is the Ca2+ sensor for Ca2+ -dependent inactivation of L-type calcium channels. *Neuron.* **22**, 549-58.

Phillips, A. M., Bull, A. and Kelly, L. E. (1992). Identification of a Drosophila gene encoding a calmodulin-binding protein with homology to the trp phototransduction gene. *Neuron.* **8**, 631-42.

Poggi, A., Rubartelli, A. and Zocchi, M. R. (1998). Involvement of dihydropyridine-sensitive calcium channels in human dendritic cell function. Competition by HIV-1 Tat. *J Biol Chem.* **273**, 7205-9.

Pragnell, M., De Waard, M., Mori, Y., Tanabe, T., Snutch, T. P. and Campbell, K. P. (1994). Calcium channel beta-subunit binds to a conserved motif in the I-II cytoplasmic linker of the alpha1-subunit. *Nature.* **368**, 67-70.

Ptacek, L. J., Tawil, R., Griggsm, R. C., Engel, A. G., Layzer, R. B., Kwiecinski, H., McManis, P. G., Santiago, L., Moore, M. and Fouad, G. (1994). Dihydropyridine receptor mutations cause hypokalemic periodic paralysis. *Cell.* **77**, 863-8.

Putney, J. W. J. (1986). A Model Receptor-regulated Calcium Entry. *Cell Calcium* **7**, 1-12.

Raghu, P., Colley, N. J., Webel, R., James, T., Hasan, G., Danin, M., Selinger, Z. and Hardie, R. C. (2000). Normal phototransduction in Drosophila photoreceptors lacking an InsP(3) receptor gene. *Mol Cell Neurosci.* **15**, 429-45.

Randriamampita, C. and Tsien, R. Y. (1993). Emptying of intracellular Ca2+ stores releases a novel small messenger that stimulates Ca2+ influx. *Nature* **364**, 809-814.

Rapp, P. E. and Berridge, M. J. (1981). The control of transepithelial potential oscillations in the salivary gland of Calliphora erythrocephala. *J.exp.Biol.* **93**, 119-132.

Regulski, M. and Tully, T. (1995). Molecular and biochemical characterization of dNOS: a Drosophila Ca2+/calmodulin-dependent nitric oxide synthase. *Proc Natl Acad Sci U S A.* **92**, 9072-6.

Ren, D., Xu, H., Eberl, D. F., Chopra, M. and Hall, L. M. (1998). A mutation affecting dihydropyridine-sensitive current levels and activation kinetics in Drosophila muscle and mammalian heart calcium channels. *J Neurosci.* **18**, 2335-41.

Reuss, H., Mojet, M. H., Chyb, S. and Hardie, R. C. (1997). In vivo analysis of the drosophila light-sensitive channels, TRP and TRPL. *Neuron.* **19**, 1249-59.

Robitaille, R., Bourque, M. J. and Vandaele, S. (1996). Localization of L-type Ca2+ channels at perisynaptic glial cells of the frog neuromuscular junction. *J Neurosci.* **16**, 148-58.

Rosay, P., S.A., D., Yu, Y., Sozen, A., Kaiser, K. and Dow, J. A. T. (1997). Cell-type specific calcium signalling in a Drosophila epithelium. *J Cell Sci.* **110**, 1683-92.

Rosenthal, A., Rhee, L., Yadegari, R., Paro, R., Ullrich, A. and Goeddel, D. V. (1987). Structure and nucleotide sequence of a Drosophila melanogaster protein kinase C gene. *EMBO J.* **6**, 433-41.

Sadighi Akha, A. A., Willmott, N. J., Brickley, K., Dolphin, A. C., Galione, A. and Hunt, S. V. (1996). Anti-Ig-induced calcium influx in rat B lymphocytes mediated by cGMP through a dihydropyridine-sensitive channel. *J Biol Chem.* **271**, 7297-300.

Sambrook, J., Fritsch, E. F. and Maniatis, T. (1989). Molecular cloning: A laboratory manual: Cold Spring Harbour Press.

Schafer, S., Rosenboom, H. and Menzel, R. (1994). Ionic currents of kenyon cells from the mushroom body of the honeybee. *J.Neurosci.* **14**, 4600-4612.

Scott, K., Sun, Y., Beckingham, K. and Zuker, C. S. (1997). Calmodulin regulation of Drosophila light-activated channels and receptor function mediates termination of the light response in vivo. *Cell.* **91**, 375-83.

Scott, K. and Zuker, C. S. (1997). Lights out: deactivation of the phototransduction cascade. *Trends Biochem Sci.* **22**, 350-4.

Scott, K. and Zuker, C. S. (1998). Assembly of the Drosophila phototransduction cascade into a signalling complex shapes elementary responses. *Nature.* **395**, 805-8.

Sessa, W. C., Harrison, J. K., Barber, C. M., Zeng, D., Durieux, M. E., D'Angelo, D. D., Lynch, K. R. and Peach, M. J. (1992). Molecular cloning and expression of a cDNA encoding endothelial cell nitric oxide synthase. *J Biol Chem.* **267**, 15274-6.

Sheu, Y. A., Kricka, L. J. and Pritchett, D. B. (1993). Measurement of intracellular calcium using bioluminescent aequorin expressed in human cells. *Anal Biochem.* **209**, 343-7.

Shieh, B. H. and Niemeyer, B. A. (1995). A novel protein encoded by the InaD gene regulates recovery of visual transduction in Drosophila. *Neuron.* **14**, 201-10.

Shieh, B. H., Zhu, M. Y., Lee, J. K., Kelly, I. M. and Bahiraei, F. (1997). Association of INAD with NORPA is essential for controlled activation and deactivation of Drosophila phototransduction in vivo. *Proc Natl Acad Sci U S A.* **94**, 12682-7.

Shortridge, R. D., Yoon, J., Lending, C. R., Bloomquist, B. T., Perdew, M. H. and Pak, W. L. (1991). A Drosophila phospholipase C gene that is expressed in the central nervous system. *J Biol Chem.* **266**, 12474-80.

Sinkins, W. G., Vaca, L., Hu, Y., Kunze, D. L. and Schilling, W. P. (1996). The COOH-terminal domain of Drosophila TRP channels confers thapsigargin sensitivity. *J Biol Chem.* **271**, 2955-60.

Sinnegger, M. J., Wang, Z., Grabner, M., Hering, S., Striessnig, J., Glossmann, H. and Mitterdorfer, J. (1997). Nine L-type amino acid residues confer full 1,4-dihydropyridine sensitivity to the neuronal calcium channel alpha1A subunit. Role of L-type Met1188. *J Biol Chem.* **272**, 27686-93.

Skaer, H. (1996). Cell proliferation and development of the Malpighian tubules in Drosophila melanogaster. *Exp Nephrol.* **4**, 119-26.

Smith, L. A., Peixoto, A. A., Kramer, E. M., Villella, A. and Hall, J. C. (1998). Courtship and visual defects of cacophony mutants reveal functional complexity of a calcium-channel alpha1 subunit in Drosophila. *Genetics.* **149**, 1407-26.

Smith, L. A., Wang, X., Peixoto, A. A., Neumann, E. K., Hall, L. M. and Hall, J. C. (1996). A Drosophila calcium channel alpha1 subunit gene maps to a genetic locus associated with behavioral and visual defects. *J Neurosci.* **16**, 7868-79.

Snutch, T. P., Tomlinson, W. J., Leonard, J. P. and Gilbert, M. M. (1991). Distinct calcium channels are generated by alternative splicing and are differentially expressed in the mammalian CNS. *Neuron.* **7**, 45-57.

Sozen, M. A., Armstrong, J. D., Yang, M., Kaiser, K. and Dow, J. A. T. (1997). Functional domains are specified to single-cell resolution in a Drosophila epithelium. *Proc Natl Acad Sci U S A.* **94**, 5207-12.

Stortkuhl, K. F., Hovemann, B. T. and Carlson, J. R. (1999). Olfactory adaptation depends on the Trp Ca2+ channel in Drosophila. *J Neurosci.* **19**, 4839-46.

Tanabe, T., Takeshima, H., Mikami, A., Flockerzi, V., Takahashi, H., Kangawa, K., Kojima, M., Matsuo, H., Hirose, T. and Numa, S. (1987). Primary structure of the receptor for calcium channel blockers from skeletal muscle. *Nature.* **328**, 313-8.

Thorn, P. (1996). Spatial domains of Ca2+ signaling in secretory epithelial cells. *Cell Calcium* **20**, 203-214.

Tortorici, G., Zhang, B. X., Xu, X. and Muallem, S. (1994). Compartmentalization of Ca2+ signaling and Ca2+ pools in pancreatic acini. Implications for the quantal behavior of Ca2+ release. *J Biol Chem* **269**, 29621-29628.

Vallee, N., Briere, C., Petitprez, M., Barthou, H., Souvre, A. and Alibert, G. (1997). Studies on ion channel antagonist-binding sites in sunflower protoplasts. *FEBS Lett.* **411**, 115-8.

Vennekens, R., Prenen, J., Hoenderop, J., Bindels, R., Droogmans, G., Nilius, B. (2001). Pore properties and ionic block of the rabbit epithelial calcium channel expressed in HEK 293 cells. *J. Physiol*, **530.2** 183-191.

Wessing, A. and Eichelberg, M. (1978). Malpigian tubules, rectal papillae and excretion. In *The genetics and biology of Drosophila.*, vol. IIc eds M. Ashburner and T. R. F. Wright), pp. 1-42. London: Academic Press.

Wicher, D. and Penzlin, H. (1997). Ca2+ currents in central insect neurons: elctrophysiological and pharmacological properties. *J.Neurophysiol.* **77**, 186-199.

Wong, F., Yuh, Z. T., Schaefer, E. L., Roop, B. C. and Ally, A. H. (1987). Overlapping transcription units in the transient receptor potential locus of Drosophila melanogaster. *Somat Cell Mol Genet.* **13**, 661-9.

Xie, Q. W., Cho, H. J., Calaycay, J., Mumford, R. A., Swiderek, K. M., Lee, T. D., Ding, A., Troso, T. and Nathan, C. (1992). Cloning and characterization of inducible nitric oxide synthase from mouse macrophages. *Science.* **256**, 225-8.

Xu, X. Z., Chien, F., Butler, A., Salkoff, L. and Montell, C. (2000). TRPgamma, a drosophila TRP-related subunit, forms a regulated cation channel with TRPL. *Neuron.* **26**, 647-57.

Xu, X. Z., Choudhury, A., Li, X. and Montell, C. (1998). Coordination of an array of signaling proteins through homo- and heteromeric interactions between PDZ domains and target proteins. *J Cell Biol.* **142**, 545-55.

Yagodin, S., Hardie, R. C., Lansdell, S. J., Millar, N. S., Mason, W. T. and Sattelle, D. B. (1998). Thapsigargin and receptor-mediated activation of Drosophila TRPL channels stably expressed in a Drosophila S2 cell line. *Cell Calcium.* **23**, 219-28.

Yeoman, M., Brezden, B., Benjamin, P. (1999). LVA and HVA Ca2+ currents in ventricular muscle cells of the *Lymnaea* heart. *J. Neurophysiol.* **82,** 2428-2440

Yang, M. Y., Armstrong, J. D., Vilinsky, I., Strausfeld, N. J. and Kaiser, K. (1995). Subdivision of the Drosophila mushroom bodies by enhancer-trap expression patterns. *Neuron.* **15**, 45-54.

Yang, M. Y., Z., W., M.R., M., Dow, J. A. T. and Kaiser, K. (2000). A novel Drosophila alkaline phosphatase specific to the ellipsoid body of the adult brain and the lower Malpighian (renal) tubule. *Genetics.* **154**, 285-97.

Zhang, J. F., Ellinor, P. T., Aldrich, R. W. and Tsien, R. W. (1996). Multiple structural elements in voltage-dependent Ca2+ channels support their inhibition by G proteins. *Neuron.* **17**, 991-1003.

Zheng, W., Feng, G., Ren, D., Eberl, D. F., Hannan, F., Dubald, M. and Hall, L. M. (1995). Cloning and characterization of a calcium channel alpha 1 subunit from Drosophila melanogaster with similarity to the rat brain type D isoform. *J Neurosci.* **15**, 1132-43.

Zocchi, M. R., Rubartelli, A., Morgavi, P. and Poggi, A. (1998). HIV-1 Tat inhibits human natural killer cell function by blocking L-type calcium channels. *J Immunol.* **161**, 2938-43.

GLASGOW
UNIVERSITY
LIBRARY